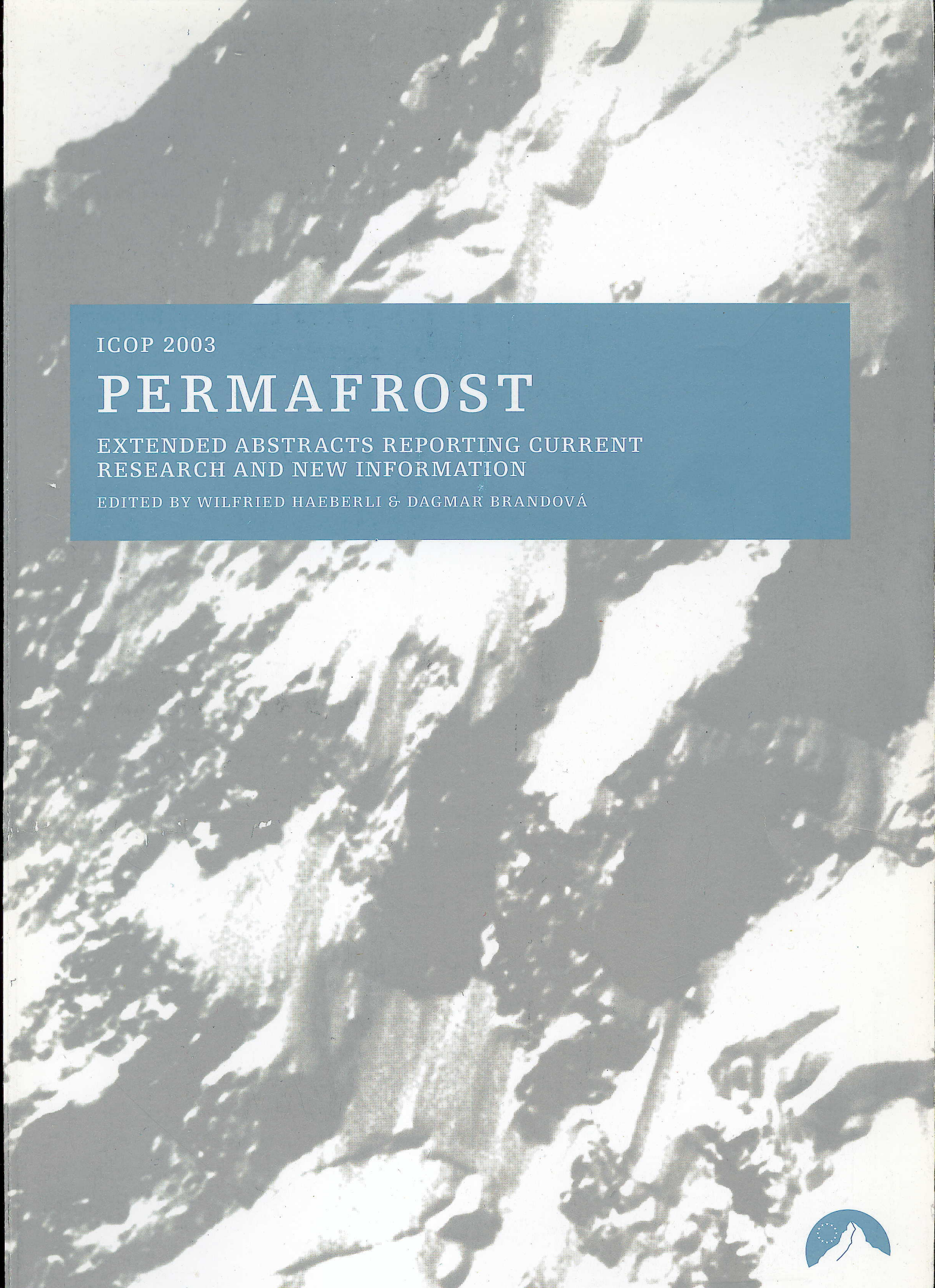

ICOP 2003

PERMAFROST

EXTENDED ABSTRACTS REPORTING CURRENT RESEARCH AND NEW INFORMATION

EDITED BY WILFRIED HAEBERLI & DAGMAR BRANDOVÁ

8th International Conference on Permafrost
Zurich, Switzerland,
20 – 25 July 2003

Extended Abstracts Reporting Current Research and New Information

edited by
Wilfried Haeberli and Dagmar Brandová

Glaciology and Geomorphodynamics Group
Geography Department, University of Zurich
Switzerland

Preface

There is a well-established tradition to prepare and print the Proceedings of the International Conferences on Permafrost (ICOP) in advance, enabling participants to take their volumes home from the meeting. As a consequence of this, papers have to be submitted, reviewed, corrected and finally edited ahead of the conference and in time for all the work to be published and delivered. In order to encourage presentation and discussion of ongoing activities and latest results, the possibility was introduced for the 8th International Conference to present posters on current research and new information. The present volume contains the extended abstracts of those posters which were personally presented at ICOP 2003 in Zurich, Switzerland, 20 – 25 July 2003. Corresponding 2-page contributions had to be submitted in early spring 2003 and were subject to a simplified yes/no-review process by the organizing committee. Our thanks go to the conference sponsors, to the authors for their excellent collaboration, to Perscheng Assef and Margit Haeberli Vunder for their help with editing and formatting, to Susan Braun, Marcia Phillips, Sarah Springman and Ivan Woodhatch for their help with English smoothing, to Andi Kääb for organising the posters and to Martin Hölzle for planning and final preparation of the printing.

Wilfried Haeberli and Dagmar Brandová

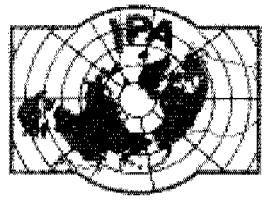

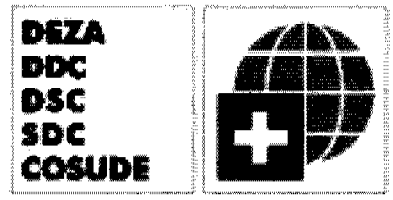

Conference Sponsors

Principal Sponsor

International Permafrost Association (IPA)	http://www.geodata.soton.ac.uk/ipa/

Co-Sponsors

European Science Foundation (ESF)	http://www.esf.org/
International Commission on Snow and Ice (ICSI)	http://geowww.uibk.ac.at/research/icsi/
International Glaciological Society (IGS)	http://www.spri.cam.ac.uk/igs/home.htm
International Society for Soil Mechanics and Geotechnical Engineering (ISSMGE)	http://www.issmge.org/
Permafrost and Climate in Europe in the 21st Century (PACE21)	http://www.cf.ac.uk/earth/pace/
Swiss Academy of Sciences (SANW)	http://www.naturalsciences.ch/
Geoforum Switzerland of SANW	http://www.geoforum.ethz.ch/
Glaciological Commission of SANW	http://www.sanw.glazko.sanwnet.ch
Swiss Geomorphological Society of SANW	http://www.sanw.ch/exthp/sgmg/
Swiss Academy of Engineering Sciences (SATW)	http://www.satw.ch/indexd.html

Funding Sponsors

Main Funding Sponsor

Swiss Agency for Development and Cooperation (DEZA)

Co-funding Sponsors

Airbornescan, Switzerland
BHP Billiton Diamonds, Canada
Department of Geography, University of Zurich, Switzerland
Geobrugg/Fatzer Protection Systems, Switzerland
Helibernina, Switzerland
Institute for Geotechnical Engineering, ETH Zurich, Switzerland
Migros Culture-Percentage, Switzerland
Solexperts, Switzerland
Stump Bohr Drilling Company, Switzerland
Swiss Academy of Sciences
Swiss Academy of Engineering Sciences
Swiss Alpine Club
Swiss Cablecars
Swiss Federal Institute for Snow and Avalanche Research
Swiss Federal Office for Water and Geology
Swiss National Cooperative for the Disposal of Radioactive Waste

Extended Abstracts

Kamchatka: mountain permafrost, volcanoes and life

A.A.Abramov, S.N.Buldovich, *V.A.Shcherbakova, K.S.Laurinavichius, **E.M.Rivkina, L.Kholodov and D.A.Gilichinsky

Department of Geocryology, Moscow State University, Moscow, Russia

**Institute of Biochemistry & Physiology of Microorganisms, Russian Academy of Sciences, Pushchino, Moscow Region, Russia*

***Soil Cryology Laboratory, Institute of Physicochemical & Biological Problems in Soil Science, Russian Academy of Sciences, Pushchino, Moscow Region, Russia*

According to the NASA point of view, one way to have liquid water on Mars at shallow depths would be through subglacial volcanism. Such volcano-ice interactions are feasible nowadays beneath the polar ice caps of Mars, or even within the adjacent permafrost at the margins of the ice caps. This is why one of the Earth's models which may come close to extraterrestrial environments is represented by active volcanoes in permafrost areas. The main question is whether volcanoes and associated environments can be ecological niche for microbial communities, and whether these bacteria can survive in permafrost. For this reason, our study was carried out on the volcano Ploskii Tolbachik, situated in Kamchatka – a unique peninsula in the east of Russia. It is one of the largest modern volcanic regions with widespread glaciers and permafrost at high altitudes. Large parts of the glaciers are well studied, cold and situated at altitudes higher than 3000 m a.s.l. (Kotlyakov 1997). Permafrost in the region, however, has received little attention; on the basis of air temperatures, continuous permafrost can be assumed to occur above 1800-2000 m a.s.l. and to reach a thickness of 50-400 m (Zamolodchikova 1989). In a generalized way, and based on new data obtained from drilling on the slopes of the volcano in the summer of 2002, preliminary results relating to microbiological and biogeochemical analyses are presented.

One 54 m deep borehole was drilled in 1978 at a site where the Large Tolbachik Fissure Eruption (LTFE; Fedotov 1984) broke through in 1975/76. In addition, we drilled a series of boreholes and pit-holes at different altitudes between 800 and 2600 m a.s.l. on the slopes of the active volcano Ploskii Tolbachik. The boreholes were placed in different landscape conditions, and had depths ranging from 5 to 15 m. The permafrost samples for microbiological analysis were obtained by slow rotary drilling without the use of solutions or drilling mud. The surface of the extracted cores was trimmed away with a sterile knife. Then the samples were immediately plated on a specially-fitted nutrient medium. The main part of the core was divided into sections, placed in presterilized aluminum cans, sealed and placed in frozen storage. Samples were taken for ice content, gas, chemical and textural composition. After completion of drilling, the boreholes were closed during a week and then borehole temperatures were measured.

Based on these field measurements and on other published data (Zamolodchikova 1989), it is possible to suggest the following scheme of permafrost distribution on Ploskii Tolbachik slopes (Fig. 1). The borehole 5/02, located in the forest zone (~800 m a.s.l.), has no permafrost. We can explain this by the fact that the trees tend to retain snow. In fact, snow depths in the forest can reach 2 m and more, whereas in the absence of trees snow depth averages 0.5 to 0.8 m, and hardly depends on wind redistribution. Enhanced snow depth in forests effectively protects the soil surface from strong winter cooling and enables seasonal freezing only. Borehole 6/02 drilled above the timberline at an altitude of 900 m a.s.l. is in the zone of seasonal freezing, too. Because of lower snow cover, however, the remains of seasonally frozen ground with a thickness of 0.5 m were encountered at a depth of 1.5 to 2 m.

Borehole "MARS-7/02" was drilled from the surface of a tefra plateau at about 1100 m a.s.l. in the belt of discontinuous permafrost occurrence. The thickness of the active layer is about 1.5 to 2 m. The mean annual temperature of the frozen

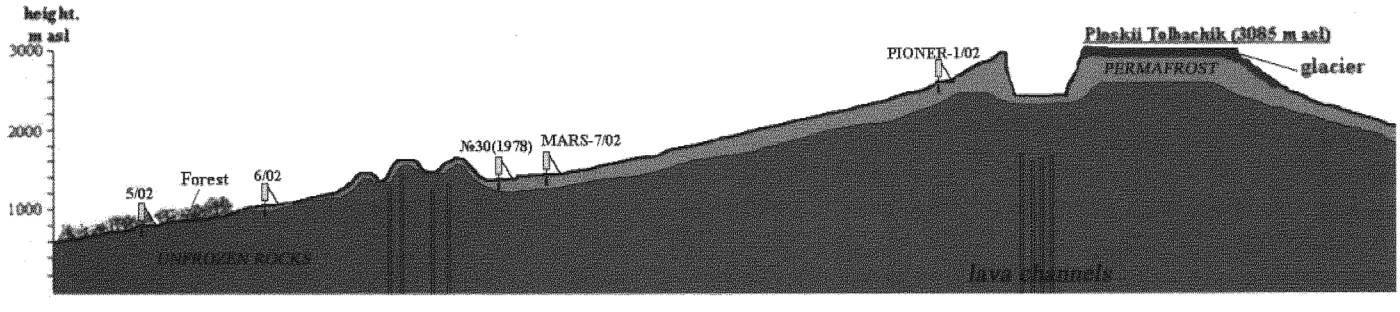

Figure 1. A schematic cross-section of the volcano Ploskii Tolbachik with the drilled boreholes. The thickness of the permafrost is estimated and not drawn to scale.

rocks is between 0 and -1° and permafrost thickness up to 50-60 m. Borehole 30 drilled three years after LTFE at about 1000 m a.s.l. revealed 54 m of frozen rocks. It is interesting to note that the textural description of this borehole indicated combined piroclastic deposits from LTFE in the upper 16 m in the summer of 1975. In 1978, these deposits had become completely frozen (Andreev 1982). Model calculations show that such deposits with a low heat conductivity need considerable time for complete freezing (~8-9 yr). We cannot completely explain this phenomenon yet.

Borehole "PIONER-1/02" was drilled at an elevation of 2600 m a.s.l. from the surface of a weathered basalt flow. Permafrost here probably has a continuous distribution pattern and a low mean annual temperature around -7 °C; its thickness can reach 100-150 m. Local taliks can be found where thermal waters exist and in the central part of the active volcano.

For better estimates of probable permafrost thickness in the region, a numerical simulation using the program "WARM" for the temperature field at the time of LFTE (1975 yr) was conducted. The model dimensions of the Ploskii Tolbachik volcanic complex are 25 km long and 25 km deep. The upper boundary condition is given by the mean annual surface temperature calculated using an altitude lapse rate of 0.5°C/100 m. In glacierized terrain were taken the boundary condition of III type (i.e. combination of mean annual air temperature and coefficient of heat transfer between atmosphere and rocks through ice with an estimated thickness of 100 m). At the lower boundary, located on the depth 25000 m, was set heat flux 80 mW/m^2. On the depth 20000 m was set the magma reservoir (3 km in diameter), with temperature 1200°C. Thermal properties of the rocks were taken from the literature data (Komarov et al. 1996; Table 1).

Table 1. Thermal properties of rocks used for simulation.

	Basalt	Volcanic dross
λT, W/m* K	2.9	0.3
λf, W/m*K	3.5	0.6
C_T, Kkal/m^3*K	600	300
C_F, Kkal/m^3*K	500	400
Q_F, Kkal/m^3	5000	1000

With the results of the simulation it is possible to conclude that the volcanic eruption causes instantaneous temperature rises of up to 1000-1200°) but constitutes short-lived effects. The main effects are concentrated at the surface and within high atmospheric layers. Thus, it is not likely that such eruptions will greatly reduce the thickness of the permafrost, any effects will remain localized. Increased heat flux in areas of modern volcanic activity, on the other hand, results in considerable reduction of permafrost thickness underneath glaciers, thereby probably inducing the formation of zones with positive subglacial temperatures and basal glacier melting. The subsurface temperature field at the the Ploskii Tolbachik volcano has a non-stationary character, because it could not fully adjust between eruptions.

The existence of frozen rocks on the investigated volcano is a function of elevation rather than latitude. As a consequence, it should be attributed to mountain permafrost conditions. In the investigated region, continuous permafrost with a thickness of about 50 m starts to occur at an elevation higher than 1400-1500 m a.s.l. Maximum permafrost thickness can probably reach 200-250 m at 3000 m a.s.l.

The analysis shows that frozen samples extracted from borehole 7/02 and representing young volcanic deposits contain viable microorganisms and, among them, thermophilic anaerobic bacteria. Moreover, biogenic methane (up to 1100-1900 μlCH_4/kg soil) was found in these samples. Thermophiles had never been found before in permafrost. The present study therefore demonstrates that the only way for thermophilic bacteria to appear within frozen volcanic horizon is during eruption from volcanoes or from related subsurface geological strata. The most important conclusion is that (1) thermophilic bacteria might survive in permafrost and even produce biogenic gases, and that (2) terrestrial volcanic microbial communities might serve as exobiological models for hypotheses on existing ancient microbiocenoses, i. e., extraterrestrial habitats that may possibly be found under anoxic conditions around volcanoes on Mars or other planets.

ACKNOWLEDGEMENTS

This work was supported by the Russian Foundation of Basic Research (grant 01-05-05-65043) and the NASA Astrobiology Institute Program.

REFERENCES

Andreev, V. 1982. Permafrost in Tolbachik eruption region. Questions of Kamchatka geography 8: 98-99 (in Russian).

Fedotov, S. (ed.) 1984. Large Tolbachik Fissure Eruption Kamchatka 1975-1976. Moscow: Nauka (in Russian).

Komarov, I. et al 1996. Heat- and mass-exchange properties of rocks. In: E. Ershov (ed.), Lithogenous Geocryology. Moscow State University publisher (in Russian).

Kotlyakov, V. (ed.) 1997. World atlas of snow and ice resources . Moscow: Nauka (in Russian).

Zamolodchikova, S. 1989. Kamchatka region. In: Ershov, E. (ed.), Geocryology of USSR. East Siberian and far East: 380-389. Moscow: Nedra (in Russian).

Verifying modelling approaches: high mountain permafrost and its environment

M. Avian

Department of Geography and Regional Sciences, University of Graz, Austria

INTRODUCTION

The Ankogel Mountains are a highly glacierized area in the easternmost part of the Hohe Tauern Range in Carinthia (Fig. 1). The test site encloses 98 km^2 including the main peaks of the Ankogel (3246 m) and the Hochalmspitze (3360 m). Glaciers cover an area of 12.1 km^2 and shows wide retreat zones.

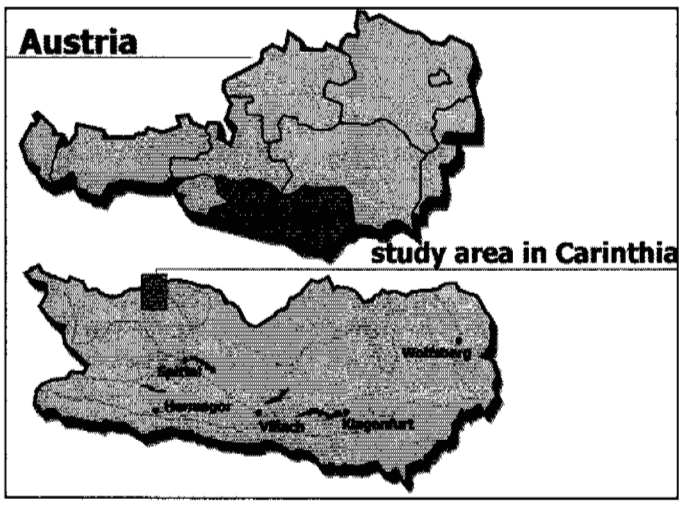

Figure 1. Location of the study area in Austria.

METHODOLOGY

The distribution of permafrost was modelled by an adaptation of the programme PERMAKART, using the GIS Arc-Info (Haeberli et al. 1996). The main point is to receive information about slope, aspect and elevation. The result is a supposed distribution of permafrost in the study area with the classes "permafrost probable", "permafrost possible" and "no permafrost". The modelling of potential incoming short wave radiation (PSWR) was done by using the programme ERDAS-Imagine. Shadows that are cast by topographic features on the surrounding surface were not calculated.

Remote sensing data are the basis for the mapping of the distribution of snow patches, vegetation and rock glaciers. Snow patches were mapped by using colour orthophotographs (as at: August 1998), Keller (1994) shows an investigation, in which a significant correlation between 493 snow patches and the occurrence of permafrost was detected. Infrared orthophotographs are a common data set for investigating vegetation. A useful classification in connection with the investigation of permafrost could only be carried out by visual interpretation. In connection with their percentage of soil cover, three classes of vegetation were used: uniform vegetation (over 90%,), transition vegetation (20 to 90%,), and island vegetation (below 20%). The background is the assumption that a solid cover of vegetation excludes permafrost in the underground. The occurrence of active rock glaciers is an obvious sign for permafrost.

RESULTS

As the distribution of exposition is homogenous it is a good basis for further analysis. The modelled classes of the distribution of permafrost were renamed for the reason of empirical results in the Hohe Tauern Range (Lieb 1998) from "permafrost possible" to "potential sporadic permafrost (PSP)" and from "permafrost probable" to "potential discontinous permafrost (PDP)" (see Tab. 1). The model of the PSWR shows a satisfying overall view and a good correspondence of areas with a PSWR under 53 kJ/m^{2}a and PDP.

The main part of the study is to compare the results of the modelling with the information received from the study area. 684 snow patches with an area of altogether 108 ha were counted in the study area (average altitude: 2635m). At first sight there is no significant relation between PDP and the occurrence of snow patches (Tab. 2), but a closer look shows that nearly all snow patches which are not situated in potential permafrost areas, occur in direct neighborhood with PDP and PSP.

29.3% of the study area are covered with vegetation, the relation between potential permafrost and vegetation provides a clear result: although there is a high percentage of soil cover with vegetation in this high mountain area, only a marginal zone of overlapping with PDP in an area of 0.9 hectares and 0.06% can be seen (Table 3). Rock glaciers can only be found in the southern part of the study area. Seven are active, one is inactive and eight are fossile. The model shows a good correlation with the catchment area of blocks, but does not mainly correspond with the lobes of the rock glaciers.

Table 1. Areas of generated permafrost classes.

	area in km²	area in %
no permafrost	58.3	59.7
PSD	15.3	15.7
PDP	24.0	24.6
sum	97.6	100.0

Table 2. Snow patches according to potential permafrost areas.

	area in km²	area in %
no permafrost	0.37	34.5
PSD	0.37	34.0
PDP	0.34	31.5
sum	1.08	100.0

Table 3. Areas of vegetation classes and overlapping with potential permafrost areas.

	area in km²	area in %	Overlapping %	
			PDP	PSP
uniform veg.	17.9	62.3	0.05	1.33
transition veg	8.6	30.1	0.12	9.86
island veg.	2.1	7.6	2.30	19.06
sum	28.6	100.0		

The final step is to generate a most probable lower borderline for permafrost including all results with a last visual interpretation of the geological situation (coarse debris). The adaptation uses the modelling of potential permafrost areas as a basis, the results of the distribution of vegetation correct the limit as well as the distribution of snow patches. A visual interpretation of the orthophotographs includes areas of coarse debris in the neighborhood of potential permafrost areas. The modelling of PSWR is only a check in a higher scale. The final result is an area of 35.16 km², that are 36% of the study area, which can be seen as potential permafrost areas. In April 2002 BTS-measurements were carried out in two small test sites in the south east of the study area. The results correspond very well with the most likely lower borderline for permafrost.

CONCLUSION

The model of the distribution of permafrost provides wide areas of potential permafrost, including almost the entire glacier areas. All the relations can be summarised as follows:

1. Although there is a superficial discrepancy between the assumption and mapping results of snow patches, a closer look provides valuable improvement.
2. Closed vegetation cover excludes potential permafrost in the study area with a probability of 99,96%.
3. All catchment areas of active rock glaciers are situated in potential permafrost areas.
4. The result of modelling the potential incoming short wave radiation shows a good connection to potential permafrost.

Crosschecking of results shows good correlations between the modelling results and the results from mapping for the Eastern part of the Alps. Valuable improvements can be derived in using the distribution of snow patches and geological patterns.

ACKNOWLEDGEMENTS

I wish to thank Mr. Gerhard Lieb and Ms. Michaela Nutz for critical review, also Mrs. Christine Lazar for improving the English and Mr. Stefan Lieb, Mr. Markus Frei, Mr. Wolfgang Sulzer as well as Mr. Alexander Avian for critical comments.

REFERENCES

Haeberli, W., Hoelzle M., Dousse, J.-P., Ehrler, C., Gardaz, J.-M., Imhof, M., Keller, F., Kunz, P., Lugon, R. and Reynard, M. 1996. Simulation der Permafrostverbreitung in den Alpen mit geographischen Informationssystemen. Arbeitsbericht NFP 31, Hochschulverlags-AG an der ETH Zürich , 58 p.

Keller, F. 1992. Automated mapping of mountain permafrost using the programm PERMAKART within the Geographical Information System ARC-Info. Permafrost and Periglacial Processes, Vol. 3(2): 133-138.

Keller, F. 1994. Interaktionen zwischen Schnee und Permafrost, Eine Grundlagenstudie im Oberengadin. Versuchsanstalt für Wasserbau, Hydrologie und Glaziologie der ETH Zürich, 145 p.

Lieb, G.K. 1998. High-mountain permafrost in the Austrian Alps. – Permafrost, 7th International Conference on Permafrost, Yellowknife (Canada), Proceedings: 663-668.

The role of cosmoplanetary climate cycles in Earth's cryolithosphere evolution

V.T. Balobaev and V.V. Shepelev

Melnikov Permafrost Institute, SB RAS, Yakutsk, Russia

We believe that different climate-forming global factors have a resonance type of relationship. The conceptual model of manifestation of this effect on the global climate system is shown in Figure 1. This model is based on the assumption that periods and amplitudes of the temperature variations caused by separate global factors are constant in time. The presented model takes into account four main climate-forming factors: one cosmoplanetary variation with a period of 200 Ma and three astroplanetary variation with periods of 100, 40.7, and 20 ka. The variation curve of the longer cycle is taken as the base level for variations of the shorter climate-forming cycle. The superposition of harmonics involved in the calculation of climate-forming cycles highlights distinct peaks corresponding to periods of phase coincidence of individual temperature variations. This effect, which we called thermoresonance, causes significant periodic cooling and warming of the global climate.

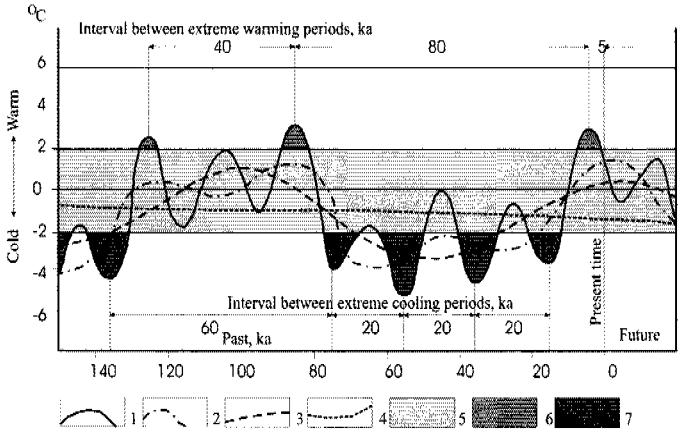

Figure 1. Conceptual model of the integral dynamic correlation between the main global factors of climate formation during the past 150 ka. (1) curve of a 20-ka cycle caused by precession of the Earth's axis; (2) curve of a 40.7-ka cycle caused by variations in the obliquity of the rotation axis with respect to the ecliptic plane; (3) curve of a 100-ka cycle caused by variations in the eccentricity of the Earth's orbit; (4) curve of an about 200-Ma cycle related to the rotation of the solar system around the galactic centre; (5) area of optimal climatic conditions; (6) periods of extreme warming; (7) periods of extreme cooling.

The amplitudes of harmonics strongly vary and the highest of them, especially those of 40-ka and 20-ka cycles, distinctly indicate the resonance amplification. Since the Earth's climate system is excited and less stable during the strongest temperature decrease or increase in the 100-ka cycle, the 40- and 20-ka cycles exert a resonance effect. It should be noted that extreme cold periods in our model generally agree with glacial periods in the Late Pleistocene reconstructed from seafloor sediment data (Steig 1998).

Using the proposed concept of the thermoresonance effect, an attempt can be made to reconstruct the climate for the whole Phanerozoic Eon spanning the past 570 Ma. Figure 2 shows a scheme constructed with consideration for the thermoresonance effect between two main cosmoplanetary climate-forming factors with periods of 1.3 Ga and 200 Ma and spanning the past 700 Ma of the Earth's evolution.

Of special interest for permafrost-researchers is to reveal the possibility of formation and dynamics of cryogenic processes in different periods of the Phanerozoic which was relatively warm in the Earth's history that had served as the base for a vigorous development of a biosphere. The preceded Proterozoic was significantly colder, what determined the existence of large glaciations whose traces are found in sediments of this epoch. The Cambrian (570-500 Ma ago), that is the first period of the Phanerozoic, was warm and without permafrost what is connected not only with 200-Ma cycle (Fig. 2) but with favourable location of lithospheric plates on the Earth's surface as well. The largest continent of that time, Gondwana, was located in subtropical latitudes, and smaller plates were in the equator zone. The poles were located in water areas of open oceans, and negative temperatures were not observed on the Earth's surface of the whole planet.

In the Ordovician (500-440 Ma ago) the planetary climate was significantly colder (Fig. 2). By the end of this period, Gondwana transferred to the South Pole. This determined the initiation of a thick continental glaciation,

whose traces occur in Africa. Frozen grounds developed at a third part of Gondwana (Africa and South America).

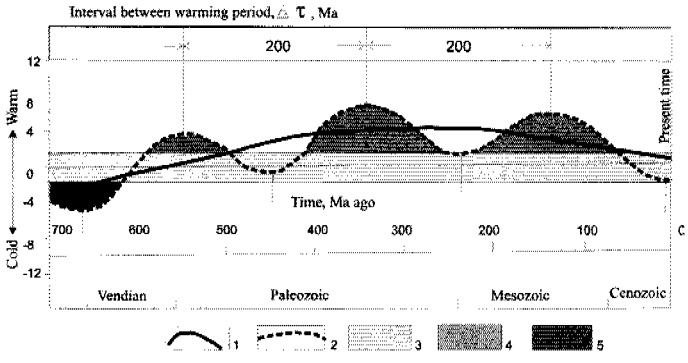

Figure 2. Scheme of the correlation between two main cosmoplanetary factors responsible for the Earth's global climate. (1) curve of the 1.3-Ga cycle caused by rotation of our galaxy around the mega-galactic centre; (2) curve of a 200-Ma cycle caused by rotation of the solar system around the galactic centre; (3) area of optimal climatic conditions; (4) extreme warming period; (5) extreme cooling periods.

The water areas of the North Pole could have seasonal icings only. The global warming occurred in the Silurian (440-410 Ma ago). The Gondwana continent left the South Pole and transferred to the equator. Thin frozen grounds could occur just on a small part of this continent (South America). The area of their development and the thickness increased by the end of the Silurian due to drifting of Gondwana to the South Pole.

The cycle of global warming (440-300 Ma ago) coinciding with the periods of the Devonian and the Carboniferous was one of the warmest cycles on the Earth. It was accompanied by a vigorous development of vegetation. The addition of small lithospheric plates to the second supercontinent, Laurasia, occurred in this epoch, and at the end of this epoch Gondwana joined with Laurasia into a single supercontinent Pangea. There was no glaciation though, Gondwana and later a significant part of Pangea were located near the South Pole throughout this period. However, considerable daily and annual fluctuations of temperature and its transitions through 0°C was to be observed due to a large area of the continent and location of its parts in high latitudes. At the end of the Carboniferous (350-285 Ma ago), when the global temperature began to decrease, negative mean annual temperatures and frozen grounds appeared in the south part of Pangea. Then the continental glaciation began near the South Pole (Antarctica, South Africa, Australia). The strongest cooling of the Earth wasobserved at the boundary of the Permian (285-230 Ma ago) and the Triassic (230-195 Ma ago). It was connected with the global climate cooling and unfavourable location of Pangea relative to the poles. The south of Pangea was covered with ice (Antarctica), and the south of the continent contained permafrost.

The subsequent cycle of a global warming occurred in the Jurassic (195-137 Ma ago) and the Cretaceous (137-67 Ma ago, Fig. 2). By that time Pangea was divided into Gondwana and Laurasia and then into smaller blocks, of which present continents were formed later. The reasons that Gondwana moved to the latitudes of 20° from the South Pole and that both poles of the Earth occurred in the ocean resulted in a greater increase of the global temperature. Mean global temperature at that time was 8°C higher than the present. All of this eliminated the possibility of formation of permafrost on the Earth and glaciation centres.

At the end of the Cretaceous, a new cold epoch developed on the Earth. Compared to the Late Cretaceous, temperature decreased by 2-4°C at the middle of the Paleogene (65-23 ka) and was 4-5°C higher than the present at the end of the Paleogene. Fast decrease of the global temperature was due to the fact that Antarctica firmly established at the South Pole. Formation of the Antarctic circumpolar stream at the beginning of the Neogene resulted in glaciation of Antarctica, which continues to the present (Monin and Shishkov 1979). In the northern hemisphere first sheet glaciations are dating by 3 Ma ago, and the ice cover in the Arctic Ocean appeared 0.7-0.8 Ma ago. Probably, at the same time the permafrost formed in the northern hemisphere.

Therefore, positive phase of the 1.3-Ga climate cycle, including practically the entire Phanerozoic, is terminating. This indicates that the next 500-600 Ma on our planet will be a kingdom of cold and ice. However, this does not exclude short-term warming periods related to astro- and geoplanetary temperature-forming factors and their resonance amplification.

REFERENCES

Monin, A.S. and Shishkov, Yu.A. 1979. Climate history (Istoriya klimata) (in Russian). Leningrad: Gidrometeoizdat.

Steig, E. 1998. Synchronous climate changes in Antarctica and the North Atlantic. In Science 282: 92-95.

Terrestrial biosphere modelling in permafrost regions

*C. Beer, *W. Lucht, **C. Schmullius and M. Gude*

Department of Geography, University of Jena, Germany

**Potsdam Institute for Climate Impact Research, Potsdam, Germany*

***Department of Geography, University of Jena, Germany*

INTRODUCTION

Besides CO_2 inversion modelling, Dynamic Global Vegetation Models (DGVMs) are suited for investigating the terrestrial component of the global carbon balance. These models are icreasingly of particular interest due to their potential for predicting the impacts of the biosphere upon future concentrations of atmospheric CO_2. Because water availability in plants is one of the key stimuli for vegetation growth, DGVMs combine the carbon with the water cycle.

Our research is conducted within the framework of the SIBERIA-II project funded by the European Commission (Contract No. EVG2-2001-00008, http://www.siberia2.uni-jena.de). In this work, the impact of hydrological conditions on the carbon cycle in permafrost regions of Northern Eurasia is investigated. For this purpose, a permafrost module built upon previous work of Venevsky (2001) following the equations of Anisimov et al. (1997) is presented as an extension of the Dynamic Global Vegetation Model LPJ (Lund-Potsdam-Jena; Sitch 2000).

MODEL DESCRIPTION

LPJ uses 4 carbon and 2 soil layers (0.5 m and 1.5 m depth). Input of LPJ are basic climate and soil data (air temperature, precipitation, sunshine duration, soil texture) on a spatial resolution of 0.5° times 0.5°. To provide dynamic variables of the carbon cycle such as Net Primary Production (NPP) or Leaf Area Index (LAI) in a daily time step, LPJ begins by computing hydrological variables such as soil moisture and evapotranspiration.

In permafrost regions the hydrology is completely altered by our new permafrost module. Soil moisture is strongly dependent on daily thaw depth in the present. As a simplification, we assume that the course of daily thaw depth and air temperature resembles a sine curve. This leads to the following equation for calculating the daily thaw depth:

$$Z_{thaw} = \begin{cases} Z_{\max} \cdot \sin\left(\dfrac{2\pi \cdot (t - t_{spring})}{4 \cdot \tau_{pos}}\right), & T > 0 \\ Z_{\max} - \left(Z_{\max} \cdot \sin\left(\dfrac{2\pi \cdot (t - t_{spring} - \tau_{pos})}{4 \cdot \tau_{pos}}\right)\right), & T < 0 \end{cases}$$

Z_{thaw} - daily thaw depth

$Z_{\max}$ - max thaw depth

t - current day

t_{spring} - start of spring

τ_{pos} - duration of days while $T > 0$

T - air temperature

The zonation of permafrost (Fig. 1) is obtained by assuming that TTOP (Temperature at TOP Of the Permafrost) is below 0 °C in permafrost regions following Smith (2002). This zonation will be compared with that obtained by means of the frost-index of Anisimov and Nelson (1997).

OUTLOOK

To investigate the impact of permafrost hydrology on the terrestrial carbon cycle, different outputs of LPJ with and without the permafrost module are compared with in situ measurements or Earth Observation data, e. g., growing stock volume, NPP, or LAI in Siberia between 90° and 110° East. A lower value of biomass and NPP is expected when permafrost hydrology is taken into consideration, and it is anticipated that more reliable values for NPP and NEP (Net Ecosystem Production), can be obtained, which in turn will lead to a more precise global carbon balance.

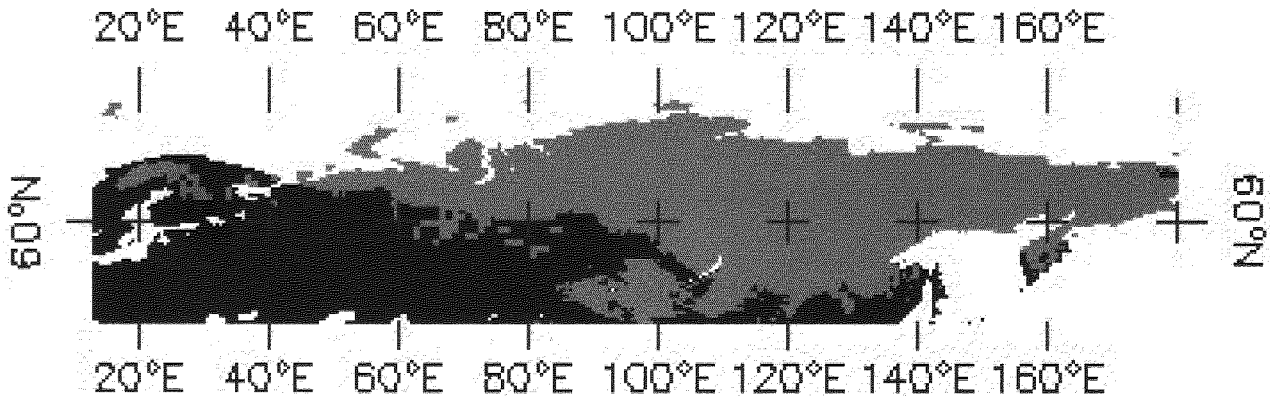

Fig. 1: Permafrost distribution (grey) in the Eurasian hemisphere as modelled using the LPJ routine

REFERENCES

Anisimov, O.A. Shiklomanov, N.I., and Nelson, F.E. 1997. Global warming and active-layer thickness: results from transient general circulation models. Global and Planetary Change 15: 61-77.

Anisimov, O.A. and Nelson, F.E. 1997. Permafrost zonation and climate change in the northern hemisphere: results from the transient general circulation models, Climatic Change 35: 241-258.

Sitch, S. 2000. The role of vegetation dynamics in the control of atmospheric CO_2 content. Dissertation, Lund University, Lund, Sweden

Smith, M. W. and Riseborough, D.W. 2002. Climate and the limits of permafrost: A Zonal Analysis. Permafrost and periglacial Processes 13: 1-15.

Venevsky, S. 2001. Broad-scale vegetation dynamics in north-eastern Eurasia – observations and simulations, PhD Thesis, Universität für Bodenkultur, Wien.

Combining water chemistry and geophysical investigations with assessment of chemical denudation rates in the Latnjavagge drainage basin, arctic-oceanic Swedish Lapland

*A. A. Beylich, E. Kolstrup, *U. Molau, **T. Thyrsted, ***N. Linde, L. B. Pedersen and ****D. Gintz*

Department of Earth Sciences, Environment and Landscape Dynamics, Uppsala University, Uppsala, Sweden
**Botanical Institute, Plant Ecology, Gothenburg University, Gothenburg, Sweden*
***Harbacken, Stavby, Alunda, Sweden*
****Department of Earth Sciences, Geophysics, Uppsala University, Uppsala, Sweden*
*****Institute for Geological Sciences, AB Hydrogeology, Free University of Berlin, Berlin, Germany*

In 1999 a monitoring programme was started in an arctic-oceanic drainage basin, Latnjavagge (9 km^2, 950 – 1440 m a.s.l.; 68°20`N, 18°30`E), with the objective to quantify the sediment budget and the relevant denudation processes as dependant on environmental parameters (Beylich in press). With regard to chemical denudation rates several factors such as topography, climate, lithology, regolith thickness and ground frost are of importance, so that as a consequence, different methods need to be combined in order to assess the chemical denudation. Once an integrated approach is applied, it is possible to analyze chemical denudation rates for clearly-defined landscape units such as confined fluvial drainage basins (Beylich 2002).

The Latnjavagge drainage basin in the periglacial Abisko mountain area is characterized by a homogeneous lithology (mica shists). Water balance, water chemistry and radio magnetotelluric geophysical investigations were integrated with assessment of regolith thickness along selected profiles as well as of ground frost conditions within the catchment. In combination with direct field observations, the geophysical profiles demonstrated the presence of very thin regolith in most of the investigated areas, yet in some parts the bedrock was located deeper and was not detected locally at 40 m depth. The low resistivities found along the profiles in the geophysical investigation showed that frozen ground was not found around 1000 m a.s.l. in late August (Beylich *et al.* subm.b). Permafrost in the area seems to be restricted to areas above 1000 m a.s.l. Water chemistry and total dissolved solids (TDS) of precipitation, snowpack and surface water have been analyzed on samples collected at 25 selected sites within Latnjavagge (Beylich *et al.* subm.a). Additionally, daily discharge and yield of dissolved solids have been calculated for several subcatchments (Beylich *et al.* subm.c). Water laboratory analyses of 205 samples taken in the field included the components Ca^{2+}, Mg^{2+}, Na^{+}, K^{+}, Fe^{2+}, Mn^{2+}, Cl^{-}, NO_3^{-}, SO_4^{2-} and PO_4^{3-}, with SO_4^{2-} and Ca^{2+} being the dominant ones in the surface water (Beylich *et al.* subm.a). The salt concentrations and chemical denudation in this arctic-oceanic periglacial environment were found to be low with a mean annual chemical denudation rate for the entire catchment of 5.4 t/(km^2 yr) (Beylich *et al.* subm.c).

Comparison of the water chemistry data from different sampling sites and subcatchments by means of cluster analysis shows that there are significant differences within the area: In areas of shade, longer snow cover, frozen ground and thin regolith, the salt concentrations over the summer were perceptible but so low that salts brought into the basin from precipitation and melting snow could be clearly detected in the surface water. The highest salt concentrations were found at a radiation-exposed west facing, vegetated, moderately steep slope with relatively thick regolith that was thawed already from the time of snowmelt in early June. In such well-drained sites with continuous subsurface water flow a maximum of contact between water and mineral particles can take place (Beylich *et al.* subm.a). The concentration values revealed differences in the rate of thawing of frozen ground between shaded areas and/or areas at higher altitude on the one hand, and radiation-exposed areas on the other. A comparison with the results from Kärkevagge a few kilometres to the northwest as well as from other periglacial locations indicates that the chemical denudation values from Latnjavagge are fairly representative of periglacial oceanic environments, more so than the values from the Kärkevagge catchment (Beylich *et al.* subm.a). The investigation in Latnjavagge stresses the importance of spatial variability within even small catchments of homogeneous lithology as it demonstrates that salt concentrations from different subareas can differ substantially depending on exposure to radiation, duration of snow cover and frozen ground conditions, regolith thickness, and also on vegetation cover and slope angle as factors steering water turbulence and retention of drainage (Beylich *et al.* subm.a).

REFERENCES

Beylich, A. A., 2001. Slope denudation, streamwork and relief development in two periglacial environments in East Iceland and Swedish Lapland. Transactions, Japanese Geomorphological Union, 22 (4), C-23

Beylich, A.A. in press. Sediment budgets and relief development in present periglacial environments – a morphosystem analytical approach, Hallesches Jahrbuch für Geowissenschaften, A.

Beylich, A.A., Kolstrup, E., Thyrsted, T., Gintz, D., subm.a. Water chemistry and its diversity in relation to local factors in the Latnjavagge drainage basin, arctic oceanic Swedish Lapland, Geomorphology.

Beylich, A.A., Kolstrup, E., Thyrsted, T., Linde, N., Pedersen, L.B., Dynesius, L., subm.b. Chemical denudation in arctic-alpine Latnjavagge (Swedish Lapland) in relation to regolith thickness as assessed by radio magnetotelluric (RMT)-geophysical profiles, Geomorphology.

Beylich, A.A., Molau, U., Luthbom, K., Gintz, D., subm.c. Rates of chemical and mechanical fluvial denudation in an arctic-oceanic periglacial environment, Latnjavagge drainage basin, northernmost Swedish Lapland, Arctic, Antarctic, and Alpine Research.

Analysis of permafrost thickness in Antarctica using VES and MTS data

*E. Borzotta and *D. Trombotto*

*Unidad de Geofísica, *Unidad de Geocriología*

Instituto Argentino de Nivología, Glaciología y Ciencias Ambientales (IANIGLA)

CONICET, Casilla de Correo 330, 5500 Mendoza, Argentina

Frozen ground thicknesses measured in the NE of the Antarctic Peninsula (Seymour and James Ross Islands; Fig. 1) and estimations of permafrost thicknesses for the same areas are being compared and analyzed using (a) vertical electrical soundings data (VES), (b) mean annual air temperature,and (c) steady geothermal heat flows as inferred from magnetotelluric soundings (MTS).

In the present study, as part of a more exhaustive study in progress, estimations of steady heat flows are made, which could contribute to a better understanding of the cryogenic processes in the area.

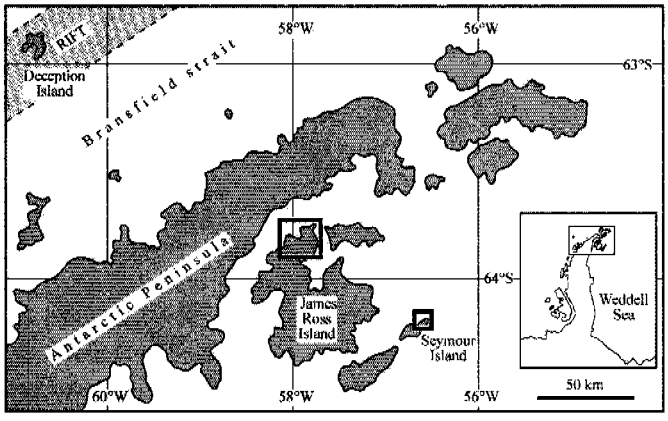

Figure 1. Antarctic Peninsula. The frames indicate the zones where permafrost studies were performed (Seymour and James Ross Islands).

Seymour and James Ross Islands are located in the Weddell Sea, next to the Antarctic Peninsula, at about 64°S and 57°W. Both are part of the Larsen Basin located eastward of the Antarctic Peninsula. Upper Cretaceous marine sediments outcrop in the south portion of Seymour Island and Tertiary sediments at the north. This island is free of ice cover. James Ross Island is a Plio-Pleistocene volcanic island with recent activity at its eastern border and around 70% of its surface is covered by glaciers. At Seymour Island, a mean annual air temperature (MAAT) of –9.4°C was estimated at 200 m a.s.l. (upper terrace) from a ten-year temperature recording (1971-1980). Temperatures at 10 m depth were measured during the 1976-1981 period in the snow on James Ross Island (Dalinger Dome and Mt. Haddington), which let to estimate a MAAT of –13°C at about 1410 m, on average, and –5°C at 35 m a.s.l. where geophysical studies were conducted later by Fukuda and others (Fukuda et al. 1992).

The first magnetotelluric soundings (MTS) in Seymour Island were carried out in its northern section (upper terrace) in 1979 and 1980 (Fournier et al. 1980, Del Valle et al. 1982), describing the Larsen Basin only below 600 m depth; thus it was not possible to study the permafrost. Results showed a very conductive layer (saline) below the frozen ground with 40 Siemens of conductance. A basin basement at 5.2 km depth is also shown by these data and a conductive layer (possible asthenosphere) is suggested in the upper mantle at longer periods with a top at 63 km depth.

In 1992, three MT soundings were made in James Ross Island (Brandy Bay and Hidden Lake). Results showed a conductance below the frozen ground one order of magnitude higher than below the frozen ground at Seymour Island: 40 Siemens in Seymour Island, 315 Siemens in James Ross Island. As in the case of Seymour Island, a possible asthenosphere is also suggested for James Ross Island with a top at 61 km depth. Distortions present in the apparent resistivity curves and the volcanic nature of this island, with recent activity, lead us to suspect the existence of a possible magma chamber seated between 6.8 km and 14 km depth in the crust at NW of James Ross Island. These electromagnetic studies performed in Seymour and James Ross Islands were not able to describe the permafrost directly.

Vertical electrical soundings (VES), particularly dedicated to studying the permafrost, were conducted on Seymour and James Ross Islands in the summer 1989-1990 (Fukuda et al. 1992). These studies were carried out at different terraces observed by these authors. In Seymour Island, 200 m of frozen ground thickness was estimated in the upper terrace (around 200 m a.s.l.), 105m in the middle terrace (around 50 m a.s.l.) and 35m in lower terrace at 5 m a.s.l. Maximum resistivities of about 720 to 800 Ωm were measured in frozen ground by these authors (Fukuda et al. 1992). In a general context, the thickness of the active layer in Seymour Island could be

estimated at 0.35 to 0.60m. In the same campaign, four VES were carried out in the ice-free northwestern region of James Ross Island. Shallower thicknesses of frozen ground than those estimated at Seymour Island were estimated in this case: 40 to 45 m in the upper terraces (around 21 to 35 m a.s.l.), 3.4 m in the middle terrace (around 10 to 17 m a.s.l.) and 5.8 m in the lower terrace at about 3 to 5 m a.s.l. Resistivities between 1000 and 4000 m were obtained, with a thickness of the active layer approximately 0.70 to 1.45 m (Fukuda et al. 1992).

From the depths of conductive layers in the crust and the upper mantle determined by MT soundings, a gross estimation of the regional geothermal heat flow - in steady condition - may be obtained, and consequently, the geothermal gradient and the permafrost thickness in equilibrium to the present MAAT can be estimated. In the present current study at Seymour and James Ross Islands, the frozen ground thickness - measured using VES - and the estimated permafrost thickness, obtained considering homogeneous medium and steady heat flows inferred from MT soundings results, are being compared and analyzed.

Empirical exponential formulas correlate the geothermal heat flows and the depths of conductive layers determined using MTS (Adam 1978). These expressions are based principally on information published in Adam (1976), corresponding to the East of Europe and Russia, involving platforms and geo-dynamically active regions. Considering 63 km as the suggested depth of the asthenosphere in Seymour Island (also suggested by the MTS performed in James Ross Island), a heat flow of 78 mW/m^2 is estimated in this island ($1\mu cal/cm^2sec. \approx 42$ mW/m^2). If the magma chamber, suggested by the MT study, really exists in James Ross Island its presence will increase the heat flow at surface. In fact, considering the top of this chamber at 6.8 km depth - according to MT results - a heat flow of 148 mW/m^2 is estimated using the expressions mentioned. The heat flow values, thus estimated, should only be considered as approximations of the steady geothermal heat flows corresponding to these regions. It is important to mention the presence of a rift at the Bransfield Strait located 200 km to northwest from Seymour Island, where heat flows higher than 220 mW/m^2 were measured.

In order to estimate the geothermal gradient in the permafrost of Seymour and James Ross Islands, a thermal conductivity obtained in the laboratory (1.883 W/m °K) was used corresponding to two samples of frozen sands with about 87-94% of water. In this way a geothermal gradient of 0.04 °C/m is estimated for Seymour Island and 0.079 °C/m for James Ross Island. Taking into account the MAAT for both islands: -9.4 °C for Seymour Island at 200 m a.s.l., (where the VES study gave 200 m of frozen ground thickness) and -5.0 °C for James Ross Island at about 35 m a.s.l. (where the VES study gave 40 to 45 m of frozen ground thickness), we obtain 235 m and 63 m as the estimated permafrost thickness corresponding to Seymour and James Ross Islands respectively.

Because of the high conductivity below the frozen ground put in evidence at both islands by MTS, the presence of a cryopeg at the base of the frozen ground is very probable. Therefore, the estimations of the permafrost thickness made in these islands (235 and 63 m) are consistent with the thickness of frozen grounds obtained by VES (200 and 45 m). The differences could be attributed to a cryopeg.

Although the permafrost thickness in equilibrium, thus estimated, may contain uncertainties, its comparison with the frozen ground thickness - corresponding to both studied islands - seems to suggest a state approaching equilibrium. This result means that the soil would have been uncovered by ice and with approximately stable climatic and geological conditions for a period of time long enough to reach this state.

REFERENCES

Adam, A. 1976. (ed.). Geoelectric and Geothermal Studies (east - central Europe, Soviet - Asia). KAPG Geophysical Monograph. Akadémiai Kiado, Budapest.

Adam, A. 1978. Geothermal effects in the formation of electrically conducting zones and temperature distribution in the Earth. Phys. Earth Planet. Inter. 17: 21-28.

Del Valle, R.A., Demichelli, J., Febrer, J.M., Fournier, H.G., Gasco, J.C., Irigoin, H., Keller, M., Pomposiello, M.C. 1982. Résultats de deux campagnes magnétotelluriques faites dans le Nord la Péninsule Antarctique en 1979 et 1980. IX e Réun. Ann. Sci. de la Terre, Paris, Soc. Géol. Fr. ...dit., Paris.

Fournier, H., Keller, M., Demichelli, J., Irigoin, H. 1980. Prospeccion magnetotelurica en la isla Vicecomodoro Marambio, Antartida. Direc. Nac. del Antartico, Inst. Antart. Argentino, Buenos Aires, Contribucion 235: 38-43.

Fukuda, M., Strelin, J., Shimokawa, K., Takahashi, N., Sone, T., Trombotto, D. 1992. Permafrost occurrence of Seymour Island and James Ross Island, Antarctic peninsula region. In: Y. Yoshida et al. (eds.), Recent Progress in Antarctic Earth Science: 745-750.

Living microorganisms in Siberian permafrost and gas emission at low temperatures

A. Brouchkov, M .Fukuda, K. Asano, M. Tanaka and F. Tomita

Hokkaido University, Sapporo, Japan

Permafrost is a source of greenhouse gases. Thus thawing of the frozen soils affects conditions of the global carbon cycle. Organic material in the thawing permafrost decays quickly, releasing carbon dioxide and methane in the process.

Long-term soil incubation experiments in flasks containing soil samples and nitrogen in the air have shown a slow production of methane in different frozen soils at -5°C. Soils were over-saturated with water. There was an increase in methane content in the air of the flasks, especially in the first 20-50 days of the experiments (Brouchkov and Fukuda 2002). The change in methane content occurred according to the logarithmical law in samples of modern soils from Yakutsk, Russia and Hokkaido (Tomakomai), Japan; the rates of methane production decrease with time (Table 1).

Table 1. Change of methane content (ppmv) in the air of the flasks during an incubation experiment at -5°C

Days	Tomakomai soil	Yakutsk soil
0	1.09	0.85
22	1.80	2.00
50	1.89	2.07
390	3.15	3.10

Micro-organisms could be responsible for microbial methane formation in permafrost: according to recent studies, methane and gas hydrates are widely distributed in there and appear to be of a biogenic origin. Colonies of micro-organisms were discovered that survived the incubation period lasting longer than 1 year at –5°C; they were able to undergo anaerobic growth at room temperature in GYP medium; 16S rDNA was amplified by PCR.

However, calculations of the amount of methane produced in permafrost based on short-term experiments are difficult. The production could be discontinued under certain conditions. The temperature is not stable: it could be suggested that methane production increases at higher temperatures. The type of soil, organic material and water content are also essential to microbial activity. In spite of the obvious possibility of methane production at low temperatures, long-term forecast of methane content in frozen soils is problematic.

Permafrost soils contain micro-organisms (Friedmann 1994, Gilichinsky and Wagener 1995); isolated from the world for many years, they might be still active. Techniques for sampling in permafrost for microbiological studies are not well-established. The requirement is for biological cleanliness and absolute avoidance of contamination while the sample is brought to the surface and during subsequent handling of the sample. Fieldwork done in 2001-2002 in Yakutsk, Eastern Siberia, has shown that the permafrost at temperature of -5°C contains living fungi identified as *Penicillium echinulatum* (Figure 1).

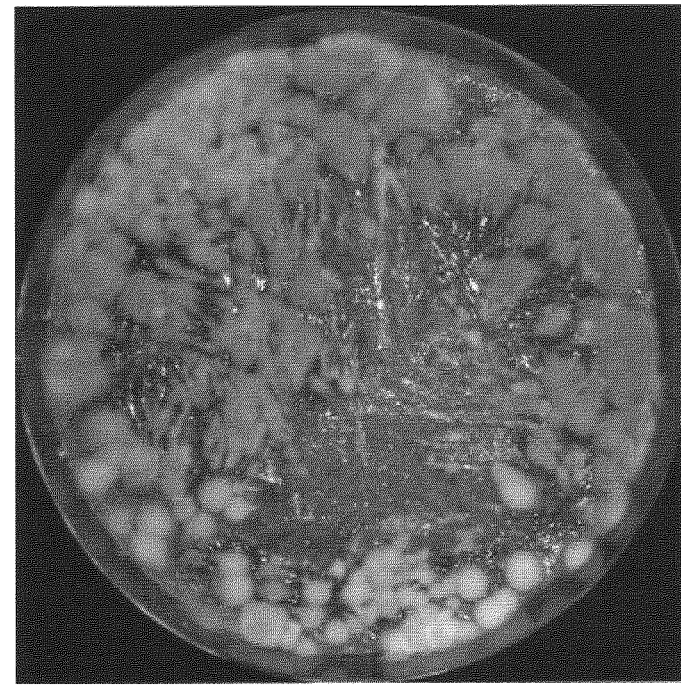

Figure 1. Growth of *Penicillium echinulatum*, new strain PF at -5°C; 11th month of incubation, PDA medium (Potato Dextrose Agar)

The genera *Penicillium* are widespread and found in soil. Fungi are responsible for the biodegradation of organic material; this could be considered as one of their important practical applications. Some fungal species grow at low temperatures, below 0°C. However, there is no information concerning the fungi which may grow in underground permafrost at temperatures below 0°C during a long time throughout their life cycle.

The identification of permafrost fungi as *Penicillium echinulatum* was based on morphological characteristics and a nucleotide sequence analysis of enzymatically amplified

18S rDNA, internal transcribed spacer (ITS) region including 5.8S rDNA and D1/D2 at the 5' end of the large subunit (26S) rDNA. The fungi were able to grow at positive and negative temperatures. The optimum temperature for the growth of *P. echinulatum* was estimated as 15-20°C, yet they were able to grow at the negative temperature of -5°C (Figure 1). Fungi colonies on MEA grow rather rapidly, attaining a diameter of 20 to 35 mm in 7 to 9 days at 20°C.

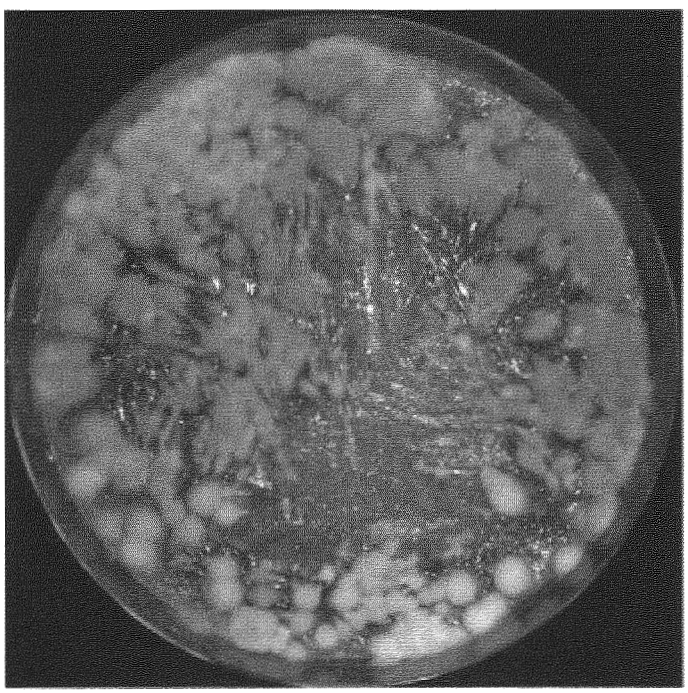

Figure 2. Micro-organisms from permafrost of Mammoth Mountain, aged approximately 3 million years; growth at temperature of +20°C

Sampling of permafrost exposures in Aldan river valley (Mammoth Mountain, Eastern Siberia), in one of the oldest regions of permafrost on Earth (possibly aged about three million years) was done. Blocks of frozen soil and ice sized approximately 20x20x20 cm in size were cut from exposures and taken frozen to Sapporo. Frozen wood of the same age was also sampled.

Micro-organisms have been discovered (Figure 2). They were able to grow at both aerobic and anaerobic conditions. For the sequence analysis DNA was extracted using the ISOPLANT set (Nippon Gene) and following the manufacturer's instructions. Preliminary results of sequencing and analysis of the evolutionary tree of the micro-organisms show that they are most related to *Bacillus anthracis*.

Understanding these permafrost organisms and their relationship to their cold environment, especially to unfrozen water common in frozen soils (Williams and Smith 1989), has immediate practical implications. The fact that viable bacteria occurring at significant depths in permafrost can be prompted to reproduce, presents imaginative possibilities, for example for the decontamination of buried contaminants. The living micro-organisms in permafrost, in common with other extremophiles (Ashcroft 2000), apparently have special mechanisms of repair of cell structures, necessary for their survival (Brouchkov and Williams 2002). A comparative study of structure and biochemical features of permafrost's micro-organisms to those of known soil micro-organisms could reveal this mechanism.

REFERENCES

Ashcroft, F. 2000. Life at the Extremes. HarperCollins.

Brouchkov, A.V. and Fukuda, M. 2002. Preliminary Measurements on Methane Content in Permafrost, Central Yakutia, and some Experimental Data. Permafrost and Periglacial Processes 3: 187-197.

Brouchkov, A.V. and Williams, P.J. 2002. Could microorganisms in permafrost hold the secret of immortality? What does it mean? In: Contaminants in Freezing Ground. Collected Proceedings of 2nd International Conference. Cambridge, England, Part 1: 49-56.

Friedmann, E. I. 1994. Permafrost as microbial habitat. In: D. A. Gilichinsky (ed.): Viable Microorganisms in Permafrost. Russian Academy of Sciences, Pushchino, Russia: 21-26.

Gilichinsky, D. and Wagener, S. 1995. Microbial Life in Permafrost: A Historical Review. Permafrost and Periglacial Processes 6: 243-250.

Williams, P.J. and Smith, M.W. 1989. The Frozen Earth, Cambridge: Cambridge University Press.

Natural risk evaluation of geocryological hazards (the Varandey Peninsula coast of the Barents Sea)

I.V. Chekhina and F.M. Rivkin

Industrial and Research Institute for Engineering of Construction, Moscow, Russia

INTRODUCTION

It is known that the intense technological impact on the Russian Arctic coast caused by industrial engineering results in the intensification of natural and origination of new geocryological processes. Therefore, prediction of development of geocryological processes is part and parcel of geotechnical survey.

The intensity of geocryological processes can be estimated only on the basis of complex engineering geocryological studies. Therefore, the creation of information databases on the basis of engineering geocryological studies is an element of primary importance for solving the complex of problems of environmental management.

In this connection, it becomes possible and necessary to automate construction of different engineering geocryological maps using geoinformation systems (GIS). This makes it possible not only to solve traditional problems of engineering survey but also to map natural risks and to assess the possibility of appearance of geocryological processes and their intensity.

METHODS AND RESULTS.

Results of the engineering geocryological studies performed on the Varandey Peninsula were used as base information to estimate the intensity of geocryological processes.

The electronic database of geocryological conditions was compiled on the basis of these studies. The database includes such attributes as engineering geological regions, which were distinguished taking into account the geomorphological position, genesis and lithology of soils. Moreover, physical (moisture, ice content, density, etc.) and thermal (heat capacity, thermal conductivity, etc.) properties of thawed and frozen soils were also taken into account. Each region distinguished was indexed depending on geocryological conditions.

The database has a two-level architecture. Data obtained as a result of the field studies and laboratory determination of soil properties is combined at the first level. The second level includes generalized information, namely first-level data and information obtained from publications. Since the second-level database includes information from different sources, all input parameters are tested for mutual consistency.

As a result, the compiled (summarized) database provides the complete set of properties necessary for analyzing the environmental quality in each of the distinguished regions. The structure of the obtained database is correlated with the scheme of zoning and is factually the legend to the map.

Natural risks of such geocryological hazards as frost heaving, soil settlement upon thawing, thermal erosion, landslides, and cryogenic appearances were evaluated based on the compiled database. Ice content and salinity of soils were also estimated in order to assess the complexity of the area.

The rule base (analytic relationships for scores) and program module for calculating scores were created in order to evaluate natural risks of geocryological hazards. The module for calculating scores from analytic relationships makes it possible to determine an appearance risk of exogenous geocryological processes (Dan'ko, 1982; Lovchuk, 1990). A certain score is assigned to each cryogenic processes depending on the obtained index value. The score system is based on risk evaluations of each geocryological process (Armand, 1975).

Thus, two evaluation tables were obtained. These tables make it possible to differentiate regions, distinguished during the engineering geocryological zoning, using the number of exogenous processes and the degree of appearance risk of geocryological hazards. The first evaluation table has been compiled using the total number of available hazardous exogenous processes (frost heaving, soil settlement upon thawing, thermal erosion, landslides, and cryogenic appearances) and ignoring the appearance risk in the regions distinguished. The second evaluation table reflects the total appearance risk of the processes in each of the region, additionally including estimation of ice content and salinity of soils. The total score of complexity of each geocryological region is given for the most hazardous process, assuming that its effect will be higher than the effect of the remaining processes.

As a result, all engineering geocryological regions were differentiated with respect to the degree of the appearance risk of hazardous processes in the following way: most hazardous, medium hazardous, and least hazardous. Data of both summary tables were reduced to the electronic engin-

eering geocryological map, which is directly related to the database.

The electronic database of the key site of the Varandey Peninsula, which includes the engineering geological characterization of the natural environment, was created as a result of the performed studies. The algorithm was constructed for evaluating natural risks of appearance of such geocryological hazards as frost heaving, soil settlement upon thawing, thermal erosion, landslides, and cryogenic appearances and for estimating ice content and salinity of soils.

Two evaluation maps of the key site of the Varandey Peninsula were constructed on the basis of the elaborated technique:

- Map of zoning with respect to the appearance risk of the most hazardous geocryological process (Fig. 1);
- Map of distribution of exogenous geocryological processes (Fig. 2).

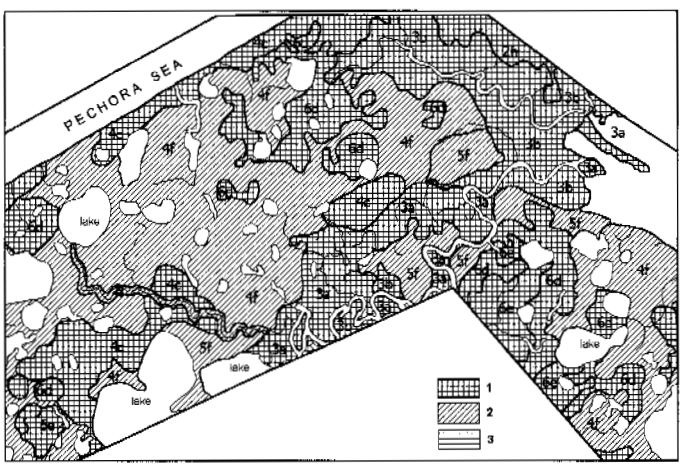

Figure 1. Map of zoning of the key site of the Varandey Peninsula with respect to the appearance risk of the most hazardous geocryological process.
1 - most hazardous; 2 - medium hazardous; 3 - least hazardous.

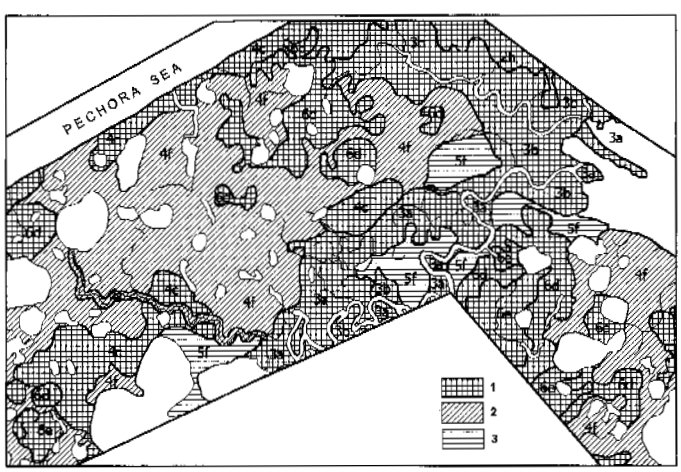

Figure 2. Map of distribution of exogenous geocryological processes at the key site of the Varandey Peninsula.
1 - most hazardous; 2 - medium hazardous; 3 - least hazardous.

CONCLUSION

The system for interpreting results of geotechnical survey, using electronic maps, electronic databases, and program modules, has been created as a result of the performed studies in order to evaluate the distribution of exogenous processes. The elaborated system can be used to map natural risks and to construct prediction maps of development of hazardous exogenous processes.

ACKNOWLEDGEMENT

This work is supported by Russian Coast Protection Program and INTAS grant 2332.

REFERENCES

Armand, D.L. 1975. Landscape Science, Moscow: Mysl'

Dan'ko, V.K. 1982. Regularities of Development of Thermal Erosion in Northwestern Siberia, Cand. Sci. (Geol.-Min.) Dissertation, Moscow.

Lovchuk, V.V. 1990. Cryomorphogenesis of Subarctic Lowlands in Western Siberia: Backgrounds of a Topography Cryomorphological Analysis, Methods of Engineering Geocryological Survey, Moscow: VSEGINGEO.

AIGEO working group "Past distribution of the periglacial environment in the Italian mountain chains: reconstructions based on the study of relict forms"

*Alessandro Chelli, *M. Pappalardo and A. Ribolini*

Dipartimento di Scienze della Terra, Università di Parma, Parma, Italy

** Dipartimento di Scienze della Terra, Università di Pisa, Pisa, Italy*

A working group within the Italian Association of Geomorphologists started its activity at the end of 2002. A number of Italian researchers, engaged in studies on the periglacial environment and often dealing with relict forms, decided to get together in order to actively compare their study objects and methods.

In Italy, landforms related to periglacial processes have been recognized for a long time (Capello 1960) and permafrost distribution in the present and throughout the Quaternary has recently been reconstructed by means of typical landforms (e.g. rock glaciers; Dramis and Guglielmin 1999). However, many other landforms, e.g., different types of inactive scree, common mainly in the Apennine chain and in Sardinia, were identified in the past and considered as "periglacial". Although displaying different characteristics with regard to parent material, texture, form, position and extension, they have some features in common: they are located on moderately steep slopes, are made of a coarse debris that may be mixed with fine material and they have no sedimentary features typical of fluvial or gravitational landforms; in all cases they are not related to present-day geomorphic processes. In the literature they were classified mainly as *éboulis ordonnées, gréze liteée* and block streams/fields.

The working group members intend to collect evidence in order to clarify the true genetic environment of such landforms: whether they are really periglacial, or whether just cryogenic weathering and frost shattering can be responsible for coarse sediment supply, in the absence of even sporadic permafrost. The possibility that other weathering processes have been responsible for the formation of such deposits, and that the action of gravity or running waters in the transport of weathered material has until now been misunderstood, will be carefully examined.

In fact, stratified scree is no longer strictly considered a typical periglacial landform, as multiple processes can be evoked for its genesis (Van Steijn et al. 1995). Moreover, block streams, presently being studied as active forms in extreme environments (very cold and arid), were recognized to be convergent, in their relict form, with other, non periglacial, types of landforms (Boelhouvers et al. 2002).

Another aim of the working group is to employ typical periglacial landforms in their relict state (e.g., rock glaciers and wedge casts) for Quaternary paleoclimatic reconstructions in Italian low altitude mountain environments.

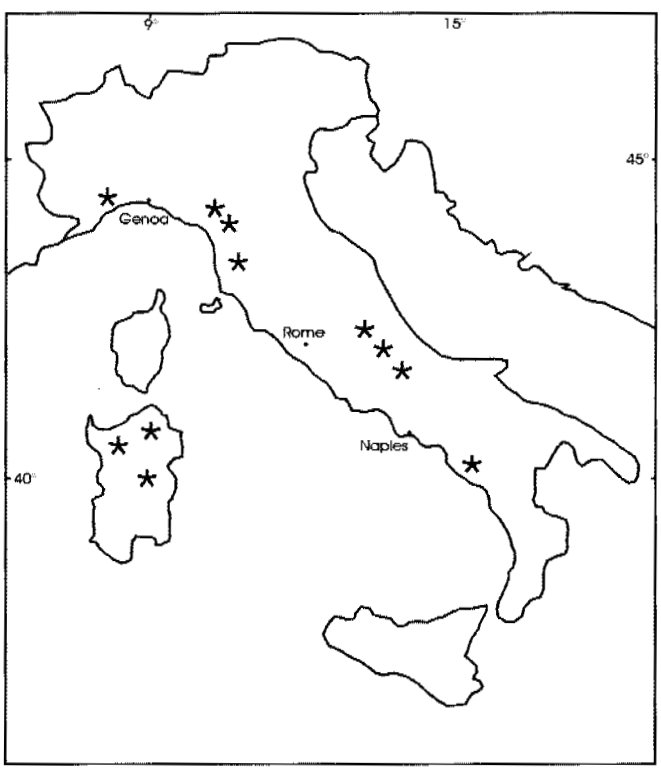

Fig. 1 Location of the study areas.

Study areas were established (Fig. 1) and a preliminary illustration of the deposits concerned permitted the members to compare the different typologies. Within the category of block streams/fields study cases were selected in Sardinia, Tuscany and Western Liguria. Sites with slope deposits of likely cold climate environment were enclosed both from the Northern Apennines (Parma and Reggio Emilia sectors) and from the Central (Abruzzo and Molise) and Southern Apennines (Cilento), as well as from Sardinia. Active landforms testifying to the present-day transition from glacial to periglacial environment in the Gran Sasso area (Central Apennines), especially lobated debris indicating permafrost creeping processes, will be included among the investigation objects. Their analysis

can be important, in fact, for making a comparison with the studied relict forms.

The first goal of the working group will be the creation of a work sheet in order to perform a description of the different deposits with identical methods. Micromorphological techniques and image analysis, successfully employed by some of the members on single deposits, will be extended wherever possible. Further work will focus on the chronological aspect of the matter and the necessity of finding a suitable dating method that permits comparison of the ages of the studied bodies.

After four years' activity, the goal of the working group is to define the role that frost weathering had in sediment supply, the role of frost creep and gelifluction processes in the material accumulation, and the relationship between the climate under which such landforms were created and the distribution of mountain permafrost.

Working Group Members: A. Bini (Università di Milano), N. Casarosa (Provincia di Pisa), A. Chelli (Università di Parma), M. Coltorti (Università di Siena), P. Farabollini (Università di Camerino), M. Firpo (Università di Genova), M. Guglielmin (ARPA Lombardia), E. Miccadei (Università di Chieti), M. Pappalardo (Università di Pisa), M. Pecci (ISPESL Roma), T. Piacentini (Università di Chieti), F. Scarciglia (Università della Calabria), C. Queirolo (Università di Genova), R. Raffi (Università di Roma "La Sapienza"), A. Ribolini (Università di Pisa), S. Sias (Università di Sassari), C. Tellini (Università di Parma).
The abstract volume of the Working Group first meeting is available upon request.

REFERENCES

Boelhouvers J., Holness S., Meiklejohn I. and Sumner P. 2002. Observations on a blockstream in the vicinity of Sani Pass, Lesotho highlands, Southern Africa. Permafrost and Periglacial Processes 13(4): 251-257.

Capello C.F. 1960. Terminologia e sistematica dei fenomeni dovuti al gelo discontinuo. G. Chiappichelli, Torino.

Dramis F. and Guglielmin M. 1999. Permafrost investigations in the Italian mountains: the state of the art. In Paepe R. & Melnikov V. (eds.), Permafrost response on economic development, environmental security and natural resources, Kluver Ac. Publishers: 259-273

Van Steijn H., Bertran P., Francou B., Hétu B. and Texier J.P. 1995. Models for the genetic and environmental interpretation of stratified slope deposits: review. Permafrost and Periglacial Processes 6: 125-146.

Active layer dynamics in Greenland, Svalbard and Sweden

*H. H. Christiansen, *J. H. Åkerman and **J. Repelewska-Pekalowa*

Institute of Geography, University of Oslo, Norway

** Institute of Physical Geography and Ecosystems Analysis, University of Lund, Sweden*

***Department of Geomorphology, University of Maria Curie-Sklodowska, Poland*

INTRODUCTION

Four sites with the longest active layer monitoring records in high arctic NE Greenland and Svalbard, and in alpine Sweden are compared. In the Greenland Sea, deep-water formation occurs bringing warm surface water from the south. This provides a relatively mild climate at high latitudes. Meteorological data and GCMs all suggest that climatic changes at high latitudes are amplified as compared to lower latitudes. Therefore, active layer monitoring and its relationship to climatic variations in Greenland, Svalbard and northern Scandinavia are of high relevance for monitoring and study.

The active layer monitoring sites are located at Abisko, northern Sweden, 68°N 19°E, at Calypsostranda, 77°N 15°E, and at Kapp Linne, 78°N 13°E, both at Svalbard, and at Zackenberg, 74°N 21°W, NE Greenland. We discuss intersite and interannual variations in active layer thickness and its potential relationship to summer air temperature represented by thawing degree days.

This abstract was developed as a result of the CALM synthesis workshop held in November 2002 at the University of Delaware, USA.

SITE DESCRIPTIONS

At Abisko, data on active layer thickness were obtained beginning in 1978 at eight valley palsa bog grids at 380-480 m a.s.l., and at three intermontane depression grids at 850-950 m a.s.l., each with 121 measuring points (Brown et al., 2000). At Kapp Linne, monitoring was initiated in 1972 at ten 100 x 100 m grids on raised marine terraces at 4-59 m a.s.l., nine on dry mineral soils and one in a peat-covered area, each with 25 randomly sampled measuring points until 1994, and after that with 121 points (Brown et al. 2000). At Calypsostranda, active layer monitoring started in 1986 at 23 individual points on raised marine terraces at 2-40 m a.s.l. These points adequately represent the average landscape active layer thickness based on a total of 300 measuring points (Repelewska-Pekalowa 2002). At Zackenberg, a grid of 100 x 100 m, with 121 measuring points was established in 1996 on ground moraine at 36 m a.s.l (Christiansen 1999). All sites are located in open flat landscapes with average landscape snow cover thickness and duration conditions. Meteorological stations operated since grid establishment at the Zackenberg Station 25 m from the Zackenberg grid; until 1976 and again from 1996 at Isfjord 0.5-5 km from the Kapp Linne grids; at the Hornsund Station, which is 68 km south of Calypsostranda; and at the Abisko Station 3-50 km from the Abisko grids. In the last 20-25 years there has been an increase (1-2 °C) in summer temperatures from the Abisko and Longyearbyen, Svalbard stations. This warming has, however, not occurred in Greenland.

DATA AND DISCUSSION

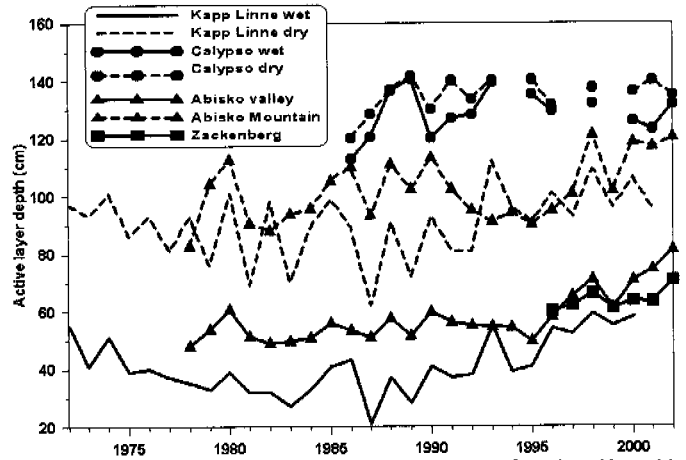

Figure 1. Active layer thickness (cm) at Abisko in Sweden, Kapp Linne and Calypsostranda at Svalbard and at Zackenberg in NE Greenland. No data was collected from the Calypsostranda sites in 1994, 1997 and 1999.

At the Abisko valley site, active layer thickness was stable around 55 cm from 1978 to 1995, and increased to around 80 cm since then (Fig. 1). In the Abisko Mountains the active layer thickness varied from 85 to 120 cm during the measuring period, with the largest values in the last five years. The Kapp Linne sites show decreasing active layer thickness until 1987 and then increasing, with the dry sites varying around 75 to 110 cm, and the wet sites from

25 to 95 cm. The thickest active layer in the region occurs at Calypsostranda, varying only from 115 to 140 cm for both wet and dry sites. There is no trend in active layer thickness at Calypsostranda. At Zackenberg the active layer is only 60 to 70 cm thick. This is the smallest value in mineral soil, and this site, with its relatively short record, also has the smallest interannual variation of the four sites.

A common pattern of interannual active layer thickness variation exists from 1997 to 2000 (Fig. 1). The Calypsostranda sites were not monitored during all these years, but data from the monitored years fit the pattern. In 1980 and 1988 the Kapp Linne and Abisko sites have peaks in the active layer thickness, but this was not seen at Calypsostranda in 1988. In 1989 the active layer thickness was reduced for all Kapp Linne and Abisko sites, but thickest during the recording period at Calypsostranda, while in 1990 all Kapp Linne and Abisko sites peaked, when Calypsostranda sites were small.

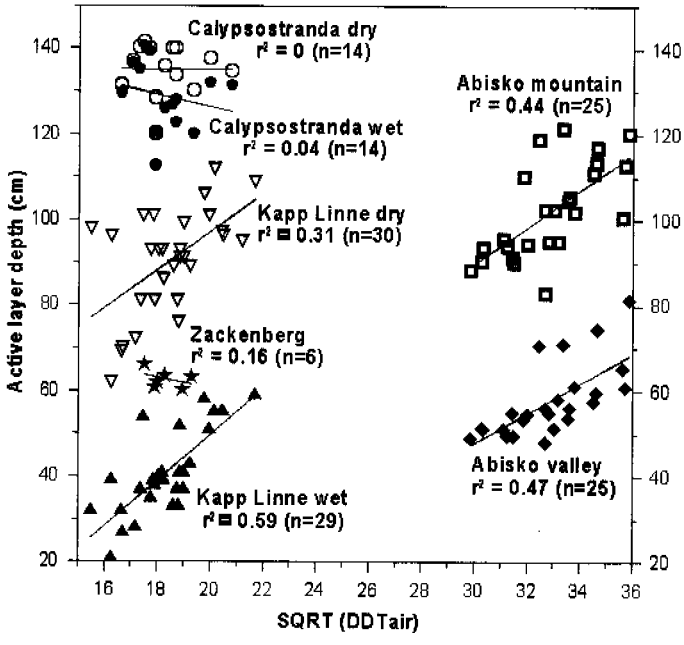

Figure 2. Active layer depth and the square root of thawing degree days of the air temperature at the closest meteorological stations at the four sites.

To investigate the relationship between active layer thickness and summer air temperature, thawing degree days (DDT) were calculated using the closest meteorological station for each four investigated sites in the years with active layer measurements (Fig. 2). There is a positive correlation for the Kapp Linne and Abisko sites, and particularly for the peat bog sites, but none for the Zackenberg and Calypsostranda sites.

The main intersite difference in active layer thickness between Greenland, Svalbard and Sweden primarily reflects climatic and material differences. Both peat sites at Abisko and at Kapp Linne have a generally shallow, 20-70 cm active layer, while the mineral soils here have thicker active layers of 80-120 cm. The active layer in the peat site at Kapp Linne is thinner than the Abisko alpine peat sites, while the active layer in the Abisko Mountains is slightly thicker than at the mineral sites at Kapp Linne. The shallow Zackenberg active layer in mineral soil of 60-70 cm is comparable to the peat sites in Svalbard and northern Sweden. The shallow Greenlandic active layer reflects the East Greenland Current carrying arctic water masses south along East Greenland, causing relatively colder summers here than at Svalbard and in northern Scandinavia.

On Svalbard, Calypsostranda is located only 58 km south of Kapp Linne, and both sites are located on raised marine terraces of the west coast. However, the active layer at the Calypsostranda sites is significantly thicker than even at the Kapp Linne mineral sites. The Hornsund and Kapp Linne summer air temperatures are within the same range, have equal overall interannual variations, but with the Hornsund values slightly lower than the Kapp Linne, particularly since 1995. During the active layer monitoring period, summer air temperatures have been rising mainly since 1998 at Kapp Linne, but not as significantly at Hornsund. Whereas the active layer increased at Kapp Linne already from 1988, there is no increase in active layer thickness at Calypsostranda. This combination of information indicates that local conditions at both sites have a larger control on active layer thickness than summer air temperature. This is in agreement with what has been found for other CALM sites (Brown et al. 2000).

None of the locations have a significant correlation between active layer thickness and DDT, stressing that the control by local factors are as strong as the influence from summer air temperature. It is also possible that other meteorological conditions could influence the active layer thickness as much as the summer air temperature. This remains to be investigated. The interannual active layer thickness variation pattern from 1997 to 2000 for all sites show similar response, presumably controlled by some regional effect, however, not by the air temperature alone.

REFERENCES

Brown, J., Hinkel. K.M., and Nelson, F.E. 2000. The Circumpolar Active Layer Monitoring (CALM) Program: Research Designs and Initial Results. Polar Geography, 24: 165-258.

Christiansen, H.H. 1999. Active layer monitoring in two Greenlandic permafrost areas: Zackenberg and Disko Island. Danish Journal of Geography, 99: 117-121.

Repelewska-Pekalowa, J. 2002. CALM – Site P1- Calypsostranda.7.

Åkerman, J.H. 1980. Studies on Periglacial Geomorphology in West Spitsbergen. Meddelanden från Lunds Universitets Geografiska Institution Avhandlingar LXXXIX.

Could the current warming endanger the status of the frozen ground regions of Eurasia?

*S.M. Chudinova, S.S. Bykhovets, V.A. Sorokovikov, D.A. Gilichinsky, *T-J. Zhang and R.G. Barry*

Soil Cryology Laboratory, Institute of Physicochemical and Biological Problems in Soil Science, Russian Academy of Sciences, Pushchino, Moskow oblast, Russia

**Natinal Snow and Ice Data Center, University of Colorado, Boulder, USA*

INTRODUCTION

The current rise in air temperature that started in the second part of the 1960s in the northern territory of Russia takes place predominantly in the cold period (Watson et al. 1998). However, a number of impacts induced by climate warming, such as reduction of the permafrost area and changes in thickness of the active layer, etc., are determined mainly by changes in ground temperature during the warm period. Changes in ground temperature reflect not only changes in air temperature but also combined impacts from many other climatic factors. The seasonal trends of ground temperature do not necessarily correspond with the trends observed for air temperature (Gilichinsky et al. 1998). Zhang et al. (2001) found that abundant rainfall under global warming may lead to a decrease in summer ground temperature. Therefore, the actual danger of an air temperature increase can be assessed only on the basis of direct determination of changes in ground temperature. This work investigates the vast regions of Eurasia, where the current warming represents a potential danger.

METHODS

The investigation was made for the period 1969-1990, for which the most comprehensive data on ground temperature are available. Linear trends were used to estimate tendencies in the time series of ground and air temperature. Analysis was performed for the mean annual ground temperature, mean annual and monthly air temperature, as well as ground temperature averaged over the summer (June-August), winter (December-February), spring (March-May), and autumn (September- November) periods. Ground temperature was measured at depths of 40, 160 and 320 cm. Best-fit linear trends were calculated for individual stations. Regions with different responses of seasonal ground temperature to the air warming were thereby delimited (Fig. 1). Then, time series of average trends of ground temperature were calculated for each region by the method of polygon area averaging. Trends of ground temperature equal to 0.04°C/year and above are significant at the 0.05 level.

RESULTS

A correspondence between changes in the time series of annual air and ground temperature has been identified down to a depth of 320 cm for the territory under investigation. Maximum trends of air temperature, and hence maximum trends of annual ground warming down to 320 cm are observed for the territories with permafrost and seasonally frozen ground in the West Siberian Plain (region IV), the central Siberian plateau (region VI), and the mountains of Transbaikalia (region VIII). Here, trends of ground temperature at the three depths analyzed average 0.07-0.06, 0.05-0.08, 0.05-0.06°C/year, respectively. Annual ground warming is practically absent in the zones of discontinuous permafrost in Pribaikal'e (region VII) (0.01-0.03°C/year) and the seasonally frozen grounds of Far East (region X) (0.0-0.02°C/year), and over vast territory occupied by continuous permafrost to the east of the Lena River (region XI) (-0.01-0.0°C/year). This reflects an absence of any significant increase in the annual air temperature time series in these regions.

The relationship between mean seasonal time series of air and ground temperature is more complicated. In the taiga zone of the Russian Plain (regions I and II), changes in ground temperature are controlled mainly by air temperatures of the warm period (Chudinova et al. 2001). In the northern and middle taiga zones (region I), in spite of the predominant increase in winter air temperature, the major rise in ground temperature is observed in the warm period (Fig. 1b), which is dictated by the strong rise in air. The absence of summer air warming in the southern taiga (region II) results in the absence of a ground temperature increase during the whole year.

In the Ural mountains (region III) and West Siberian Plain, a strong rise in air temperature in both the warm and the cold periods results in large positive trends in both winter and summer (0.08-0.10°C/year) ground temperature (0.07-0.10 in the upper layers and 0.04-0.08°C/year in the lowest one). In the vast permafrost zone of East Siberia (regions VI, VII, VIII, and XI), trends in the ground temperature time series are determined mainly by changes in winter air temperature. The effect of changes in summer air temperature extends only down to 40 cm. Therefore, in accordance with air temperatures trends in this region, ground temperature increases in the cold period (autumn-winter-spring) and remains unchanged, or decreases, in summer (Fig. 1). The largest significant rise in ground temperature in the cold period (winter-spring), down to a depth of 320 cm, characterizes the central Siberian Plateau and mountains of Transbaikalia, averaging 0.10-0.08°C/year. The summer trend of ground temperature in these regions is zero or negative to a depth of 40 cm. Below, due to winter warming, trends of ground temperature become positive and reach 0.05-0.06°C/year. Trends at individual stations can differ strongly from the average estimates. Therefore, we attempted to ascertain whether this increase takes place at stations where permafrost exists from a depth of 160-320 cm. Our analysis shows the absence of significant trends in mean monthly ground temperature, both at the boundary of the thaw layer and in the permafrost. The maximum decrease in summer ground temperature is observed over the vast discontinuous permafrost zone in region XI. A strong rise in air temperature in February and March cannot offset this cooling with depth. Thus, changes in permafrost status in this region have not occurred.

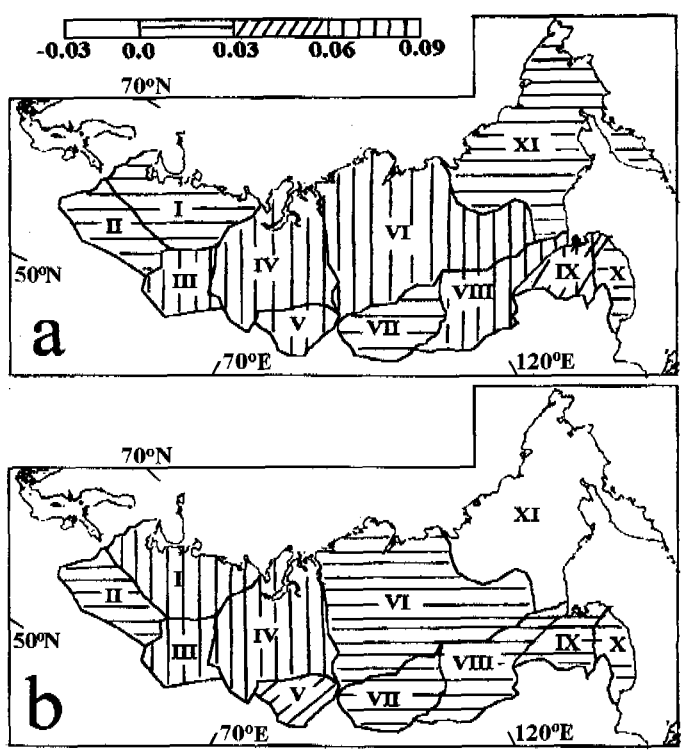

Figure 1. Regions (I-XI) with different linear trends of ground temperature at a depth of 40 cm for (a) winter and (b) summer.

CONCLUSION

Despite a significant rise in winter and annual ground temperature in the vast territory of East Siberia, no significant effect on the permafrost status is apparent. Based on the results obtained, attention should be focused on the West Siberian Plain, where extensive territories are occupied by permafrost and peatland. Changes in the temperature regime of these ecosystems can have both negative and positive consequences (for example, for agriculture). The West Siberia Plain is the region of Russia most sensitive to global air change (Anisimov 2001). Therefore, changes observed in the ecosystems (especially peatlands) of West Siberia may be of interest for other regions of the world where similar changes are taking place.

ACKNOWLEDGEMENT

This work was supported by the Russia Foundation for Basic Research (02-05-64597) and in part by NSF-OPP (9907541 & 0229766).

REFERENCES

Anisimov, O.A. 2001. Predicting patterns of near-surface air temperature using empirical data. Climatic Change 50: 297-315.

Chudinova, S.M., Bykhovets, S.S., Fedorov-Davydov, D.G., et al. 2001. Response of temperature regime of Russian North to climate changes during second half of 20th century. Earth Cryosphere 5(3): 63-69 (in Russian).

Watson, R.T. Zinyowera, M.C. and Moss, R.H. (eds). 1998. The Regional Impacts of Climate Change. An Assessment of Vulnerability. IPCC, Cambridge University Press.

Zhang, T, Barry R.G., Gilichinsky, D.A., Bykhovets, S.S., et al. 2001. An amplified signal of climatic change in ground temperatures during the last century at Irkutsk, Russia. Climatic Change 49: 41-76.

Gilichinsky, D.A., Barry, R.G., Bykhovets, S.S. et al. 1998. A century of temperature observations of soil climate: methods of analysis and long-term trends. In A.G. Lewkowicz & M. Allard (eds), Permafrost; Proc. the 7th intern. conf., Yellowknife, 23-27 June, 1998, Université Laval: 313-17.

Snow effects on recent shifts (1998-2002) in mean annual ground surface temperature at alpine permafrost sites in the western Swiss Alps

R. Delaloye and M. Monbaron

Department of Geosciences, Geography, University of Fribourg, Switzerland

INTRODUCTION

The ground temperatures at several alpine permafrost sites have been monitored for the last five years. The data analysis highlights the effects of both duration and thickness of the snow cover on the mean annual ground surface temperature (MAGST).

The calculation of MAGST is frequently used for estimating the occurrence of permafrost. Nevertheless, as weather conditions may dramatically fluctuate from one year to another, MAGST is susceptible to large interannual changes, which can lead to significant misinterpretation of the data. The snow conditions represent a key factor governing the short-term variations in MAGST. Concerning the amplitude of these variations, Vonder Mühll et al. (1998) relate, for instance, a MAGST drop of more than 2°C at a depth of 0.6 m in a borehole over a one-year interval. However, the spatial variability of the temporal evolution of MAGST still remains poorly documented. The present work reports observations made at both regional and local scales.

SITES AND METHOD

The analyzed data stem from five sites, each less than 1 km^2 wide, and located within a radius of 20 km in the western Swiss Alps. The regional climatic conditions are transitional between the humid northwestern façade of the Alps (Mont-Blanc), the southern quite mediterrannean side of the alpine range, and the drier inner parts of Valais. The Sanetsch site is an exception as it is directly located on the northern and wetter border of the Alps.

Depending on the site, 4 to 22 mini-dataloggers (UTL-1) have recorded the temperature at 2-hour intervals, the first ones since October 1997. The annual series are adjusted on the zero curtain phases. The resulting accuracy of measurement is +/-0.15°C. The UTL-1 have been positioned immediately below the ground surface in order to be protected from direct solar radiation, i.e., at a depth of between 10 and 70 cm, depending on the ground granulometry and on the definition of the surface.

REGIONAL SCALE

Figure 1 provides a regional overview of the behaviour of the MAGST. For each site, the values correspond to the average of all the UTL-1. A first observation is that the MAGST is relatively high for permafrost terrain, frequently above 0°C. This could be see as an effect of climate warming, with the potential for a rapid degradation of permafrost. More probably, however, these high temperatures indicate a "thermal offset" between the surface and the top of the perennially frozen ground, a matter that still requires further study of mountain permafrost.

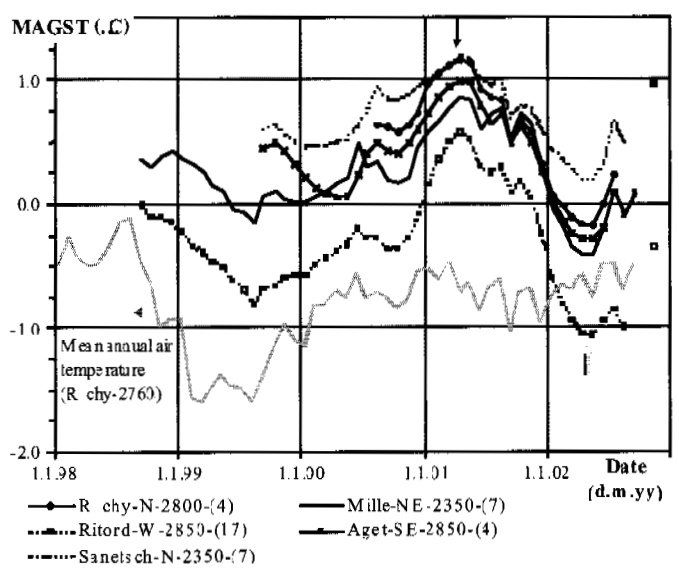

Figure 1. Monthly running MAGST during the period 1998-2002. For each site, the values correspond to the average of n UTL-1 and are placed at the end date of the annual interval. Legend: site-aspect-mean elevation-n. Black and white dots indicate the extreme values of MAGST calculated for all sites together, the arrows show the date when they occurred.

Figure 1 also shows that the interannual evolution of the MAGST looks quite similar for every site. An increase in the values from the end of 1999 until April 2001 was followed by a strong decrease during the next 12 months. On average, over the 41 available UTL-1, the drop in MAGST reached 1.4°C between April 2001 and April 2002. The maximum decrease obtained for a single datalogger was 3.1°C, the

minimum only 0.3°C. The shift in ground surface temperature was not accompanied by any significant change in mean annual air temperature (MAAT, Fig. 1). Indeed, interannual differences in snow covering caused this thermal drop.

Important snowfalls occurred relatively early in autumn 2000 and then protected the ground from winter cooling. The effect on MAGST was an increase towards the maximal values recorded during the five-year monitoring period. The spring of 2001 was again characterized by subsequent snowfalls which caused a relative delay in the snowmelt in comparison with the previous year. In response, MAGST began to decrease. The autumn of 2001 was not snowy and was followed by very cold weather in December and early January. Which resulted in especially cold ground temperatures. In April 2002, MAGST at all sites reached their lowest levels in the last 5 years at least.

A detailed comparison of the different sites reveals some peculiarities which can be attributed to local differences in interannual snow conditions.

LOCAL SCALE

The example illustrated on Figure 2 shows the effect of interannual changes in snow conditions on the MAGST at a very local scale.

The four UTL-1 involved were located on a complex of push-moraines. In contrast with both the preceding and the following years, the winter of 2000/01 was characterized by predominantly southerly winds which drastically modified the snow distribution in the area. As a result, the spatial pattern of the MAGST was inversted during 2001. The coldest places at the end of 2000 became the warmest a few months later, before being the coldest again in 2002. While the contrasted thermal evolution at Ri-19 and Ri-20 can be easily explained by their location on opposite sides of a pass, the behaviour of Ri-21 and Ri-22 appears to be due to the presence of plurimetric-sized ridges and furrows at that place. Variations in the redistribution of snow by wind over a very short distance – a few metres – is seen as being responsible for this peculiar thermal behaviour.

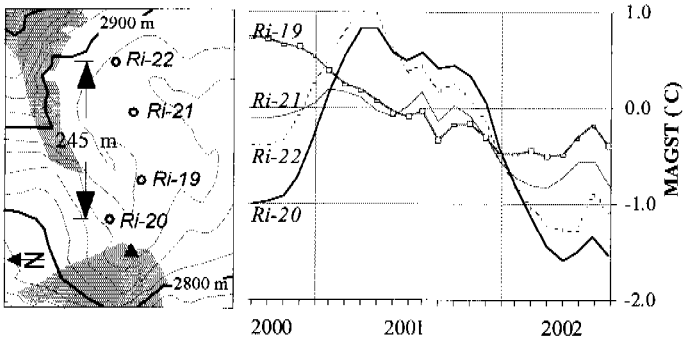

Figure 2. Monthly running MAGST near the Six Rouge pass at the Ritord site. On the location map, the white area corresponds to loose sediments (mainly push-moraines). Outcropping bedrock is drawn in grey. The Six Rouge is the small summit west of Ri-19.

CONCLUSIONS

The analyzed data illustrate the interannual influence of snow conditions on the annual ground temperature. MAGST can vary sharply both in time and space without any change in MAAT.

Interannual variations in snow cover conditions at a regional scale can induce strong changes in the ground surface temperature, which can be as high as 1.5°C for

MAGST calculated over an entire area. Locally, or in mountainous regions subject to more dramatic interannual shifts in weather conditions than in the western Swiss Alps, interannual changes in MAGST could be expected to be much higher.

Interannual differences in predominant winds can result locally in completely different snow cover distribution which in turn has an influence on the spatial pattern of MAGST.

The above conclusions indicate in particular that single-year measurement of the MAGST in high mountain areas must be very carefully interpreted.

REFERENCE

Vonder Mühll, D., Stucki, T. and Haeberli, W. 1998. Borehole Temperatures in Alpine Permafrost: A Ten-Year Series. Proceedings of the 7th International Conference on Permafrost, Yellowknife, Canada. 1089-1095.

Dangerous engineering-cryogenic processes at work in the urban territories of Russia's permafrost zone

E. A. Domnikova

Moscow State University, Faculty of Geography, Moscow, Russia

INTRODUCTION

Vast territories in Russia are located in permafrost zones. Large natural resources are concentrated there and consequently many buildings and facilities have been constructed. Perennially frozen grounds are unstable with temperature fluctuations and readily change their condition from frozen to thawed and vice versa. These changes are followed by a dangerous intensification of geocryogenic processes with negative consequences for the geoecological situation.

Cryogenic processes are geological processes which are related to the perennial and seasonal freezing of rocks (Kudrjavtsev 1978).

The following main groups of natural cryogenic processes, differing in their directions of influence and their specific manifestations in Far North landscapes, can be singled out: processes connected with warming effects on permafrost (thermokarst, thermoerosion); processes caused by cooling influences on the ground such as thawed-ground freezing or additional ice segregation in frozen ground (frost heave, cryogenic cracking); specific cryogenic processes (slope processes, the process of cryogenic weathering and the formation of frozen grounds under specific salt conditions).

Natural cryogenic processes increase with industrial development in permafrost zones and often new engineering-cryogenic processes arise. In a lot of cases these engineering-cryogenic processes produce disastrously negative influences on the environment, buildings and structures.

All engineering-cryogenic processes can be divided into two major types: those having a natural analog and their counterparts that have no complete natural analog. The first type includes activated natural cryogenic processes and also those caused by anthropogenic activity but also occurring under natural conditions. The second type embraces processes that are not found in nature.

To classify the processes belonging to the first type we can use the groups cited for natural cryogenic processes but adjusted for technogenic impact. Given below is a classification of engineering-cryogenic processes that have no natural analog since these processes are most widespread in industrially developed territories of the permafrost zone.

Technogenic heating of the ground is a process that increases the temperature of the perennially frozen rock. This process is intensified in industrially developed territories if the needs of local environment are violated by the maintenance of the facilities.

Technogenic salting of the ground is the process whereby pollutants coming into the active layer alter the properties of the ground. Frequently, under such conditions of deep thawing within the boundaries of cities and settlements cryopegs arise – unfrozen strongly mineralized horizons with below zero temperatures. Technogenic salting results in the active destruction of the foundation material (Grebenets et al.1997).

TECHNOGENIC INUNDATION

Most frequently, technogenic inundation is caused by leaks from engineering structures. This process weakens the ground structure and lowers its strength. It often involves ground ice which leads to thermokarst and thus deforming structures and foundations (Fig.1).

Figure 1. The process of technogenic inundation. Yamburg, 2000.

DESTRUCTION OF CONCRETE BY FROST

The concrete of foundation pillars and supports is slowly destroyed under repeated freezing – thawing conditions of the moisture contained in the pores, microcrevices and caverns (Grebenets 1995). When the water contained in the cracks is converted into ice it expands and widens the crack that is undergoing the freezing. This major factor, producing negative effects on the foundation material, is increased as the depth of thawing increases due to elevated ground temperatures caused by technogenic sources of heating.

It would seem advisable to classify not only the engineering-cryogenic processes but also the degree of their impact. This whole set of factors, leading to increasing engineering-cryogenic processes, can be conditionally divided into two groups: passive effects on the perennially frozen rocks and active effects on the perennially frozen rocks. Thus, all the engineering-cryogenic processes can be divided into two groups: engineering-cryogenic processes that only emerge under active effects on perennially frozen rocks and engineering-cryogenic processes that emerge even under passive effects on perennially frozen rocks.

Various engineering-cryogenic processes occur with different intensities under the same conditions of technogenic effect. It would seem relevant to single out four different categories of intensity:

1. Engineering-cryogenic processes with no marked effects;
2. Engineering-cryogenic processes producing low intensity effects;
3. Engineering-cryogenic producing high intensity effects;
4. Engineering-cryogenic processes producing disastrous effects;

Engineering-cryogenic processes can be controlled by stopping or neutralizing the processes of the technogenic impact, or by taking special engineering measures so that the geosystem reverts to its natural state, or by building new properties to the requirements of the geoecology and geocryology. Once this has become possible, engineering-cryogenic processes are considered to be controllable. If not, they are uncontrollable.

Studies of the dynamics of dangerous engineering-cryogenic processes, during the industrial development of the area have revealed their great dependence on regional geocryologic peculiarities as well as on the character and intensity of the technogenic impacts applied. The map "The Intensification of Engineering-Cryogenic Processes on the Urban Territories of Russia's Permafrost Zone" (1:15'000'000) has been created for the first time. It has been based on the "Geocryological Map of the USSR" and the following parameters were taken into consideration:

The character of the permafrost rocks in the area (solid. unsolid); whether it is flat or mountainous territory; the permafrost ground temperature and the level of zero annual amplitude; the population of an inhabited area; the type of industrial development and the predominant engineering-cryogenic processes.

The problems of stable developments in permafrost zones are very important now.

REFERENCES

Kudrjavtsev, V.A. 1978. General Geocryology. Moscow State University Publisheryouse (in Russian).

Grebenets, V.I., Kerimov, A.G.-o. and Savtchenko, V.A. 1997. Stability of foundation in cryolitic zone under the condition of technogenic inundation and salting. Publications Committee of XIV ICSMFE (ed). Proc. XIVth Int. Conference on Soil Mechanics and Foundation Engineering, Hamburg, 6 – 12 September 1997: 113-114. Rotterdam: Balkema.

Grebenets V.I. 1995. Heat regime operation of frozen grounds on urban areas. New constructions of foundaments and methods of foundament preparation [Novyye konstruktsii fundamentov I metody podgotovki osnovaniy]. VNIIOSP Proc., vol. 95. Moscow: 66-79 (in Russian).

Environmental maps of the Russian Arctic as a base for the segmentation of the coastline and the analyses of coastal dynamics

D. S. Drozdov and Yu. V. Korostelev

Earth Cryosphere Institute, SB RAS, Russia

During the past years coastal dynamics in the Arctic Seas have been studied under different aspects by various scientific divisions and organizations. The main task of the project is to investigate fundamental scientific questions concerning coastal dynamics in the Eurasian Arctic by using Geographic Information System (GIS) technology – mapping, zoning and monitoring of the caostal exogenic processes, based on geosystem principles.

Modern conditions and dynamics of the natural geosystem in northern regions with permafrost areas exist and constantly change, influenced by natural factors and anthropogenic activities. To study the influence of these factors, several GIS have been developed which can be applied to produce cartographical models of the main components of the geosystem. Digital environmental maps at global, regional and local scales are the most significant form of spatial realization of these models. Various prognostic, eco-geological and environmental maps were created and are being further developed at the present time.

The GIS technology can be used to handle a geocryological data base correlated with particular polygons on the map and to create digital landscape, engineering-geocryological, eco-geological, environmental, etc. maps. The GIS technology also supports monitoring needs, especially in the case of significant human activity. If a forecasting algorithm is accepted based on designed scripts of natural dynamics and economic activity, the GIS and monitoring system may represent not only modern data, but also prognostic information on environmental parameters.

To analyze the dynamics of the Russian Arctic coastal zone a set of digital landscape and Quaternary geology maps with scales of 1:4 000 000 - 1:2 500 000 for the hard copy are currently being developed. The first draft of these maps (Fig.1) was published within the framework of the CAVM project (Drozdov et al. 2001, Walker et al. 2002). According to the recommendations of the Arctic Coastal Dynamics (ACD) project (Rachold et al. 2002) and the Russian World Ocean project, the mapped areas will be enlarged and more details on landscape and geological units will be provided, especially along the coastline. Several climatic zones from forest-tundra to central taiga will be included in the mapped area and new types of landscape and geological units with different lithology and permafrost extent appear on the map. The consequent reprocessing of the source and derived maps, of satellite imagery and of the data base have to pass through several iterations.

The basic information which is needed to create the environmental-geological GIS is collected in small-scale graphic documents presented in the literature and in archives. The most important information can be taken from maps published by I.S.Gudilin in 1980, G.S.Ganeshin in 1976, J.Brown and others in 1997 and E.S.Melnikov and others in 1999. Additionally, the results of own research and the processing of remote sensing information were used.

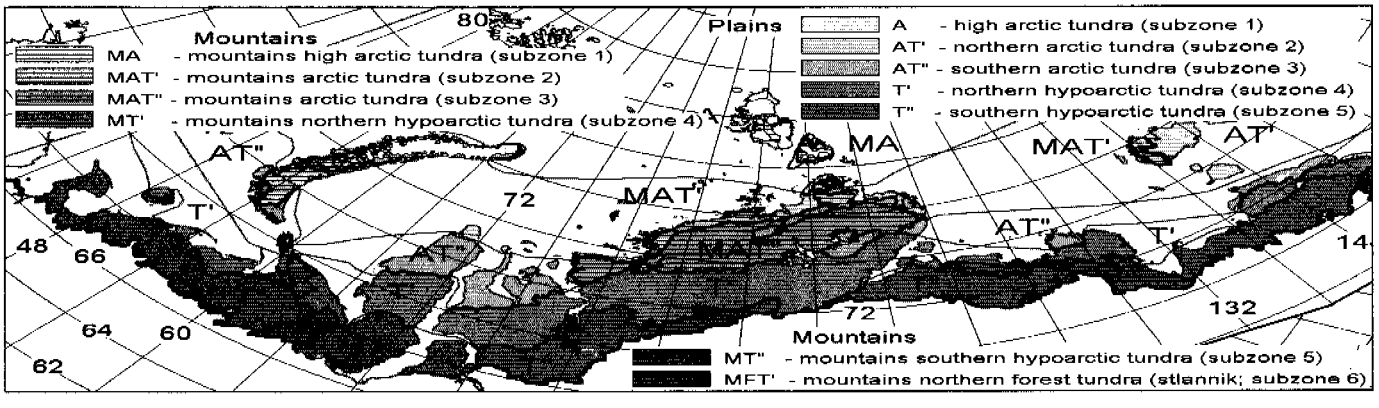

Figure 1. The landscape map of the Russian Arctic coastal zone: Climatic zonal, subzonal and altitudal-longtitudal landscape units.

The major part of the information needed for the analyses of coastal dynamics can be extracted from the landscape map of the Russian Arctic coastal zone which provides a subdivision of landscape unit types. This principle of unit types is widely used for drawing up landscape, geocryological and environmental-geological maps of the northern territories of Russia. It can be applied for all scales, the only differences are the dimensions of the examined and displayed landscape and geological units. In the case under discussion, case we deal with the units of largest dimension. Each landscape - forming attribute affects on-shore exogenic processes including coastal dynamics. The main landscape forming controls are the following:

- Location of the area in the particular natural-climatic zone or subzone (e.g., arctic tundra, northern forest-tundra, central taiga, etc.).
- Location of the territory in units of altitude zoning (i.e., plains, plateau, mountains).
- Genesis and main morphological attributes of relief (e.g., landscapes of marine plains and terraces, glacial landscapes, erosive-denudation landscapes of mountains and piedmonts, etc.).
- Characteristics of sediments: lithology of soils and petrography of rocks (e.g., clay, sand, debris material, karst-able and non-karstable bedrocks, etc.).

Each of the listed attributes has to be mapped and the overlay of all these maps represents the final landscape map, which serves as the base for spatial characteristics of modern geological processes. Formally, all lines on the obtained landscape map can be estimated as the boundaries of common range. For convenience of analysis, however, it is useful to organize the boundaries in the order mentioned for the landscape-forming controls where the boundaries of natural-climatic zones are the most important and the boundaries of ground types are least important.

The landscape and surface geology maps obtained serve as a graphical base to make segmentation of the Russian Arctic coastlines for description and analysis of coastal processes and for further assessment of coastal dynamics (Fig. 2).

At the present time, segmentation of one coastal zone is practically completed. Each segment is to be supplied with a table of appropriative data according to the appropriate legend – the ACD classification template. This work is currently being performed by specialists from different institutes and organizations involved in the ACD project.

ACKNOWLEDGEMENTS

This study is supported by INTAS (grant 01-2332) and RFFI (grant 01-05-64256).

REFERENCES

Circum-Arctic map of permafrost and ground ice conditions. 1997. Edited by J. Brown, O.J. Fenians, Jr., J.A. Heginbottom, E.S. Melnikov – IPA. US Geological Survey.

Drozdov D.S., Ananjeva (Malkova) G.V. 2001. Landscape Map of the Russian Arctic. // Forth Int. Circumpolar Arctic Veg. Map. Work: Moscow, April 10-12: 43-45.

Melnikov E.S. (ed.) et al., 1999: Landscape map of Russia permafrost at scale 1:4 000 000. Tyumen. Earth Cryosphere Institute SB RAS *(in Russian)*.

Rachold, V., Brown, J., Solomon, S. 2002. Arctic Coastal Dynamics - Report of an International Workshop, Potsdam (Germany) 26-30 November 2001, Reports on Polar Research 413, 103 pp.

Walker D.A. et al. 2002. The circumpolar Arctic vegetation map. – Remote Sensing, V.23, #21: 4551-4570.

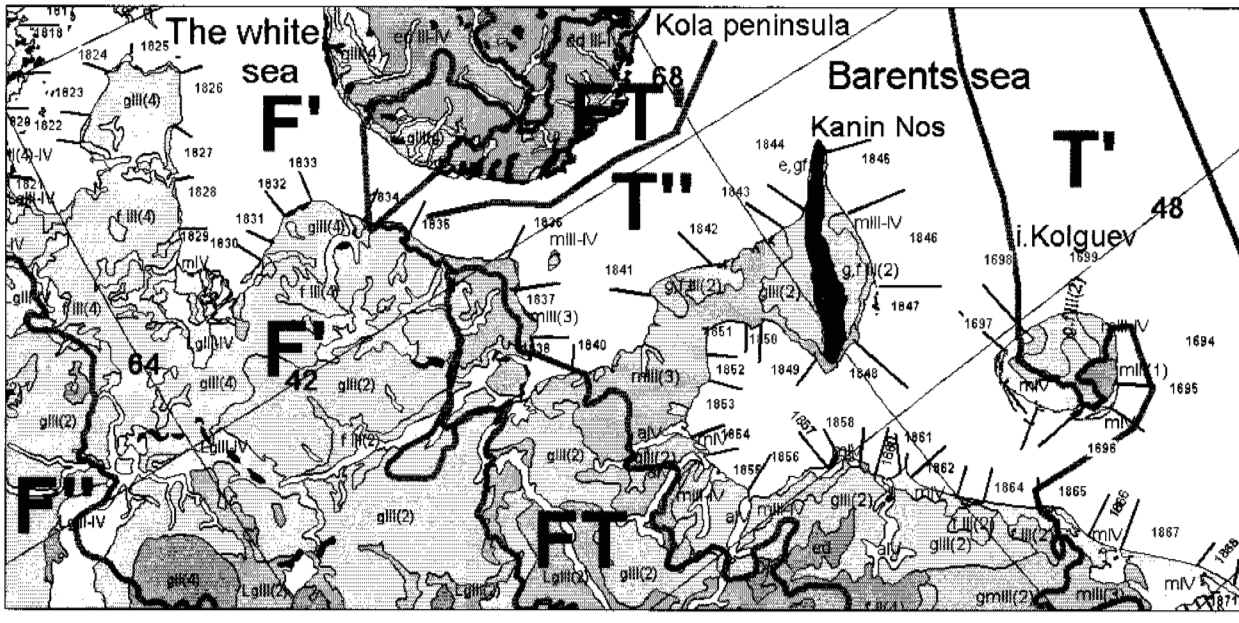

Figure. 2. The segmentation of the Russian Arctic coastal zone based on landscape and surface geology maps.

Use of BTS measurements and logistic regression to map permafrost probability in complex mountainous terrain, Wolf Creek, Yukon Territory, Canada

M. Ednie and A.G. Lewkowicz

Department of Geography, University of Ottawa, Canada

Many thousands of square kilometers of north-western Canada are underlain by mountain permafrost. At present, even the most up-to-date permafrost maps of this area are at scales which classify whole regions as sporadic or widespread discontinuous permafrost, thereby ignoring the influence of elevation and exposure. In order to provide baseline data for assessment of the effects of future climate change and to assist with mineral development, a simple methodology is needed to measure and identify permafrost distribution in this complex mountainous terrain. The BTS (basal temperature of snow) method, widely employed in the European Alps (e.g. Hoelzle et al. 1993) and elsewhere, could be of great use in this context since it allows the development of a model of permafrost likelihood within a GIS. However, a thick, stable snow cover (at least 80 cm deep) is required to insulate the ground from atmospheric temperature variations in order to use BTS temperatures as indicators of permafrost. Studies of the thermal influence of the relatively thin and wind-blown snow cover that is typical of northern Canada (e.g. Granberg 1973) have led to skepticism among some researchers as to the potential efficacy of the BTS method in this region. Consequently, to our knowledge, this is the first attempt to test the BTS method to map mountain permafrost in North America.

Our study was carried out in the Wolf Creek research basin, 20-30 km south of Whitehorse in an area mapped as part of the sporadic discontinuous permafrost zone. The basin has an area of almost 200 km^2 at elevations of 750 to 2250 m a.s.l. and a vegetation cover that changes from boreal forest to alpine tundra as elevations increase. The annual air temperature at Whitehorse is –0.7°C (1971-200) at 703 m a.s.l. and a value of -4°C was measured from 2001-02 at an elevation of 1235 m within the basin.

The methods used to evaluate the efficacy of the BTS methodology to predict the probable distribution of permafrost in this complex mountainous terrain were as follows:

1) A geo-referenced set of 396 BTS measurements were collected within the basin in March-April 2001 and 2002. Miniature data loggers installed in fall 2000 showed that stable minimum temperatures at the snow-ground interface were reached at both times of measurement, as required for the BTS methodology.
2) A map of potential incoming solar radiation for the basin was developed using a 30 m digital elevation model and the Solar Analyst extension (Fu and Rich 1999) in Arcview 3.2. The proportion of incoming radiation modeled as direct beam was set using cloud cover data from Whitehorse.
3) Measured BTS values were regressed against elevation and the modeled potential incoming solar radiation and gave a statistically significant relationship with an r^2 of 0.37. This value is comparable to those from European investigations (Gruber and Hoelzle 2001). The scatter in the graph of measured vs. modeled BTS values (Fig. 1) likely derives from variables that are not included in the modeling, such as albedo and vegetation cover.
4) We determined the relationship between modeled BTS and permafrost distribution, rather than employing the categories used in the European Alps. In late July-August 2002, holes were augered or pits were excavated at a total of 200 sites with a range of elevations and slope orientations to verify the presence or absence of frozen ground. Frozen ground encountered within 2 m of the surface, or predicted from instantaneous temperature profile measurements to be present in this layer, was taken to be an indication of permafrost.
5) Logistic regression (e.g. Pereira and Itami 1991) was used to evaluate the relation between the modeled BTS values and the permafrost distribution identified in the excavations. A cluster of points from a confined valley in the central part of the basin were significant outliers and indicated that permafrost was present there at relatively low elevations. It is believed that these resulted from winter air temperature inversions which are common in the Wolf Creek basin. These points were excluded from the analysis. Traditional BTS results (e.g. Hoelzle et al. 1993) are given as

qualitative values (permafrost improbable, permafrost possible, and permafrost probable) whereas logistic regression allows for the calculation of quantitative probabilistic values of permafrost distribution based on BTS (Figure 2). For Wolf Creek, there is a >90% probability of permafrost at modeled BTS values <-5°C, and <10% probability of permafrost at BTS values >-1.1 °C.

6) A preliminary probability permafrost map of Wolf Creek basin was produced (not shown). From the analysis, about 40% of the basin is underlain by permafrost.

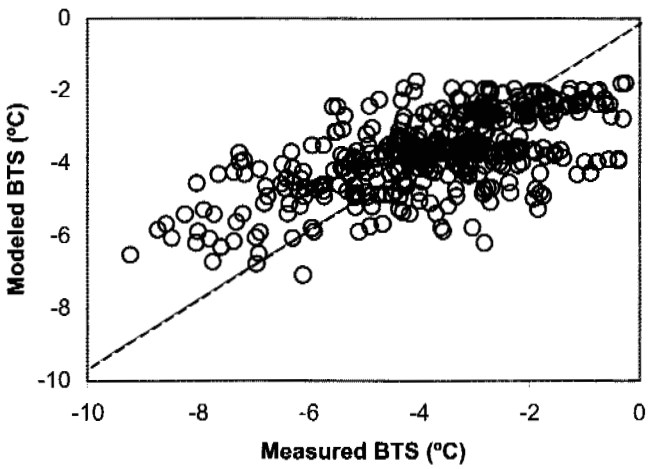

Figure 1 Measured BTS versus modeled BTS values.

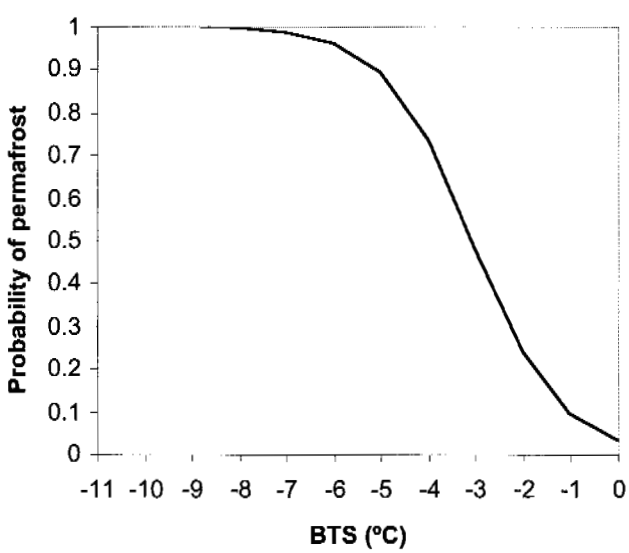

Figure 2: The probability of permafrost curve.

We conclude that BTS modeling to predict permafrost is possible in mountainous parts of the Yukon Territory and that a quantitative probabilistic approach is the most logical given the variable terrain, vegetation and snow cover in this basin and elsewhere. Future research is needed to identify the topographic characteristics of mountain valleys that may experience air temperature inversions and to incorporate such characteristics into a permafrost prediction model. In addition, the relationship between BTS values and permafrost probability (Fig. 2) needs to be tested in other parts of the Yukon Territory.

REFERENCES

Fu, P. and Rich, P.M. 1999: Design and implementation of the Solar Analyst: an Arcview extension for modeling solar radiation at landscape scales. Accessible at: http://www.esri.com/library/userconf/proc99/proceed/papers/pap867/p867.htm

Granberg, H.B. 1973: Indirect mapping of the snow cover for permafrost prediction and Schefferville, Quebec. In Proceedings of the Second International Conference on Permafrost, North American Contribution, Yakutsk, USSR. Washington, DC: National Academy of Science Publication; 113-120.

Gruber, S. and Hoelzle, M. 2001: Statistical modeling of mountain permafrost distribution: local calibration and incorporation of remotely sensed data. Permafrost and Periglacial Processes 12: 69-77.

Hoelzle, M., Haeberli, W. and Keller, F. 1993: Application of BTS measurements for modeling mountain permafrost distribution. In Proceedings of the Sixth International Conference on Permafrost, Beijing. South China University of Technology, Beijing. Vol.1: 272-277.

Pereira, J.M.C. and Itami, R.M. 1991: GIS-based habitat modeling using logistic multiple regression: A study of the Mt. Graham red squirrel. Photogrammetric Engineering & Remote Sensing 57(11): 1475-1486.

Modeling the influence of moisture variations on physical rock weathering processes in Antarctica: proposed investigations and preliminary results

C. Elliott

Geography Department, University of Canterbury, Christchurch, New Zealand

The primary objective of the proposed research is to quantify the role of moisture in the weathering of rock in a cold environment such as Antarctica. It is being conducted to fulfill the requirements of a Ph.D. Although primarily focussed on physical weathering processes, some investigations of the potential role of chemical and biological weathering will also take place. Specifically, the research aims to develop a model to predict changes in weathering rate, for a particular rock type, along a temperature and moisture gradient on the Victoria Land Coast, Antarctica (Figure 1A). One of the more challenging aspects of investigations into rock weathering is the complexity of factors involved and Antarctica is an ideal environment to undertake such research as its low moisture (at least in the area under consideration here) and extremely low temperatures enable some of these factors to be excluded or minimized.

Despite the fact that the weathering of rock is a fundamental landscape process, the important role that moisture plays in weathering, although recognized, has not yet been quantified. For example, there has been no systematic study of how increasing quantities of moisture may influence the type of process operating. Nor, apart from the work of Prick (1997), have attempts to quantify the influence of changing moisture availability on weathering rates been made. With one or two notable exceptions (e.g. Matsuoka 1991), very few rock weathering studies have attempted to develop models that will predict weathering rates. A series of simulations will be conducted on rock samples from four locations in the field using an environmental cabinet and the effects of moisture isolated from other factors. The use of an environmental cabinet and speeded-up climatic cycles is a well-established technique for measuring weathering rates (e.g. Warke and Smith 1998). However, in this study the climatic cycles to be used in the laboratory will be based on field observations of temperature and moisture regimes *within* the rock, rather than those using air temperature, for example. To achieve this, water baths will be used to provide the moisture levels necessary and the cabinet fitted with a lamp as an artificial 'sun' to enable the rock surface temperatures to be achieved.

An empirically-based mathematical model will then be developed that will predict changes in weathering rate depending on changes in moisture in the rock. The weathering rate will be estimated by both measuring changes in the weight of the samples and using a non-destructive sonic technique to detect changes in strength (e.g. Fahey and Gowan 1979), after a specific number of cycles.

Four locations along the Victoria Land Coast have been identified to undertake the fieldwork: Victoria Valley, Gneiss Point, Terra Nova Bay and Cape Hallett (Fig. 1B). These locations enable both a coast-to-inland perspective (between Victoria Valley and Gneiss Point at approximately 77.5 °S), as well as a 5° latitudinal gradient (between Gneiss Point at 77.5 °S and Cape Hallett, at 72.5 °S) to be investigated. Hourly recordings of surface and subsurface (45 mm, 90 mm) rock temperature measurements from mid-October to mid-January will be made using thermocouples and dataloggers. One-minute temperature measurements will also be taken during each visit (i.e., in mid-October and mid-January) in order to determine whether any thermal gradients likely to induce insolation weathering have occurred. Year-round measurements will be attempted during the second field season in 2003/04.

Surface moisture sensors will provide measurements of hourly surface moisture data, and relative humidity probes will enable subsurface moisture regimes to be determined (at 45 mm and 90 mm depths). The latter technique has not yet been used to measure subsurface moisture content in the field in rock weathering studies, but has been used successfully for measuring moisture content in concrete. These measurements are recorded manually and so can only be undertaken during the times of visits.

These techniques represent a unique aspect of this research, as previous studies, such as those undertaken by Hall (1986), have measured average moisture content of rock samples left in the field rather than investigating levels of moisture at different depths in the rock. In addition, macro-climatological data (air temperature, relative humidity, wind speed and direction) provided through existing Automatic Weather Stations will be analyzed.

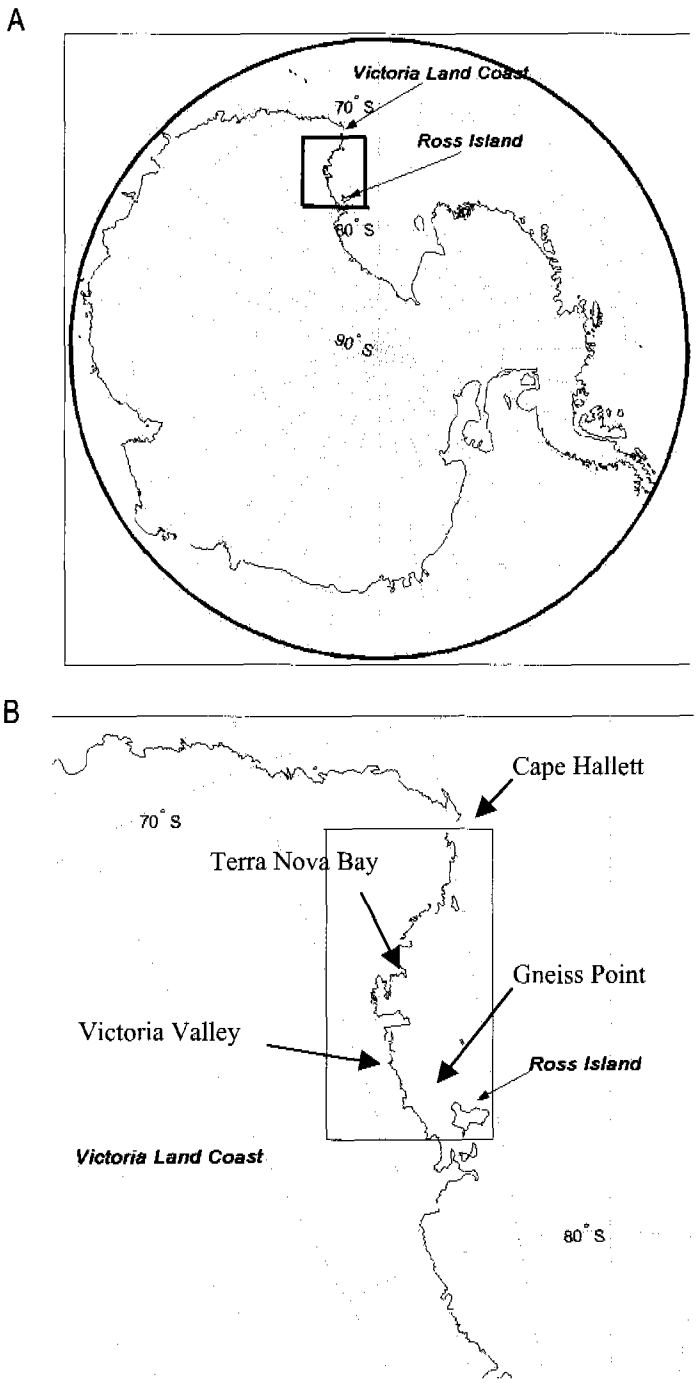

Figure 1. (A) General location of field sites in relation to the Antarctic continent (B) The Victoria Land Coast indicating the four field sites at Victoria Valley, Gneiss Point, Terra Nova Bay and Cape Hallett. Not to scale.

The first fieldwork season has just been completed at Gneiss Point and Victoria Valley and rock temperature and moisture data successfully captured. Initial results give a clear indication of the different temperature regimes between the October and January recordings, as well as the changes in moisture levels at the different depths within the rock. Mean moisture levels between October 2002 and January 2003, although similar between depths for each period, show significant differences between periods (Table1) and during the course of the day (Figure 2).

Table 1: Mean vapor densities at Gneiss Point October 2002 and January 2003 at 45 mm and 90 mm depth in the rock

Depth of Probe	Vapor Density (gm/m²)	
	October 2002	January 2003
45 mm	1.4	5.1
90 mm	1.2	5.2

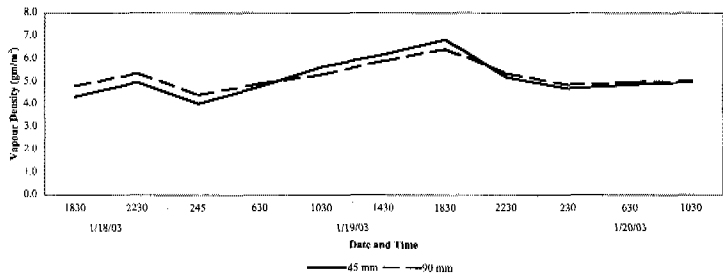

Figure 2. Vapor densities for the Gneiss Point Site at 45 mm and 90 mm depths in January 2003 indicate that the 90 mm vapor densities are greater than the 45 mm vapor densities during the evening and early morning, but are less than the 45 mm ones during the day.

REFERENCES

Fahey, B. D. and Gowan, R.J. 1979. Application of the sonic test to experimental freeze-thaw studies in geomorphic research. Arctic and Alpine Research 11(2): 253-260.

Hall, K. 1986. Rock moisture content in the field and laboratory and its relationship to mechanical weathering studies. Earth Surface Processes and Landforms 11: 131-142.

Matsuoka, N. 1991. A model of the rate of frost shattering: application to field data from Japan, Svalbard and Antarctica. Permafrost and Periglacial Processes 2: 271-281.

Prick, A. 1997. Critical degree of saturation as a threshold moisture level in frost weathering of limestones. Permafrost and Periglacial Processes 8: 91-99.

Warke, P. A. and Smith, B.J. 1998. Effects of direct and indirect heating on the validity of rock weathering simulation studies and durability tests. Geomorphology 2: 347-357.

The lower discontinuous permafrost boundary in the Argentera Massif (Maritime Alps, Italy): insight from rock glacier geo-electrical soundings

*D. Fabre, * A. Ribolini, P. R. Federici and M. Pappalardo*

Laboratoire Interdisciplinaire de Recherche Impliquant la Géologie et la Mécanique (LIRIGM), Université Joseph Fourier, France

** Dipartimento di Scienze della Terra, University of Pisa, Pisa, Italy*

The rock glaciers of the Argentera Massif are located in the southernmost part of the European Alps, only 50 km from the Mediterranean Sea. Glacial and periglacial reconstructions in this Alpine region indicate out a rock glacier formation mainly during the Younger Dryas and Subboreal cold phases (Finsinger and Ribolini 2001 and references therein). In this marginal area of the Alps, transitional climate between Mediterranean and more continental conditions made uncertain the evaluation of rock glacier activity, that in some cases seems controlled by local microtopography and meteorology (Federici et al. 2000). Recently, Surface Ground Temperature (SGT) of some rock glaciers (Ribolini 2001), allowed to site the Lower Discontinuous Permafrost Boundary (LDPB) at about 2,600 m a.s.l., which is slightly lower than the one proposed for the southern French Alps in the opposite flank of the mountain chain (Evin and Fabre 1980).

To improve this evaluation, during the years 2001-02 geo-electrical soundings were conducted on four rock glaciers (namely: Bassa Margot, Agnel, Portette and Prefouns), selected at mean elevations ranging between 2,450 m and 2,700 m, thus proximal to the inferred LDPB. All the analyzed rock glaciers belong to the Gesso Basin in the southeastern Argentera Massif.

The Schlumberger method was adopted (with AB/2 max ranging from 20 to 70 m), using an apparatus (MAATEL BM1) working at DC 2000 V of max power. This device was calibrated on the Murtel rock glacier in Switzerland, where a mechanical sounding through the permafrost is available (Fabre and Evin 1990). Previous soundings in the southern French Alps (Assier et al. 1996 and references therein) evidenced a typical active rock glacier vertical profile of resistivity: a) surface layer without permafrost (5,000-20,000 Ωm), b) ice-saturated sediments (permafrost) with resistivity ranging from tens of thousand up to million of Wm, and c) bedrock or not frozen basal sediment (1000-10,000 Ωm).

Two longitudinal profiles in the upper-middle part (BM1, BM2) and a transversal one (BM3) in the lower part were performed on the Bassa Margot rock glacier. The results (Fig. 1) indicate presence of permafrost with medium-high ice content layers in the upper-middle part, while in the lower one unfrozen sediments were found.

The Portette rock glacier also shows high resistivities. In the upper part transversal profile (PO1), data are consistent with a 5 m thick permafrost level with a medium ice content (110,000 Ωm), overlaying a 20 m thick of permafrost with an higher ice content (~1 MΩm). Similar resistivities in the vertical distribution results from the transversal profile in the lower part (PO2) (Fig. 1).

The three transversal profiles (PR1, PR2, PR3) performed on the Prefouns rock glacier show the presence of permafrost, with thick layers characterized by low to medium ice contents. Here, the results of the soundings are consistent with a permafrost thickness of 20 m overlaid by a few metres of sediments with little ice content (Fig. 1).

Agnel rock glacier was investigated by means of only one transversal profile (AG), because of its limited areal extension. The resistivity distribution found (Fig. 1) suggests a thin layer of permafrost (1 to 7 m depth), with low ice content (70,000 Ωm) probably not in equilibrium, characterized by a temperature near the melting point (T > -1 °C)

Considering that the rock glaciers studied could be considered representative of all the rock glaciers that are present in the Argentera, a speculation about activity elevation can be proposed. Sectors of rock glacier developed above 2,600 m are affected by permafrost, up to 20 m thick and with medium-high ice content (20 to 40 %). Rock glaciers at elevations ranging between 2,450 and 2,600 m are affected by thin/relict permafrost layers. Below 2,450 m it is unlikely to find permafrost, except for very isolated, sheltered sites.

On the basis of these results, the Argentera Massif can be considered the southernmost discontinuous permafrost environment of the Alps, whose lower boundary corresponds to about 2,600 m a.s.l.

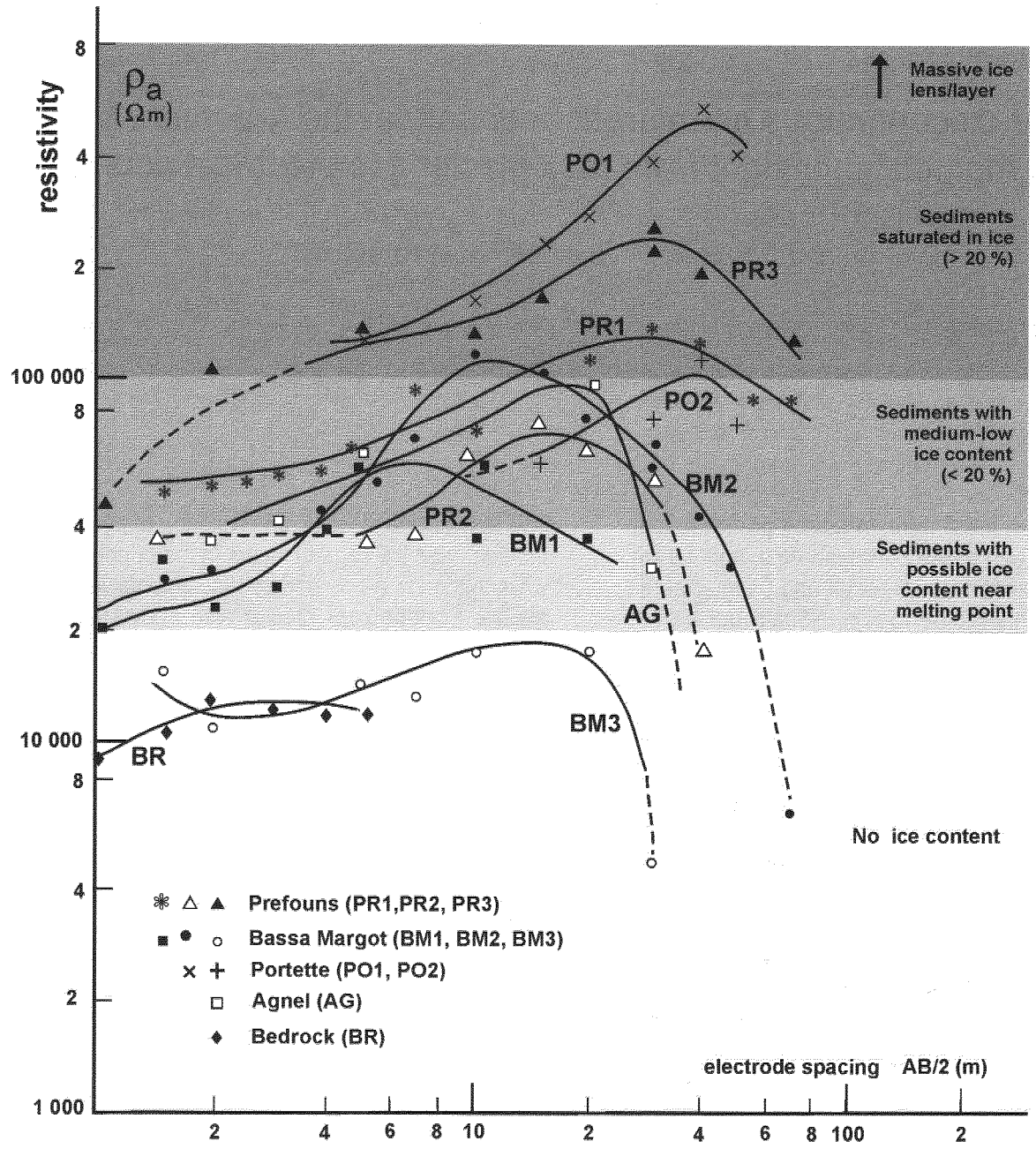

Figure 1. Results of DC resistivity soundings

REFERENCES

Fabre, D. and Evin, M. 1990. Prospection électrique des milieux à très forte résistivité: le cas du pergélisol alpin. Proceeding of Sixth International Congress of the International Association of Engineering Geology, Pays-Bas: 8.

Assier A., Fabre, D. and Evin, M. 1996. Prospection électrique sur les glaciers rocheux du cirque de Ste-Anne. Permafrost and Periglacial Processes 7: 53-68

Finsinger, W. and Ribolini, A. 2001. Late glacial to Holocene deglaciation of the Colle del Vei del Bouc-Colle del Sabbione Area (Argentera Massif, Maritime Alps, Italy-France). Geografia Fisica e Dinamica Quaternaria 24: 141-156.

Federici, P.R., Pappalardo, M. and Ribolini, A. 2000. On the ELA and lower limit of discontinuous permafrost boundary in the Maritime Alps (Italian side). Atti Accademia delle Scienze di Torino 134: 23-29.

Ribolini, A. 2001. Active and fossil rock glaciers in the Argentera Massif (Maritime Alps): Surface ground temperatures and paleoclimatic significance. Zeitschrift für Gletscherkunde und Glazialgeologie 37: 125-140.

Using catchment soils to establish the provenance of high arctic pond sediments: Truelove Lowland, Devon Island, Canada

*L.A. Fishback and *R.H. King*

Scientific Coordinator, Churchill Northern Studies Centre, Canada

**Department of Geography, The University of Western Ontario, London, ON, Canada N6A 5C2*

INTRODUCTION

High arctic ecosystems have been identified as critically sensitive areas in terms of global changes because of the strong negative feedback mechanisms that create sensitivity to the effects of greenhouse warming. Lakes and ponds in these regions have been identified as "sensitive bellweath-ers" of these changes (Douglas et al. 2000). Ponds are de-fined as water bodies that freeze to the bottom each winter whereas lakes maintain an unfrozen water column during the winter months.

The preservation of the paleo-environmental record in arc-tic pond sediments has been found to be more complete than anticipated (Douglas et al. 2000). However, such paleo-environmental reconstructions tend to be far more effective in determining past stages of the water body than providing indi-cations of environmental changes in the surrounding catch-ment areas.

This research attempts to address the catchment condi-tions with respect to pond sediment records by gaining a bet-ter understanding of the physical, chemical and mineralogical signal of catchment processes and identifying the presence of this signal in the adjacent high Arctic pond sediments.

STUDY AREA

Truelove Lowland (75o40'N, 84o35'W) is one of a series of coastal lowlands with high biological diversity located on northeastern Devon Island, Nunavut, Canada. As a result of isostatic emergence following the last glaciation, a series of raised beaches was formed (King 1991). These features are topographic barriers that have trapped water resulting in the formation of approximately 530 ponds and five lakes (ap-proximately 20% of the Lowland area) (King 1991). Pooh Pond in the central Lowland and the adjacent raised beach were selected for this study.

METHODS

The sediments of Pooh Pond, a large, 1.2 m deep, freshwa-ter pond were characterized using four short sediment cores (< 0.40 m) taken from a variety of water depths in a transect from shore to deepest area of the pond. Sediments were cored using a modified corer (id = 51 mm) and fractioned at 50 mm intervals. Fractions were analyzed using chemical fractionations and selective extractions to characterize the sediments and differentiate between materials from the catch-ment and the water body, as well as establishing indicators of specific catchment processes.

Major soil inspection pits were excavated in a catena comprising four landscape units within the catchment. Soil ho-rizons from each pit were sampled in duplicate in the field and processed with the pond sediment cores. A data set was compiled of similar biogeochemical variables for pond sedi-ment and soils and tested for normalcy. A series of multivari-ate statistics were used to investigate the provenance of the pond sediments.

RESULTS AND DISCUSSION

A 14C pond sediment basal date of 5980 ± 40 yrs BP (Beta-162840) from 0.32 m depth was comparable to a predicted emergence date for Pooh Pond, indicating a freshwater origin of pond sediments collected. The lack of biogeochemical stratigraphy in these pond sediment cores was most likely due to cryoturbation or wave-induced turbation of the sedi-ments that act to homogenize the unfrozen sediments. An ANOVA of the physical and chemical characteristics of the four cores demonstrated a significant difference between the four cores. These differences indicate the importance of local sedimentary environments in the pond and the difficulty of single core characterization of pond sediments.

The four soil types investigated on the raised beach are formed on poorly stratified gravelly carbonate-rich beach de-posits (Lev and King 1999). Soils on the raised beach crest were poorly developed with desert pavement at the surface and a thin A horizon overlying a coarse parent material with carbonate pendants and particle caps. Brunification dominates the soils in the upper and lower foreslope as indicated by the Na-pyrophosphate extractable Fe in the soils in Table 1. These soils are more developed with high organic carbon contents, a thin Bm horizon and an overall finer texture. Contemporary translocation of Fe and Al in the lower foreslope soil solu-

tions was indicative of incipient podzoliza-tion. Soils at the slope base are waterlogged with accumu-lated organic matter over a gleyed silty parent material with high concentrations of Mn and Fe.

Table 1: Extractable Fe as an indicator of brunification in soil horizons in the raised beach soils.

Soil Type [1] (Landscape Unit)	Soil Horizons [1]	Fe_p [2] (% wt)
Regosolic Static Cryosol (Raised Beach Crest)	Ahk	0.050
	Cca	0.025
	Ck2	0.020
Brunisolic Eutric Static Cryosol (Upper Foreslope)	Ah	0.080
	Bmk	0.050
	Ck1	0.035
	Ck2	0.025
Brunisolic Eutric Turbic Cryosol (Lower Foreslope)	Ahy	0.110
	Bmy	0.115
	Cky1	0.025
	Cky2	0.030
Gleysolic Turbic Cryosol (Meadow)	Ofy	0.210
	Ckgy	0.050

1 as determined by the Canadian Soil Classification System, 1998.
2 Na-pyrophosphate extractable Fe to represent organically chelated Fe in the B horizon in % of soil weight.

Cluster analysis was used to classify the raised beach soil horizons into four groups to create a reference set for comparison with the pond sediments. The 'unknown' pond sediments were classified into the soil groups using a discriminant function analysis (DFA). The inorganic pond sedi-ments were classified predominantly with soil horizons showing some weathering. This DFA also identified the most discriminating variables in classifying the pond sediment with the soils as total organic carbon, organically chelated Fe, Al and Mn and 'plant available' elements (Mehlich III extract).

A second cluster analysis of the entire soil and pond sediment data set resulted in separate groups of pond sedi-ments and soil horizons with the exception of one group. This group contained soil horizons from the toe of the slope and from the pond sediment core closest to the shore highlighting the localized connection of soils and pond sediments.

CONCLUSIONS

Soil profile morphologies reflected a variety of pedogenic and cryogenic processes within a soil catena across a raised beach in Truelove Lowland. These processes included brunification and incipient podzolization.Sediments from the adjacent Pooh Pond were heterogeneous and the characteri-zation of these sediments based on single cores was difficult. Biogeochemical analyses indicate that Pooh pond sediments are predominantly catchment-derived in origin.

This research indicates that while these pond sediments are derived mostly from catchment soil material, it is difficult to establish provenance based on the biogeochemistry of sediment alone. Pond sediments are a result of a number of genetic processes operating together to produce a unique material. Modification of the catchment-derived material dur-ing transport and deposition obscures the catchment signal and therefore influences the interpretation of the sediment re-cord.

REFERENCES

Agriculture and Agri-Food Canada, Soil Classification Working Group. 1998. The Canadian Soil Classification System. Agri-culture and Agri-Food Canada Publication 1646 (Revised).

Douglas, M.S.V., Smol, J.P. and Blake, W.Jr. 2000. Summary of paleolimnological investigation of high arctic ponds at Cape Herschel, east-central Ellesmere Island, Nunavut. In M. Garneau and B. Alt (eds.), Environmental Response to Climate Change in the Canadian High Arctic. Geological Survey of Canada Bulletin 529.

King, R.H. 1991. Paleolimnology of a polar oasis, Truelove Low-land, Devon Island, NWT, Canada. Hydrobiologia 214: 317-325.

Lev, A. and King, R.H. 1999. Spatial variation and soil development in a high arctic soil landscape: Truelove Lowland, Devon Is-land, Nunavut, Canada. Permafrost and Periglacial Processes. 9: 35-46.

Atmospheric and geothermal conditions during thermal contraction of ice wedges, Bylot Island, eastern Canadian Arctic archipelago

D. Fortier and M. Allard

Centre d'études nordiques, Université Laval, Québec, G1K 7P4

We studied thermal contraction cracking of ice-wedge polygons located on a terrace bordering a glacio-fluvial outwash on Bylot Island (73^0 09'38"N, 80^0 00'43,2" W). Previous studies showed that the polygons of the study site are composed of a syngenetic ice-rich accumulation of *in-situ* grown peat and wind-blown silts (Fortier and Allard 2001).

Air and ground temperature conditions preceding the rupture of electric cables buried in the active layer over ice wedges were analyzed for the period 1997 to 2002. Frost cracking (breaking of electric cables 5 mm o.d.) occurred from November to March with the largest number of breaks (45%) taking place in January, during the polar night. Due to the absence of solar radiation, air temperature variations are closely linked to the thermal properties of the air masses. In the Bylot Island region and in north-eastern Baffin Island, the atmospheric depressions in the winter come mainly from the south (Maxwell 1981). Analysis of wind data recorded over the study site showed that frost cracking of ice wedges occurred mainly following the incursion and persistence of eastward and southward cold weather accompanied by winds of varying strength from the Byam Martin mountains and Navy Board Inlet.

The rate of geothermal contraction in the polygons is related, in a non-linear way, to the length, range and speed of the cooling of the air temperature, the thickness of the snow cover, the sediment types and the ice content of the ground (MacKay 1993, MacKay and Burn 2002). Crack openings occur when contraction deformation by creep in ice wedges is not fast enough to release the mechanical tensions created by the thermal contraction of the terrain.

From 1997 to 2002, the mean daily air temperature on days when cracking occurred was -36 °C, with air temperatures ranging from -27 to -40 °C. Frost cracking of the ground (electric cable ruptures) occurred a few hours to a few days after a drop in the mean hourly air temperature in the order of 7.9 °C over an average of eighteen hours at a mean air cooling rate of -0.45 °C/h. Maximum cooling rate was -0,9 °C/h when air temperature quickly dropped by 18.6 °C in less than 24 hours (12-2000). Fifteen of the nineteen cracking events occurred when the mean daily air temperature was stationary or rising slightly since the preceding day. This is due to the penetration time of the cold wave into the snow cover and the frozen ground. Table 1 shows air temperature cooling rates during the days before selected frost cracking events, for the 1997 to 2002 period.

Table 2 shows mean, maximum and minimum ground temperature occurring during frost cracking days. During cracking episodes, the mean temperature at the ground surface (-2 cm) was -22.9 °C (1997-2002) and ranged from -14.7 °C to -29 °C. Geothermal data obtained from a thermistor cable, installed in permafrost in 1999, reveal that mean daily ground temperature at the top of permafrost (40 cm under the ground surface) during frost cracking events (13) was -18.6 °C (2000-2002) and varied from -23.8 °C to -12.8 °C.

YEAR	DAY / MONTH	ATCR (°C / h)
1997	21 - 22/02 **(24)**	-0,61 (-8,5°C/14h)
1997	13 - 14/03 **(15)**	-0,44 (-6,2°C/14h)
1997	14 - **15/03**	-0,43 (-6,9°C/16h)
1998	10 - **11/01**	-0,55 (-9,4°C/17h)
1999	22/ 01 **(26)**	-0,21 (-4,9°C/23h)
1999	23 - 24/02 **(26, 27)**	-0,36 (-9,3°C/26h)
1999	24 - 25/02 **(26, 27)**	-0,58 (-7,0°C/12h)
1999	25 - **26/02**	-0,47 (-4,7°C/10h)
1999	26 - **27/02**	-0,31 (-4,0°C/13h)
2000	02 - 03/01 **(7)**	-0,37 (-7,1°C/19h)
2000	06/01 **(7)**	-0,84 (-4,2°C/05h)
2000	21/01 **(23)**	-0,53 (-5,8°C/11h)
2000	**23/01**	-0,69 (-6,2°C/09h)
2000	12/02 **(13)**	-0,33 (-7,3°C/22h)
2000	30/11 - **01/12**	-0,71 (-12°C /17h)
2000	04 - 5/12 **(6)**	-0,27 (-6,8°C/25h)
2000	09 - **10/12**	-0,93 (-18,6°C/20h)
2001	17 -**18/12**	-0,51 (-14,2°C/28h)
2001	08 - 09/01 **(11)**	-0,51 (-12,7°C/25h)
2001	13/01 **(15, 16)**	-0,69 (-5,5°C/08h)
2001	14/01 **(15, 16)**	-0,19 (-3,6°C/19h)
2001	04/02 **(5)**	-0,51 (-7,2°C/14h)
2001	26 - 27/11 **(28)**	-0,36 (12,4°C /34h)
2001	27 - **28/11**	-0,26 (5°C / 19h)

Table 1. ATCR : air temperature cooling rate preceding selected frost cracking events of the 1997 to 2002 period. Frost cracking days in bold.

DEPTH	MIN	MAX	MEAN
0 cm	-28,95	-14,67	-22,65
- 10 cm	-26,38	-14,09	-20,86
- 20 cm	-24,84	-13,21	-19,58
- 30 cm	-24,54	-12,85	-19,06
- 40 cm	-23,83	-12,76	-18,55
- 80 cm	-22,08	-11,67	-17,06
- 120 cm	-20,61	-11,2	-15,88
- 160 cm	-19,1	-1,22	-14,37
- 200 cm	-17,86	-9,57	-13,38
- 300 cm	-15,3	-8,76	-11,74

Table 2. Mean, minimum and maximum daily ground temperatures (°C) at given permafrost depths, during frost cracking days (2000-2002).

Cracking episodes that occurred from 2000 to 2002 had a mean thermal gradient in the active layer (0-40 cm) of 10.9 °C/m that varied from 3.9 to 18.8 °C/m. Deeper down, the mean thermal gradient was 3.34 °C/m (1.1 to 5.5 °C/m) between 40 and 100 cm, 3.12 °C/m (-2.1 to -4.3 °C/m) between 1 and 2 m and 1.64 °C/m (0.7 to 3.25 °C/m) between 2 and 3 m. According to our analysis of the mean ground cooling rate occurring at different depths before frost cracks opened in 2000-2002, the maximum cooling zone was primarily located in the active layer, most of the time being in the upper part close to the surface (table 3). Between 0 and 20 cm, the mean daily ground cooling rate was -0.25 °C/day and varied from -0,1 to -1,1 °C/day. Since the tensile strength of the ice-rich peaty loess is greater than the tensile strength of wedge ice, frost cracks probably initiated at or near the top of permafrost, i.e., the top of the wedges. (Lachenbruch 1962).

DEPTH	MDGCR
Surface	-0.25
10 cm	-0.21
20 cm	-0.19
30 cm	-0.19
40 cm	-0.17
80 cm	-0.15
120 cm	-0.12
160 cm	-0.09
200 cm	-0.09
300 cm	-0.07

Table 3. Mean daily ground cooling rate (MDGCCR; °C/day) at given permafrost depths during frost cracking days (2000-2002).

REFERENCE

Fortier, D. and Allard, M. 2001. Cryostratigraphy and chronology of syngenetic ice wedge polygons, Bylot Island, Canadian Arctic archipelago. Proceedings 31st international Arctic workshop, University of Massachussetts: 31-32.

Lachenbruch, A.H. 1962. Mechanics of thermal contraction cracks and ice wedge polygons in permafrost. Geological Society of America, New-York: 69.

MacKay, J.R. 1993. Air temperature, snow cover, creep of frozen ground, and the time of ice-wedge cracking, western Arctic coast. Canadian Journal of Earth Sciences 30: 1720-1729.

MacKay, J.R. and C.R. Burn. 2002. The first 20 years (1978-1979 to 1998-1999) of ice-wedge growth at the Illisarvik experimental drained lake site, western Arctic coast, Canada. Canadian Journal of Earth Sciences 39: 95-111.

Results of a first study on tree growth and soil characteristics at a cold site located below the limit of discontinuous alpine permafrost

*M. Freppaz, L.Celi, *V. Stöckli and M. Phillips*

Swiss Federal Institute for Snow and Avalanche Research, Davos Dorf, Switzerland and Laboratory Research Center on Snow and Alpine Soils, Italy

**Swiss Federal Institute for Snow and Avalanche Research, Davos Dorf, Switzerland*

INTRODUCTION

Scree slopes with particularly cold ground temperatures at low elevations have been known for centuries in Switzerland. They were termed 'wind holes', 'ice holes' or 'weather holes' by local farmers who recognized the potential of such locations for cooling milk and butter during the hot summer months. The sites are generally steep scree slopes located at the foot of high cliffs.

Studies effected over the past 50 years have demonstrated that the ground is not frozen as a result of a cold microclimate at these locations, but that it occurs due to a particular underground air circulation phenomenon and due to the presence of an insulating vegetation cover (Delaloye and Reynard 2001).

A particularly interesting and important characteristic is that despite their occurrence in montane areas, these sites have subalpine and alpine vegetation, and that some plants, in particular spruce (Picea abies L. Karst) display signs of severely limited growth. The soils generally reveal a high organic matter content, with the formation of a humus mor type at the surface.

In this preliminary study we analyzed the main properties of these cold soils and of tree growth in order to elaborate the first hypotheses about the contribution of soil characteristics to the reduced plant growth.

METHODS

The Creux du Van in the Swiss Jura, at 1200 m a.s.l., where the patches of dwarf trees are especially well developed, was selected as a test site. To compare soil characteristics and tree growth in areas with different evidence of permafrost occurrence the site was divided into two strata, corresponding to the prevailing tree growth form: I) stunted forest, and II) normal spruce forest.

In each of the two strata a spot was selected where a soil profile was dug and tree cores were sampled. The distance between the two sampling points, situated at the same elevation and aspect, was about 50 m.

Around each soil profile in every stratum, three trees of representative sizes were selected. The height of the trees was estimated and the tree stems were cored perpendicular to their axes at heights of 30 cm above the ground. In the laboratory, the wood cores were processed with the usual dendrochronological methods (Schweingruber 1988).

To record soil temperature, thermistors combined with dataloggers (UTL-1) were buried in pairs in the two soil profiles at a depth of about 30 cm (Oa horizon). The loggers recorded the temperature throughout the period November 2001 to November 2002.

The soil pH was determined in a 1:20 soil-water suspension. Total soil carbon and nitrogen were measured using a THERMOQUEST NC 2005 combustion analyzer. The microbial biomass C and N were determined by the fumigation technique. Humic acids (HA) and fulvic acids (FA) were extracted from the soil and the elemental C and N content determined. The N availability was determined by anaerobic incubation of soil samples under water in closed containers at 40°C for 7 days.

RESULTS AND DISCUSSION

The analysis of tree ring patterns revealed that the smallest trees of stratum I exhibit ages around 90 years, despite their small size (mean height = 3 m). Trees in stratum II are distinctly larger (mean height = 25 m), older (124 years) and have much more rapid growth rates.

Soil profiles typically exhibit an upper soil horizon (Oi) of a fibric humus type, an intermediate horizon (Oe) of a hemic humus type and a lower horizon comprising a sapric humus type (Oa), which filled the interstices between blocks of limestone.

According to the thickness of the active layer, estimated at 2 m under the dwarf trees (Delaloye and Reynard 2001), the soil was classified as gelic Histosol (stratum I) (ISSS Working Group RB. 1998). The depth of the active layer under the normal forest was estimated

greater and the soil was classified as sapric Histosol (stratum II).

In both strata the humus type in the Oi and Oe horizons comprises mainly Sphagnum residues, which actively acidify the soil upper horizons and hence are responsible for the low pH (4.2 - 4.3). The pH in the Oa horizon of all three strata is higher than in the upper horizon, reaching values of 7.3 to 7.4.

Mean soil temperature (Oa horizon) between November 2001 and November 2002 (Fig. 1) was higher in stratum II (+3.43 °C) than in stratum I (+2.63 °C) as expected by the depth of the active layer.

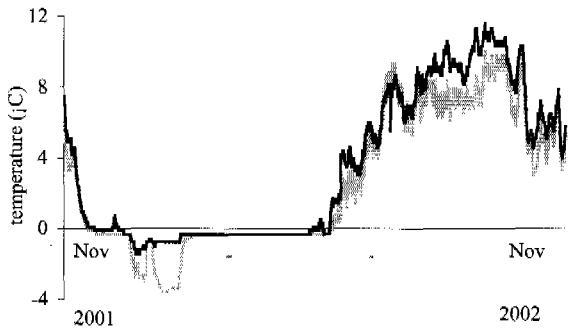

Figure 1. Soil temperature recorded in the two soils (Oa horizon) (stratum I grey; stratum II black) from November 2001 to November 2002. Average values of the 2 loggers in each stratum.

Soil organic matter content is high in both strata, due to the low soil temperature which may have contributed to reducing the C decomposition rate. The Corg and Norg concentrations of the Oa horizon were respectively equal to 382 g C kg-1 and 15.9 g N kg-1 in stratum I and 428 g C kg-1 and 12.9 g N kg-1 in stratum II. In the Oa horizon of stratum I the C and N content of the humic fraction (70.3 g C kg-1; 7.53 g N kg-1) was lower than in stratum II (103.6 g C kg-1; 8.08 g N kg-1), revealing how temperature might affect the biochemical pathways and decomposition in addition to their metabolic rates (Dalias et al. 2001).

The microbial C and N pools are significantly lower in stratum I (1.1 g C kg-1; 0.12 g N kg-1) than in stratum II (17.5 g C kg-1; 2.50 g N kg-1).

The N availability assessed by incubation under anaerobic waterlogged conditions was equal to 29.2 mg N kg-1 in stratum II and 14.8 mg N kg-1 in stratum I. The amount of mineralizable N obtained in stratum II is in the range of values previously determined for coniferous forest soils (Myrold 1987) while in stratum I it is significantly lower, revealing a limited N availability to plants.

From these preliminary results it appears that in stratum I the low soil temperature recorded affects the soil biological activity, influencing the biochemical pathways and reducing the nutrient availability to plants. In stratum II, less affected by frost conditions, the humification process carried out by the microbial biomass is more pronounced and influences the quality of the soil organic matter. The N availability is higher and may contribute to explaining the greater tree growth rate.

To test these hypotheses, and to better understand soil chemical status and plant reaction, further investigations are underway.

REFERENCES

Dalias, P., Anderson, J.M., Bottner, P. and Couteaux, M.M. 2001. Long-term effects of temperature on carbon mineralisation processes. Soil Biology & Biochemistry 33: 1049-1057.

Delaloye, R. and Reynard, E. 2001. Les éboulis gelés du Creux du Van (Chaîne du Jura, Suisse). Environnements périglaciaires (Association Française du Périglaciaire) 8: 118-129.

ISSS Working Group RB. 1998. World Reference Base for Soil Resources. International Society of Soil Science (ISSS), International Soil Reference and Information Centre (ISRIC) and Food and Agriculture Organization of the United Nations (FAO). Report No.84, Rome, 91.

Myrold, D. 1987. Relationship between microbial biomass nitrogen and a nitrogen availability index. Soil Science Society of America Journal 51: 1047-1049.

Schweingruber, F.H. 1988. Tree Rings: Basics and Application of Dendrochronology. D. Reidel Publishing, Dordrecht.

Spatial and temporal observations of seasonal thawing in the Northern Kolyma lowlands

*D. G. Fyodorov-Davydov, V. A. Sorokovikov, A. L. Kholodov, V. E. Ostroumov, S. V. Gubin and D. A. Gilichinski, *N. S. Mergelov, **S. P. Davydov and S. A. Zimov*

Soil Laboratory, Institute of Physicochemical and Biological Problems in Soil Science, Russian Academy of Sciences, Pushchino, Moscow Region, Russia

**Soil Geography Laboratory, Institute of Geography, Russian Academy of Sciences, Moscow, Russia*

***Northeast Science Station, Pacific Ocean Institute of Geography, Russian Academy of Sciences, Far East Branch, Chersky, Russia*

Between 1996 and 2002, 15 sites (100x100 m, Fig. 1) were established in the Kolyma lowlands within an area of 250x300 km for active-layer monitoring (Brown et al. 2000). Eleven of the sites represent different tundra subzones: arctic (Kuropatochya River), typical (Cape Chukochiy, Yakutskoe Lake) and southern tundra (Chukochya River, Alaseya River, Konkovaya River, Segodnia pingo, Ahmelo Lake). The sites differ also in lithology of parent materials, which accounts for the differing appearance of the landscape in various sectors of the region. Observations started at some sites in 1989.

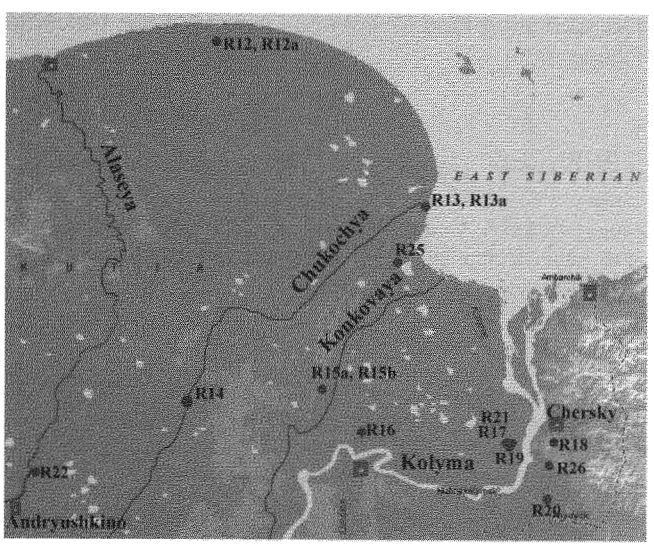

Figure 1. Map of the measurement sites: R12A - Kuropatochya River (top of the Edoma), R12B - Kuropatochya River (slope of the Edoma), R13 - Cape Chukochiy (Edoma), R13A - Cape Chukochiy (alas), R14 - Chukochya River, R15A - Konkovaya River (alas), R15B - Konkovaya River (Edoma), R16 - Segodnya pingo, R17 - Akhmelo Channel, R18 - Mountain Rodinka, R19 - Glukhoe Lake, R20 - Malchikovskaya Channel, R21 - Ahmelo Lake, R22 - Alazeya River, R25 - Yakutskoe Lake.

Ice-rich sediments of the Edoma formation (loess-icy complex) are widespread in these northwestern lowlands. These deposits were subjected to intensive thermokarst development during the Holocene optimum, which has resulted in the creation of deep depressions or alases. Thermokarst, alongside with hydraulic erosion, creates high relief with considerable changes in elevation between watersheds (edomas), alases and river terraces. Moundy micorelief is common on watersheds and slopes. Vegetation is represented by low shrub-grass-moss, grass-moss-dryas or cottongrass-moss-osier associations. The soil cover consists of complexes with typical cryozems [Glacic Haploturbels, Typic Haploturbels] and peaty-weakly gleyic soils [Glacic Aquiturbels, Typic Aquiturbels]. In alas valleys or depressions, various polygonal bogs with peaty-duff [Typic Aquorthels], peaty-gleyic, peat-gley [Typic Aquorthels] and peat [Sphagnic Fibristels, Typic Fibristels, Typic Sapristels] soils are formed.

Ice-poor sand depositions of the Khallerchinskaya tundra (Ahmelo Lake, Segodnia pingo) were also influenced by thermokarst processes. Furthermore, they initially occupied lower hypsometric levels than the Edoma surfaces. All these processes resulted in considerable peneplaneization of the surface, a general landscape waterlogging, with an extremely high abundance of lakes and assoicated migration. Because of the moundy microrelief, higher landscape drainage is common in the southern part of the area. Zonal biogeocenoses on sandy deposits have low mound-hummocky microrelief, low shrub–lichen associations and podzolized podbur [Spodic Psammoturbels] as the zonal soil subtype. Polygonal bogs vegetation is represented by moss, grass-moss and moss-lichen-grassy associations, the soil cover consists of peat-duff or peat-duff-gleyic soils [Psammentic Aquorthels].

The northern taiga subzone is represented by Gluhoe Lake and Mountain Rodinka. Low mound-hummocky nanorelief, low shrub-lichen larch open forests and weakly podzolized sandy podbur [Spodic Psammorthels, Spodic Psammoturbels] are common for the first site; moss-shrub larch open forests and gleyic loamy cryozem [Typic Haploturbels] are formed at the second one.

The Ahmelo and Malchikovskaia Channels sites were established on the floodplains biogeocenoses with high heterogeneity. These sites cover both drained parts of river terraces and different floodplain bogs. On river flood terraces with moundy microrelief, calamagrostis associations and sod-gleyic soils [Typic Umbriturbels] are developed. Among floodplain bogs, sedge-cotton grassy plant

associations with peat-gley soils [Typic Aquorthels] and comarum-sedge associations with peaty-gley soils [Typic Aquorthels] prevail.

The lithology of the parent sediments leads to significant differences in the depth of active layer between the north-east and north-west zonal tundra ecosystems of Kolyma lowland: Dry sands thaw 2-3 times deeper than the moist Edoma loams. The differences are considerable, also for the zonal sandy soils (Ahmelo Lake) and soils of polygonal bogs (Segodnia pingo) (Table 1).

Table 1. The mean depth of active layers for Kolyma lowland sites.

Sites	Years					
	1996	1998	1999	2000	2001	2002
R12A	37	-	-	-	-	-
R12B	27	-	-	-	-	-
R13*	-	-	36	34	38	44
R13A**	-	-	-	31	38	38.5
R14	43	41	38	41	-	-
R15A**	39	25	32	-	36	32
R15B*	38	-	36	-	32	-
R16	38	-	30	-	-	39
R17	44	43	-	45	47	48
R18	45	72	74	75	75	76
R19	72	65	67	72	73.5	78
R20	54	48	52	46	50	47
R21	85	70	83	84	84	91
R22	-	46	46	-	-	50
R25	-	-	23	37	38	47

*- top of the edoma
** - alas.

In tundras of the western part of the Kolyma lowlands, the climatic zonality is given at weekly intervals but still leads to some increase in thaw depths from north to south in soils of watersheds and slopes. In arctic tundras, the mean long-term active-layer depth varied between 32 and 37 cm, in typical tundras between 36 and 38 cm, and in southern tundras between 35 and 47 cm. The comparison of two sites at Cape Chukochiy revealed greater thaw depths on the upland watersheds than on waterlogged alas lowlands. At the same time, in the basin of Konkovaya River, warming effects could be due to a thicker snow cover in winter on the alas than on the watershed.

The soils of floodplains, both at the boundary between tundra and taiga (Ahmelo Channel) and in the northern taiga (Malchikovskaia Channel) differ from zonal soils at the same latitude with a considerably smaller active layer depth.

The 1989-2002 data do not show any directional trends in the changes of the active layer thickness (Fig. 2). However, this relatively long time series indicates the dependence of active layer depths on summer temperature. The increase of thaw depth in the last three years (2000-02) corresponds with high average summer (June-August) temperatures (11.3-12.1°C) at most sites (Table 1). In the years (1998-99) with lower temperatures (8.3-9.8°C) the soil thawed to a considerably shallower depth. This tendency is better expressed for the zonal tundra sites (Cape Chukochiy, Yakutskoe Lake, Alaseya River, Ahmelo Lake) and northern taiga (Gluhoe Lake, Mt. Rodinka) biogeocenoses, and least pronounced for intrazonal ones (Ahmelo Channel, Segodnia pingo). A relation between active layer depth and air temperature at the intrazonal sites of Konkovaya River (alas) and Malchikovskaya Channel is not evident.

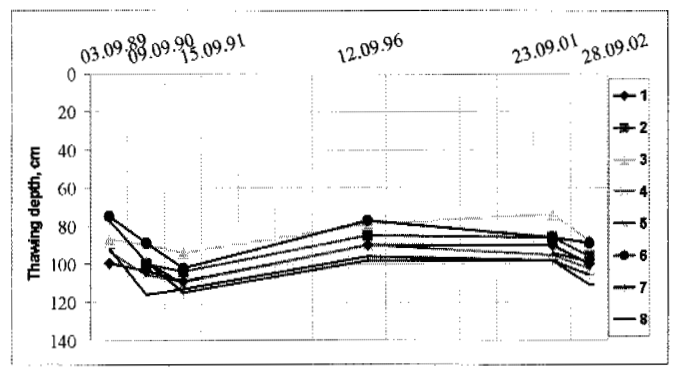

Figure 2. The 1989-2002 changes of the maximal active layer thickness on different microrelief forms (sandy tundra soils at Ahmelo Lake).

ACKNOWLEDEMENT

This report was developed as a result of the CALM synthesis workshop held in November 2002 at the University of Delaware.

REFERENCES

Brown, J., Hinkel K. M. and Nelson, F. E. 2000. The Circumpolar Active Layer Monitoring (CALM) Program: Research Designs and Initial Results. Polar Geography 24 (3): 165-258.

Landscape indication of permafrost degradation in Central Siberia

S.P.Gorshkov and M.A.Tishkova

Moscow State University, Moscow, Russia

One of the systems that is very responsive to climate warming is the periphery of the permafrost zone, i.e., the area of high temperature (– 0.1° - – 1.0°C) permafrost. It is important to know what is happening and what will happen to the permafrost and permafrost landscapes in the coming decades.

During the last 5-6 years the table of high-temperature permafrost in the lower reaches of the Stony Tunguska River has descended 1 m or deeper. Degradation takes place on about 90% of the total permafrost area is in that region.

According to the elaborated classification (Gorshkov, et al., 2003) sensitive, or the least resistant, permafrost is associated with the sites of low top surfaces (altitudes about 200-250 m) and gentle slopes (steepness about 2-3°). The largest areas of such permafrost are situated in the field of Pleistocene moraine and lacustrine-glacial deposits. Both are represented by thin sands, aleurite, loam and clays, sometimes with boulders. These dynamic permafrost landscapes are swampy, with low sparse (canopy 40-50%) cedar pine-spruce taiga forests with some birches and larches, sometimes with firs, on peaty-gley permafrost soils with moss-and-underbrush ground cover and reindeer lichens in places. Solifluction is identified by the presence of tilted trees ("drunken forest") and gaps (so-called "ruptures-windows") of 1-2 meters in diameter and 0.5-0.6 meters in depth, which disturb the turf-plant layer. Usually gaps are filled with water during warm periods and have a viscous-flow clay mass at the bottom. Almost all above-mentioned landscape features are also typical to the areas covered by birch forests. One important difference is the distribution of trees. Two, three, four, sometimes five or six and even seven-eight birches from 8 to 15 meters high grow together like big bushes. They alternate with small wet lawns.

At the end of the summers of 1995-1997, the thickness of the active layer was not more than 0.8-1.0 m in the mentioned landscapes. But during the same period of 2002 it was about 1.2-1.5 m and sometimes 1.9 m and deeper. The gaps were mostly without water. The rate of active layer thickness increase is estimated to be 10-15 cm/year during 1998-2002. Sites of heat-deficient slopes, glaces, and glacis floodplains are characterized by the presence of more resistant permafrost. Under forest vegetation at these sites we observed the permafrost table at a depth of 0.5-0.8 m. We suppose that the active layer thickness increased not more than 0.2-0.3 m during last four years. More pronounced changes occurred in areas located near thermokarst ponds and where forests or dense bush groves are absent. In the first case the permafrost table is located at a depth of 1.0 and 1.3 m underneath holes and hummocks. In the second case geocryological changes have not been so significant.

Three types of permafrost sites are the most resistant. These include kurums and «hanging» peat bogs of heat-deficient slopes, as well as forested floodplains of major rivers.

Figure 1. Overgrowing kurum edge on the left slope of the Rybnaya River valley in its middle reaches

Kurums could probably be transferred to the previous category (Fig. 1). An increasing number of blocks in unstable positions is typical for kurums. Furthermore, many blocks and spaces between them are being covered with lichens. Water, which flowed at the base of the block horizon has disappeared. The cold air between the blocks became warmer. It seems that during the last several years a lowering of the permafrost table took place at kurum

sites. Perhaps ice disappeared from the base of kurums in some places.

The geocryological situation remains without apparent changes at hanging bog sites. The position of the permafrost table is approximately at the former level: about 0.4-0.5 meter under holes and 0.7-0.8 m under hummocks.

Permafrost is most stable at sites of boggy forested flood-plains in the largest river valleys of the region. This was proved by the investigations carried out in the valleys of Kulinna, Stolbovaya, Vorogovka and Stony Tunguska rivers (Fig 2). At these sites the depth of permafrost table is about 0.2-0.3 m under holes and reaches 0.4-0.5 m under hummocks.

Figure 2. Floodplain under birch taiga on peaty-boggy permafrost soils on the left bank of the Stolbovaya River in its lower reaches. Several trees have been tilted under the impact of ice drift during the flood in the spring of 2002.

Thus the following processes can be singled out as likely responses to climate warming:

1) increase of the active layer thickness and intensification of solifluction processes;
2) local replacement of solifluction processes by landslide mass movement in the areas of active river erosion;
3) frequent falling of trees with creeping root system. This usually happens where the hydromorphic clays having a viscous-plastic consistence reach a thickness of about 1.5 m or more
4) presence of trees with bent trunks and vertical tops;
5) improvement of drainage on top surfaces and adjacent gentle slopes (water disappeared from rupture-windows; it is often absent in fissures-ruptures);
6) increase in the number of blocks in unstable positions on the surface of kurums as well as of size and number of reindeer moss patches;
7) exhaustion of ground rills under block cover of kurum
8) signs of noticeable warming thoroughly of underground kurum space after water supplying decrease;
9) possible lowering of the permafrost table in kurum stows;
10) intensification of thermokarst processes;
11) wide development of long-frozen rocks which can indicate recent permafrost degradation in places;
12) occurrence of young fir-tree stands within burnt areas previously covered with different coniferous species.

During the last few years, a considerable increase in active layer depth has occurred in the permafrost landscapes of Central Siberia. Degradation takes place on about 90% of the permafrost area in the region.

Intensification of solifluction and thermokarst is associated with this process as well as transformation of kurums. Degradation of high temperature permafrost is possible in places. However, several types of sites which are most resistant to global warming do not show clear responses to current climate change. Nevertheless the above-mentioned processes, particularly solifluction, can be considered as "trigger" mechanisms representing a large-scale response to global warming in the studied region.

ACKNOWLEDGEMENT

This research is carried out within the framework of RFBR project 05-01-64901.

REFERENCE

Gorshkov, S., Vandenberghe, J., Alexeev, B., Mochalova, O. and Tishkova, M. 2003. Climate, permafrost and landscapes of middle yenisei region. Faculty of Geography of M.V.Lomonosov Moscow State University, Moscow, (In Russian and in English).

New permafrost studies at Lake Hövsgöl, north-central Mongolia

*C. Goulden, *N. Sharkhuu, Ya. Jambaljav, **B. Etzelmüller, E. S.F. Heggem, ***V. Romanovsky, ****R. Frauenfelder, A. Kääb, *****L. Ariuntsetseg, N. Saruul and S. Tumentsetseg*

Mongolian Institute, Academy of Natural Sciences, Philadelphia, U.S.A.

**Institute of Geography, Mongolian Academy of Sciences, Ulaan Baatar, Mongolia*

***Department of Physical Geography, University of Oslo, Oslo, Norway*

****Geophysical Institute, University of Alaska, Fairbanks, U.S.A.*

*****Glaciology and Geomorphodynamics Group, Department Geography, University of Zurich, Zurich, Switzerland*

******Hövsgöl GEF project, Geoecology institute, Mongolian Academy of Sciences, Ulaan Baatar, Mongolia*

Lake Hövsgöl in northern Mongolia occupies a north-south aligned tectonic basin at the southern end of the Baikal Rift System at an elevation of 1645 m, in a biogeographic and ecological transition zone from taiga forest to steppe and at the southern edge of the continuous permafrost zone (Fig. 1). Hövsgöl is a Mongolian Long Term Ecological Research network site (Goulden et al. 2000). In 2002 a research program funded by a five-year grant from the Global Environment Facility to the Geoecology Institute of the Mongolian Academy of Sciences was initiated to define the impacts of deforestation, nomadic pasture use, and climate change on soil and permafrost conditions, and plant and animal diversity. Analysis of long-term temperature data from the Hatgal meteorological station at the south end of the Lake indicates that annual temperatures have warmed by about 1.5 °C since 1963.

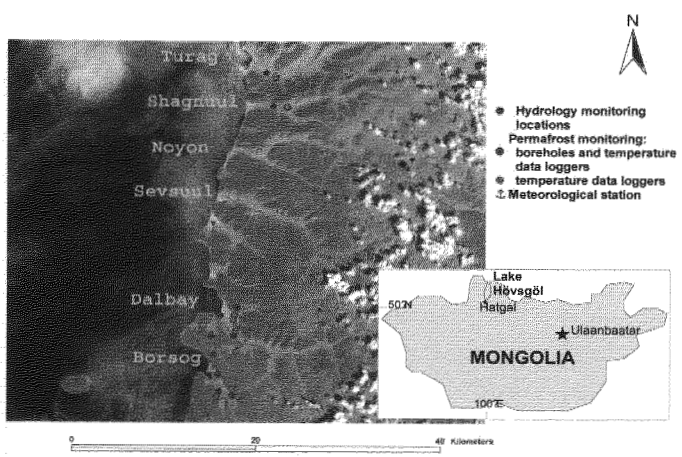

Figure 1. Key map and study area of Lake Hövsgöl GEF monitoring and research valleys. The area lies on the eastern shore of the lake.

Six valleys along the northeastern shore of the Lake have been selected for study, ranging from the heavily grazed northern valleys, Turag (51° 17'46" N, 100°47'51"E) and Shagnuul, south of Hanh, Noyon and Sevsuul with moderate grazing, and Dalbay and Borsog (50°58'24"N, 100°44'54"E) valleys in the south with little or no grazing pressure (Fig. 1). This gradient of pastoral use allows us to define impacts of climate change in the south, and its combined effects with pastoral use in the north on biodiversity and ecosystems. The valleys have a similar alignment, flowing from east to west, with north-facing forested slopes covered by larch (*Larix sibirica*) and south-facing mixed forest and steppe slopes and steppe valley bottoms. Two meteorological stations monitor climate conditions, one in Dalbay Valley, and the second at Hatgal.

The goals of the permafrost studies are to define the distribution and temperature of permafrost, the depth of active layers in detail, and begin a monitoring program of soil and permafrost temperatures in each of the valleys. In June 2002, N. Sharkhuu drilled six boreholes to a depth of six meters at different topographic locations in the Borsog and Dalbay valleys. In late August to early September 2002, studies of the distribution of permafrost and active layer depths were initiated, and temperature data loggers were placed in two watersheds to add to information gained from boreholes for monitoring soil and permafrost temperatures in the study area (Fig. 1, Etzelmüller et al. 2001).

Sandy soils dominate on slopes but thick sequences of lake sediment layers cover the valley bottoms. 1D resistivity soundings were carried out at four sites, and 2D resistivity tomography at ten sites in the field. Resistivities were generally low, calibration with borehole temperatures indicate permafrost conditions at resistivities close to 1 kΩm, while ice-rich sediments in the valley bottoms showed resistivities up to 10 kΩm. The results have shown that permafrost occurs on north-facing slopes and in valley bottoms. Permafrost thickness in the valley bottoms is estimated to be between 10 and 15 m, while active layer thickness was around 3-5 m on dry locations and down to below 1 m in wet, vegetation-covered sites. South-facing slopes have little or no permafrost. In valleys where intense grazing occurs, soils are very dry, resulting in relatively high resistivities even in the active layer. In these

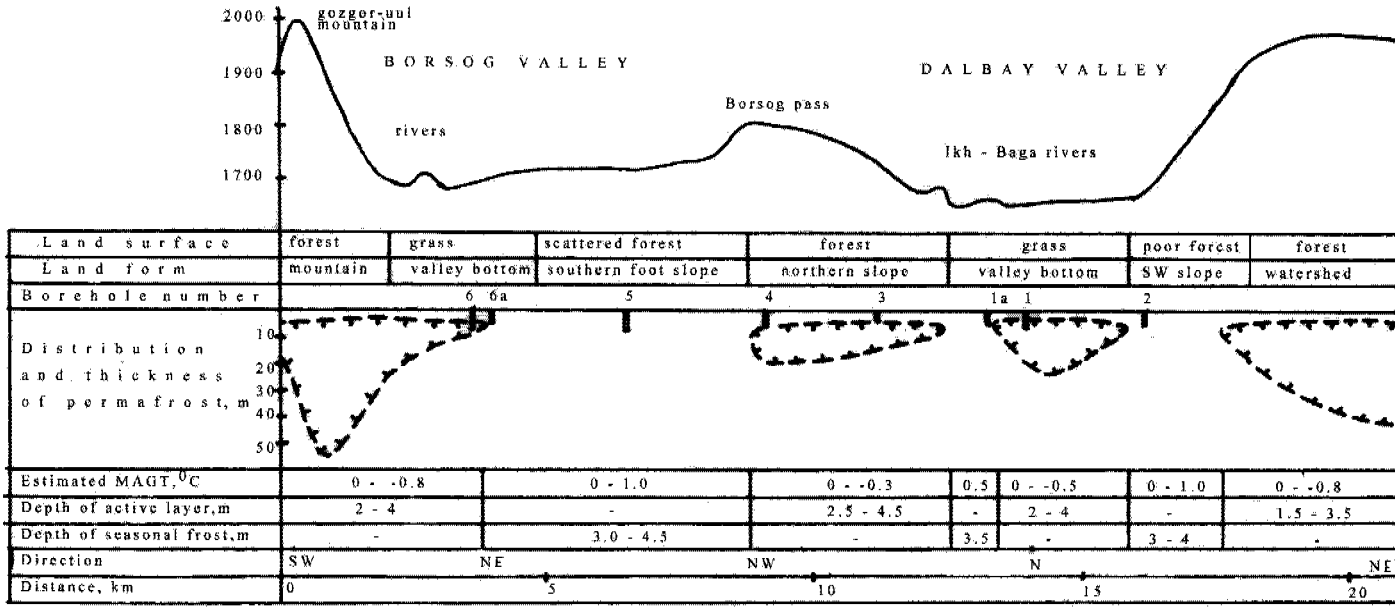

Figure 2. Preliminary permafrost profile of Borsog and Dalbay valleys, Lake Hövsgöl, northern Mongolia (from N. Sharkhuu). For an overview of recent permafrost changes in Mongolia, see Sharkhuu (2003).

areas, more borehole information is required; additional boreholes will be drilled in early 2003 (Fig. 2).Two MRC soil temperature measurement probes were installed at the two meteorological stations, one on the north-facing slope in the Dalbay River valley, and the other at the Hatgal meteorological station. These temperature probes will provide year-round hourly soil temperature data at eleven different depths (approximately every 10 cm), starting at the ground surface and down to one meter. These data, together with temperature data from the deeper boreholes, will be used for calibration of a numerical thermal model developed by the Permafrost Lab, Geophysical Institute, UAF (Romanovsky et al. 1997, Romanovsky and Osterkamp 2001). The site-specific calibrated models will be applied to the entire period of available meteorological data from this region to reconstruct the permafrost temperature dynamics within different landscape units.

Transects for the study and monitoring of plant taxa and biomass growth, terrestrial insects, birds, mammals, and stream flow, water chemistry and aquatic biology have been set across each valley and longitudinally along the streams. Detailed studies in Borsog Valley show that increased soil moisture occurs on lower slopes associated with permafrost and plant and insect taxa and biomass vary with soil moisture. In Turag and Shagnuul with very dry soil, grazing may have affected permafrost conditions, plant biomass is low but plant taxa number is high apparently due to an increase in the number of xerophytic plant taxa. Experimental studies will begin in 2003 to study the impact of plant cover on soil and permafrost temperature.

REFERENCES

Etzelmüller, B., Hölzle, M., Soldjørg Flo Heggem, E., Isaksen, K., Mittaz, C., Vonder Mühll, D., Ødegard, R. S., Haeberli, W. and Sollid, J. L. 2001. Mapping and modeling the occurrence and distribution of mountain permafrost. Norsk Geografisk Tidskrift, 55(4): 186-194.

Goulden, C. E., J. Tsogtbaatar, Chuluunkhuyag, W. C. Hession, D. Tumurbaatar, Ch. Dugarjav, C. Cianfrani, P. Brusilovskiy, G. Namkhaijantsen and R. Baatar. 2000. The Mongolian LTER: Hövsgöl National Park. Korean J. Ecol. 23:135-140.

Romanovsky, V.E., Osterkamp, T.E. and Duxbury, N. 1997. An evaluation of three numerical models used in simulations of the active layer and permafrost temperature regimes, Cold Regions Science and Technology. 26 (3): 195-203.

Romanovsky, V. E. and Osterkamp, T. E. 2001. Permafrost: Changes and Impacts, in: R. Paepe and V. Melnikov (eds.), Permafrost Response on Economic Development, Environmental Security and Natural Resources, Kluwer Academic Publishers: 297-315.

Sharkhuu, N. in press. Recent changes in the permafrost of Mongolia. Proceedings, 8th International Conference on Permafrost. Zurich, Switzerland.

Snow-free ground albedo derived from DAIS 7915 hyperspectral imagery for energy balance modeling in high-alpine topography

*S. Gruber, *D. Schläpfer and M. Hoelzle*

Glaciology and Geomorphodynamics Group, Department of Geography, University of Zurich, Switzerland

**Remote Sensing Laboratories, Department of Geography, University of Zurich, Switzerland*

INTRODUCTION

In alpine topography, air temperature, solar radiation, snow cover height and duration exhibit a strong lateral variability. Statistical models (e.g. Gruber and Hoelzle 2001) are only partially able to approximate these processes with a limited number of input variables such as mean annual air temperature and simulated solar irradiation. Physically-based distributed modeling of the vertical energy balance can realistically simulate complex interactions of several variables as demonstrated by Stocker-Mittaz et al. (2002). Their model PERMEBAL simulates the daily vertical energy balance, based on ground characteristics and meteorological time series. The required base data such as albedo, emissivity and roughness length is needed for every grid cell and must therefore be measured or accurately estimated. During snow-free conditions in summer when energy input to the ground is largest, the daily albedo mean is nearly constant. Remote sensing is the only way to provide corresponding spatial data fields. This study uses imaging spectrometry together with geo-atmospheric correction techniques to measure albedo in a complex topography. The test site is the Corvatsch area, Upper Engadin, Switzerland, where the model PERMEBAL was developed.

METHODS AND MEASUREMENTS

Albedo is defined as the ratio of outgoing over incoming radiation and, for climatological purposes, it is usually considered in the wavelength interval of about 300 to 2500 nm, outside of which solar irradiation is small. For periglacial surfaces without snow cover, albedo usually lies between 0.1 and 0.3. In the determination of albedo with remote sensing, ground reflected radiance as well as irradiance needs to be quantified. As a consequence, a well-known and well-calibrated sensor is needed together with accurate characterization of the atmosphere and solar illumination geometry. Because of the high spatial variability of surface characteristics and illumination, all auxiliary and image data must be accurately referenced.

In a raw image, sun-exposed slopes will generally appear brighter than other areas. Haze in a valley may lighten-up the valley bottom. However, these differences largely reflect the influence of atmospheric and illumination conditions but not the surface property under investigation. The geo-atmospheric correction needs to account for this effect and convert an at-sensor radiance image to reflectance. However, this reflectance (i.e. hemispherical-directional reflectance factor, HDRF) is still not suitable to describe albedo because the reflectance of natural objects usually exhibits a pronounced angular anisotropy. It is mathematically described by the bi-directional reflectance distribution function (BRDF). Multiangular observations of a target and the use of a BRDF model is necessary to quantitatively take into account angular anisotropy. Alternatively, BRDF effects can be corrected using empirical models. Both approaches are used in this study to derive spectral albedos for each band. Broadband albedo can then be calculated by spectral integration.

On 14 August 2002, the test area was covered by three flight lines of the imaging spectrometer DAIS7915 under cloud-free conditions. The airborne DAIS7915 sensor has 72 bands between 500 and 2500 nm and seven additional infrared bands.

PROCESSING AND RESULTS

The system calibrated data has been geometrically corrected using the software PARGE (Schläpfer & Richter, 2002). Aircraft position and attitude as well as a digital elevation model are used to reconstruct the ground-sensor geometry and precisely locate individual pixel footprints. The final pixel size is 10 m and the standard errors in horizontal accuracy were below 5 m. Atmospheric correction has been performed for the image bands between 500 and 2500 nm wavelength using the software package ATCOR4 (Richter and Schläpfer 2002). The effects of path radiance, transmittance and direct and diffuse solar flux in complex topography are accounted for.

In one experiment, the BRDF effect is empirically corrected based on illumination geometry and using the algo-

rithm provided by ATCOR4. The correlation between solar illumination intensity and the derived albedo serves as a means to evaluate the removal of topographic effects as, in theory, they should be virtually independent. Figure 1 demonstrates the success in removing the effects of illumination and BRDF. The analysis is based upon 56,000 pixels of periglacial surfaces without snow. During this empirical correction, however, the quantifiable physical basis for the albedo product is lost. A comparison with field measurements from one site gives good agreement, 280 pixels on the Murtèl rock glacier had an albedo of 17.1 ± 1.4% and the snow-free albedo derived from a CM3 pyranometer (0.3 - 3 µm) is 17% (Stocker-Mittaz et al. 2002).

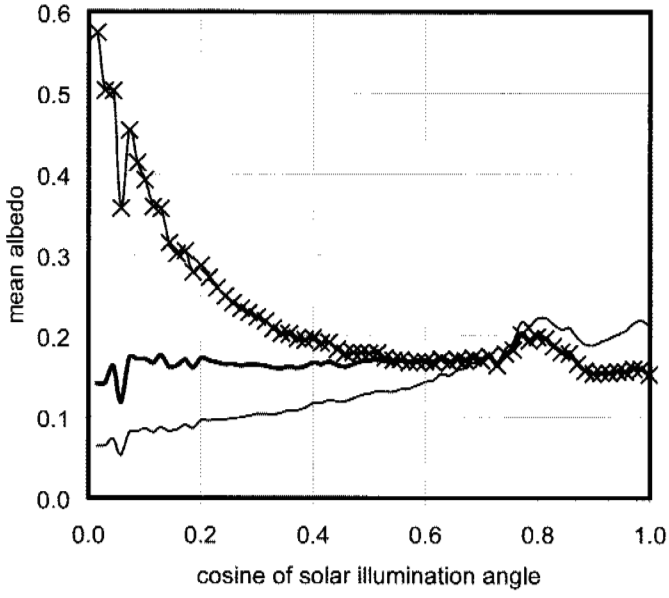

Figure 1. Dependence of albedo on solar illumination without topographic correction (thin line), with topographic correction (crosses) and with topographic correction and empirical BRDF compensation (thick line).

In a second experiment (see Gruber et al. 2003 for details) a BRDF model was fitted to the data and the effects of angular anisotropy were explicitly corrected. The parameterization of albedo by a BRDF model provided the opportunity to investigate the influence that angular anisotropy has on the net short-wave radiation in a complex terrain. This was achieved by coupling the energy-balance model PERMEBAL to a BRDF-based model of albedo. Using meteorological data of the Corvatsch area, direct and diffuse downwelling short-wave radiation as well as solar incidence angles were parameterized hourly for the entire year 1999. Slope angles between 0 and 50° north- and south facing were simulated. The solar incidence angle and the ratio of diffuse and direct radiation served as input for the parameterization of albedo. The diurnal variation of albedo measured by the climate station could successfully be reproduced using this combination of remote sensing data and PERMEBAL. Unfortunately, the accuracy of the derived albedo is between 15 and 25%, only. It was demonstrated that the same surface material has a distinctly different albedo on slopes of different orientation due to the dependence of albedo on solar incidence angles. This difference is up to 25% and, therefore, an angular parameterization of albedo should be considered in complex terrain for accurate models of net short-wave radiation.

CONCLUSION AND OUTLOOK

The derivation of accurate albedo in complex terrain is still subject to large errors, especially because of the difficulty to quantify the BRDF for each pixel. The dependence of albedo on solar incidence angle can lead to distinctly different albedo values for the same surface in differing topographic situations. This makes research into angular anisotropy of albedo especially interesting for energy-balance modeling in complex topography. The variability ranges of albedo as well as the achieved benefit to model accuracy can now be assessed based on the data generated in this project. The two BRDF corrections using an empirical model and a BRDF model can be compared. Furthermore, the data generated in this campaign will be used to assess the error inherent in derivations of albedo from operational orbiting satellites such as Landsat, SPOT or ASTER.

ACKNOWLEDGEMENTS

This work has been supported by the Swiss National Science Foundation project "Analysis and Spatial Modelling of Permafrost Distribution in Cold-Mountain Areas by Integration of Advanced Remote Sensing Technology". The EU-funded project HySens gave additional support.

REFERENCES

Gruber, S. and Hoelzle, M. 2001. Statistical Modelling of mountain permafrost distribution - local calibration and incorporation of remotely sensed data. Permafrost and Periglacial Processes 12(1): 69-77.

Gruber, S., Schlaepfer, D. and Hoelzle, M. 2003. Imaging Spectrometry in High-Alpine Topography: The Derivation of Accurate Broadband Albedo. Proc. the 3rd EARSeL Workshop on Imaging Spectroscopy, Oberpfaffenhofen, May 13-16 2003.

Richter, R. and Schläpfer, D. 2002. Geo-atmospheric Processing of Airborne Imaging Spectrometry Data Part 2: atmospheric/topographic correction. International Journal of Remote Sensing 23: 2631-2649.

Schläpfer, D. and Richter, R. 2002. Geo-atmospheric Processing of Airborne Imaging Spectrometry Data Part 1: Parametric Orthorectification. International Journal of Remote Sensing 23: 2609-2630.

Stocker-Mittaz, C., Hoelzle, M. and Haeberli, W. 2002. Modelling alpine permafrost distribution based on energy-balance data: a first step. Permafrost and Periglacial Processes 13(4): 271-282.

Permafrost conditions in the starting zone of the Kolka-Karmadon rock/ice slide of 20 September 2002 in North Osetia (Russian Caucasus)

*W. Haeberli, C. Huggel, A. Kääb, *A. Polkvoj, **I. Zotikov and **N. Osokin*

Glaciology and Geomorphodynamics Group, Department of Geography, University of Zurich, Switzerland

**Geological Survey, Environment Department, North Osetia, Vladikavkas*

***Russian Academy of Sciences, Moscow*

On the evening of 20 September 2002, a large rock/ice slide took place in the norh-northeast wall of the summit of Dzhimarai-khokh, northern slope of the Kazbek massif, Northern Osetia, Russian Caucasus. Large parts of the debris covered Kolka Glacier at the foot of the slope sheared off as a consequence of the main impact and enlarged the initially detached mass by about 60 million m^3 of snow/firn/ice, debris, morainic material and water. After sliding down at an average speed of about 200 km/h along a path of 18 km, the moving mass was strongly compressed at the narrow entrance of the Genaldon gorge (ca. 1300 m a.s.l.), ejecting a mudflow which continued for another 15 km into the Giseldon valley. The compressed avalanche deposit dammed local rivers and led to the formation of several lakes. The largest of these lakes inundated parts of the village of Saniba at the orographic right valley side near Karmadon and constituted a growing threat to the population of the downvalley town of Gisel (Kääb and others 2003, Popovnin and others in press).

The situation necessitated the immediate establishment of an observation/alarm system at the dammed lakes in order to protect downvalley settlements from potential floods and avoid unnecessary evacuation or uncontrolled reactions of inhabitants. At the same time, the potential for an immediate repetition of similar or even larger accidents from the mountain slope had to be assessed. This involved interpretation of photographs collected by the authorities during reconnaissance flights by helicopter together with some best-guesses about thermal aspects related to firn, ice and permafrost conditions in the starting zone. The fact that two large slides from the same slope but with considerably shorter runout distances had occurred in 1902 – almost exactly 100 years ago – constituted an important aspect of this assessment.

The avalanche starting zone as depicted in Figure 1 was approximately 1 km wide and was located between about 4300 m and 3500 m a.s.l. A roughly estimated total of some 4 million m^3 of steeply inclined metamorphic rock layers were detached to a depth of about 40 m, entraining a similar thickness/volume of snow, firn and glacier ice. The dip of the bedrock layers, as visible in the detachment zone after the event, was less than the inclination of the now-exposed slope surface: outcropping of steeply inclined bedrock layers in the lower part of the affected slope (arrow in Fig. 1) could have constituted an important geological influence on stability conditions. The primary cause of the instability must have been within bedrock rather than surface ice. As bedrock stability can be especially low in warm or degrading permafrost (Davies and others 2001), thermal conditions affecting ice and water within rock fissures are likely to have exerted major and detrimental influence.

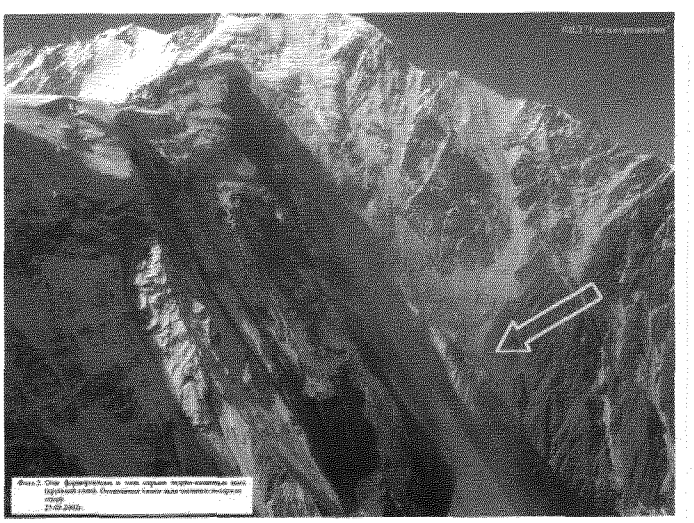

Figure 1. Starting zone of the Kolka-Karmadon rock/ice slide in the north-northeast wall of the summit of Dzhimarai-khokh. Arrow points to steeply inclined bedrock layers.

A weather station near Karmadon was run between 1962 - 1987, showing a mean annual air temperature (MAAT) of 5.9°C. Assuming a warmer recent MAAT of about 7°C at 1300 m a.s.l., and a MAAT-lapse rate of 0.6 ± 0.1°C/100m, present-day mean annual air temperature can be estimated at -6 ± 2°C at the lower and -11 ± 3°C at the upper end of the detachment zone. The existence of active rock glaciers in the region (Fig. 2) indeed confirms that the lower boundary of discontinuous mountain per-

mafrost is around 2500 m a.s.l., where MAAT is slightly below 0°C. Direct minilogger measurements in the Alps (Gruber and others 2003) indicate that mean annual rock temperatures tend to be somewhat higher than air temperatures extrapolated from weather stations. This effect, however is to some degree compensated for by the fact that the affected slope is oriented away from the sun and hence will be colder than average. In the absence of any direct measurements or numerical model results, bedrock surface temperatures in the detachment zone may be estimated at about -5 to -10°C, indicating bedrock conditions of cold permafrost after the event.

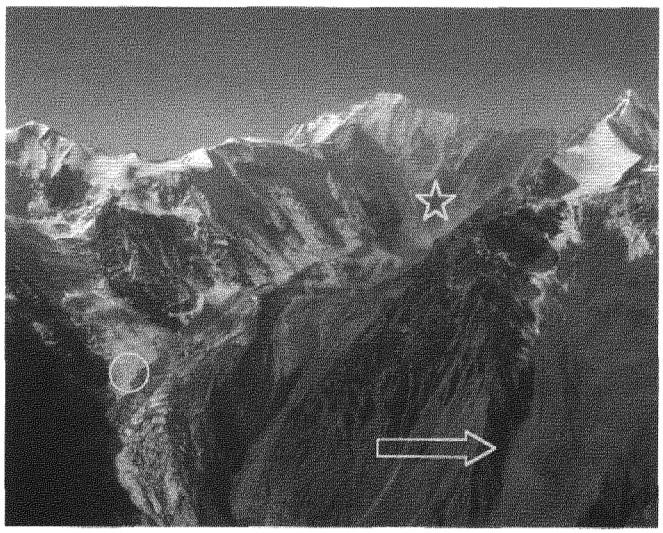

Figure 2. Upper avalanche path of the Kolka-Karmadon rock/ice slide, the summit of Dzhimarai-khokh and the detachment zone are in the background. An active talus-derived rock glacier (arrow) is seen in the lower right corner. Note steam/dust (?) cloud at the foot of the slope where Kolka glacier has been sheared off (star) and overriden tongue of Maili glacier (circle). Kazbek volcano would be to the left.

During the years before the event, the slope had been covered by a number of well-developed, spectacular hanging glaciers. Such firn/ice bodies are known to have a complex distribution of englacial temperatures: while vertical/impermeable cliffs, where ablation takes place through ice breaking off, can be as cold as the surrounding bedrock, permeable firn layers underneath the less inclined upper surface with snow accumulation are strongly warmed up by latent heat from percolating and refreezing meltwater. In areas with MAAT exceeding -10 to -12°C, firn is usually temperate and the ice/bedrock interface behind the cold cliff remains at phase equilibrium temperature, a pattern, which introduces deep-seated thermal anomalies within the underlying bedrock (Haeberli and others 1997). It is, therefore, highly probable that the detachment zone at Dzhimarai-khokh was in a complex condition of relatively cold/thick permafrost combined with warm if not unfrozen parts and meltwater flow in very steeply inclined materials with most heterogenous permeability. This situation favouring high and strongly variable water pressures was further complicated by the fact that hot springs are known to occur in this volcanic region of the Kazbek massif: the steam/dust (?) clouds visible on most photographs, and the strong sulphur odour mentioned by reconnaissance teams, documents that thermal water surfaces in the critical zone.

The answer to the question about the potential for an immediate repetition of a similar or even larger event was based on the facts that (1) the elimination of hanging glaciers with warm firn areas had reduced the load on the slope and eliminated the main meltwater source, (2) the exposed bedrock would now be subject to strong cooling and deep freezing, (3) the sheared-off ice/debris volume of Kolka glacier had made large mass increase at the foot of the slope impossible and (4) the path of the 20 September event with its heavy destruction was practically inaccessible anyway. It was concluded that the threat from a possible repetition at the same site and in the immediate future of an even bigger accident could be considered minimal but that instabilities in the remaining parts of the slope could continue and should be observed accordingly. The build-up over long time intervals of hanging glaciers with complex thermal conditions, in combination with thermal water in the region and the specific geological setting (steeply inclined rock layers, volcanic/geothermal processes), could explain the "quasiperiodicity" of events at a century time scale. Effects of potential future atmospheric warming would also have to be taken into account for the coming decades.

ACKNOWLEDGEMENT

The presented work resulted from collaboration with the the Government of North Osetia and the Academy of Sciences, Moscow, as part of a project directed and funded by the Swiss Development Corporation - Humanitarian Aid.

REFERENCES

Davies, M., Hamza, O. and Harris, C. 2001. The effect of rise in mean annual air temperature on the stability of rock slopes containing ice-filled discontinuities. Permafrost and Periglacial Processes 12: 137-144.

Gruber, S., Peter, M., Hoelzle, M., Woodhatch, I. and Haeberli, W. 2003. Surface temperatures in steep Alpine rock faces - a strategy for regional-scale measurements and modelling. Proceedings of the 8th International Conference on Permafrost, Zurich, Switzerland.

Haeberli, W., Wegmann, M. and Vonder Mühll, D. 1997. Slope stability problems related to glacier shrinkage and permafrost degradation in the Alps. Eclogae geologicae Helvetiae 90: 407-414.

Kääb, A., Wessels, R., Haeberli, W., Huggel, C., Kargel. J.S. and Khalsa, S.J.S. 2003. Rapid Aster imaging facilitates timely assessments of glacier hazards and disasters. EOS 13/84: 117, 121.

Popovnin, V.V., Petrakov, D.A., Toutoubalina, O.V. and Tchernomorets, S.S., 2003. Catastrophe glaciaire 2002 en Ossetie du Nord. Unpublished french translation, original article to appear in Earth Cryosphere VII (1).

The thermal regime of the coarse blocky active layer at the Murtèl rock glacier in the Swiss Alps

S. Hanson and M. Hoelzle

Glaciology and Geomorphodynamics Group, Department of Geography, University of Zurich, Switzerland

Energy balance measurements on the Murtèl rock glacier in the Upper Engadine in the Swiss Alps have shown that the sum of all measured components indicate a non-zero energy budget (Mittaz et al. 2000). This pattern was seen both in 1997 and in 1998 with positive deviations in the winter months and negative deviations during the summer. Already at this time it was suggested that the imbalance of the energy exchange fluxes may be explained by unmeasured advective energy fluxes within the active layer. Furthermore, a de-coupling between the surface temperature and the temperature within the active layer of the rock glacier was recognized which does support this interpretation.

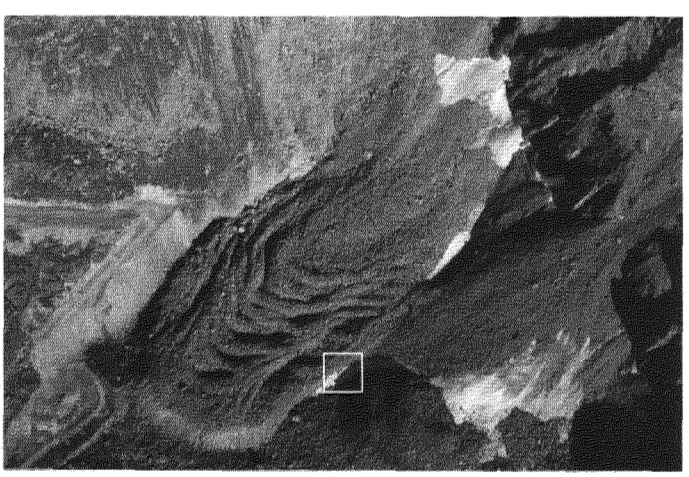

Figure 1. The Murtèl rock glacier. The square indicates the position of the measuring site. Photo: C. Rothenbuehler

The existence of permafrost in the Alps is strongly influenced by incoming short-wave radiation and snow cover thickness and durations. Prediction of present and future permafrost distribution in the Swiss Alps is based mainly on the prediction of the extent of these factors. However, the above-mentioned result may indicate processes related to permafrost conditions, especially in coarse blocky material, that are not fully accounted for today and could be important in coupling the atmosphere to the ground when applying climate change scenarios.

Haeberli (2000) stated that due to pronounced lateral energy fluxes in inclined active layers consisting of coarse blocks, pronounced differences can exist between mean annual temperatures at the surface and at the permafrost table, respectively. Harris and Pedersen (1998) suggest that the air moving through the voids between the large blocks play a significant role in modifying the thermal regime of the blocky surface material. They showed, like Humlum (1997), how the active layer protects the permafrost core acting like a thermal filter when snow cover is thin or absent and low wind speeds prevail. The summer warming of the permafrost surface is prevented by the trapped cold air between the boulders in the active layer to the benefit of the permafrost. Furthermore evaporative cooling in summertime keeps the temperature in the active layer low. A reverse of these processes caused by an abrupt increase in air temperatures within the active layer has also been reported. Humlum (1997) pointed out the scenario with high wind speed and absence of snow cover where forced ventilation caused by wind pumping disturbs the pattern and an introduction of relatively warm air can have a deepening effect on the active layer. Latent heat release caused by refreezing of meltwater during spring can possibly also play an important role in heating up the active layer.

The importance of each of these non-conductive processes is highly dependent upon local site conditions and is also highly variable. Many of the non-conductive processes are seasonal and effective only during periods of phase changes when the driven gradient near the ground surface is relatively large. In the context of global warming, a better understanding of the non-conductive processes in the active layer of alpine permafrost and how these are related to seasonal alterations is required in order to comprehend and anticipate the influence of climate changes in the Alps.

The year 2002 featured two very different cold periods with snow cover. The winter of 2001/2002 was very cold and dry. The snow did not arrive before late January 2002 and the snow cover was thin and discontinuous. This led to open voids between the boulders during the whole winter, allowing free connection between the atmosphere

and the active layer. The winter of 2002/2003 started already in October 2002 with heavy snowfall that covered the blocky surface completely with several meters of snow that lasted the year out. The thick snow cover sealed off any exchange between the active layer and the atmosphere. These two situations give an unique opportunity to compare two extreme conditions on the snow cover's influence on the processes governing the energy fluxes in the active layer.

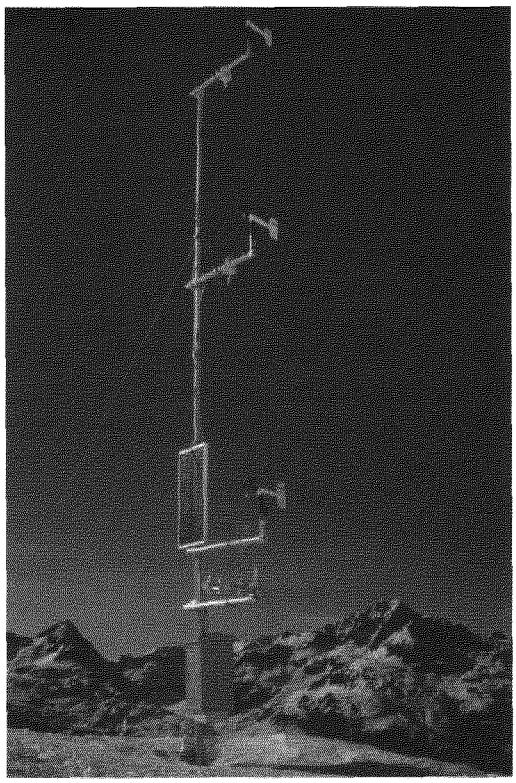

Figure 2. The energy balance climate mast on the Murtèl rock glacier. Photo: M. Hoelzle.

The aim of this project is to discuss the thermal regime of an active layer at a high resolution in a coarse bouldery environment in an alpine discontinuous permafrost setting. A fully-equipped energy balance station has been logging data every 30 minutes at the Murtèl rock glacier during the entire year of 2002. In the same period, seven thermistors placed within the active layer of the rock glacier were measuring temperatures at a 5-minute scale. Two of these thermistors were measuring the air temperature between the blocks. The remaining five thermistors were drilled into the blocks. With the comparison of the meteorological observations and the recorded temperature within the active layer, a discussion is presented and data provided of the processes that govern the state of the active layer. Indications of non-conductive processes are analyzed in detail with the temperature gradient within the active layer, and the cumulative daily heat accumulation at the surface and within the active layer itself.

REFERENCES

Haeberli, W. 2000. Modern research perspectives relating to permafrost creep and rock glaciers: a discussion. Permafrost and Periglacial Processes 11: 290-293.

Harris, S. A. and Pedersen, D. E. 1998. Thermal regime beneath coarse blocky material. Permafrost and Periglacial Processes 9: 107-120.

Humlum, O., 1997: Active layer thermal regime at three rock glaciers in Greenland. Permafrost and periglacial processes, 8: 383-408.

Mittaz, C., Hoelzle, M. and Haeberli, W. 2001. First results and interpretation of energy-flux measurements of Alpine permafrost. Annals of Glaciology 31: 275-280.

Detection of permafrost structure by transient electromagnetic method in Mongolia

*K. Harada, *K. Wada and **M. Fukuda*

Miyagi Agricultural College, Sendai, Japan

**Mitsui Mineral Development Engineering Co., Ltd., Tokyo, Japan*

***Institute of Low Temperature Science, Hokkaido University, Sapporo, Japan*

Field observations were carried out in order to examine the applicability of the transient electromagnetic (TEM) method to detection of permafrost structure in a discontinuous permafrost area of Mongolia.

In Mongolia, frozen ground occupies nearly 63% of the total territory of this country, and the thickness of permafrost varies between 5 and 200 m (Choibalsan 1998). The TEM survey was made in Nalaikh (47°45' N, 107°15' E), which is located in the suburbs of Ulaanbaatar, central Mongolia, in November 1998. Around this area, permafrost is discontinuously distributed and the mean annual air temperature ranges between –4 and 0 °C (Choibalsan, 1998). Bedrock around this area is consisted of schist and sandstone. Volcanic ash and Quaternary deposit are above it for approximately 300 m. The soil profile up to 6.8 m is clay and silt confirmed by the boring survey made in November 1998.

The TEM survey was conducted near a borehole, named #524. The measuring station interval was 10 m and the length of the profile was 100 m, named St. 2900 - St. 3000. St. 3000 was located 100 m from the borehole #524. A central induction measurement configuration was used in this site. The measurements were performed by using the transmitter loop of 60 x 60 m. The transient data were recorded using PROTEM 47 TEM system by Geonics Limited with a receiver coil having an effective area of

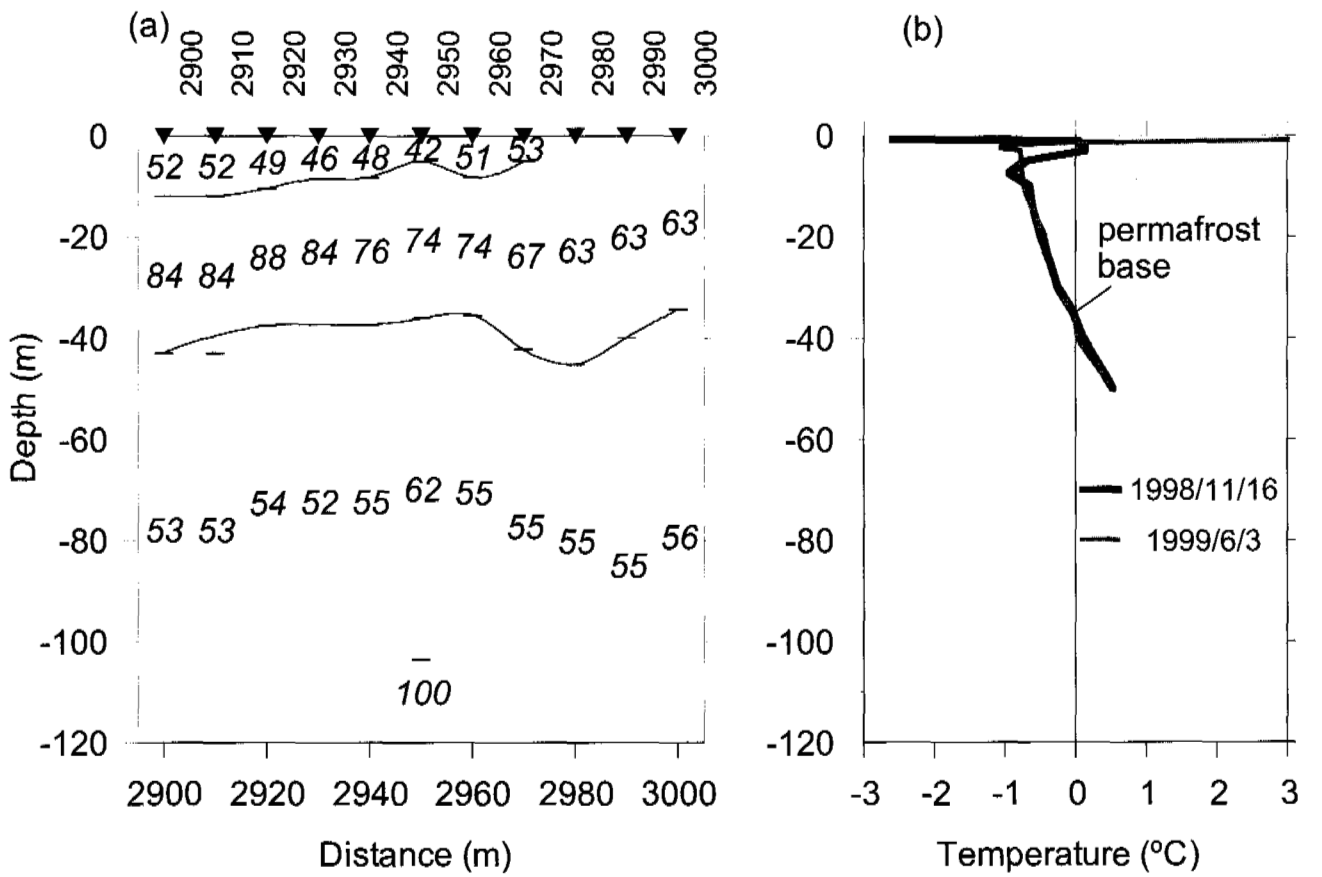

Figure 1. (a) Layered earth section near borehole #524 and (b) temperature profile in the borehole, Nalaikh. Values in figure (a) show resistivity in ohm-m.

31.4 m². At the borehole #524, the ground temperature to the depth of 50 m was measured on 16 November 1998 and 3 June 1999. Based on the temperature profiles, the permafrost base was located at the depth of 36.4 m (Fig. 1b).

The resistivity structures near the borehole #524 are shown in Figure 1 (a). Three- or four-layered structures were obtained between St. 2900 and St. 2970. Rather low resistivity values (40-100 ohm-m) were found, and the variation of resistivity value was small. The first and third layers had the lowest resistivity values, 42-62 ohm-m. The resistivity value of the second layer was higher than that of the other layers. At the stations between St. 2980 and St. 3000, a two-layered resistivity structure was estimated. The resistivity values of the first and second layers were almost constant, 63 and 55 ohm-m, respectively. The difference of resistivity between the first and second layers was very small. The lower boundary of the first layer ranged from 34 m to 45 m deep.

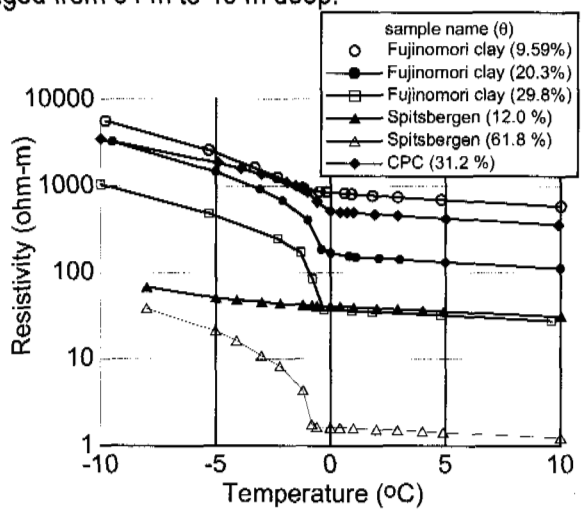

Figure 2. Electrical resistivity of soil samples. q is volumetric water content (after Harada and Yoshikawa 1996; Harada and Fukuda 2000; Harada et al. 2000). Spitsbergen is the soil sample obtained from Spitsbergen and CPC is from Caribou-Poker Creeks, Alaska.

The surface layer represented permafrost as confirmed by the boring survey. From the observation at the nearest station of the borehole #524, St. 3000, the lower boundary of the first layer was located at the depth of 34.2 m from the best-fit model and the allowable depth ranged between 23 m and 74 m based on the equivalence analysis. The lower boundary of the best-fit model, 34.2 m, was in good agreement with the depth of permafrost base obtained from the ground temperature profiles, 36.4 m. Therefore, this boundary indicates the permafrost base.

The observational results show that the difference in resistivity values between the frozen and unfrozen layers was very small. This small difference may have been caused by the low water content. Choibalsan (1998) reported that Mongolian permafrost is generally characterized by low to moderate ice contents. Figure 2 represents the relationship between resistivity values of fine-grained soils and temperature obtained from the laboratory experiments (after Harada and Yoshikawa 1996, Harada and Fukuda 2000, Harada et al. 2000). The experimental results show that the resistivity difference of the fine-grained soil is small due to the presence of unfrozen water, , especially in case of low water content. Furthermore, the measured ground temperature shows above –1 °C below the depth of 10 m. As a resistivity of frozen soil is a function of temperature, the resistivity difference becomes small in this study site.

From the field observation, it is noted that the best-fit model obtained by the TEM survey represents the permafrost structure precisely at this site, even though the difference in resistivity between frozen and unfrozen layers is small.

REFERENCES

Choibalsan, N. 1998. Characteristics of permafrost and foundation design in Mongolia. In Proceedings of 7th International Conference on Permafrost: 157-160.

Harada, K. and Fukuda, M. 2000. Characteristics of the electrical resistivity of frozen soils. Seppyo 62: 15-22 (in Japanese with English abstract).

Harada, K., Wada, K. and Fukuda, M. 2000. Permafrost mapping by transient electromagnetic method. Permafrost and Periglacial Processes 11: 71-84.

Harada, K. and Yoshikawa, K. 1996. Permafrost age and thickness near Adventfjorden, Spitsbergen. Polar Geography 20: 267-281.

Application of a capacitively coupled resistivity system for mountain permafrost studies and implications for the interpretation of resistivity values

*C. Hauck, and *C. Kneisel*

Graduiertenkolleg Natural Disasters & Institute for Meteorology and Climate Research, University of Karlsruhe, Germany

**Institute for Physical Geography, University of Würzburg, Germany*

INTRODUCTION

Geophysical techniques have become more and more popular to determine the physical properties of frozen ground, as they are comparatively cheap and easy to apply on most kinds of permafrost terrain. Within the large variety of geophysical techniques, electric and electromagnetic methods are especially well suited for permafrost studies, as resistivity increases with increasing ice content (or decreasing unfrozen water content), enabling the determination of ice content and ground ice characteristics in principle. However, in practical applications a number of technical limitations often prohibit a reliable assessment of the ice content. Among these, the influence of the electrical contact of the electrodes (in DC resistivity surveys) and the influence of data inversion of the measured apparent resistivities are probably the most important. Data inversion includes the problem of equivalence, which may be addressed by giving ranges for the resistivity values of the various layers (e.g. Kneisel 1998), and the influence of inversion parameters, which may change resistivity values over up to one order of magnitude (Hauck et al. 2003).

In this contribution we would like to address the discrepancy of resistivity results obtained through different measurement techniques by comparing data from several resistivity surveys along the same profile in the eastern Swiss Alps. Hereby, a capacitively coupled resistivity system (OhmMapper, Timofeev et al. 1994), which has been successfully applied on Arctic permafrost, is applied on more heterogeneous mountain permafrost terrain. The applicability of this new instrument was evaluated in comparison to a standard multichannel resistivity system.

METHODS AND DATA ACQUISITION

The OhmMapper (Geometrics) is a capacitively coupled resistivity meter that measures the electrical properties of the subsurface without the galvanic coupling of ground electrodes used in traditional resistivity surveys. A simple coaxial-cable array with transmitter and receiver sections is pulled along the ground. An alternating current is induced in the earth at a particular frequency by the transmitting dipole. The resulting voltage coupled to the receiver's dipole is measured. In flat or easily accessible terrain data collection is faster than when using conventional DC resistivity systems. Further details are given in Timofeev et al. (1994).

The DC resistivity tomography technique has been used increasingly in permafrost studies in recent years. The details of the method and the peculiarities of its application to mountain permafrost are described in many recent publications (e.g. Marescot et al. 2003, Hauck et al. 2003) and will not be repeated here.

The test sites of this study are located in the *Bever* valley (eastern Swiss Alps, see Kneisel et al. 2000) and on a non-frozen grass field near St. Moritz, which was used as reference area. DC resistivity measurements were conducted with a SYSCAL Junior Switch system with Wenner and Dipole-Dipole configurations. The OhmMapper surveys were conducted in Dipole-Dipole configuration using the same array geometries as for the SYSCAL surveys.

RESULTS

Whereas very similar results were obtained with both methods on the flat grass field of the non-frozen reference area (not shown here), difficulties were encountered on the steep and heterogeneous terrain in the Bever valley. The surface is vegetated by small trees and bushes and covered partly by medium-sized boulders, which makes towing the OhmMapper system a difficult task, as the antenna dipoles tend to get stuck between boulders and bushes. In addition, downslope towing is only manageable if a second person is holding the end of the line in order to prevent uncontrolled tumbling or misalignment of the dipole antennas (which is also the case on snow-covered slopes).

Figure 1 shows the survey results for both methods in comparison to the DC resistivity survey conducted in 1998 (Kneisel et al. 2000). All results are shown as a horizontal variation of electrical resistivity along the survey line. In principle, the 2002 results of the OhmMapper and the DC resistivity survey (SYSCAL) with Dipole-Dipole configuration

should be the same, as measurements were taken on the same day, at the same location and with the same survey geometry. Even though the general resistivity distribution is similar, the OhmMapper results (Fig. 1a) have much larger noise content than the SYSCAL data (Fig. 1b). This is mostly due to difficulties in keeping the correct distance between receiver and transmitter, as well as the correct orientation of the dipole antennas due to the steep and uneven terrain. Besides and possibly more important, the absolute values of apparent resistivities are systematically lower for the OhmMapper (1 kΩm) than for the SYSCAL (4 kΩm). In contrast, it is seen that the differences between the SYSCAL Dipole-Dipole and Wenner results (Figs. 1b and 1c) and the Wenner results obtained in different years (1998 and 2002, Fig. 1c) are less variable than between OhmMapper and SYSCAL (Figs. 1a and 1b) obtained at the same time and at the same locations.

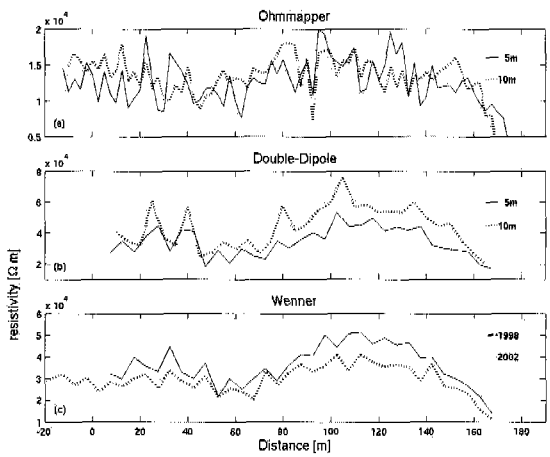

Figure 1. Comparison of apparent resistivity variation along the survey line in the *Bever* valley for (a) OhmMapper, (b) SYSCAL Dipole-Dipole array for 2 different spacings and (c) Wenner array from 2 different years.

The discrepancies between SYSCAL and OhmMapper are larger the higher the resistivity values. Plotting the apparent resistivity values obtained with the OhmMapper system against the corresponding apparent resistivity values of the SYSCAL system, systematic differences are seen for resistivity values above 500 m with smaller values for the OhmMapper system (Fig. 2). This systematic discrepancy is more pronounced the larger the resistivities. For very high resistivities the OhmMapper values reach less than for the values obtained with the SYSCAL system.

The possible reason is quite likely found in the different electrical coupling methods of both techniques. The high contact resistances typically found in mountain permafrost terrain result in larger apparent resistivities than obtained with capacitively coupled instruments (OhmMapper) or electromagnetic induction systems, where no coupling is needed at all. In most mountain permafrost applications only relative resistivity variations are needed, as the aim is to detect lateral or vertical resistivity anomalies indicating the presence of frozen material. However, when comparing data from different locations, care has to be taken as absolute resistivities may be overestimated due to resistive surface characteristics at specific locations.

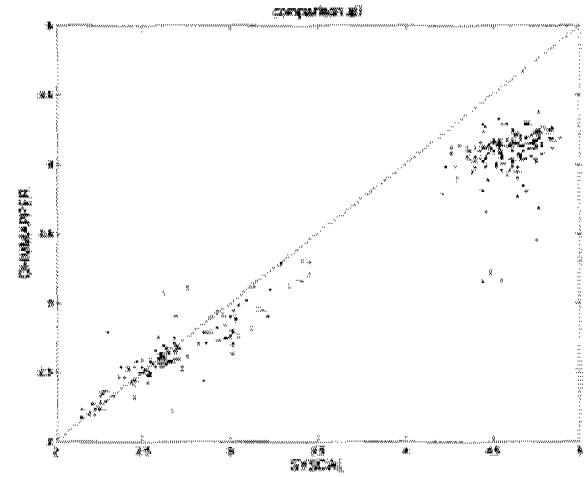

Figure 2. Comparison of measured apparent resistivity values obtained with SYSCAL and OhmMapper. Values are given in $\log_{10}$(Wm).

REFERENCES

Hauck, C., Vonder Mühll, D. and Maurer, H. 2003. Using DC resistivity tomography to detect and characterize mountain permafrost. Geophysical Prospecting 51 (in press).

Kneisel, C. 1998. Occurrence of surface ice and ground ice/permafrost in recently deglaciated glacier forefields, St.Moritz area, eastern Swiss Alps. Proc. of the 7th Int. Conf. on Permafrost, Yellowknife, Canada: 575-581.

Kneisel, C., Hauck, C. and Vonder Mühll, D. 2000. Permafrost below the timberline confirmed and characterized by geo-electric resistivity measurements, Bever Valley, eastern Swiss Alps. Permafrost and Periglacial Processes 11: 295-304.

Marescot, L., Loke, M.H., Chapellier, D., Delaloye, R., Lambiel, C. and Reynard, E. 2003. Assessing reliability of 2D resistivity imaging in permafrost and rock glacier studies using the depth of investigation index method. Near Surface Geophysics 1(2): 57-67.

Timofeev, V.M., Rogozinsky, A.W., Hunter, J.A. and Douma, M. 1994. A new ground resistivity method for engineering and environmental geophysics. Proc.of the SAGEEP, Annual Meeting: 701-715.

Combining and interpreting geoelectric and seismic tomographies in permafrost studies using fuzzy logic

*C. Hauck and *U. Wagner*

Graduiertenkolleg Natural Disasters & Institute for Meteorology and Climate Research, University of Karlsruhe, Germany

**Graduiertenkolleg Natural Disasters & Institute for Program Structures and Data Organization, University of Karlsruhe, Germany*

INTRODUCTION

For many problems in periglacial and glaciological studies, but also for other environmental, engineering and archaeological problems, geophysical investigations are the main source of information concerning the structure and characteristics of the subsurface. In particular, the ability to gather 2-dimensional information about the subsurface material is considered the main advantage of geophysical techniques as opposed to the single-point information through boreholes. However, the indirect nature of geophysical surveys, where material properties like water content, pore size or temperature have to be inferred from the measured physical variables such as electrical resistivity, can be considered a major drawback for the application of geophysical methods in applied geosciences. Nevertheless, the uncertainty in the interpretation of geophysical data sets is seldom explicitly treated in geophysical applications.

In order to address this uncertainty, a model approach using fuzzy logic is presented in this contribution, which is based on expert knowledge about a particular problem. The problem is taken from the area of ground-ice detection, where a large variety of geophysical methods has been applied in recent years (e.g. Vonder Mühll et al. 2001, Hauck and Vonder Mühll 2003). Generally, more than one method is used in order to get a multivalued data set and to facilitate data interpretation (e.g., DC resistivity and refraction seismics). However, due to the non-uniqueness of the inversion results and the range of possible values for most earth materials, the interpretation of the data set can be very ambiguous.

FUZZY MODEL

Fuzzy logic is an extension of a multivalued logic, where classes of objects have unsharp boundaries and membership is a matter of degree. It is a convenient way to map an input space to an output space, especially if a quantitative output is required from imprecise input variables. In this case the input space is comprised by the results from the geophysical surveys (e.g., electrical resistivities or seismic P-wave velocities) and the output space is the "degree of ice content" (but not the ice content itself), that is the possibility of ground-ice occurrence.

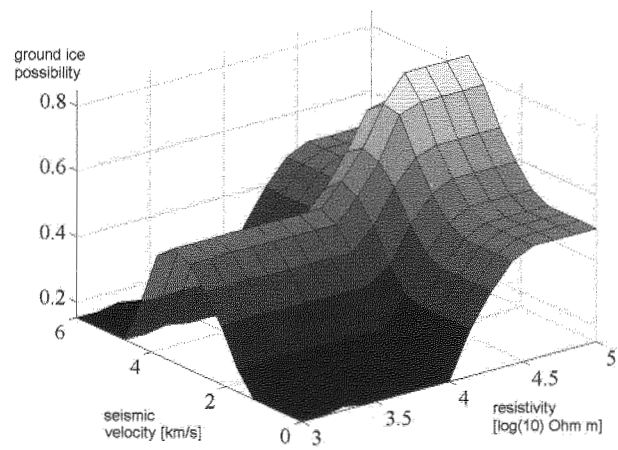

Figure 1. Decision surface for the fuzzy inference system for ground ice detection. Each value of seismic velocity (in km/s) and the logarithm of electrical resistivity (in $\log_{10}$(Wm)) is associated with a degree of possibility for ground ice (z-axis).

The fuzzy inference system used in this study is of the so-called Mamdani-type (Mamdani and Assilian 1975) and is based on nine rules, all linking low, medium and high resistivity and velocity values to a corresponding output (low, medium and high ice content). A practical view of the rule system is shown as decision surface (Fig. 1), where each pair of resistivity and velocity data point is associated with a possibility of ground-ice occurrence. High resistivity values and medium seismic velocities around 3500 m/s (velocity for pure ice) are associated with a high possibility of ice occurrence, as can be seen from Fig. 1. Due to the exponential increase of resistivity with decreasing and negative temperature, the logarithm of resistivity is used in the model.

RESULTS

The decision surface and the corresponding fuzzy model are tested using a synthetic data set of resistivity and seismic data pairs (Fig. 2). Both data sets are comprised of 4 regions with high, medium and low resistivity and velocity values, respectively, where only the upper right hand corner represents values consistent with the material properties of ice. Accordingly, the resulting model output shows a region of high possibility for ice occurrences in this part, whereas the possibility is low for all other regions. This outcome would have been difficult to predict by "manual" inspection of the resistivity and seismic distribution alone, as the two patterns are notably different.

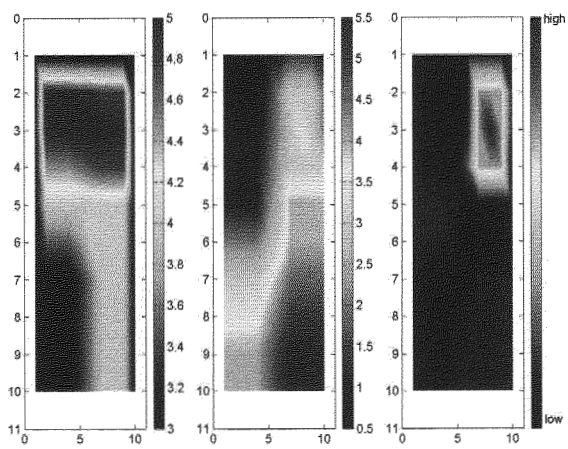

Figure 2. Resistivity (left, in $\log_{10}(\Omega m)$) and seismic velocity (center, in km/s) of the synthetic data set, and fuzzy model output (right, possibility of ground ice).

As can be seen from Figure 2, the fuzzy model can be applied to detect areas with high possibility for ground-ice occurrence from joint resistivity-velocity data sets. In an initial evaluation study, the model was applied to several field data sets from anomalously cold low altitude sites in the midlands of Central Europe and the Alps, where permafrost is sporadic or absent in general. However, ground ice may be present in isolated patches with specific microclimatic conditions (Kneisel et al. 2000, Gude et al. 2003). First results show anomalies with an enhanced possibility for ground-ice occurrence in comparison to the neighbouring areas. Even though neither the probability nor the actual ice content can be determined by the model, the possibility for ground ice can be quantitatively compared between different the field sites.

As the fuzzy inference system and the governing decision rules can easily be adapted to different types of input data, the applicability of the fuzzy logic approach may be wide.

REFERENCES

Gude, M., Dietrich, S., Mäusbacher, R., Hauck, C., Molenda, R., Ruzicka, V. and Zacharda, M. 2003. Permafrost conditions in non-alpine scree slopes in Central Europe. 8th Int. Conf. On Permafrost, Zurich, 2003, in press.

Hauck, C. and Vonder Mühll, D. 2003. Evaluation of geophysical techniques for application in mountain permafrost studies. Zeitschrift für Geomorphologie, Suppl., special issue: geophysics in geomorphology (in press).

Kneisel, C., Hauck, C. and Vonder Mühll, D. 2000. Permafrost below the timberline confirmed and characterized by geo-electric resistivity measurements, Bever Valley, eastern Swiss Alps. Permafrost and Periglacial Processes 11: 295-304.

Mamdani, E.H. and Assilian, S. 1975. An experiment in linguistic synthesis with a fuzzy controller. International Journal of Man-Machine Studies, 7 (1): 1-13.

Vonder Mühll, D., Hauck, C., Gubler, H., McDonald, R. and Russill, N. 2001. New geophysical methods of investigating the nature and distribution of mountain permafrost. Permafrost and Periglacial Processes, 12 (1): 27-38.

The spatial extent and characteristics of block fields in Alpine areas: evaluation of aerial photography, LIDAR and SAR as data sources.

*S. Heiner, S. Gruber and *E. Meier*

Glaciology and Geomorphodynamics Group, Department of Geography, University of Zurich, Switzerland

**Remote Sensing Laboratories, Department of Geography, University of Zurich, Switzerland*

INTRODUCTION

The coarse surface layer in block fields operates as an insulating layer between the surface climate and the ground below. Often it acts as a thermal filter, insulating against the effect of surface warming but readily transmitting the effect of surface cooling (Harris and Pedersen 1998). Therefore, knowledge about the extent of coarse surfaces is important for the successful spatial application and further development of energy balance models (Stocker-Mittaz et al. 2002) or statistical models (e.g. Gruber and Hoelzle 2001).

Block fields can be mapped relatively accurately based on the manual interpretation of aerial photography because of the textural information and terrain position. This is a labor intensive process depending on the skills of the operator. This study uses high resolution aerial photography and a GIS (Geographic Information System) to automatically map the spatial extent and characteristics of block fields. The test site is the Corvatsch area in the south-eastern part of the Swiss Alps.

METHOD AND DATA

In aerial photographs, block fields are characterized by the frequency of change between dark and bright areas caused by the shadows of big blocks. Other areas are typically much more homogeneous. This effect can be used to separate blocky areas from areas with fewer blocks by using statistical methods.

On 17 September 2002, aerial photographs of the test area have been taken by the Federal Office of Topography of Switzerland. The ground resolution of these pictures is about 6 cm.

Two more methods for the remote sensing of surface roughness appear feasible and are currently under investigation: (1) a SAR (Synthetic Aperture Radar) image of JERS (Japanese Earth Resources Satellite) is currently processed and (2) a flight with a LIDAR (Light Detection And Ranging, laser altimetry) sensor on board will take place in the test area this summer. LIDAR data from a different campaign is already available for testing the methods.

The correctness of the interpretation and validation of the extracted coarsenesses is provided by transects obtained from terrestrial surveying.

PROCESSING AND RESULTS

The aerial photographs are orthorectified and imported into the GIS. Focal functions are applied on this grid. These are functions which calculate a new value for a cell using the value of this cell and its adjacent cells. Three new grids are calculated: one contains the maximum of two adjacent cells, and the second the mean of two adjacent cells. Then the difference between these two grids is calculated and the sum of ten adjacent cells is written into the central cell. As a result, areas with a high frequency of change between dark and bright cells (block fields) will show high values, whereas more homogeneous areas will be attributed lower values. Now the grid will be reclassified into the different classes of surface roughness. The last step is the resampling of the pixels to the desired resolution for permafrost modeling.

First results are satisfactory as shown in Figure 1. The block fields could be delineated and the method clearly shows the potential to distinguish between several classes of surface roughness. Problems remain in shadow areas.

CONCLUSION AND OUTLOOK

The result presented above clearly shows the potential of the method for the automatic mapping of block fields using standard GIS software packages. Problems remain to be solved in the shadow areas. The availability of this data will improve permafrost modeling.

The use of JERS SAR and LIDAR data will provide an evaluation using two more data sources. SAR will be inexpensive and provide large area coverage but only have a low spatial resolution and only be able to distinguish a limited number of roughness classes in alpine terrain. LI-

DAR will permit a high spatial resolution and accurate characterization and quantification of surface structure but requires significantly more cost and effort.

First attempts to use wavelets in the detection of surface roughness have shown interesting perspectives and applications of this method to aerial photographs and LIDAR data are underway.

Figure 1. The picture shows the area around the rockglacier Murtèl. Four classes of surface roughness are determined: highest values are found on the coarse surface of the rockglacier, whereas the homogenous surface of the skislope shows lowest values.

REFERENCES

Gruber, S. and Hoelzle, M. 2001. Statistical modelling of mountain permafrost distribution - local calibration and incorporation of remotely sensed data. Permafrost and Periglacial Processes 12 (1): 69-77.

Harris, S. and Pedersen, D.E. 1998. Thermal regimes beneath coarse blocky materials. Permafrost and Periglacial Processes 9: 107-120.

Stocker-Mittaz, C., Hoelzle, M. and Haeberli, W. 2002. Modelling alpine permafrost distribution based on energy-balance data: a first step. Permafrost and Periglacial Processes 13(4): 271-282.

Thermal regime of coarse debris layers in the Ritigraben catchment, Matter Valley, Swiss Alps

*T. Herz, L. King and *H. Gubler*

Institut für Geographie der JLU, Giessen, Germany

**ALPUG, Davos, Switzerland*

INTRODUCTION

The objective of the current study is to investigate the microclimate within coarse debris layers in high mountain environments. To quantify the heat exchange between the local atmosphere and the near-surface ground, special attention is focused on thermal conditions. Further-more, their influence on the distribution pattern of discontinuous mountain permafrost is of specific interest. Based on the research concept and site description given in Herz et al. (in press), this poster presents and discusses the initial data gathered from the measurement equipment described below.

RESEARCH AREA

The data was recorded in close proximity to the meteorological station erected in the Ritigraben block slope (46°11´N, 7°51´E, 2615 m a.s.l.). Block sizes in this area range from 0.5 up to several cubic meters. For comparison purposes, the finer-grained substrate types known as "ski run" and "soil beneath alpine grassland" were also incorporated in the measurement programme.

MEASURING SETUP

Local climatic conditions are recorded at a meteorological station. The ground thermal regime is registered in a 30 m deep borehole (cf. Herz et al. in press).

To measure rock and air temperatures within the block layer, two types of temperature sensors were constructed. In both cases the sensor element consists of a high-precision platinum thin film thermo-meter Pt 1000 1/3DINB (LxWxH = 10x2x0.25 mm). The sensors were connected to a 5-channel-mini-logger (Type Wickenhaeuser TL_LOG5) by a half-bridge circuit. The technical components of the logger and the use of a high-precision reference resistor in the circuit guarantee excellent long-term stability of the temperature measurements with a theoretical resolution of 0.00012°C. A four-point calibration was done in an ice-water bath for 0°C or a circulated water bath controlled by an analogue calibration thermometer (resolution 0.01°C) for 10, 20 and 30°C, respectively. The calibration yielded outstanding results, so that the accuracy of temperature measurements can be indicated as within at least 0.02°C.

Rock and soil temperature sensor elements were sealed in closed high-grade steel tubes with a wall thickness of 0.2 mm. Air temperature sensor elements were fixed in open steel tubes in such a way, so that the tip of the Pt 1000 sticks out of the tube and is in direct contact with the surrounding air.

Block layer rock and air temperatures are measured in a profile of four consecutive measurement points. The profile follows the drainage way of the local micro relief. Each measurement point consists of two loggers with five rock and air temperature sensors installed at different depths. Four additional measurement points form two cross-sections to the main profile to also include other micro topographical positions in the block slope.

Surface and soil temperatures are also recorded in the substrate types, "ski run" and "soil".

INITIAL RESULTS

Hourly meteorological and daily borehole temperature data have been available since April 2002. Microclimatological data exist so far for the nine-week period from August 15th to October 18th 2002. Measurement intervals were set to 5 minutes for air temperature and 15 minutes for rock and soil temperature sensors during this period. The borehole temperature data presented in Figure 1 display a marked asymmetry. The heat input during summer penetrates down to only 3.5 m in spite of extreme temperature gradients of up to 10°C/m. A sharp bend in the maximum curve occurs at that depth. The maximum temperature remains very close to 0°C during the whole summer between 3.5 and 5 m depth. Penetration of surface cooling during winter reaches down to 14 m depth, tantamount to the depth of zero annual amplitude. These differences in ground thermal properties

between "summer" and "winter" conditions can only be explained by phase change processes at a permafrost table situated between 3.5 and 5 meters depth during summer 2002.

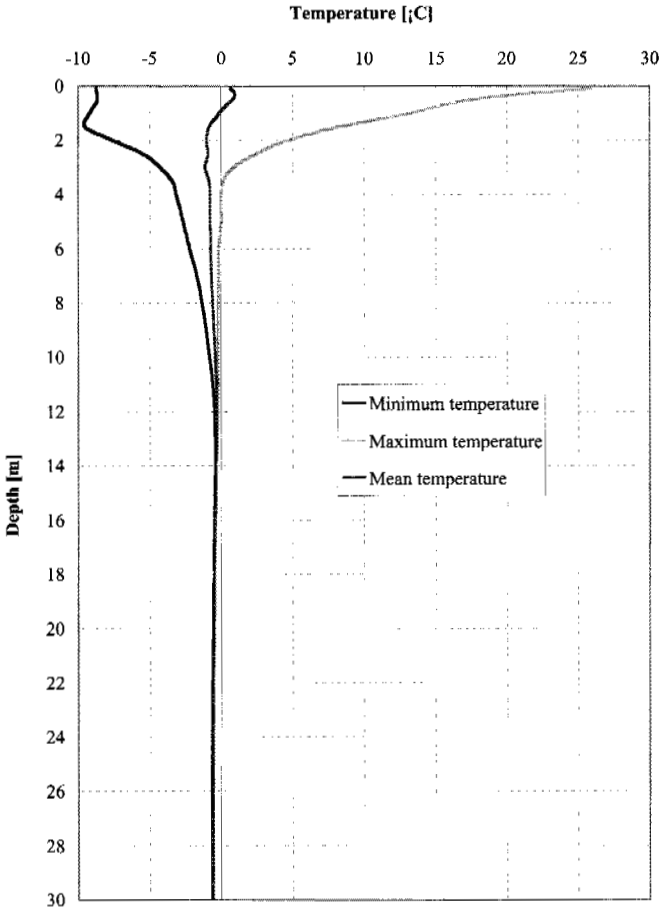

Figure 1. Ground temperature envelope, Ritigraben block slope, 2615 m a.s.l. (April 2002 – January 2003).

The resulting thermal offset in ground temperatures according to Goodrich (1978) is indicated by a mean temperature of –0.84°C at 3.5 m depth, which is 1.5°C colder than the mean temperature at 0.1 m depth. The permafrost body can be characterized as "warm" with mean temperatures of –0.37°C at depth of ZAA and –0.61°C at 30 m depth. It is remarkable, that absolute minimum temperatures were measured at 1.5 m depth, representing the bottom side of the uppermost block of the surface layer. The bottom side is obviously influenced by advective air circulation between the block layer void system and the near-ground atmosphere also under winter conditions, while its surface is protected from heat loss by the formation of a snow cover.

Figure 2 compares rock temperatures in the block layer with temperatures measured in an adjacent soil profile. The different behaviour of the two deeper curves is of special interest in this context. Rock temperatures at 140 cm depth still show a daily course, which is not detectable at a comparable depth in the soil. Altogether the temperature level in the block layer is lower than in the soil in spite of higher surface temperature values. Rock temperatures at 140 cm depth clearly correlate with the daily minima of the surface temperature course and show an immediate response on a surface temperature decrease, which is not the case for the soil.

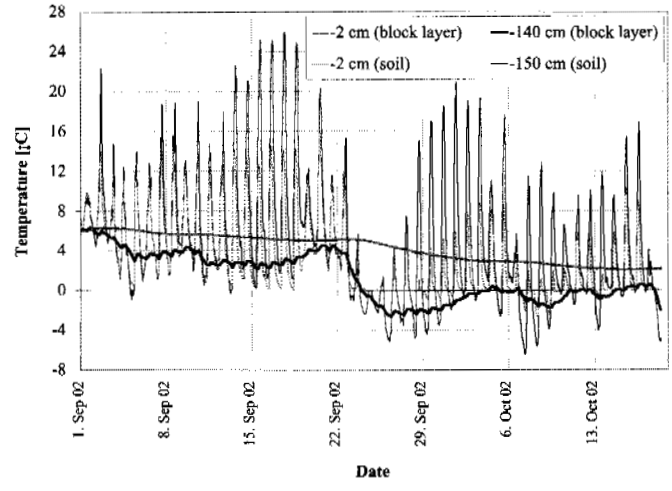

Figure 2. Comparison of block layer and soil temperatures from September 1st to October 18th, 2002.

CONCLUSIONS AND OUTLOOK

The data presented indicate that non-conductive heat transfer processes play an important role in the thermal regime of block layers. Advection of water and air in the void system between blocks is believed to be the crucial phenomenon, which is investigated in this study. Furthermore, in October 2002 five additional boreholes were drilled in the lower part of the Ritigraben block slope to investigate the rheological conditions in the catchment of the torrent.

REFERENCES

Goodrich, L.W. 1978. Some results of a numerical study of ground thermal regimes. In 3rd International Conference on permafrost, Proceedings, Edmonton, 10-13 July: 29-34.

Herz, T., King, L. and Gubler, H. in press. Microclimate within coarse debris of talus slopes in the alpine periglacial belt and its effects on permafrost. In 8th International Conference on Permafrost, Proceedings, Zürich, 21-25 July 2003.

Topographical properties of active and inactive patterned grounds in Finnish Lapland

*J. Hjort and *M. Seppälä*

Department of Geography, University of Helsinki, Finland
**Physical Geography Laboratory, University of Helsinki, Finland*

Periglacial patterned grounds are quite widespread features in Northern Finnish Lapland, especially above timberline in the zone of discontinuous permafrost. The most common types are sorted and non-sorted nets. Activity of these landforms varies from one area to another and between different types of patterned grounds. Active forms seem to be mainly located in the valleys. Respectively, inactive patterned grounds are more common on the slopes and on top of the fells (Fig. 1). In general, climate is a crucial environmental determinant of frost activity. However, when we study regions at large scale the importance of local factors such as soil, hydrology, topography, vegetation etc., becomes apparent.

The objective is to present some results of a research where active and inactive patterned grounds were studied using Geographical Information System (GIS) and statistical methods. The main aim was to compare topographical properties of active and inactive regions to see if there are any differences between these areas. Topographical parameters calculated from a digital elevation model (DEM) were used as explanatory variables in univariate analysis. The DEM with 20 m grid size was created from contours of topographic maps using Arc/Info 8.1. SPSS 9.0 software package was used in statistical analysis.

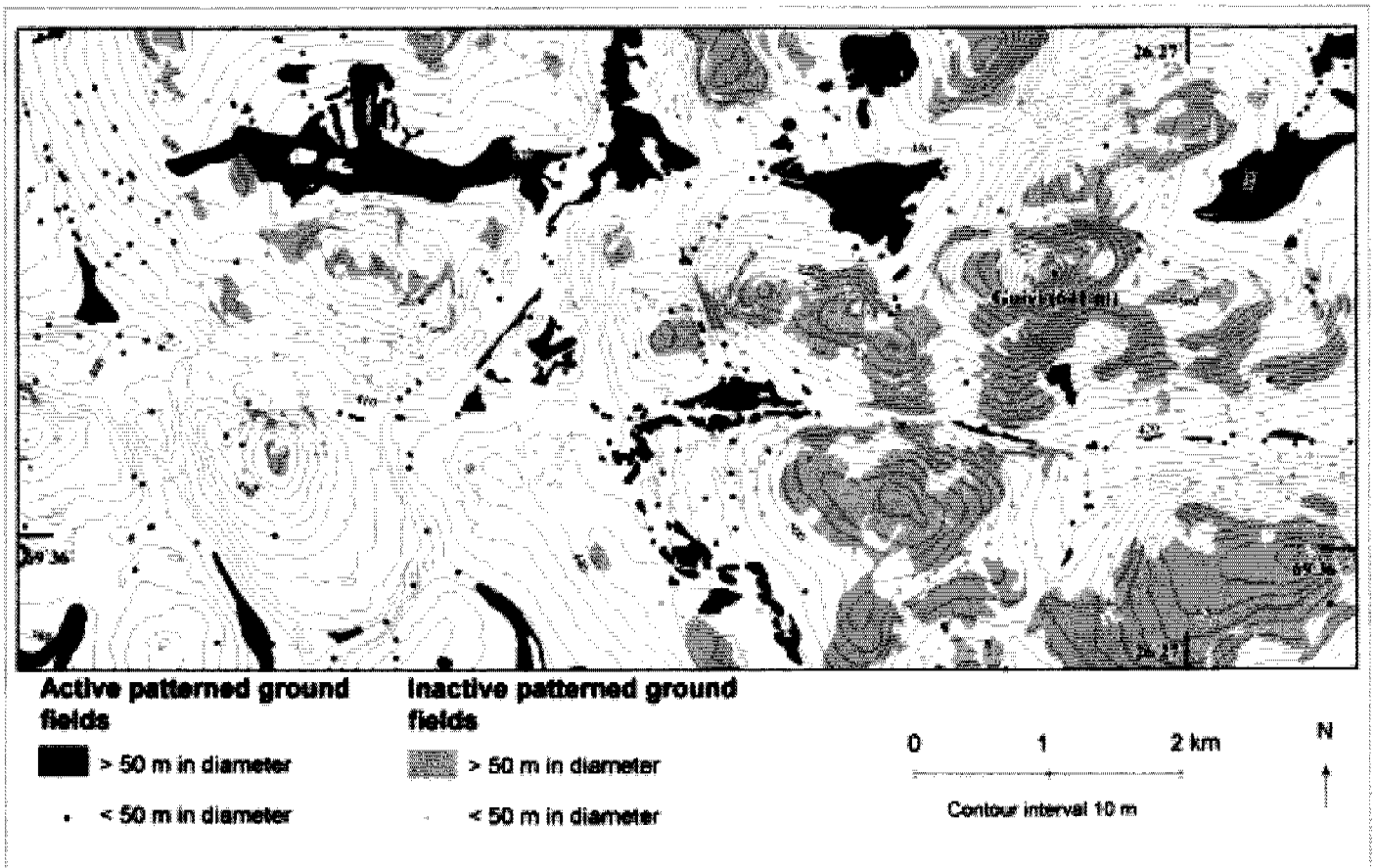

Figure 1. Distribution of active and inactive patterned grounds in a part (4.8 x 10 km) of the study area (10 x 20 km) at Paistunturit fell region in Finnish Lapland (Contours © National Land Survey of Finland, Licence number 49/MYY/03).

Table 1. Results of an univariate analysis where active and inactive patterned ground squares were compared with topographical variables calculated from DEM. Total number of the grid squares in the analysis is 745. Statistical significance is tested with the Mann-Whitney U-test.

Topographical variables	Patterned ground		Statistical significance (p)
	Active (n = 421) mean ± std	*Inactive (n = 324)* mean ± std	
Mean altitude (m a.s.l.)	392 ± 40	454 ± 49	<0.001
Mean slope angle (°)	3.4 ± 1.7	5.8 ± 2.3	<0.001
Wetness index*	5.25 ± 0.58	4.40 ± 0.51	<0.001
Proportion of flat topography (%)	33.2 ± 25.0	9.6 ± 13.3	<0.001
Proportion of concave topography (%)	54.1 ± 10.1	45.0 ± 9.7	<0.001

* Formula from Etzelmüller et al. 2001

Data were collected from an area of 200 km² (SW corner 69°28´N, 26°14´E and NE corner 69°39´N, 26°29´E) in the Paistunturit fell area of northernmost Finland. Patterned grounds were mapped in the field with a GPS-device in summer 2002 and are classified according to Washburn (1979). Mapping results were digitized on orthorectified aerial photographs. The most common landforms were non-sorted nets, sorted solifluction sheets and steps, sorted nets, non-sorted circles, non-sorted solifluction steps, sorted stripes and sorted circles. For the statistical analysis the study area was split into 800 equal-size (500 x 500 m) grid squares (see Luoto and Seppälä 2002). Every grid containing patterned grounds was classified to be active or inactive as a function of the predominant type. Activity of the patterned ground was defined visually in the field. Squares without patterned landforms were excluded. Topographical variables were calculated using Arc/Info Grid for each 25-hectare square from some of the parameters, which have been stated as significant in periglacial research (Etzelmüller et al. 2001). Highly correlated parameters were excluded from the final analysis (absolute value of the Spearman's rank correlation coefficient over 0.8). For example from mean, relative, minimum and maximum altitude only mean altitude was used in the analysis.

Results of the univariate analysis can be seen in Table 1. All the variables show statistically significant ($p < 0.001$) differences between active and inactive patterned ground squares. Active features are located in moist areas and at lower elevation with more gentle slopes. The proportion of flat topography (slope < 2°) is more than three times higher than for inactive squares. Also the proportion of concave topography is higher in active areas. From the results it can be concluded that moisture is at present one of the most important local environmental factor affecting frost activity in North Finnish Lapland with the mean annual air temperature about -2°C and precipitation c. 400 mm (Seppälä 1976; cf. Matthews et al. 1998).

REFERENCES

Etzelmüller, B., Ødegård, R.S., Berthling, I. and Sollid, J.L. 2001. Terrain parameters and remote sensing data in the analysis of permafrost distribution and periglacial processes: examples from southern Norway. Permafrost and Periglacial Processes 12: 79-92.

Luoto, M. and Seppälä, M. 2002. Modelling the distribution of palsas in Finnish Lapland with logistic regression and GIS. Permafrost and Periglacial Processes 13: 17-28.

Matthews, J.A., Shakesby, R.A., Berrisford, M.S. and McEwen L.J. 1998. Periglacial patterned ground on the Styggedalsbreen glacier foreland, Jotunheimen, southern Norway: microtopographic, paraglacial and geoecological controls. Permafrost and Periglacial Processes 9: 147-166.

Seppälä, M. 1976. Periglacial character of the climate of the Kevo region (Finnish Lapland) on the basis of meteorological observations 1962-71. Reports from the Kevo Subarctic Research Station 13: 1-11.

Washburn, A.L. 1979. Geocryology. A survey of periglacial processes and environments. 406 s. London: Arnold.

Influence of human activities and climatic change on permafrost at construction sites in Zermatt, Swiss Alps

*R. Hof, L. King, T. Herz and *S. Gruber*

Institute for Geography, Justus Liebig University, Giessen, Germany

**Glaciology and Geomorphodynamics Group, Department of Geography, University of Zurich, Switzerland*

GEOGRAPHICAL BACKGROUND AND PERMAFROST CONDITION

Zermatt is a tourist resort in the Alps with a total of 14,000 hotel beds and more than one million official overnight stays per year. The necessary infrastructure consists of installations that often reach into permafrost areas, from the sporadic zone at about 2600 m a.s.l. up to the continuous permafrost zone above 3400 m a.s.l. The unglaciated permafrost area has a large vertical extension due to the surrounding high mountain ranges that reach above 4000 m a.s.l., resulting in a dry and sunny climate and a very high glacier equilibrium line.

The infrastructure erected in the permafrost areas consists of

(a) hotels, restaurants and mountain huts,
(b) station buildings of railways, funiculars and ski lifts,
(c) other related structures such as masts, tunnels, elevators, shelters for vehicles, workshops, etc.
(d) subsurface water pipes (for drinking water, artificial snowing of ski-runs), sewage, communication and electricity lines.

Engineering geologists as well as those responsible persons for this infrastructure have become increasingly interested in the distribution and the characteristics of permafrost in the Zermatt area, as there have been problems due to permafrost degradation.

The poster gives an inventory of the existing structures on probable and proven permafrost sites and describes some problems encountered during the last 25 years, with original new temperature data.

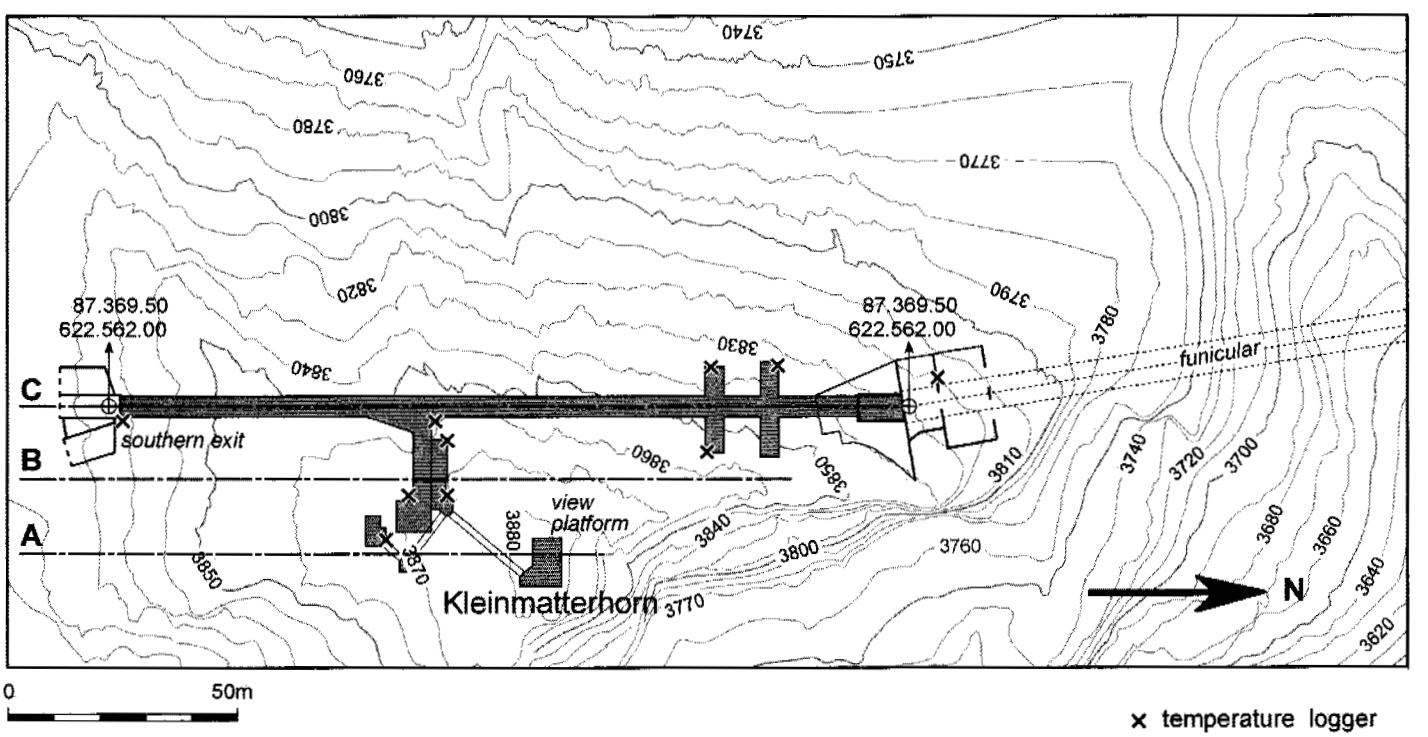

Figure 1. Map of Kleinmatterhorn mountain peak with tourist facilities (10 meter contour lines).

CONSTRUCTION SITES

Kulmhotel and Gornergrat Funicular

Gornergrat can be reached by a 9.340 km long railway line constructed between 1896 and 1898. The uppermost 500 meters were added in the year 1909 and the Kulmhotel Gornergrat was opened in 1910. The railway track and the hotel were mainly used in summer until the early Fifties. Winter skiing became more and more attractive in the Sixties when the hotel started to open also in winter. In the year 1985 two new astronomic observatories were added to the northern and southern towers and this caused a substantial additional load on the subsurface. Moreover, apartments for scientists were heated in the basement.

Soon after this, the northern tower that was erected on frozen morainic material started to settle due to permafrost degradation. The subsidence between tower and hotel was controlled with geodetic measurements and strain gauges and concrete were injected into the foundation in order to stop the differential settlement. Today, ground temperature measurements show that the ground below the tower is probably not frozen for a depth of about 10 meters (the active layer at undisturbed sites is less than 2.5 meters). This must be attributed to the heating of the basement for almost 20 years. Actually, subsidence seems to have stopped.

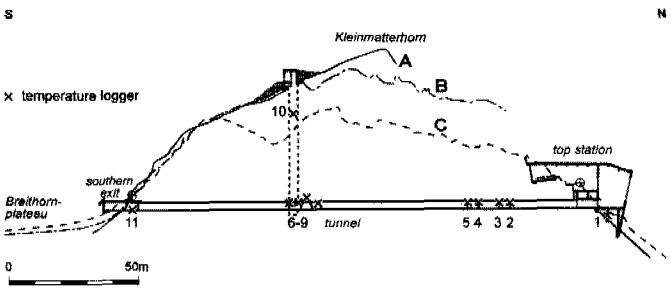

Figure 2. Kleinmatterhorn mountain top with the location of temperature loggers. The position of the cross sections A, B and C are shown in Figure 1.

Kleinmatterhorn Funicular

This funicular travels up to 3820 m a.s.l. and were constructed in 1981. It arrives at a tunnel cut in the northern wall of the mountain top (Fig. 1). At its southern exit the ski run starts down to Zermatt. Bedrock temperatures as low as –12°C were reported during the construction (Keusen and Haeberli 1983). The same temperature was measured in the near-surface rock material of the northern rockwall below the mountain top in a diploma study. The MAAT measured here was –8°C in the years 1998/99.

Today, bedrock temperatures have risen to –3 to –2°C at several localities (cf. Fig. 2). This is due to heating and to the heat brought into the tunnel by the more than 490,000 visitors per year. Additional heat is created by almost 70,000 elevator movements per year, transporting tourists to the mountain top. In summer 1997, meltwater created problems when refreezing in the elevator shaft (King et al. 1998).

In view of the considerable temperature rise in the bedrock, temperatures have been monitored since 1998 at ten different places in order to take countermeasures if necessary.

2.3 Further construction sites on permafrost

There are many more facilities erected on the permafrost (Table 1). Climatic change may further contribute to a rise in the lower permafrost limit. It should be recalled that an actual MAAT of about –1°C indicates patchy permafrost occurrences, and at less than -5°C, continuous permafrost may be expected.

Table 1. Installations on permafrost in the Zermatt area with altitudes and expected MAAT.

Name	Altitude (m a.s.l.)	MAAT (°C)
Kleinmatterhorn (station)	3820	-7,2
(elevator summit)	3883	-7,6
Testa Grigia (station)	3479	-5,3
Stockhorn (station)	3407	-4,9
Hohtälli (station)	3286	-4,2
Matterhorn Refuge	3260	-4,0
Rote Nase (station)	3250	-4,0
Kulmhotel Gornergart	3135	-3,3
Rothorn (station)	3103	-3,1
Gandegg Refuge	3029	-2,7
Trockener Steg (station)	2939	-2,2
Gornergrat rack railroad (top)	3090	-3,0

CONCLUSIONS

Degradation of permafrost due to climatic change may become a serious threat to installations at high mountain tourist resorts. This is especially dangerous when the facilities are not properly maintained. Therefore, relevant information must be improved to the managers of these installations and to the local authorities by permafrost scientists working in these areas.

REFERENCES

Keusen H.R. and W. Haeberli, W. 1983. Site investigation and foundation design aspects of cable car construction in Alpine permafrost at the "Chli Matterhorn", Wallis, Swiss Alps. In 4th International Conference on Permafrost, Proceedings, Fairbanks, 17-22 July: 601-605.

King, L. and Kalisch, A. 1998. Permafrost distribution and implications for construction in the Zermatt area, Swiss Alps. In 7th International Conference on Permafrost, Proceedings, Yellowknife, 23-27 June: 569-574.

Spatial conditions of frozen ground and soil moisture at the southern boundary of discontinuous permafrost in Mongolia

*M. Ishikawa, Y. Zhang, T. Kadota, T. Ohata and *N. Sharkhuu*

Frontier Observational Research System for Global Change, Yokohama 236-0001, Japan

**Institute of Geography, Mongolian Academy of Sciences, Ulaanbaatar 210620, Mongolia*

INTRODUCTION

As a consequence of global warming, mean annual air temperatures are predicted to increase significantly in the high latitudes, leading to changes in the distribution and geometries of permafrost on a decadal scale. Degradation and thawing of permafrost is expected to occur, especially at the southern boundaries of discontinuous permafrost, resulting in significant changes in the components of land-surface hydrology such as surface runoff, groundwater flow, soil moistures and evapotranspiration as well as those of energy balance.

The Frontier Observational Research System for Global Change has promoted a research program entitled "Observational study on the water cycle in the periphery of Eurasian snow cover/frozen ground region in relation to climate formation". The critical components of this project are to clarify and to define the hydrological roles of frozen ground with respect to land-surface hydrology. This year we focused on the spatial variations of ground thermal and moisture conditions in Mongolia at the southern boundary of Eurasian discontinuous permafrost. On the basis of the results obtained, this paper discusses the local distribution and thermal condition of permafrost, and its hydrological roles.

REGIONAL SETTING OF STUDY AREA

The Tuul river basin in the Khentei Mountains, north-east of Ulaanbaatar was selected as an area for intense observation. The topography is characterized by a significant relief with altitude ranging from 1300 to 2500 m A.S.L. Mean annual air temperature (MAAT) averaged between 1992 and 2000 was -3.5 °C at the Terelj meteorological station (1520 m A.S.L). The 20 years MAATs averaged at Zuunmod (1529 m A.S.L.) and at the Ulaanbaatar stations (1300 m A.S.L.) were close to -1.0 °C. Recent long-term air temperature observations indicate significant warming. Originally negative MAATs have sometimes become positive values after the late 1990s. Mean annual total precipitation at Ulaanbaatar station was 300 mm between 1980 and 2000, and approximately 80 % of the precipitation occurs between June and August.

In spite of such dry climatic conditions, dense forests are extensively developed mainly on the northern slopes, while pastures dominate on the southern slopes and on the flat plains.

OBSERVATIONS

Observations include measurements of ground temperatures at shallow and greater depths, of soil moisture and of hydraulic conductivity at two locations; in Shijir valley, west of the Terelj station and at the Nalaikh site. In the Shijir basin, transect measurements were carried out on steep and gentle northern forest slopes (NFSs) and on southern pasture slopes (SPSs) in the rainy season of July and during the dry season of October and November 2002. At the Nalaikh site, we drilled a borehole reaching a depth of 30 m in early October. The drill site is on the wide flat pasture plain (FPP). A ground temperature profile was measured on the 1st November. Core samples were taken at 20 cm depth intervals and used for estimating soil water contents.

RESULTS

Shijir valley (Figure 1)

Steep NFSs (sites *A*, *B*, *C*, *Q* and *R*) have large angular gravels overlain by thick organic materials composed of humus and moss, while gentle NFSs (sites *E* and *F*) dominate silt materials. Soil textures beneath SPSs were characterized by sand-gravels overlain by thin humus. The highest hydraulic conductivity (100 m/d) was found at steep NFS (site *A*). The values on other slopes ranged from 0.1 to 10 m/d. Ice lenses were visible only beneath steep NFSs only. Higher ground water tables were found at gentle NFSs.

Ground temperatures at 1.5 m depth were low on steep NFSs (reaching 0 °C at sites *A*, *B*, *C*, *Q* and *R*), but higher (ranging from 5 to 6 °C at sites *I*, *N* and *O*) on SPS. Thermal observations at greater depths in November indicated the occurrence of permafrost below a depth of 2.4 m on NFS (site *E*). On the other hand, ground temperatures at SPSs were about 5 °C at the same depths, suggesting that permafrost is absent.

High moisture contents, reaching 40 and 60 % at some depths, occurred beneath gentle NFS (sites *E, F* and *S*). At these sites, ground water tables were found at shallower depths. On the other hand, moisture contents were less than 20 % on steep NFSs (*A, B* and *C*) and SPSs (*I* and *O*).

Nalaikh site (Figure 2)

At the Nalaikh site, freezing reached a depth of 0.9 m on the 1st of November. The highest temperature (3.7 °C) occurred at 3 m depth. Below this depth, ground temperature decreased until the uppermost portion of frozen grounds was reached. Subzero temperatures (0 to -0.2 °C) occurred between 6 and 12 m depth, indicating permafrost conditions. The temperatures of sub-permafrost layers were slightly above 0 °C.

Significant differences were found in the water contents of the active layer, the permafrost and sub-permafrost layers, respectively. While water contents were less than 10 % in the active layer, those in the upper portion of permafrost were high, varying from 15 % to 27 %. The water contents in the lower portions of permafrost were from 10 to 20 % and similar to those of sub-permafrost layers.

SPATIAL THERMAL CONDITIONS OF PERMAFROST

Generally, permafrost underlies the NFSs where the incoming local energy fluxes on the surface are reduced due to slope orientation, forest shading and thermal properties of substrata. Cold permafrost with a thinner active layer occurs beneath NFSs.

Extremely warm permafrost with thick active layers sporadically occurs beneath FPPs. According to the increasing rate of ground temperature change estimated by Sharkhuu (2003), the permafrost at Nalaikh site could completely thaw during the coming 20 years.

DISCUSSION

The influence of permafrost as an impermeable layer can be well delineated and observed in comparisons with the distribution pattern of soil moisture in the Shijir valley. Water from precipitations was kept in active layers, leading to high moisture contents and groundwater levels beneath gentle NFSs. The differences in hydraulic conductivity and topography between steep and gentle NFSs enable subsurface water to flow downward laterally above the permafrost table and to stay beneath gentle NFSs, resulting in high moisture contents only beneath gentle NFSs (Fig. 1). Dry subsurface conditions on SPSs are likely to be dominated by vertical water movements, because of the absence of impermeable layers such as permafrost.

Vertical water movements also probably occur at the Nalaikh site underlain by extremely warm permafrost with dry active layers. Since the amount of unfrozen water in frozen soils increases as temperature increases to zero (*e.g.* Burt and Williams 1976), large amounts of unfrozen water are contained within the permafrost. This condition probably enables water to exchange between the bottom of the active layer and the uppermost part of the permafrost. Such permeable permafrost would not keep the overlaying active layer wet. As suggested in the unevenly distributed forest, this process may affect the land-surface hydrology even within the small areas and needs further studies with due consideration of the differences in permeability between contrasting sites with cold and warm permafrost.

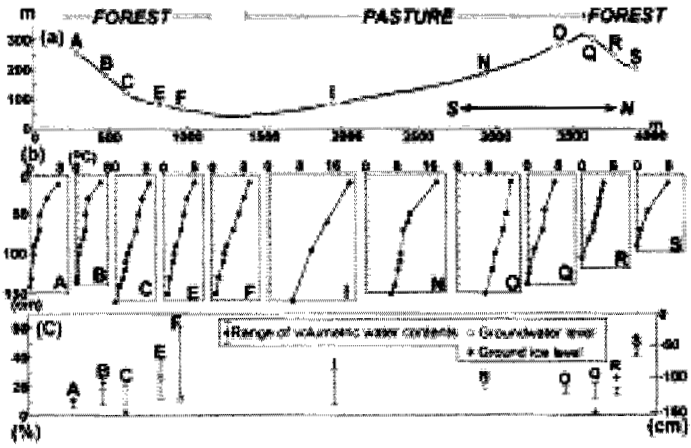

Figure 1. Spatial pattern of thermal and moisture conditions in the Shijir valley in mid-July, 2002: (a) Topography and location of each site (b) Ground temperature profiles (c) Volumetric water contents, depths of groundwater level and ground ice.

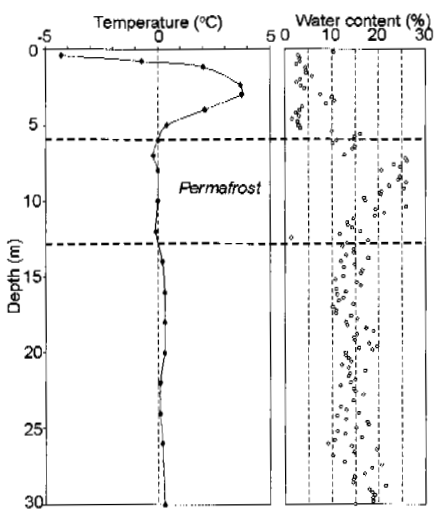

Figure 2. Thermal (1st November) and moisture (early October) profile at Nalaikh site.

REFERENCES

Burt, T. P. and Williams, P. J. 1976. Hydraulic conductivity in frozen soils. Earth Surface Processes, 1: 349-360.

Sharkhuu, N. in press. Recent changes in the permafrost of Mongolia. In: Proceedings of the 8th International Conference on Permafrost. Zürich, Switzerland.

Radio wave method for the determination of the electrical properties of permafrost in crosshole space

*V.A. Istratov, S.O. Perekalin, A.O. Kuchmin and * A.D. Frolov*

Radionda Ltd, Moscow, Russia

**Scientific Council on Earth Cryology, Russian Academy of Sciences, Moscow, Russia*

Geocryology studies are important during the construction and exploitation of engineering objects in permafrost areas. Investigations of inter-borehole space by the radio wave geo-introscopy (RWGI) method, whereby resistivity and dielectric permittivity are simultaneously defined, make it possible to ensure higher reliability when determining the forms and disposition of the geological inhomogenities within the volume under study (Borisov et al. 1993). RWGI measurements could be a reliable instrument for the delineation of the frozen - thawed sediment boundaries. This suggestion is made, first of all, because of the high dependence of formation resistivity and dielectric permittivity on the aggregate status of porous water.

The first tests in this domain were carried out in 1940 near Igarka (Eastern Siberia). These experiments have shown (Petrovsky and Dostovalov 1947) that the propagation of radio waves (up to frequency ~ 6.5 MHz) is quite possible through about 10 m of permafrost. Since this time there have been many tests using various radio wave techniques to study frozen formations. It needs to be noted that until recent years there was little evidence of a concrete technology (special equipment, procedures for field measurements, data processing, mode of result presentation etc.) to make such studies.

The physical-geological basis of the RWGI method is the relationship between the intensity of radio energy absorption along the wave path and the electrical characteristics of the soils. The coefficient of radio wave absorption (k") depends on the electromagnetic field frequency and the electrical properties of the medium:

$$k'' = \omega \left\{ \frac{\mu\varepsilon}{2} \left[\sqrt{1 + \left(\frac{1}{\rho\omega\varepsilon} \right)} - 1 \right] \right\}^{\frac{1}{2}} \qquad (1)$$

$\omega = 2\Pi f$, f is the operating frequency, μ and ε are, respectively, the absolute magnetic and dielectric permittivities, ρ is the resistivity of a medium.

In soils with a resistivity <100 Ωm, the radio wave absorption is practically not dependent on the dielectric permittivity (the medium is a quasi-conductor).
In frozen soils with high resistivity (ρ ▫ ~hundreds to thousands Ωm) and ε <30, radio wave absorption at frequencies of 30 MHz and higher depends considerably on permittivity (the medium is quasi-dielectric). When measurements are performed in an inhomogeneous medium, k" is an integral value that summarizes all the local changes in the medium absorbing properties along the wave path, or more correctly, within the most essential space for radio wave propagation (the first Fresnel zone). Having performed measurements at two fixed frequencies, it is possible to calculate the effective magnitudes of electric resistivity ρ_e and dielectric permittivity ε_e of soils within the studied intervals.

A special digital borehole radio equipment of the RWGI-2 series was designed and manufactured by "Radionda LTD" for measurements of the intensity of the electromagnetic field emitted using an electric (or magnetic) dipole antennae at the fixed frequencies of 0.061, 0.156, 0.625, 1.25, 2.25, 10.0 and 31.0 MHz. Cross-borehole measurements are usually performed following the "tomographic survey" technique, where the field is measured at each position of the transmitter in one borehole, over the whole working range of receiver displacement in the other borehole, - "in fan manner" (Fig. 1). To exclude the antenna effects of the cable, the borehole units are connected to the cable through dielectric inserts (coupler) with a fiber-optic channel and an optoelectronic converter. Besides measuring the electric (or magnetic) field intensity at the reception point and those of the current in the transmitting antenna, the equipment design makes it possible to execute transmitter tuning at each position in the borehole and to control the emission power. This makes it possible to operate in boreholes with distances of hundreds of meters from each other even with a short antennae. While processing, the measured data is corrected to exclude any differences in power emission. In the upper part of Figure 1 the scheme of RWGI-CB measurements along 6 sections with 4 boreholes (1-4) is presented as an example. The contour of the first Fresnel zone is shown for each section (between any pair of holes).

To obtain reliable final data, it is essential to secure a sufficient overlapping of these zones. To do this requires a preset and suitable operating frequency for the given con-

ditions for RWGI-CB. All this ensures the most complete and uniform studies of inter-hole space because every inhomogenity in the medium is explored at various angles.

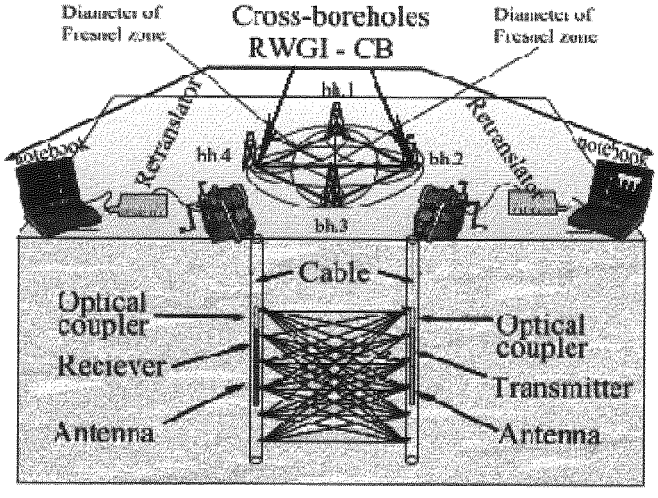

Figure 1. Principle scheme of the RWGI operation.

In the search for the absorbing properties distribution in inter-hole space, both 2-D and 3-D approaches to inverse problem solving are used. Electric anisotropy of the medium can be found from diagrams of angle dependence of absorption coefficients and can be taken into account. Using all the data obtained and taking into account spatial field characteristics, a 3D geoelectric map of the site is compiled by the technique of wave reconstruction. The map may be presented as a set of horizontal sections and arbitrarily oriented cross-sections, with isolines of ρ_e or (and) ε_e.

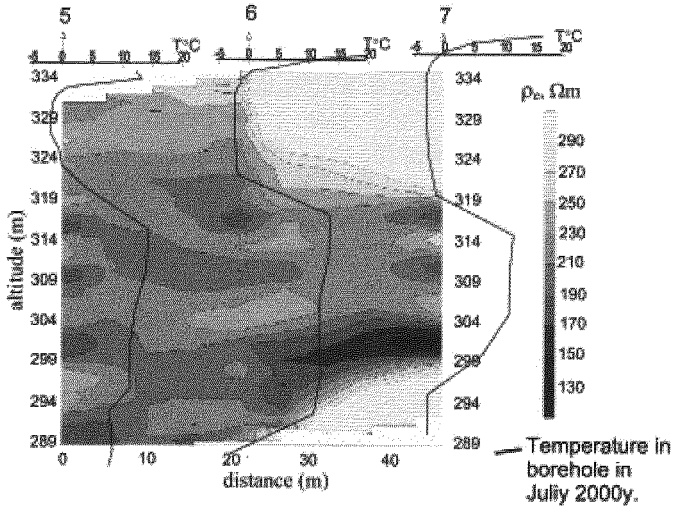

Figure 2. Example of the geoelectric section of effective resistivity (fragment of the 3D map) obtained from the field studies made by the RWGI-CB technique at the site near diamond pipe "Udachnaya".

As an example let us consider the investigations performed in order to delineate subsurface leakage channels from the Sytykan water reservoir (Yakutia). The crosshole RWGI measurements were provided using 1.25 MHz. A fragment of the geoelectrical map is shown in Figure 2. The section is orthogonal to the shoreline of the Sytykan reservoir. The temperature curves are also shown near each borehole. In is evident that by means of RVGI it is possible to extrapolate high temperature zones in an interhole media as areas of low resistivity. The most conductive zone corresponds to a leakage channel.

The briefness of this paper does not permit the discussion of the very interesting results of RVGI monitoring and the measurements of dielectric permittivity obtained at the same site (Snegirev et al. 2003).

The modern technology of RWGI measurements and associated data processing provides geocryological investigations with an appropriate resolution for engineering purposes.

REFERENCES

Borisov, B.F., Istratov, V.A. and Lysov, M.G. 1993. Method of radio wave cross-borehole geointroscopy. Patent of Russia 2084930.

Petrovskii A.A. and Dostovalov B.N. 1947 First experience of radiowave propagation in permafrost media. Proceedings of the Permafrost Institute 5: 121-160. Moscow: USSR Academy of Sciences press.

Snegirev, A.M., Velikin, S.A., Istratov, V.A., Kuchmin, A.O. and Frolov, A.D. 2003. Geophysical monitoring in permafrost areas. Proceedings of the 8th International Conference on Permafrost, Zurich, Switzerland.

Effects of volumetric ice content and strain rates on shear strength and creep rate under triaxial conditions for frozen soil samples

*M. M. Johansen and *L. U. Arenson*

Department of Civil Engineering, BYG·DTU, Technical University of Denmark, Lyngby, Denmark

**Institute for Geotechnical Engineering, Swiss Federal Institute of Technology, Zurich, Switzerland*

INTRODUCTION

Rock glaciers are special geomorphological phenomena of mountain permafrost. In some rock glaciers that have been investigated recently, a clear shear horizon has been detected (Arenson et al. 2002) in which most deformation takes place. Within an alpine environment, rock glaciers may have temperatures close to 0 °C (Vonder Mühll et al. 2003), which make them very sensitive to global warming. Even though rock glaciers in the Swiss Alps have been investigated intensively since the 1970s (e.g. Barsch 1996), there are still a lot of unanswered questions. In particular, the loss of strength of the frozen geomaterial, which might lead to stability problems of steep slopes, is expected as an effect of a warmer climate and is of major concern in Switzerland.

Therefore, a set of triaxial creep and shear tests were performed to study the effect of the volumetric ice content under natural stress conditions.

TESTS

The goal for this project was to examine mechanical response of various ice-solid mixtures from triaxial shear and creep tests. A programme was set up to test the strength under different confining pressures and for a range of strain rates as well as volumetric ice contents. The material was prepared as closely as possible to the natural conditions found in alpine rock glaciers (e.g. Arenson et al. 2002, Vonder Mühll et al., 2003) and tested at equivalent temperatures. To obtain controllable and repeatable tests, the original soil was mixed in the laboratory. Triaxial shear tests and creep tests were carried out in a cold room with a fixed temperature at the Institute for Geotechnical Engineering at the Swiss Federal Institute of Technology in Zurich. Artificially-made samples with an ice content of 30, 50, 80 and 100% by volume, respectively, were tested under changing testing parameters. The confining pressures s_3 were 50, 100 and 200 kPa and the strain rates used for the shear tests were 0.25, 2.5 and 25 mm/h. All tests were carried out at a temperature of about -1.5°C. During a test, the temperature variations were about +/-0.05 °C.

TEST RESULTS

Figure 1 shows the peak and the residual shear strength for samples with different ice contents at three different strain rates. Figure 2 shows the peak and residual shear strength for samples with different strain rates at four different ice contents.

The tests indicate that the strength of the frozen soil increases rapidly at the beginning of the test, probably due to ice strengthening, after which it reaches peak strength and drops to a lower value due to bonds cracking between the soil and the ice. The authors observed no clear trend between the strength and the confining pressure within the range of confining pressure tested, especially for ice-rich soils. A trend was recognized for soils with lower ice contents (30%). Soils with low volumetric ice content and high confining pressure showed a behaviour similar to unfrozen soils. Soil strengthening takes place due to structural hindrance of the solid particles after an initial slight strengthening of the ice with increasing solid content. This results in an increase of the strength during the test with increasing axial strain, which has also been described by other authors (e.g. Ladanyi 1981, Ting et al. 1983).

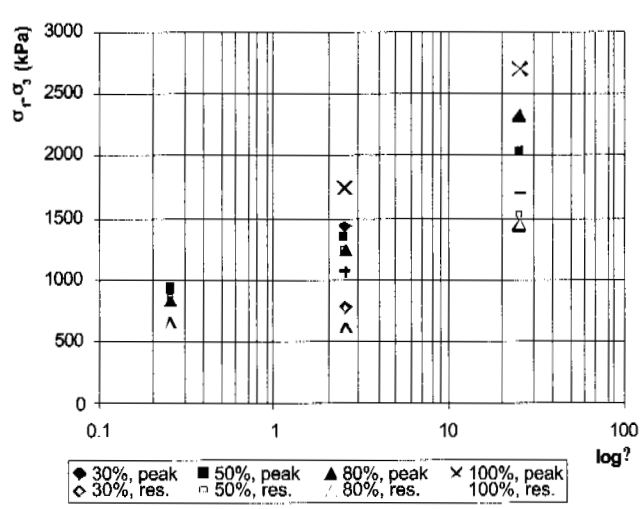

Figure 1. Shear strength (s_1-s_3) versus strain rate for different ice contents. Confining pressure s_3 = 100 kPa.

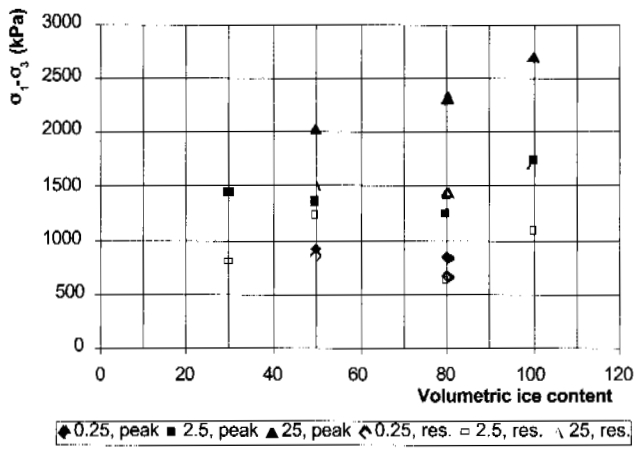

Figure 2. Shear strength (σ_1-σ_3) versus volumetric ice content at different strain rates. Confining pressure σ_3 = 100 kPa.

There is a clear trend that higher strain rates result in higher shear strengths. In general it is found that the strength increases with decreasing ice content except for the samples with 100% ice, which showed the highest strength (Fig. 1). The authors assume that this is because a different mechanism is in play. The sample showed a brittle behaviour with a sudden loss of strength after a peak value was reached.

Because of limited time, only a few creep tests were carried out. These could not be used for proper analysis. Further tests should be carried out to examine the creep behaviour of the frozen soil in more detail.

CONCLUSIONS

The following conclusions can be drawn from the tests on frozen soils presented.

Samples have to be prepared very carefully in order to achieve repeatable tests. The ends of the samples should be cut precisely and parallel to each other so that the stress is equally distributed on the surface. The technique used for sample preparation has proved to be appropriate, but an air content of about 4% was measured. To avoid air in the sample, different methods for the sample preparation should be considered.

The strength and the mechanisms of frozen soil are very dependent on the temperature. Lower temperature leads to higher strength. Small temperature differences in the soil samples and in the cold room used for tests can explain the different values for strength found for similar tests. On the other hand, small differences in the volumetric ice content might also have influenced the strength of the sample.

Due to the time limitations of this diploma project, it has not been possible to examine everything in depth. In additions, questions have arisen during the testing of the samples considering mechanical behaviour of frozen soil which are worth investigating further. The volumetric change in the samples should be examined and a better method to measure the volume of the sample should be developed.

The ice content versus shear strength should be examined in more detail. The tests were only made on samples with four different ice contents. To observe trends better, samples with different ice contents should be prepared and tested. In addition, the influence of the air in the sample and the difference between peak strength and high strain rates should be examined.

The reason for testing artificially-made samples instead of original samples extracted from a rock glacier is that it should be possible to carry out repeatable tests. This is often not possible when original samples are used, because the composition of the sample can vary and this not well recognized until after the test. Furthermore, the recovery of original permafrost samples is very expensive due to the costs of drilling and fieldwork. However, it was the intention to prepare and test the samples under similar conditions found in a real rock glacier. Further investigations on artificial soil samples may help in developing a better understanding of rock glacier dynamics.

REFERENCES

Arenson, L.U., Hoelzle, M. and Springman, S.M. 2002. Borehole deformation measurements and internal structure of some rock glaciers in Switzerland. Permafrost and Periglacial Processes 13: 117-135.

Barsch, D. 1996. Rock glaciers: indicators for the present and former geoecology in high mountain environments. Springer series in physical environment 16.

Ladanyi, B. 1981. Mechanical behaviour of frozen soils. Mechanics of Structured Media B: 205-245.

Ting, J., Martin, T. and Ladd, C. 1983. Mechanisms of strength for frozen sand. J. of Geotech. Eng. 109: 1286-1302.

Vonder Mühll, D. Arenson, L.U. and Springman, S.M. 2003. Temperature conditions in two Alpine rock glaciers. Proc. 8th Int. Conference on Permafrost, Zurich: this issue. Lisse: Swets & Zeitlinger.

Evolution of Alpine permafrost under the impact of climatic fluctuations (the results of numerical modeling)

*M. Kasymskaya, *D. Sergueev and N. Romanovskii*

Lomonosov Moscow State University, Faculty of Geology, Geocryology Department, Leninsky Gory, Russia
**Geophysical Institute, University of Alaska, Fairbanks, Alaska, USA*

Alpine permafrost is characterized by considerable spatial and temporal variability, especially near its southern boundary. To assess the evolution of alpine permafrost we used a 2-D computer-based model developed by G.S. Tipenko. This model takes into account (1) long-term climatic fluctuations, (2) the geometry of mountain relief, (3) the thermal properties of rocks and their moisture content and (4) the character of permafrost altitudinal zonality.

This model was applied to study permafrost evolution within a typical mountainous area in Southern Yakutia (Chul'man Depression) with its extremely continental climate, flat-topped mountains and a discontinuous distribution of permafrost. This area has an inverse type of altitudinal zonality, i.e., mean annual temperatures of both air and rocks rise as the absolute height increases. A profile across a mountain massif with flat-topped divide (950 m a.s.l.) and depression (750 m a.s.l.) was selected for modeling. (Fig.1)

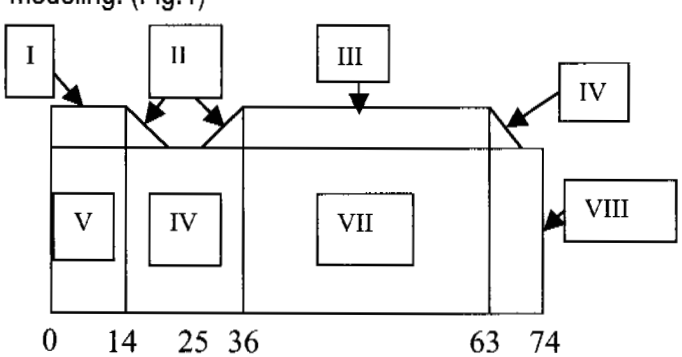

Figure 1. Chart of the model field

The new palaeogeographical scenario developed by A.V. Gavrilov for the last 120 ka was used (Fig.2) This scenario takes into account the effect of permafrost altitudinal zonality on the dynamics of mean annual ground temperatures. It was assumed that ground temperatures on the tops of plateaus (divides) rise above 0°C in the periods of maximum climatic warming.

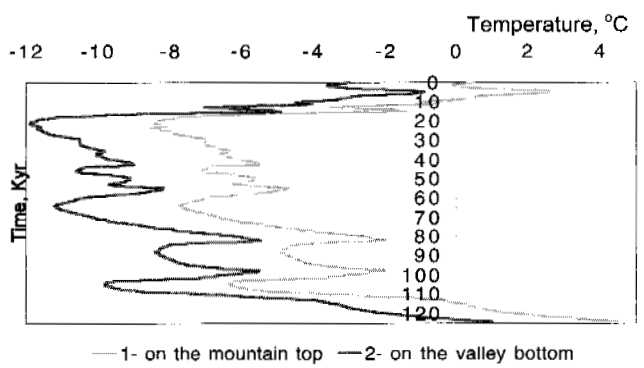

Figure.2. The curves of mean annual ground temperatures in accordance with the paleo- geographic scenario.

Numerical modeling showed that in the given type of mountains, permafrost temperatures in depressions and river valleys are substantially higher than those on watersheds. In periods of climatic warming, taliks can develop on the tops of plateaus. Thus, infiltration of atmospheric precipitation becomes possible in summer periods. It was also found that the maximum depth of permafrost is reached, with some time lag, after the minimum permafrost temperature has been attained.

The results of this modeling make it possible to estimate the effect of climatic fluctuations on the extent and depth of permafrost, as well as the amount of increase of groundwater through talik formation on local divides during phases of climatic warming. The appearance of these taliks considerably effect the groundwater and hydrological regime of local rivers, especially in the winter period.

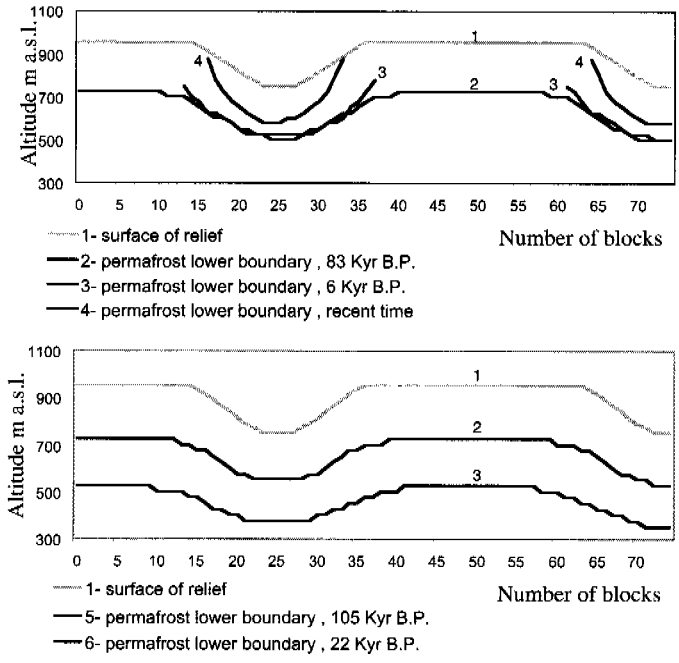

Fig.3. Surface of relief (upper boundary of alpine permafrost model) and position of permafrost lower boundary in different time periods.

REFERENCES

Sergueev,D., Tipenko, G., Romanovskii, N., Romanovsky, V., and Kasymskaya, M. 2002. Impact of Mountain Topography and Altitudinal Zonation on Alpine Permafrost Evolution and Ground Water Hydrology, AGU 2002 Fall Meeting Abstracts, San Francisco, California, USA.

Sergueev,D., Tipenko, G., Romanovsky, V., and Romanovskii, N. Mountain permafrost thickness evolution under influence of long-term climate fluctuation (results of numerical simulation). Proceedings of the 8th International Conference on Permafrost (In press).

An estimate of organic carbon input to the Arctic seas from permafrost and soils of the East Siberian coasts

A.L.Kholodov, D.G.Fyodorov-Davidov, E.M.Rivkina, S.V.Gubin, V.A.Sorokovikov, L.A. Fominikh, and D.A.Gilichinsky

Institute of Physicochemical and Biological Problems in Soil Science, Russian Academy of Science, Pushchino, Russia

Permafrost is a significant reservoir and potential source of ancient organic matter (plant remains, humified organics, etc.) and greenhouse gases (CO_2 and CH_4). Due to the degradation of permafrost as a result of coastal erosion, thermokarst formation and thawing of submarine permafrost, this organic carbon is easily released and reabsorbed again into the present biogeochemical cycle. The task of this study is to estimate possible organic input into the Laptev and East Siberia seas and atmosphere due to these processes as one objective of the IPA Arctic Coastal Dynamics program.

Investigations were carried out at three key sites: Bykovsky peninsula (129°30'E, 71°40'N.), Cape Svyatoi Nos (140°0'E 72°55'N), both in the Laptev Sea region, and Cape Chukochyi (159-55'E 70°05'N), East Siberian Sea coast. All sites are characterized by the widespread occurrence of fine-grained Quaternary sediments with large quantities of organic matter and biogases. There are two main types of landscapes associated with the deposits. One is the late Pleistocene ($l\text{-}alQ_{III}$) accumulative plain (Edoma formation or ice-complex) composed of syncryogenic ice-rich sediments. Mean annual ground temperatures within this landscape are -11 to -14°C. Shore cliffs are 20 to 40 m in height. The other type of landscape is characterized by alas depressions resulting from the thawing of ice-complex under thermokarst lakes. The alas complex includes layers of Holocene lake-boggy deposits ($l\text{-}bQ_{IV}$); layers of tabular deposits (thawed and redeposited ice complex; $tbQ_{III\text{-}IV}$), and residual ice complex (Fig. 1). Mean annual ground temperature is -9°C and the height of Laptev shore cliffs is less than 10 m but can reach 20 m along the East Siberian coast.

One of the main processes in this region is coastal erosion. The length of eroding shores of the Laptev Sea is 1000-1300 km, and for the East-Siberian Sea up to 2000 km. The rate of coastal retreat is 2-6 m/year (Are 1998). According to data obtained for the Cape Chukochyi at the East Siberian Sea, the coast has retreated at an average rate of 4.5 m/year during the past 18 years. Another important process which takes place in the region is erosion of the sea floor. This process is most active on the shallow shelves near the coast and on the seabed of former islands that were destroyed by erosion over the past centuries.

Total content of organic carbon was determined on dry soil samples using the wet oxidation method. Volumetric total C_{org} content for massive frozen soil was calculated on the basis of an assumed soil density (1700 kg/m^3). Calculations were carried out using a volumetric ice content of 75% for the ice complex and of 50% for the alas complex.

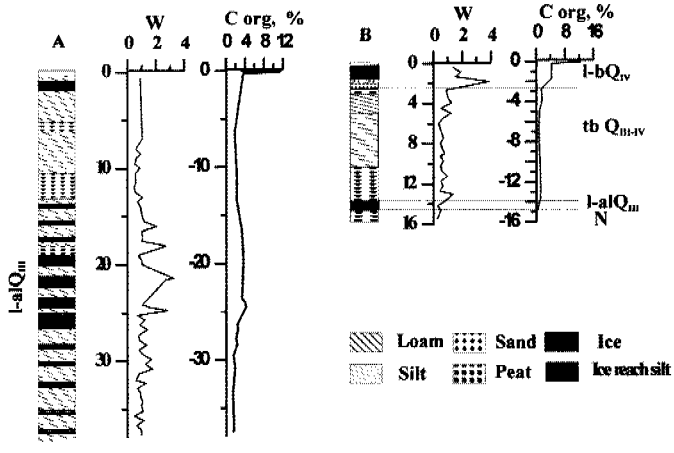

Figure 1. Texture, water and carbon contents of ice complex deposits (A) and alas complex (B) on Bykovsky Peninsula.

Supply of C_{org} for the different relief forms was determined for the active layer at the CALM sites R13, and R13A (Brown et al. 2000). Thickness of the active layer was taken as 0.5 m for hummocks, 0.4 for spot medallions, 0.3 m on the slope of hummocks, and 0.1 m in cracks. Soil density was assumed as 150-200 kg/m^3 for organic horizons, 800 kg/m^3 for mineral horizons in the upper part of the profile, and 1700 kg/m^3 for the lower part (Fig. 2). Results of the calculation of total C_{org} in frozen deposits and modern soils are given in Table 1.

It was determined that 1 m^3 of ice complex contains 5-12 kg of C_{org} Due to erosion of 1 m^2 of coastal territory, an amount of 25 to 425 kg of C_{org} can be delivered into Arctic seas.

Deposits of the alas complex are characterized by a similar total C_{org} (8-12 kg/m^3). The main part of organic

supply (75%) in these deposits is concentrated in upper parts of the section which are composed of lake-bogy sediments. Tabular deposits have less organic matter relative to the initial ice complex. Average organic content in a 50m thick section of massive ice complex on the Bykovsky peninsula is 22 kg/m^3, but a 10 m section of tabular deposits contains 3 to 10 kg/m^3. Thus, due to thawing of the ice complex during development of the thermokarst lake, decay of up to 50% of the organic matter took place (Fig. 1).

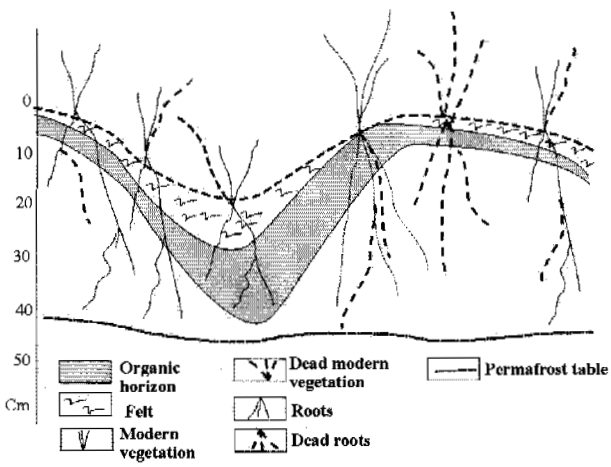

Figure 2. Typical profile of modern soil (Cape Chukochyi).

Table 1. Content of organic carbon in frozen deposits and modern soil of Laptev and East Siberian coastal zone.

Borehole	Deposits	Average TOC, kg/m^3
Bykovsky peninsula		
1-01	l-alQ$_{III}$	11.2
2-01	N-l-bQ$_{III-IV}$	12.2
Svyatoy Nos cape		
3-01	l-alQ$_{II-III}$	5.5
4-01	Q$_{II-III}$	3.4
Chukochyi cape		
2-91	mQ$_I$	71.1
3-91	lQ$_{III-IV}$	8.2
4-91	mQ$_{II-III}$	8.6
5-91	lQ$_{III-IV}$	11.2
6-91	lQ$_{III-IV}$	24.7
8-91	lQ$_{III-IV}$	11.0
10-91	l-alQ$_{III}$	5.9
Modern soil (Chukochyi cape)		
Edoma	Hummock	19.6
	Spot medallion	14.8
	Hummock slope	24.5
	Crack	5.6
Alas	Hummock	21.7
	Spot medallion	25.3
	Hummock slope	23.1

For the modern soils of the Edoma surface of Cape Chukochyi, the content of C_{org} is in the range of 5-9 kg/m^3. For alas depressions it is 7.5-11.5 kg/m^3. Similar values of C_{org} for sites along the Bering Sea coast (Svyatoi Lavrenty Cape) were obtained by D. Zamolodchikov (see abstract in this volume for site discussion). The average supply of total C_{org} in modern vegetation is about 1 kg/m^2.

On the widespread marine terraces, river deltas and alas depressions of Northeast Russia, where the bluff height is not more than 5 m, the total C_{org} input to the Arctic seas from modern soils is comparable with the C_{org} from cliffs. Total amounts of C_{org}, delivered to the Arctic seas due to coastal erosion of the Laptev and East Siberian seas can be up to 0.8 million tons/year or more, including 0.01 million tons of modern vegetation, 0.03 and more of modern soil, and more than 0.75 buried in permafrost. These values are comparable with the input from river discharge (0.85 million tons/year) (Danyushevsky 1990).

Due to the erosion of marine banks, the organic carbon could also be released into the atmosphere. The concentration of CH_4 in permafrost varies from 2 to 40 ml/kg and of CO_2 from 1 to 20 ml/kg; it should be noted that carbon dioxide is ubiquitous while the occurrence of methane is determined by the genesis of the deposits and by the type of cryogenic stratum. For example, the ice complex on the East Siberian coast is free of methane, while the alas complex contains 20 to 30 ml/kg of CH_4. We have calculated the amount of methane which could be released after thawing and abrasion of the Cape Chukochyi alas outcrops (with sediments containing 30 ml CH_4/kg and outcrop sizes being up to 1 km in length, – up to 20 m in height and with coastal retreat amounting to -1 m). The resulting value is close to 0.4 tonnes.

ACKNOWLEDGEMENTS

These investigations were carried out as a part of Russian Academy of Sciences "World Ocean" program and supported by the Russian Foundation for Basic Research (2003). The modern soil depths of thawing and organic matter content were studied within the framework of the NSF-supported CALM project (Brown et al. 2000).

REFERENCES

Are F. 1998. The contribution of shore thermo-abrasion to the Laptev Sea sediment balance. In Proceedings of the 7th Intern. Conference on Permafrost. Yellowknife, Canada: 25-31.

Brown J., Hinkel K.M. and Nelson, F.E. 2000. The Circumpolar Active Layer Monitoring (CALM) program: Research designs and initial results. Polar Geography 24 (3): 165-258.

Danyushevsky A. (ed) 1990. Organic substance of bottom sediments in polar zone of World Ocean. Leningrad, "NEDRA" (in Russian).

Long-term monitoring of borehole temperatures and permafrost-related data for climate change research and natural hazard management: examples from the Mattertal, Swiss Alps

*L. King, R. Hof, T. Herz and *S. Gruber*

Institut für Geographie, Justus Liebig-Universität Giessen, Germany

**Glaciology and Geomorphodynamics Group, Department of Geography, University of Zurich, Switzerland*

INTRODUCTION

Mattertal and neighbouring Saastal are certainly amongst the best investigated areas in the Alps with regards to permafrost distribution and natural hazard management. An extremely steep topography and traffic routes to touristic sites (e.g., Zermatt, Saas Fee) have led to intense research efforts by transport authorities and scientists in order to minimize risks for the population and tourists and to acquire the data necessary for natural hazard assessment and protection. Moreover, long-term temperature monitoring in deep boreholes and continuous climate measurements provide valuable data for permafrost distribution modelling and climate change research.

BOREHOLE MONITORING FOR CLIMATE CHANGE RESEARCH

Three boreholes have provided us with significant data concerning subsoil rock temperatures. The locations and the characteristics of the two boreholes on the Stockhorn plateau and the borehole at Ritigraben are shown in Table 1. The temperature curves vary considerably, mainly due to their respective positions and surface structures. Permafrost thickness is expected to be approximately 170 meters (Stockhorn Plateau) and more than 30 m (Ritigraben), respectively. The temperature curves show evidence of climatic warming during the last decades, however, the separation of topographic from transient effects in complex topography is a challenging task. The two boreholes at the east-west running crest of the Stockhorn show a very strong effect of exposure to permafrost characteristics. On the plateau and close to the northern face of the ridge –2,5° C have been measured at 30 metres depth, however, only –0,9° C were recorded at the southern face.

The Stockhorn and Ritigraben boreholes provide data for long-term monitoring of permafrost temperatures, an important source of data for climatic change research. In the high mountain areas of Europe, this idea was initiated by the EU project PACE (Permafrost And Climate in Europe) and the network is maintained by its ESF-sponsored continuation, PACE-21. The data is also integrated into international or national databases as GTN-P or PERMOS (PERmafrost MOnitoring Switzerland), forming a basis for global comparative research.

CLIMATE MONITORING AND PERMAFROST MODELLING

Long-term data gathered by the Inter-cantonal Measurement and Information System (IMIS, ENET) for avalanche warning provides permafrost-related information such as air and ground temperatures, precipitation, snow depth, global radiation, wind speed and wind direction in the Mattertal. These stations are often located in permafrost areas, as the 0°C-isotherme in the Mattertal lies slightly above 2600 m a.s.l. (Tab. 2).

In connection with information taken from DTMs, aerial photography, satellite imagery and research undertaken at the Giessen Institute for Geography (Gruber 2000; Philippi et al., in press), this climate information forms an excellent database for further permafrost modelling (Gruber and Hoelzle 2001) using a Geographical Information System (GIS). A field check with BTS measurements was done in March 2003. It is intended to implement this data into a neuronal network as this could prove to be a valuable tool for a better modelling of permafrost.

MONITORING FOR NATURAL HAZARD MANAGEMENT

The strong variability of climatic parameters in this relatively dry and continental climate may lead to extreme climatic events that could trigger catastrophic mass wasting processes due to the extremely steep topography of the whole Valais region. The increasing frequency of natural hazard events are a matter of great concern to the local, regional and national authorities. Great attention is therefore paid to the assessment and management of natural hazards.

More and more, it is realized that permafrost plays an important direct or indirect role in the assessment and prevention

of these hazards (Herz et al. in press). The responsible authorities and research organizations therefore support applied research of the mudflow origins in permafrost areas and the origin of unexpected water releases, the installation of early warning devices in mudflow canyons, the monitoring of degrading permafrost and the examination of the stability of avalanche protection structures in permafrost areas.

Table 1. Borehole Stockhorn Plateau and Ritigraben, location and borehole characteristics.

Stockhorn	Ritigraben	
Co-ordinates	45°59'00" N 07°49'05" E	46° 10' 27" N 07° 50' 56" E
Altitude	3410 m a.s.l.	2615 m a.s.l.
Slope inclination	8° S	14° NW
Date of Drilling	August 2000	October 2001
Borehole depth	100 m / 30 m	30 m
Permafrost thickness	170 m (approx.)	>30 m
Active layer depth	3.1 m	3.8 m
ZAA / MAGT	17.7 m/-2,5°C	14 m/-0,37°C
Active layer	bedrock	boulders

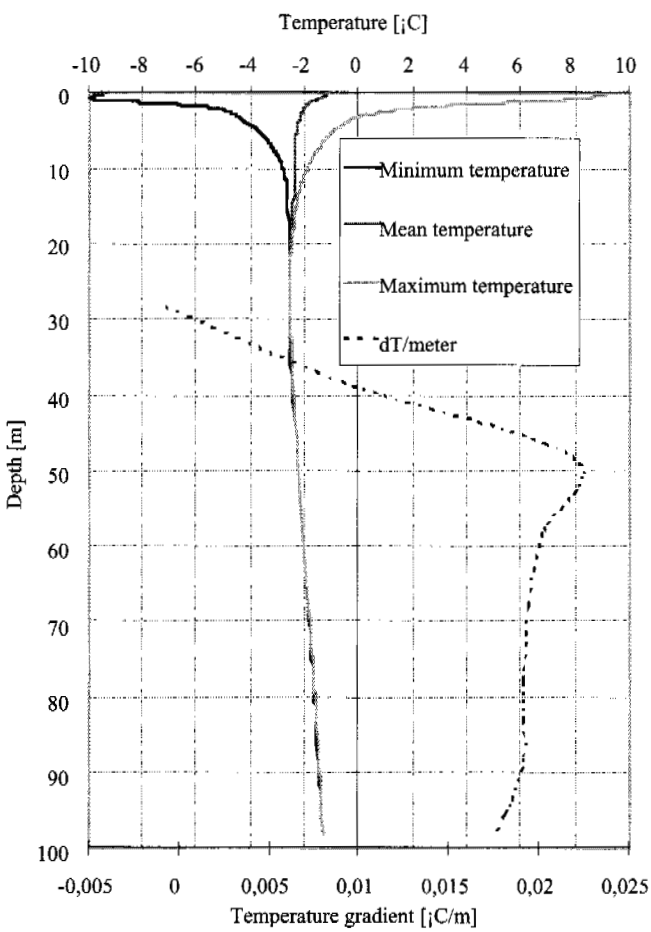

Figure 1. Rock temperatures and thermal gradient of the 100 meter deep Stockhorn borehole (01-10-2001 to 30-09-2002).

An early warning device has been installed in the Ritigraben gully above St. Niklaus. In the event of a debris flow it would automatically cause the main road in the valley to be closed. In a further step it is intended to use precipitation data from the weather station at the Ritigraben borehole as an early warning parameter, that is located close to the starting point of the debris flows.

Table 2. Selected IMIS and ENET-Climatic stations used for modelling purposes in the Matter valley.

Name 2001	Altitude	MAAT
Gornergrat snow station	2950m	-2,1°C
Gornergrat wind station	3130m	-2,7°C
Saas Platthorn	3246m	-3,9°C
Saas Schwarzmies	2810m	-1,3°C
Saas Seetal	2480m	+0,5°C
St. Niklaus Ob. Stelli Glacier	2910m	-1,6°C
Zermatt Platthorn	3345m	-4,5°C
Zermatt Triftchumme	2750m	-0,6°C

CONCLUSIONS

Long-term monitoring of permafrost temperatures in deep boreholes and the analysis and interpretation of climate data forms a valuable source of information for climate change research and permafrost distribution modelling. This information can also be used for natural hazard detection and protection.

REFERENCES

Gruber, S. 2000. Slope instability and permafrost – a spatial analysis in the Matter valley, Switzerland. – unpublished diploma thesis, Institute for Geography, University of Giessen, Germany.

Gruber, S. and Hoelzle, M. 2001. A statistical modelling of mountain permafrost distribution: a local calibration and incorporation of remotely sensed data. Permafrost and Periglacial Processes 12 (1): 69-77.

Herz, T., King, L. and Gubler, H. (in press). Microclimate within coarse debris of talus slopes in the alpine periglacial belt and its effects on permafrost. 8th International Conference on Permafrost, Proceedings, Zürich, 19-25 July 2003.

Philippi, S., Herz. T. and King, L. (in press): Near-surface ground temperature measurements and permafrost distribution at Gornergrat, Matter valley, Swiss Alps. - Poster Abstract. - In: 8th International Conference on Permafrost, Proceedings, Zürich, 19-25 July 2003.

Destruction of coasts on the Yugorsky Peninsula and on Kolguev Island, Russia

*A. I. Kizyakov and * D. D. Perednya*

Earth Cryosphere Institute SB RAS, Tyumen, Russia

**Moscow State University, Faculty of Geography, Russia*

Cryolithological, environmental and climatic features which determine coastal processes were investigated at the western coast of the Island Kolguev (Barents Sea) in summer 2002 and at the central part of the Yugorsky Peninsula coast (Kara Sea) in the summers of 1999, 2001 and 2002 (Cherkashov et al. 1999, Kizyakov et al. 2002, Perednya et al. 2002). Coasts at both sites consist of frozen sandy-clayey deposits enclosing tabular (massive) ground ice. Such tabular ice bodies control the formation of thermodenudational cirques as characteristic landforms: such thermocirques develop in slopes where tabular ground ice is found near the surface. They are formed by a variety of processes: thermokarst, coastal and lateral thermoerosion, retrogressive thaw slumps and earth flows.

The observed key sites differ in the activity of hydrodynamic processes. The western coast of Kolguev Island is open to wave action and the dynamically active ice-free period at the Barents Sea is longer than in the Kara Sea. At the Yugorsky key site, the hydrodynamic processes are weaker as a result of a very short ice-free period: the Kara Sea is completely covered with ice from October to May. Drift ice stays practically all summer. These conditions determine the character and dynamics of coastal destruction at the study sites.

Coastal bluffs on Kolguev Island are up to 40-50 m high. The coasts are of thermoerosion type, directly affected by waves. Bluffs are steep to overhanging. At the slope foot wave-erosion niches are formed and often remain partially filled with snow. The beach is narrow, up to 10 m wide and the bluff edges are dissected by numerous gullies which reflect a polygonal pattern (Fig. 1).

The three investigated coastal thermocirques are 200-400 m long (along the coast), and up to 200 m wide (landward). Analysis of the shoreline is done based on field inspection and aerial images from 1948 and 1968. Coastal retreat averages 3-4 m/year (Perednya et al. 2002).

One of the thermocirques formed after 1968. The retreat rate of its scarp was therefore no less than 5 m/year. Older thermocirques, however, are much less active and most likely retreat at a rate of less than1 m/year. At the Yugorsky key site, coastal bluffs have relative heights from 12 up to 29 m. Coasts are of the thermoerosion-thermodenudation type

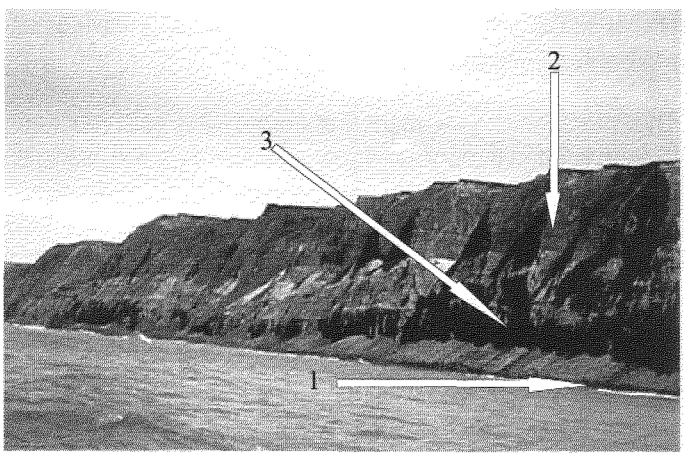

Figure 1. Smooth-faced wave-eroded coastal bluffs of Kolguev Island. A narrow beach (1), steep to overhanging bluffs (2) and wave-eroded niches (3) at the slope foot are common on the western coasts. Numerous gullies at the bluff edges reflect polygonal patterns.

and wave-erosion niches are not formed (Fig. 2). A complex of thermodenudation slope processes destroys coastal bluffs. Sediments are washed away by tides and most actively by storm surges after having been deposited on a beach. These sediments are involved in a shore-parallel drift directed west-to-east. In 2001, a monitoring network was established at a thermocirque scarp edge. The dynamics of long-term coastal retreat and thermocirque growth was recorded based on a comparison of field and remote-sensing data. Interpretation of aerial images from 1947 was combined with an analysis of topographic maps compiled using images from 1967.

The topographic survey of thermocirques and coastal-bluff edges was performed by theVNIIOceangeology Institute, St-Petersburg in 2001 (Kizyakov 2002, Kizyakov et al. 2002). The scarp most actively retreating from 1947 to 2001 was analysed and the retreat rate determined as 0.6 to 1 m/year, while the coastal-bluff retreat amounted to 1.3 - 1.6 m/year. The topographic survey enabled the compilation of a digital terrain model in SURFER software, which provided a reconstructed topography of the area prior to thermocirque formation and formed the basis forcal culating the sediment input from the thermocirque in 54 years. According to these calculations (Tab. 1), the thermocirques on the Yugorsky

coast increase the sediment yield, because the scarp edges are curved and thus longer than the shoreline for the smooth-faced bluffs.

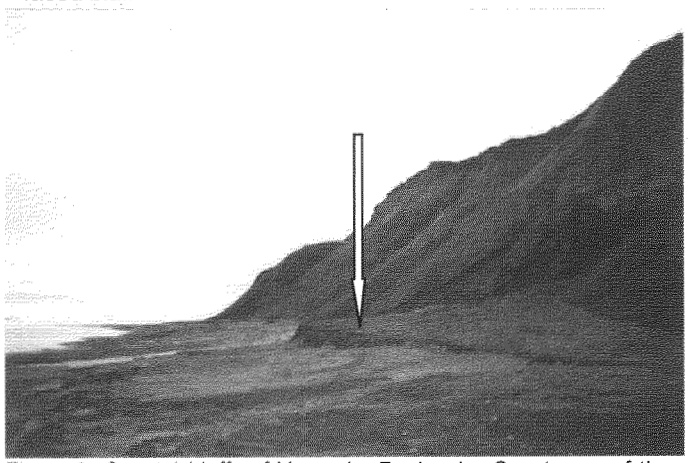

Figure 2. Coastal bluffs of Yugorsky Peninsula. Coasts are of thermoerosion-thermodenudation type. Arrow points to a wave-eroded sandy-silty fan formed due to the sediment yield from a gully.

The corresponding sediment flux from a vast catchment area is concentrated through a narrow exit. On average, sediment input from thermocirques appeared to be approximately 3 times as high as from the smooth-faced coastal bluffs. The total input of thermocirques for a large portion of the coast is rather low because the latter occupy only about 6% of the Yugorsky shoreline.

Table 1. The rate of retreat due to coastal thermoerosion and thermodenudation at the Yugorsky Peninsula and sediment yield per km of the shoreline

Destructive processes	Retreat rate m per year	Sediment yield m^3 per year
Coastal thermoerosion and falls at the coastal bluffs	1.3-1.6	30100
Complex of thermodenudation processes in thermocirques	0.6-1.04	89000

Thus, the western coast of Kolguev Island is of the thermoerosion type, and collapses as a result of direct mechanical and thermal wave influence. The coast of Yugorsky Peninsula in its central part, however, is of the thermoerosion-thermodenudation type and collapses mainly due to slope thermodenudation processes. At both study sites, thermocirques develop within smooth-faced slopes by thawing of tabular ground ice. The coastal retreat on Yugorsky Peninsula for the smooth-faced bluffs is slower by a factor of two than on the western coast of Kolguev Island. Active thermocirques of Kolguev Island are developing up to 5 times faster than on Yugorsky Peninsula. The development of thermocirques in the coastal zone increases the sediment yield per metre of a shoreline.

This points toward more active destruction of the Kolguev site in the western aspect of the study coast of Kolguev Island and specific hydrodynamic features (longer ice-free period, more wave action) of the Barents Sea.

ACKNOWLEDEMENT

The study was performed within the framework of the INTAS projects, grants 01-2329 and 01-2211.

REFERENCES

Cherkashov, G.A., Goncharov, G.N., Kizyakov, A.I., Krinitsky, P.I., Leibman, M.O., Persov, A.V., Petrova, V.I., Solovyev, V.A., Vanshtein, B.G. and Vasiliev, A.A. 1999. Arctic coastal dynamics in the areas with massive ground ice occurrence. Report of an International Arctic Coastal Dynamics Workshop, Woods Hole, 2-4 November 1999. Geological Survey of Canada Open File 3929.

Kizyakov, A.I., Perdnya, D.D., Firsov, Yu.G., Leibman, M.O. and Cherkashov G.A. 2002. Character of the costal destruction and dynamics of the Yugorsky Peninsula coast. Arctic Coastal Dynamics 3rd Workshop Proceedings, Oslo, 2-5 December 2002, (in press).

Kizyakov A.I. 2002. The forms of Kara Sea coasts destruction in conditions of widespread tabular ground ice. Extreme phenomena in cryosphere: basic and applied aspects. Abstracts of the International Conference, Pushchino, 12-15 May 2002. Pushchino: ONTI PNC RAS.

Perdnya, D.D., Leibman, M.O., Kizyakov, A.I., Vanshtein, B.G. and Cherkashov, G.A. 2002. Coastal dynamics at the western part of Kolguev Island, Barents Sea. Arctic Coastal Dynamics 3rd Workshop Proceedings, Oslo, 2-5 December 2002, (in press).

New insights of mountain permafrost occurrence and characteristics in recently deglaciated glacier forefields through the application of electrical resistivity tomography

C. Kneisel

University of Wuerzburg, Department of Physical Geography, Wuerzburg, Germany

INTRODUCTION

Different geophysical methods have been applied successfully in mountain regions to detect mountain permafrost. Since geo-electrical methods are most suitable for investigating the subsurface with distinct contrasts in conductivity and resistivity, DC resistivity soundings constitute one of the traditional geophysical methods which are standardly applied in permafrost research to confirm mountain permafrost over many years. During recent years advances have been achieved in using the traditional methods but with more powerful instruments and modern data processing algorithms which enable two-dimensional surveys and data processing (Vonder Mühll et al. 2001).

The study sites are situated in the Upper Engadine, eastern Swiss Alps, in the vicinity of St. Moritz (46°30'N, 9°50'E). Numerous rock glaciers are obvious geomorphological indicators of the discontinous distribution of alpine permafrost. Various aspects of mountain permafrost have been investigated in the past decades with the main focus on rock glacier permafrost. Discontinuous permafrost is encountered above 2400 m a.s.l. The investigation of permafrost in glacier forefields at high altitudes in the Upper Engadine was performed during recent years using one-dimensional geo-electrical soundings as the standard geophysical technique to detect mountain permafrost. The results of numerous measurements confirmed the local presence of perennially frozen ground and ground ice in the investigated glacier forefields (Kneisel 1998, 1999).

On heterogeneous ground conditions the interpretation of one-dimensional soundings can be difficult, as lateral variations along the survey line can influence the results significantly. The sounding curve produces an average resistivity model of the survey area, but individual anomalies such as small permafrost lenses will not show explicitly in the results. Hence, the interpretation is limited with respect to the characteristics and the local distribution pattern. Recently, two-dimensional electrical resistivity tomography which overcomes this problem using multi-electrode systems and two-dimensional data inversion was applied in the same glacier forefields and at the same location confirming the assumptions made by the one-dimensional vertical soundings.

The motivation of this contribution is to illustrate the opportunities and potentials of two-dimensional DC resistivity tomography for periglacial geomorphology providing a more detailed characterization of the subsurface as compared to the results obtained by traditional one-dimensional vertical soundings.

METHODS

For the one-dimensional geo-electrical soundings a *GGA30 Bodenseewerk* instrument was used. Three-layer models were calculated which are assumed to represent the most probable case with respect to the local geomorphological situation. For the interpretation of one-dimensional data the assumption is made that the subsurface consists of horizontal layers and that the resistivity changes only with depth but not horizontally. The typical one-dimensional geo-electrical sounding curve obtained on alpine permafrost shows a three-layer model with an increase of resistivity at shallow depth representing the active layer and the permafrost underneath, followed by a sharp decrease of resistivities at greater current electrode distances representing the unfrozen ground beneath. For the two-dimensional electrical tomographies a SYSCAL Junior Switch system was applied. The surveys were conducted using the Wenner configuration.

Resistivity values of frozen ground can vary over a wide range depending on the ice content, the temperature and the content of impurities. The dependance of resistivity on temperature is closely related to the amount of unfrozen water. Perennially frozen silt, sand, gravel or frozen debris with varying ice content show a wide range of resistivity values between 5 kWm to several hundred kWm (Haeberli and Vonder Mühll 1996).

RESULTS

The resistivity sounding profile shown in Figure 1 was measured in a high altitude glacier forefield using the symmetrical Schlumberger configuration. The graph shows only a slight

increase of the resistivity values. A three-layer model inversion was performed suggesting a first layer of 3 to 7 m representing the active layer and a second layer with a thickness of about 10 to 25 m. The resistivity values obtained for this middle layer (between 20 km and 35 km for equivalent models), lie in the range of perennial frozen ground and suggest a shallow permafrost occurrence at this site. The third layer with better conductivity represents the unfrozen ground underneath.

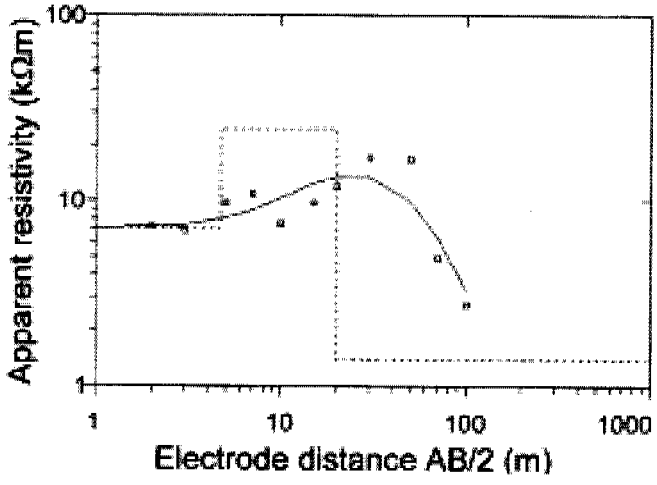

Figure 1. One-dimensional DC resistivity sounding profile

This shape of geoelectrical sounding graphs is considered to be typical of permafrost in glacier forefields. Similar curves have also been measured in other investigated forefields. With the special conditions in glacier forefields, permafrost occurrences can be assumed to be shallow, "warm" and thus, rich in unfrozen water, what can explain the comparatively low apparent resistivity values (Kneisel 1999). Figure 2 illustrates the results of the two-dimensional resistivity survey performed at the same location where the one-dimensional geoelectrical soundings were performed in the previous study which already indicated a permafrost occurrence. The dark grey colors represent perennially frozen ground. Through the one-dimensional sounding similar thickness of the active layer and depth of the permafrost were obtained. However, since one-dimensional geoelectrical soundings produce only an average resistivity model of the survey area, the lenticular high-resistive areas as shown in the 2-D image could not be deduced.

Additionally, topography was incorporated in the inversion, resulting in a more realistic interpretation of the obtained resistivity image of the subsurface. This is especially evident in the depression between station 45 and 55 where the active layer is markedly thinner due to the late-lying snow. Here, the potential of electrical resistivity tomography for geomorphological investigations compared to one-dimensional soundings is shown clearly, as a more sophisticated interpretation of the subsurface can be derived. Furthermore, the opportunity for a real mapping over larger areas is a major advantage for geomorphological studies.

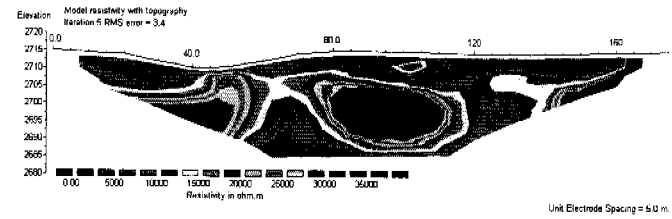

Figure 2. Resistivity tomogram of a Wenner survey with mountain permafrost

The described examples from two surveys in the periglacial environment illustrate that electrical resistivity tomography is a powerful tool to determine the structure of the subsurface at different resolutions, depending on the electrode spacing and array geometry employed. For a reliable interpretation of the survey results, knowledge of the geomorphological and geological setting is essential. Further details of applicability of different array geometries, advantages and disadvantages of the electrical resistivity tomography and its application to various geomorphological studies are given in Kneisel (2003).

REFERENCES

Haeberli, W. and Vonder Mühll, D. 1996. On the characteristics and possible origins of ice in rock glacier permafrost. Z. f. Geomorph. N.F. Suppl. 104: 43-57.

Kneisel, C. 1998. Occurrence of surface ice and ground ice/permafrost in recently deglaciated glacier forefields, St. Moritz area, Eastern Swiss Alps. 7th International Conference on Permafrost, Yellowknife, Canada. Proceedings: 575-581.

Kneisel, C. 1999. Permafrost in Gletschervorfeldern - Eine vergleichende Untersuchung in den Ostschweizer Alpen und Nordschweden. Trierer Geographische Studien 22.

Kneisel, C. in press. Electrical resistivity tomography as a tool for geomorphological investigations – some case studies. In: L. Schrott, A. Hoerdt and R. Dikau (eds.). Geophysical methods in geomorphology. Z. f. Geomorph., Suppl.

Vonder Mühll, D., Hauck, C., Gubler, H., McDonald, R. and Russill, N. 2001. New geophysical methods of investigating the nature and distribution of mountain permafrost with special reference to radiometry techniques. Permafrost and Periglacial Processes 12: 27-38.

Evidence of paleotemperature signals in mountain permafrost areas

*T. Kohl and *S. Gruber*

Geophysical Institute, ETH Zürich, Switzerland

**Glaciology and Geomorphodynamics Group, Department of Geography, University of Zurich, Switzerland*

INTRODUCTION

In Alpine environments ground temperature changes may have a significant effect on permafrost. As a consequence, future warming is likely to lead to increased instability in mountain permafrost terrain. However, field studies of thaw-related slope instability are hampered by the natural variability of geomorphic processes, both in space and time. To quantify the impact of recent climate variation, borehole temperature measurements were taken using 30 thermistors at the 3400 m high Stockhorn in the central part of the Swiss Alps. The measurements show non-linear thermal profiles, with pronounced near-surface temperature deviations from the deeper thermal gradient. Although climatic-induced temperature effects seem to be evident, other topography-induced thermal signals cannot be excluded. The present analysis aims at the investigation of coupled transient and topography effects which should also elucidate the significance of temperature measurements in alpine terrains.

METHOD

The investigation was conducted using the FE code FRACTure (Kohl and Hopkirk 1995). One of the features of this code is the integration of complex topography and surface condition into a robust and reliable numerical code. The FE-forward scheme is now linked with the UCODE computer program which can be broadly used for various applications. In combination, UCODE and FRACTure perform inverse modelling, posed as a parameter-estimation problem, by calculating parameter values that minimize a weighted least-squares objective function using non-linear regression. With this tool complex multi-dimensional inversion studies can be theoretically accomplished. However, numerical instability and nonuniqueness represent well-known problems in inverse modelling, and obtaining useful results can become more difficult for highly heterogeneous conditions. Therefore, the problem was focused on properties that seem to have the major impact on the near-surface temperature field: surface temperature distribution and accurate topography representation. The analysis of these near-surface energy fluxes is therefore represented by a two-dimensional homogeneous model assuming constant basal heat flow at 3.5 km depth below the Stockhorn but with transient surface temperature variation. The model included 20,000 nodes. The mesh was strongly coarsened from surface (<5 m distance between nodes) to greater depth (100 m distance). Topography was taken at 10 m distance from a DTM along a N-S running profile of the Stockhorn.

RESULTS

Figure 1 illustrates typical temperature curves along the selected profile. The influence of changing surface temperature (due to different altitude, surface, radiation) is well visible at z=0 m and the influence of topography is shown by the different curvature. It becomes clear that

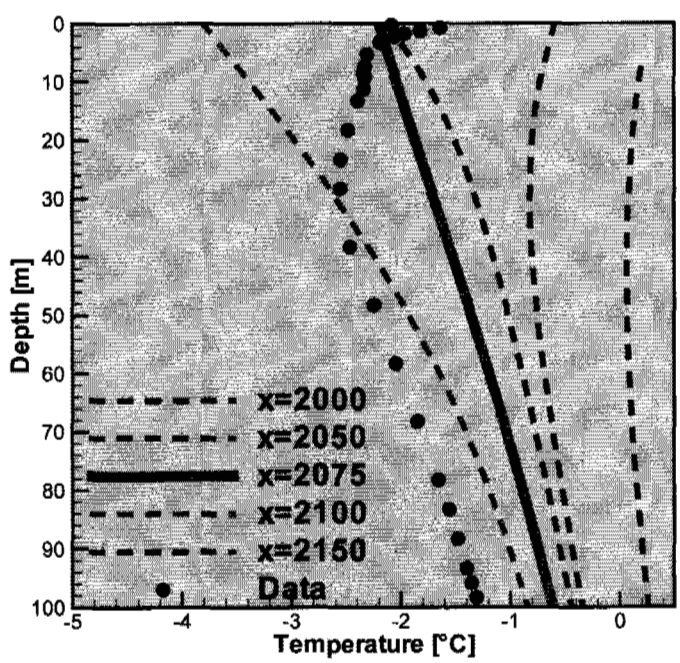

Figure 1. Temperature profiles along selected sites: the measured temperature data are given by black dots, the T-profile at x=2075m represents the calculated temperature from steady-state assumptions.

only a small displacement of the borehole location would result in completely different T(z) profiles. Under steady-state conditions, the results are nearly independent of thermal conductivity along the borehole depth. To account for transient effects, a climatic time series from a nearby study (Böhm et al. 2001) was initially superimposed on the surface temperature. When performing 2nd order regression on these strongly varying data, basically a 1.3°C warming between 1900 and 2000 can be identified, between 1800 and 1900 surface temperature did not change drastically. However, our calculations have shown better fits with a more pronounced warming in the last 50 years. Figure 2 illustrates the additional curvature in the T(z) profile due to climatic warming.

CONCLUSION

Our analysis has demonstrated that the ground surface temperature distribution is highly sensitive to the shallow (~100 m deep) subsurface temperature field. In alpine terrains, energy fluxes can even be totally dominated by topography without any influence of basal heat flow. Under these circumstances, temperature measurements need to be carefully designed and located at those points which are less sensitive and which provide the most useful data. Our procedure can also be applied successfully to further locations to optimize different configurations and temperature logging devices at specific sites.

REFERENCES

Böhm R., Auer I., Brunetti M., Maugeri M., Nanni T. and Schöner W. 2001. Regional temperature variability in the European Alps 1760 - 1998 from homogenised instrumental time series. International Journal of Climate 21: 1779-1801.

Kohl T. and Hopkirk R.J. 1995, "FRACTure" a simulation code for forced fluid flow and transport in fractured porous rock. Geothermics 24(3): 345-359.

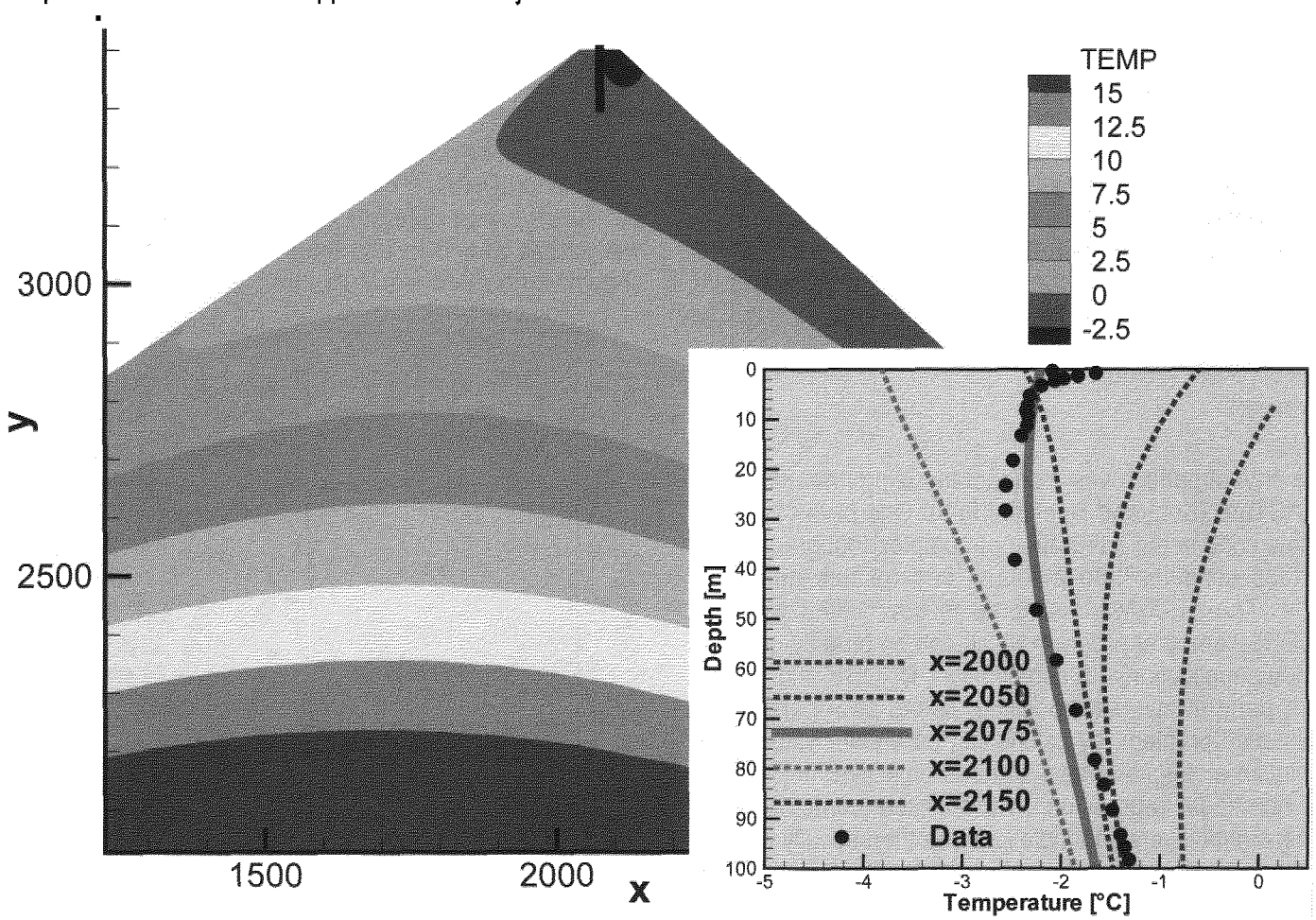

Figure 2. Temperature field from a transient calculation. The nearly vertical geotherms at Stockhorn peak illustrate the dominant role of topography.

Hydrological modelling of (sub)arctic river systems: responses to climate change

E. Koster, R. Dankers and S. van der Linden

Centre for Geo-ecological Research, Department of Physical Geography, Utrecht University, Utrecht, The Netherlands

PERMAFROST HYDROLOGY

Hydrologic modelling of river regimes is restricted by our poor knowledge of permafrost-related processes and by a paucity of data (Woo 2000). Frozen ground is relatively impermeable, especially when ground ice content is high. Warm spring temperatures melt the bulk of the snowpack within a few days or weeks, while the soils are still frozen. The closer to the summer solstice, the greater the incoming solar radiation so that the spring thaw is often intense (Woo 2000), leading to overland flow as the rate of melt exceeds infiltration capacity. When the active layer thickness increases towards the end of the thawing season, infiltration rates increase and surface runoff is correspondingly reduced. Not surprisingly, the annual catchment water balance in permafrost areas often shows a high runoff/precipitation ratio. Typical values range from 0.7-0.8 in high-Arctic polar deserts to 0.4-0.6 in sub-Arctic tundra regions and wetlands because of higher evaporation (Woo 2000). However, wide variations in ratios do occur between different catchments. During summer with greater thaw depth, depleted groundwater stores, and increased evapotranspiration, the hydrograph will respond less markedly to rainfall. Nevertheless, rainstorms may still occasionally produce strongly peaked hydrographs. In winter, river discharge is usually low or sometimes even absent. Another characteristic of the periglacial fluvial domain is the sometimes very high percent of the annual runoff that occurs within the two to three weeks of the snowmelt flood (break-up), with a corresponding concentration of sediment transfer. Finally, the presence of permafrost accentuates runoff peaks while reducing groundwater supply to river runoff and thereby base flow.

WATER BALANCE MODELLING

In the framework of two EC-funded research projects, "Barents Sea Impact Study" (BASIS) and "Tundra Degradation in the Russian Arctic" (TUNDRA), hydrological modelling studies of the Tana river in northern Fennoscandia and the Usa River as part of the Pechora basin in northern Russia were conducted (Dankers 2002, Van der Linden 2002). The hydrographs of both river systems fall within the category of the subarctic nival river regime. The Tana River catchment is 16,000 km^2 in size; mean annual discharge is only 166 m^3/sec; interannual variation is high; snowmelt runoff, with a maximum discharge as high as 3,000 m^3/sec, may contribute as much as 65 % to the total annual runoff; mean annual T varies from -0.5 to -3°C and mean annual P from ca 350-450 mm; discontinuous permafrost occurs. The Usa catchment is 93,000 km^2 in size; peak discharges vary from ca 4,000 to more than 7,000 m^3/sec; mean annual T varies from –3 to -7°C and mean annual P from 400 –800 mm; continuous, discontinuous and sporadic permafrost zones occur from north to south.

The sensitivity of the discharge of the Tana and Usa rivers to changes in climate was evaluated with hydrological models, called TANAFLOW and USAFLOW, respectively, in both cases based on a spatially-distributed water balance model (RHINEFLOW) developed for the Rhine River by Kwadijk (1993). Both models are embedded in a GIS and calculate the water balance for grid cells of 1 by 1 km; runoff is subsequently routed over a digital elevation model (DEM) of the area and accumulates at the catchment outlet. Originally designed for monthly time steps, the models have now been applied on a 10-day basis. Moreover, the USAFLOW model (Van der Linden 2002) has been adapted for cold-climate conditions by introducing variable (in space and time) separation coefficients - dividing rapid (surface) runoff from water added to groundwater storage – for continuous (1.0 ≡ 100% rapid runoff), discontinuous (0.9), sporadic permafrost (0.8) and for seasonal frost (0.6).

IMPACT OF CLIMATE CHANGE

In general, it is expected that should warming occur, permafrost will degrade, and storage capacity of the soil will increase. Consequently, there will be fewer high flow events of large magnitude, and the probability of extremely low flows will also diminish. R/P ratios will de-

crease as groundwater storage increases, but surface flow remains important during spring (Woo 2000, Van der Linden 2002). By introducing temperature and precipitation changes concurrent with state-of-the-art climate scenarios, the sensitivity of river discharge to these climate variables was established (Harding et al. 2002). Fig. 1A illustrates the change in the Tana hydrograph between a control run (simulated for the period 1980-1993) and a scenario run (simulated for the period 2070-2100), derived from the RCM HIRHAM4 model. The combined effects of increased temperatures, precipitation and evaporation result in a distinctly earlier timing (by about 20 days) of the runoff peak, which is also slightly higher. The latter is due to the somewhat larger snow mass, in spite of the shorter snow season, and reduced sublimation. Although smaller in amounts, the relative increase in runoff is even larger in the rest of the year. As baseflow is higher, runoff in winter has increased in the scenario run as well. Fig. 1B illustrates the change in the Usa hydrograph for the present situation and according to a GCM HADCM2 scenario projection to the period around 2080. It shows a decrease in peak discharge. In this region the increased evaporation in summer due to a rise in temperature is not compensated by larger precipitation amounts, which causes discharge to decrease. To further improve hydrological models, the feedback effects of vegetation responses to climate change should be taken into account. In conclusion, these studies reveal that the indirect effects of climate change (e.g., vegetation and permafrost changes) on discharge in (sub)arctic areas are relatively small compared to direct effects.

REFERENCES

Dankers, R. 2002. Sub-arctic hydrology and climate change. A case study of the Tana River Basin in Northern Fennoscandia. Netherlands Geographical Studies 304, 237 pp.

Harding, R., Kuhry, P., Christensen, T.R., Sykes, M.T., Dankers, R. and Van der Linden, S. 2002. Climate feedbacks at the tundra-taiga interface. Ambio Special Report 12: 47-55

Kwadijk, J.C.J. 1993. The impact of climate change on the discharge of the River Rhine. Netherlands Geographical Studies 168, 201 pp.

Van der Linden, S. 2002. Ice rivers heating up. Modelling hydrological impacts of climate change in the (sub)arctic. Netherlands Geographical Studies 308, 174 pp.

Woo, M-K. 2000. permafrost hydrology. in: Nuttall, m. and Callaghan, T.V. (eds.): The Arctic, Environment, People, Policy. Harwood, Amsterdam: 57-96

Using BTS for mapping permafrost distribution in Apussuit, SW Greenland

L. Kristensen

Institute of Geography, University of Copenhagen, Denmark

INTRODUCTION

Permafrost in Greenland has been mapped on a national scale by Weidick (1968) and Christiansen and Humlum (2000) but no previousl attempts have been made to map mountain permafrost on a local or regional scale. Geomorphological indicators of permafrost such as pingos and rock glaciers, as well as borehole temperatures from permafrost, are reported from various locations in Greenland. On the west coast of Greenland the southernmost location of reported geomorphological indicators of permafrost is in the Sisimiut area. Here, borehole temperatures show thin permafrost at sea level.

The BTS Method (Haeberli 1973) has been succesfully used for mapping mountain permafrost in the Alps and other mountain regions but, so far, has not been used in Greenland.

SITE DESCRIPTION

The Apussuit study area covers 30 * 40 km and is located on mainland Greenland at 65°32'N, 52°22'E, 25 km NE of Maniitsoq, approximately 30 km from the outer west coast and 100 km west of the Inland Ice sheet. The area is located in a zone of discontinuous permafrost and on the border between sporadic and discontinous permafrost on Weidick's (1968) and Christiansen and Humlum's (2000) permafrost maps of Greenland. However, no previous studies on permafrost have been carried out in the area.

The Apussuit ice cap sits on a narrow plateau at 800 - 1133 m a.s.l. and measures around 110 km^2. Some of the highest mountains of western Greenland are located north of Apussuit, where large ice caps can also be found. The mountains were probably nunataks during the Quartenary glaciations (Weidick 1968). The landscape south of Apussuit has a gentler, glacially-eroded topography. Sediments are sparse due to low weathering rates of the archaic gneisses, so apart from block fields and talus slopes, geomorphological indicators of permafrost are rare. The fieldwork was carried out near a small skisport center at a nunatak in 931 m a.s.l. The mean annual air temperature at sea level is around -1°C.

METHOD

A Digital Terrain Model (DEM) with a cell size of 40 * 40 m was interpolated from 150,000 point values originating from photogrammetry of aerial photographs. The potential direct solar radiation (PR) was calculated on an hourly basis throughout the DEM and averaged over a year. The calculations include damping of the radiation through the atmosphere and shadow from the surrounding horizon.

160 BTS measurements at 81 points were recorded between 925 m a.s.l. and sea level, together with GPS location, snow depth, inclination and aspect. The measurements were made at snow depths between 85 cm and 200 cm. The mean distance between the recorded GPS point and the centre of the appropriate cell in the DEM was 15.1 m. The differences between measured and modelled inclination and aspect were 8.4° and 39.8° respectively. These differences are most likely caused by differences in scale as the parameters in the field were measured for an area covering around 10 * 10 m, whereas the cell size in the model was 40 * 40 m.

RESULTS AND DISCUSSION

130 measurements were in the "permafrost probable" BTS class (BTS < -3°C), 17 in the "permafrost possible" BTS class (-3°C < BTS < -2°C) and 13 in the "permafrost improbable" BTS class (BTS > -2°C, Hoelzle 1992). The highest located point in "permafrost improbable" BTS-class was at 283 m a.s.l.; the highest point in "permafrost possible" BTS class was measured at 478 m, whereas several points in the "permafrost probable" BTS class were found near sea level. The results are supported by borehole temperatures from the area showing permafrost at

360 m a.s.l.

The BTS measurements were analyzed with respect to altitude, PR and snow depth. Within the measured interval of snow depths, no significant relation between BTS and snow depth was found. Altitude explains 59 % of the variance in BTS and PR 25 %. However, a significant negative correlation (r = -0,33) between PR and BTS shows that the dataset is biased, indicating that areas facing south are more likely to have been sampled at low altitudes. Because of this multiple regression, using both altitude and PR as the controlling variables only improves R^2 to 66 %. The relation takes the form:

$$BTS = -0.0054 \times altitude + 0{,}028 \times PR - 5.30$$

The equation was applied to the entire study area, simulating BTS throughout the DEM. 121 BTS measurements were assigned to the appropriate BTS class, 33 were assigned to the neighbouring BTS class, whereas six were assigned to two BTS classes from the measured one. According to this relation, permafrost limits are highly influenced by radiation. Areas receiving low amounts of radiation are modelled to belong to the "permafrost probable" BTS class at sea level, whereas areas receiving maximum radiation are modelled to the "permafrost improbable" BTS class up to 250 m a.s.l. and "permafrost possible" up to 430 m a.s.l. The importance of altitude and PR in explaining BTS is comparable to findings from Jotunheimen and Dovrefjell, southern Norway (approximately 62°), though permafrost in these areas is found at higher altitudes (Ødegård 1996). Radiation is probably of much greater importance in the eastern Swiss Alps (approximately 46°, Hoelzle 1992) than in Greenland, which might reflect the lower latitude and higher amounts of radiation received in the Alps.

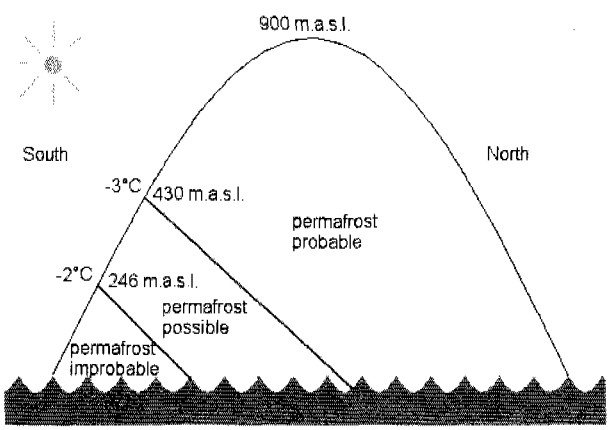

Figure 1. The effect of PR on BTS classes and permafrost limits as found by the model.

CONCLUSIONS

BTS measurements in the Apussuit region indicate widespread permafrost in the area, even at sea level. The results are supported by borehole temperatures from the area showing permafrost at 360 m a.s.l. However, multiple regression including both altitude and PR shows that the thermal regime of the ground is highly influenced by PR as permafrost-free areas or areas marginal to permafrost are found up to nearly 500 m a.s.l. where PR is high.

REFERENCES

Christiansen, H. H. and Humlum, O. 2000. Permafrost. In B. H. Jakobsen. Böcher, J. Nielsen, N. Guttesen, R. Humlum, O. and Jensen, E (eds), Topografisk Altas Grønland. København: C.A. Reitzels Forlag.

Haeberli, W. 1973. Die Basis-Temperatur der winterlichen Schneedecke als möglicher Indicator für die Verbreitung von Permafrost in den Alpen. Zeitschrift für Gletscherkunde und Glazialgeologie 9: 221-227.

Hoelzle, M. (1992). Permafrost occurrence from BTS measurements and climatic parameters in the Eastern Swiss Alps. Permafrost and Periglacial Processes 3: 143-147.

Weidick, A. 1968. Observations on some Holocene glacier fluctuatuins in West Greenland. Meddelelser om Grønland. 164(6): 1-202.

Ødegård. R. S. Hoelzle, M. Johansen, K. V. and Sollid, J. L. 1996. Permafrost mapping and prospecting in southern Norway. Norsk geogr. Tidsskr. 50: 41-53.

Measuring rock glacier surface velocities with real time kinematics GPS (Mont Gelé area, western Swiss Alps)

*C. Lambiel, *R. Delaloye, **L. Baron and R. Monnet*

Institute of Geography, University of Lausanne, Switzerland

**Dept. of Geosciences, Geography, University of Fribourg, Switzerland*

***Institute of Geophysics, University of Lausanne, Switzerland*

INTRODUCTION

Studies on rock glacier movement have been led for a long time on several sites in the Alps (e.g. Barsch 1992). Methods applied until now are essentially measurements using theodolites (e.g. Francou and Reynaud 1992) and aerial photogrammetry (e.g. Kääb et al. 1997). Rock glacier surface velocities measurements with Real Time Kinematics (RTK) GPS have been tested in the Mont Gelé area (Verbier, Swiss Alps, 46°06'N/7°17'E).

The studies were conducted on three rock glaciers, two of them (B and C) north-northeastern oriented and the third one (D) facing towards the east. Rock glacier D is mainly inactive (presence of depressed parts, no steep front, abundance of lichens), whereas rock glaciers B and C are clearly active (very steep fronts, unstable blocks, no lichens). The roots of rock glacier C are largely covered by an ice patch. The occurrence of permafrost is corroborated in all rock glaciers by many BTS measurements performed since 1993 and by continuous logging of the subsurface temperature using miniature loggers UTL-1.

In summer 1998, DC resistivity soundings and mapping lines were carried out on the rock glaciers (Reynard et al. 1999). Some of the results are presented in Figure 1. Marked differences in resistivities are primarily interpreted as differences in ice content. They also could reveal differences in temperature of the ice/rock mixture. According to Reynard et al. (1999), rock glaciers B and D contain congelation ground ice and are therefore considered as typical periglacial rock glaciers. Low resistivities (max. 50 kWm) should indicate a permafrost temperature close to the thawing point. Feature C is more complex. The presence of the ice patch at its roots and the high resistivities measured (specific resistivity of about 350 kWm) indicate the presence of massive (and colder?) ice within the rock glacier. The resistivity mapping demonstrated that there was no break between the ice patch in the rooting zone and the rock glacier (Reynard et al. 1999).

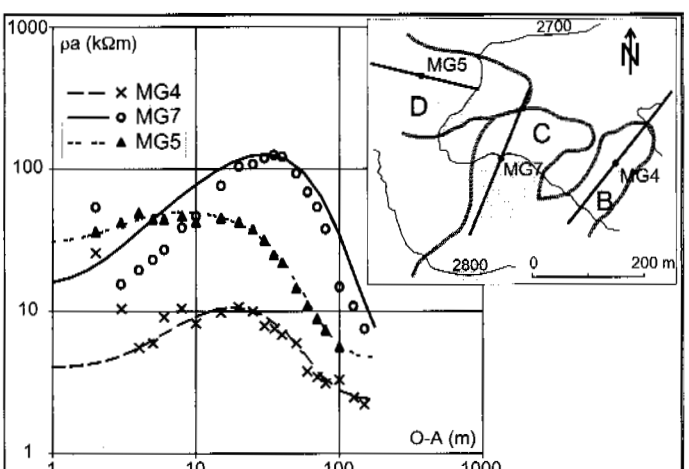

	MG4		MG7		MG5	
	Thick. (m)	ρ(kΩm)	Thick. (m)	ρ(kΩm)	Thick. (m)	ρ(kΩm)
1st layer	2.5	4	1.5	20	1.5	30
2nd layer	10	20	12	350	1.5	90
3nd layer		2.3		6	16	45
4nd layer						4.5

Figure 1. Three of the DC resistivity soundings carried out on the Mont Gelé rock glaciers (Reynard et al. 1999, modified).

METHOD

The method used to survey the rock glacier surface velocities is of Real Time Kinematics type (Leica Geosystems): two stations (reference and rover) permits the local coordinates to be localized after a few seconds with a relative accuracy of 2-3 cm in the horizontal (x, y) coordinates and 3-5 cm in the vertical coordinate (z).

In September 2000, 87 blocks were measured on the rock glaciers. Four control points were also surveyed on bedrock, i.e. at places that are not affected by movement. Only blocks that seemed to be deeply buried in the active layer (and if possible in the permafrost body) were chosen. One year later, the position of the blocks was measured again.

RESULTS AND INTERPRETATION

Results are presented in Figure 2. A spectacular difference in horizontal movements between rock glaciers B and C can be observed. Rock glacier B clearly shows the maximal surface velocities. Annual displacement is up to 125 cm a^{-1} in the central part of the rock glacier. Such values are relatively high compared to values usually obtained on rock glaciers (Barsch 1992). The lowest movements are encountered in the lateral parts of the formation. The roots show smaller velocities than the central and frontal parts of the rock glacier. Rock glacier C is also affected by movements, but to a much lesser extent. Maxima are encountered on the right side, toward the frontal part. The left side and the upper flat area appear to be more stable. Rock glacier D only shows velocities lower than 5 cm a^{-1}.

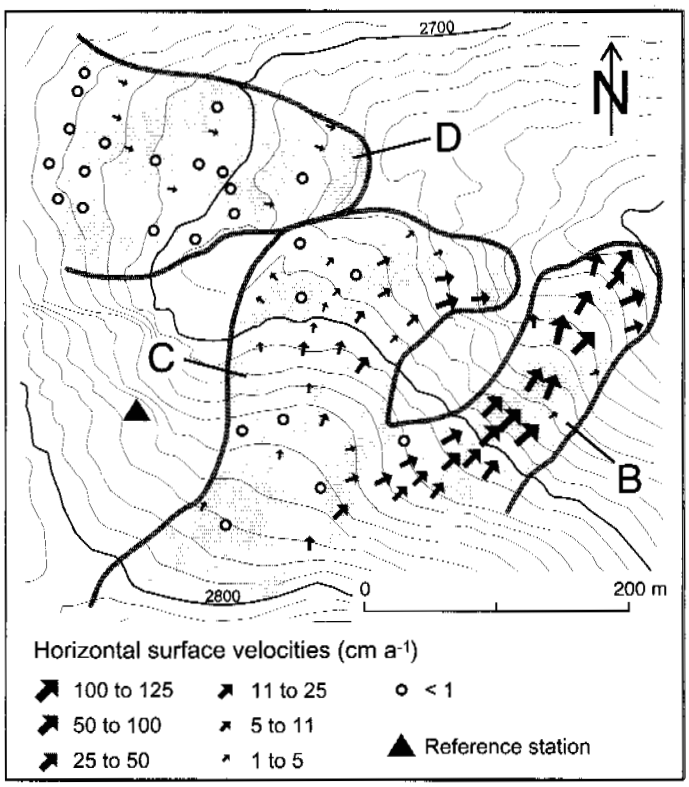

Figure 2. Horizontal surface velocities measured on the three Mont Gelé rock glaciers (Sept. 2000 – Sept 2001).

These results confirm what was assumed by geomorphologic observation: rock glaciers B and C are clearly active, whereas rock glacier D seems to be inactive. The comparison of the results with those obtained through geoelectrical prospecting shows that rock glacier B has the lowest electrical resistivity and presents at the same time the strongest surface velocities. On the other hand, rock glacier C shows high resistivities, but moves much slower than its neighbor does. This observation points out that surface velocities of rock glaciers cannot be linked to ice content. Two hypotheses are formulated to explain this great difference in surface velocities.

The first one considers the topographic position of both rock glaciers. Rock glacier B has developed on a steep and quite regular slope (~32°). Just below the roots, the slope becomes steeper. This part corresponds to the faster velocities. As no flat zone is present further down, velocities remain high. Lower velocities measured on rock glacier C, despite higher resistivities, can be explained by topography as well. The slope of the formation is much less regular and large flat areas dominate the rock glacier. The presence of obstacles (rock glacier D and an outcrop of roches moutonnées) at the front of the rock glacier can also explain the relatively low velocities of this part. This forces the rock glacier to turn with an angle of about 90° to the right. Such a change in direction probably affects the velocity of the rock glacier.

The second hypothesis refers to differences in ice/rock mixture temperature. Rock glaciers with temperature close to the thawing point would creep faster than colder rock glaciers (e.g., Ikeda et al. 2003). Nevertheless, except for the difference in electrical resistivity, there is still no further data available confirming any difference in the temperatures of both rock glaciers B and C.

CONCLUSION

RTK GPS has proved to be very efficient for rock glacier surface velocity measurements. The precision of a few centimeters is sufficient and one (long) day of work permits more than a hundred points to be measured.

This ongoing study has suggested that surface velocities of rock glaciers are not governed by ice content, but are more closely related to the topography (slope angle) of the rock glacier or to the temperature of the ice/rock mixture.

REFERENCES

Barsch, D. 1992. Permafrost creep and rock glaciers. Permafrost and Periglacial Processes 3: 175-188.

Francou, B. and Reynaud, L. 1992. 10-year surfacial velocities on a rock glacier (Laurichard, French Alps). Permafrost and Periglacial Processes 3: 209-213.

Ikeda, A., Matsuoka, N. and Kääb, A. 2003. A rapidly-moving small rock glacier at the lower limit of the mountain permafrost belt in Swiss Alps. Proceedings of the 8th International Conference on Permafrost, Zurich 2003 (in press).

Kääb, A., Haeberli, W. and Gudmundsson, G. H. 1997. Analysing the creep of mountain permafrost using high precision aerial photogrammetry: 25 years of monitoring Gruben rock glacier, Swiss Alps. Permafrost and Periglacial Processes 8: 409-426.

Reynard, E., Delaloye, R. and Lambiel, C. 1999. Prospection géoélectrique du pergélisol alpin dans le massif des Diablerets (VD) et au Mont Gelé (Nendaz, VS). Bull. Murithienne 117: 89-103.

Detection of frost heave and thaw settlement in tundra environments: application of differential GPS technology

J. Little, H. Sandall, M. Walegur and F. Nelson

Department of Geography and Center for Climatic Research, University of Delaware, Newark, USA

Geocryologists have devised several methods to measure the vertical component of frost heave and thaw subsidence. Most have employed either (a) mechanical "heavometers" that record differential movement at points or over very small (e.g. 10 m^2) areas; or (b) optical leveling, used in conjunction with specially designed platform targets. Measurements are usually made within localized coordinate systems and have rarely been related precisely to geodetic coordinate systems.

Degradation of permafrost and thaw settlement have received much attention recently in popular and global-change literature (e.g. McCarthy et al. 2001, Goldman 2002). These processes pose considerable hazard to human activities and infrastructure in high latitude regions. Recent technological advances in geodetic science have the potential to measure vertical movements accurately and rapidly, to survey relatively large areas, and to communicate survey results in precise, externally referenced coordinate systems. Among the most promising technological developments are *Differential Global Positioning Systems (DGPS).*

During summer 2001 and 2002, *post-processed stop-and-go kinematic, rapid-static carrier phase DGPS,* and a total of sixty-four specially designed heave and subsidence targets were used to record frost heave and ground subsidence at two 1 ha sites in northern Alaska. One site is at Sagwon in the northern foothills of the Brooks Range, the other at West Dock in the Prudhoe Bay oilfield on the Coastal Plain (Fig. 1). Our preliminary results indicate that post-processed rapid-static carrier phase DGPS has the ability to measure frost heave and ground subsidence at very high resolution (e.g. 1 cm).

Global Positioning Systems acquire coordinate positions through triangulation of an antenna receiver with at least four satellites. DGPS, which requires two antenna receivers, improves the accuracy to the cm scale; we used a base receiver (Trimble 4000) and a rover receiver (Trimble 4700). The inexpensive platform targets are cylindrical platforms capable of supporting a rover DGPS antenna while allowing the freedom to move vertically in response to heave or settlement. The ability to move the antenna from target to target permits acquisition of data at time scales varying from 15 to 45 seconds for stop-and-go kinematic DGPS; rapid-static DGPS requires eight to twenty minutes, but improves accuracy substantially (Little et al. in review).

The West Dock and Sagwon sites, located in the Kuparuk River basin of northern Alaska (Fig. 1), were instrumented with 32 platform targets, arranged according to a nested hierarchical sampling design (Nelson et al. 1999). The West Dock site is composed primarily of wet non-acidic tundra, and is underlain by ice-wedge polygons. The study site occupies part of a drained thaw lake basin and an adjacent section of "upland" tundra, which has better drainage. The Sagwon site occupies a section of nonacidic tundra with frost boils and patchy vegetative cover (Walker et al. 1998).

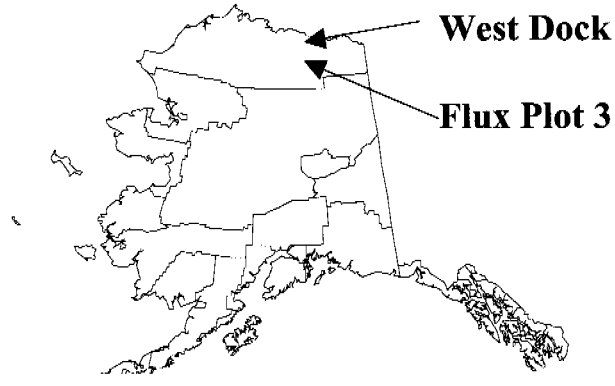

Figure 1. Map showing locations of West Dock and Sagwon (Flux 3) sites, North Slope, Alaska near the Dalton Highway.

All targets were given an arbitrary position of 10 cm at the beginning of the survey during summer 2001; Figure 2 shows heave and subsidence relative to this position. Rapid-static DGPS observations for June 2002 resulted in average surface heave of 1 cm from July 2001 (Fig. 2a) with maximum heave and subsidence of 6.7 cm and 2 cm, respectively. Although observations were recorded in July 2001 instead of August, the normal period of maximum thaw in northern Alaska, 24 of 32 targets recorded heave by June 2002. Mean values from a rapid-static DGPS survey in August 2002 were 4.3 cm lower than in June 2002.

Subsidence was recorded at 29 of 32 targets, with maximum subsidence of 15.5 cm and heave of 0.5 cm (Fig. 2a).

Heave of 1.9 cm was recorded from August 2001 to June 2002. Of the 32 targets, 24 recorded heave in June 2002 (Fig. 2b). Rapid-static DGPS from August 2002 recorded 3.3 cm of subsidence from June 2002 (Fig. 2b).

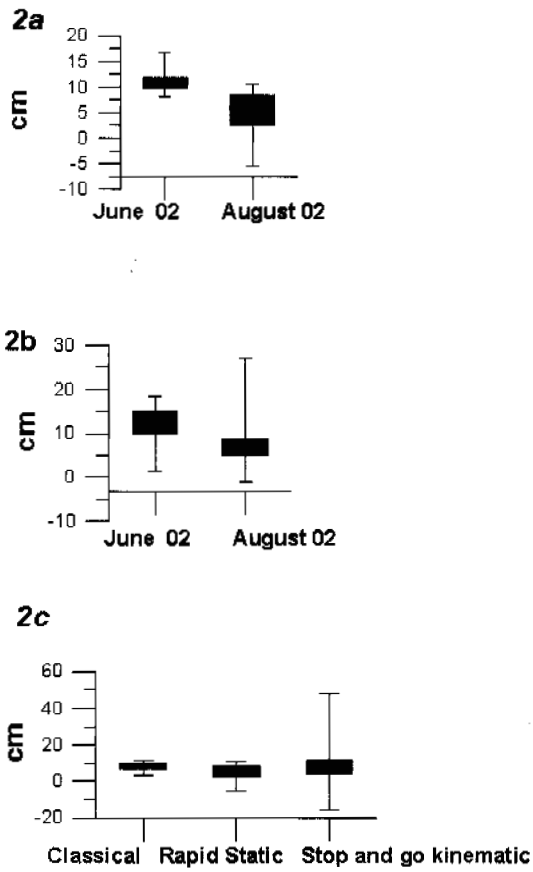

Figure 2a. Box plot depicting heave June 2002 from July 2001 at West Dock. Subsidence occurred between June and August 2002 and was detected by rapid-static DGPS. Figure 2b. Box plot showing heave and subsidence at Flux 3. Figure 2c. Box plot comparing results from traditional surveying with stop and go kinematic and rapid-static DGPS.

The use of DGPS as a stand-alone replacement for traditional survey methods (e.g., differential leveling or profile leveling) has been called into question (e.g., US Army Corps of Engineers 1996). To ascertain the degree of correspondence between DGPS and traditional survey techniques in the context of frost heave and thaw settlement, we compared results at West Dock from rapid-static and stop and go kinematic DGPS with those from a survey using profile leveling. The traditional survey, conducted in August 2002, detected mean subsidence of 2 cm, compared with results from June 2002 (Fig. 2c). Comparison of results from traditional surveying and the two DGPS techniques confirmed *that* rapid-static DGPS yields much better accuracy. Profile leveling in June 2002 averaged just 1.2 cm higher than rapid-static DGPS recorded a few days earlier, but 5 cm higher than stop-and-go kinematic (Fig. 2c). Standard deviations were 1.6 and 3.9 cm for classical surveying and rapid-static DGPS, respectively, yet were 14.2 for stop and go kinematic *DGPS* (Fig. 2c).

The close correspondence between traditional survey methods and rapid-static DGPS at West Dock indicates that frost heave and thaw can be successfully detected with the latter. As part of an ongoing project, the vertical displacement of each platform will be measured again using DGPS in summer 2003.

ACKNOWLEDGEMENTS

This paper is a contribution to the Circumpolar Active Layer Monitoring (CALM) program. We are grateful to Shad O'Neel (UNAVCO) for making DGPS equipment available for work in Alaska and for formal instruction in its use at UNAVCO's Boulder, CO facility. Professor Carmine Balascio (Department of Civil Engineering, University of Delaware) kindly provided surveying equipment for the validation work. We thank British Petroleum (Alaska) Inc. for logistical support and its Health, Safety and Environment office for access to the West Dock site. Funding was provided by the U.S. National Science Foundation under Grant OPP-0095088 to F.E. Nelson and Grant OPP-9732051 to K.M. Hinkel (University of Cincinnati). Any opinions, findings, conclusions, or recommendations expressed in this material are those of the authors and do not necessarily reflect the views of the National Science Foundation. Identification of specific products and manufacturers in the text does not imply endorsement by the National Science Foundation.

REFERENCES

Goldman, E. 2002. Even in the High Arctic, Nothing is Permanent. Science, 297: 1493-1494.

Little, J.D., Sandall H., Walegur, M.T., and Nelson, F.E in review. Application of differential GPS to monitor frost heave and ground subsidence in tundra environments. Permafrost and Periglacial Processes.

McCarthy, J.J., Canziani, O.F., Leary, N.A., Dokken, D.J. and White, K.S. 2001. Climate Change 2001: Impacts, Adaptation, and Vulnerability. Cambridge University Press, Cambridge, UK.

US Army Corps of Engineers. 1996. Engineering and Design - NAVSTAR Global Positioning System Surveying. April, 2002. http://www.usace.army.mil/usace-docs/eng-manuals/em1110-1-1003/toc.htm.

Walker, D.A., Auerbach, N., Bockheim, J.G., Chapin, F.S. I.I.I., Eugster, W., King, J.Y., McFadden, J.P., Michaelson, G.J., Nelson, F.E., Oechel, W.C., Ping, C.L., Reeburgh, W.S., Regli, S., Shiklomanov, N.I., and Vourlitis, G.L., 1998: A major arctic soil pH boundary: implications for energy and trace-gas fluxes. Nature 394: 469-472.

Permafrost and Little Ice Age glaciers relationships: a case study in the Posets Massif, Central Pyrenees, Spain

*R. Lugon, *R. Delaloye, **E. Serrano, ***E. Reynard and C. Lambiel*

University Institute Kurt Bösch, Sion, Switzerland

**Department of Geosciences, University of Fribourg, Switzerland*

***Department of Geography, University of Valladolid, Spain*

****Institute of Geography, University of Lausanne, Switzerland*

INTRODUCTION

The prospecting of ground ice in sediment deposits within a glacier forefield requires two main types of ground ice to be differentiated: pure permafrost ice (congelation ice within the ground) and debris-covered (or buried) glacier ice. DC (direct current) electrical prospecting is an easy and light technique, which allows such a distinction to be revealed in many situations (Haeberli and Vonder Mühll 1996).

Results from a geoelectrical measuring campaign in the forefield of the Posets glacier are briefly presented and discussed here. As far as we know, this is the first study treating the relationship glacier – permafrost (rock glacier) within the Little Ice Age (LIA) Pyrenean glacier forefields.

STUDY AREA

The LIA margins of the Posets glacier are located between 2900 and 3100 m a.s.l. on the eastern side of the Posets peak (3369 m a.s.l.) in the Central Pyrenees (42°39'N, 0°26'E). In 2001, the Posets glacier covered less than 0.1 km^2 (Fig. 1). It was three to four times larger during the LIA. At that time, the glacier divided into two tongues, one flowing to the east towards the Posets rock glacier, and the other to the north towards the La Paul rock glacier. The presence of permafrost in the glacier/rock glaciers complex was shown by Serrano et al. (2001) who used a set of BTS (Bottom Temperature of the Snow cover) and year-round continuous ground temperature measurements.

The bedrock beneath almost all the glacial sediment accumulations consists of a granite batholith. Hornfels resulting from contact metamorphism of Paleozoic shales surrounds the igneous intrusion and forms the greater part of the face on Posets peak overhanging the glacier cirque.

PROSPECTING METHODS

Two complementary DC resistivity techniques were applied. Vertical electrical soundings (VES) were used to estimate the stratigraphy of the ground resistivity. The dissymmetrical Hummel configuration allowed detection of shifts in ground resistivity in both branches of the soundings.

The VES were partially complemented with resistivity mapping (Wenner configuration). The technique allowed spatial changes in the measured apparent resistivity (usually 2-10 times lower than the specific resistivity for a permafrost body) to be determined at a fixed pseudo-depth.

A challenging aspect was to dispose of a sufficient electrical supply for a whole week of measuring. An OYO McOhm device (model 2115), complemented with a single lithium-lead battery (about 10 kg), was well suited as no recharge was required. This was only possible due to the use of low-intensity current (between 1 and 5 mA). Sponges soaked with salt water were used as electrodes.

RESULTS AND INTERPRETATION

Posets rock glacier

Two VES were performed on the Posets rock glacier, a 400 m long imposing sedimentary formation located at the front of the former eastern tongue of the Posets glacier (Fig.1). Five main arched ridges are clearly visible. Under a thin (1 m) active layer (20 kΩm), mainly consisting of angular hornfel clasts, an extreme resistive layer was detected (specific resistivity: 3-12 MΩm, 5-12 m thick), beneath which the resistivity falls towards a few tens of kΩm.

The spatial extension of the apparent resistivity of the second layer was mapped at a depth of about 6-9 m (AB = 37.5 m, 78 measurements). Extreme apparent resistivities, somewhere higher than 500 kΩm, were measured in the whole sedimentary complex. However, resistivities strongly decreased towards the rooting zone of the debris rock glacier where values between 50 and 100 kΩm were found.

The high resistivity of the second layer clearly indicates the presence of a massive ice layer, immediately beneath a thin layer of deposits. Such massive ice is interpreted as buried ice of glacial origin. The very high resistivity of the second layer could have made deeper layer(s) with lower resistivities undetectable, i.e., permafrost with low resistive ground ice.

La Paul rock glacier

The 400 m long La Paul rock glacier shows a typical but poorly-developed relief of permafrost creep with transversal furrows and ridges. A VES revealed the presence of an extremely resistive layer (8-25 MΩm, 5-15 m thick) below a 2 m thick active layer (30-40 kΩm). The downward branch of the VES shows the decreased resistivity of the second layer towards the frontal part of the rock glacier (1.3-5 MΩm, 5-15 m thick). As for the Posets rock glacier, geo-electrical methods could not prove nor exclude the existence of a third underlying frozen layer.

The extreme values of resistivity calculated towards the rooting zones of the rock glacier are only known to be found in cold or polythermal glaciers (buried sedimentary ice, Haeberli and Vonder Mühll 1996).

FURTHER QUESTIONS

Geo electrical measurements pointed to extreme resistivity ice in two debris rock glaciers that were prospected. Specific resitivities ranging between 1 and 25 MΩm were detected under a thin (1-2 m) active layer. The following suppositions can be made about the origin of ice within both Posets and La Paul rock glaciers.

Debris-covered glacier ice could have been incorporated in the two rock glaciers during the advance of the Posets glacier in the LIA, or former Holocene advances. Very cold subsurface temperatures measured in the deposits (Serrano et al. 2001) indicate that buried ice could easily have been preserved since the end of the LIA.

The massive ice probably superimposed former permafrost bodies, i.e., a much thicker layer of perennially frozen ground. However, such permafrost could not be detected by means of geo-electrical techniques.

The processes which have created both La Paul and Posets debris rock glaciers therefore remain in question. What is the role played by the glacier dynamic in the formation of the deposits? What is the importance of the creeping processes? Do the ridges occurring at the surface of the Posets glacier attest to advances of the Posets glacier during LIA, or do they indicate a sign of permafrost creeping?

REFERENCES

Haeberli, W. and Vonder Mühll, D. 1996. On the characteristics and possible origins of ice in rock glacier permafrost. Zeitschrift für Geomorphologie, Suppl. Bd. 104: 43-57.

Serrano, E., Agudo, C., Delaloye, R. and Gonzalez-Trueba, J.J. 2001. Permafrost distribution in the Posets massif, Central Pyrenees, Norsk Geografisk Tidsskrift-Norwegian Journal of Geography 55: 245-252.

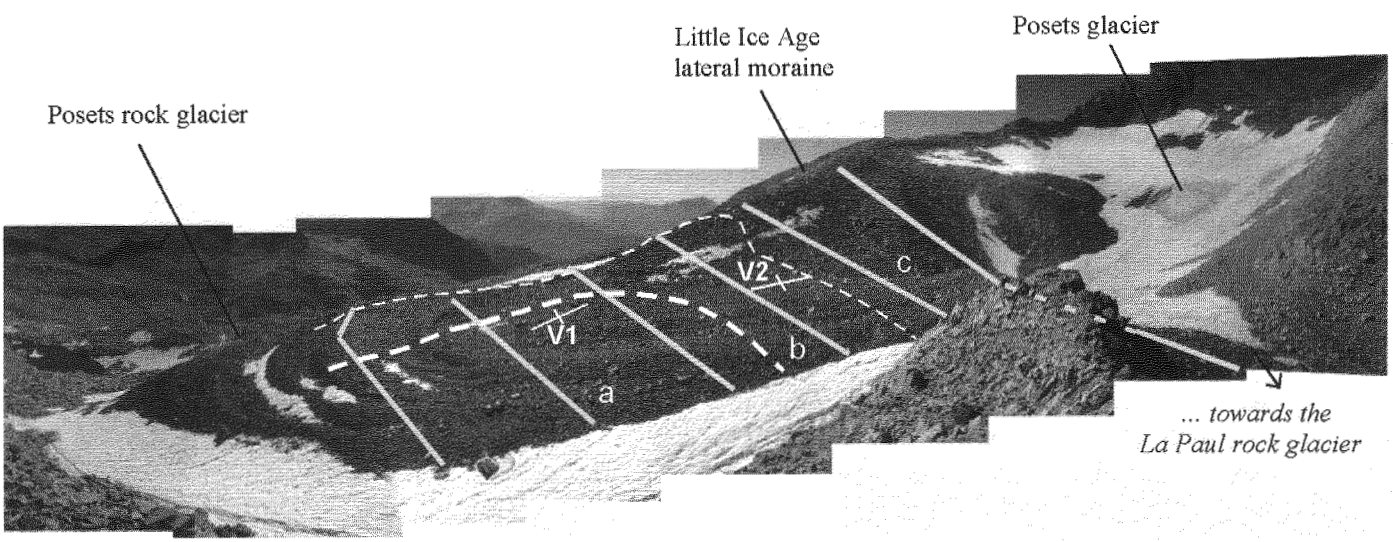

Figure 1. The Posets debris rock glacier. Photograph taken in September 2001. V1, V2: vertical electrical soundings. Resistivity mapping along the straight lines (12.5m inter-electrode spacing, 6-9 m investigation depth). Dashed lines delimit following areas: (a) apparent resistivity > 250 kΩm, (b) apparent resistivity between 80 and 250 kΩm, (c) apparent resistivity < 80 kΩm.

Borehole drilling in permafrost of an avalanche-affected slope at Flüelapass, eastern Swiss Alps

*M. Luetschg, V. Stoeckli, W. Ammann and *W. Haeberli*

Swiss Federal Institute for Snow and Avalanche Research (SLF), Davos Dorf, Switzerland

**Glaciology and Geomorphodynamics Group, Department of Geography, University of Zurich, Zurich, Switzerland*

Alpine permafrost is affected by different topographic and climatic factors. The snow cover is of high importance due to its strong insulation and albedo effects. Snow cover has a warming effect on ground temperatures during cold winter, whereas in late spring and summer, snow cover has a cooling effect (Keller 1994). This means that not only altitude and aspect but also snow-cover distribution is important with regard to the permafrost distribution; avalanches, therefore, play an important role in permafrost distribution, as they redistribute, compress and accumulate the snow: hence, at the accumulation zone of an avalanche slope, cooler ground temperatures were measured than in the passing zone higher above, due to the long remaining avalanche snow (Haeberli 1975). Thus, permafrost often occurs in the lower parts of avalanche slopes.

Such an avalanche-affected permafrost slope was found at Flüelapass, located in the eastern Swiss Alps, at an altitude of 2380 m a. s. l. The slope above the lake Schottensee is exposed towards northeast and is between 33 and 37 degrees steep at the upper part of the slope, corresponding to a typical avalanche starting zone.

Avalanches indeed occur in this slope in late winter and spring and deposit the snow at the foot of the slope. These large snow accumulations disappear later in the season than the snow on the slope above. This fact was also observed by a series of automatically-taken photographs during 1999 (Lerjen et al. 2003). Measurements of ground surface temperatures and seismic refraction soundings indicate colder temperatures and the presence of ice close to the surface in the lower third of the slope (Haeberli 1975). In summer 1999, these measurements were repeated and the active layer thickness was determined to be between 2 and 4 m in the lower part of the slope (Lerjen et al. 2003).

Ground surface temperatures in the slope and at both shores of the lake were measured during winter 2001/02.

In summer 2002, two boreholes were drilled, one (bh 1) in the avalanche starting zone (791352/180353 2500 m a. s. l.) and one (bh 2) at the foot of the slope (791500/180474 2394 m a. s. l.) to study the effect from the redistribution of snow due to avalanche events on ground temperatures. In the lower borehole (bh 2), cores containing pore ice were sporadically drilled. Figure 1-A shows the stratigraphy of the two boreholes as based on information from the experienced borehole-drilling team, and Figure 1-B presents the temperature profiles which were measured at the beginning of winter 2002/03, six weeks after the end of the drilling.

In the upper borehole (bh 1), 40 cm of humus to sandy soil was found under a dense vegetation cover (Fig. 1-A). This top layer was underlain by blocky material which contained larger blocks in the lower part. At 14.5 m depth, bedrock was encountered. The lower borehole (bh 2) differs from the upper borehole by the lack of a vegetation cover and the presence of pore ice: this ice was found between 1.8 and 8.5 m depth. Cores were drilled at the depths from 3.3 to 4.25 m and from 5.1 to 6.44 m; they contained some fragments of the pore ice. In the lower borehole, bedrock was not reached but at 20 m depth, the porous material was filled with water, indicating that the level of the lake surface was reached.

In both boreholes, inclinometer tubes were inserted to measure future deformation of the scree slope. Additional surveyings of the borehole positions (surface coordinates) are performed twice a year. Ground temperatures have been monitored continuously since October 2002.

First borehole temperature measurements at the beginning of winter 2002/03 reveal a clear difference between the two positions in the slope. In the lower borehole (bh 2), temperatures are close to 0°C (Fig. 1-B), while below 13 m, the temperature in borehole bh 2 increases to attain positive values. Note that the spatial resolution of the temperature profile in the lower part is 5 m, corresponding to the distance of the installed temperature sensors.

Since winter 2001/02, surface temperatures at four positions between the two borehole positions were measured continuously with universal temperature loggers (UTL) (Fig. 2). They show that the UTLs placed at lower altitudes close to the lower borehole position are becoming snow-free about 80 days later than in the upper part of

the slope. BTS were measured at the end of April 2002 to be – 2.8 °C in the upper part and – 3.8 °C in the lower part of the slope.

The borehole temperatures are supposed to still be somewhat affected by the effects of drilling disturbance, due to the short period between the end of drilling and the first temperature measurements presented in Figure 1-B. Results from the studies presented here will be used in comparison to modelling results, in which the situation is calculated with the one-dimensional model SNOWPACK (Bartelt and Lehning 2002). This snow-cover model was developed and extended to the underlying ground. It will be used to study the effect of snow height and snow density on ground temperatures in the avalanche starting zone and at the foot of the slope.

Borehole temperature measurements, surveys of snow cover characteristics and snow distribution and numerical simulations will give a better understanding of the effect of avalanches on permafrost distribution in avalanche slopes.

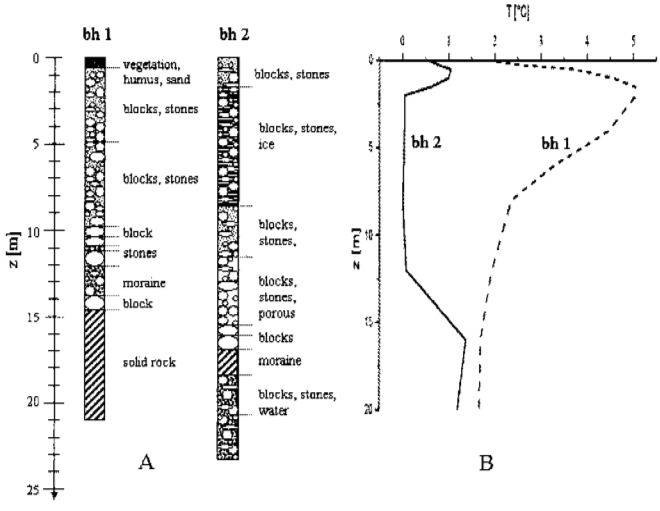

Figure 1. Stratigraphy of the the upper borehole (bh 1) and the lower borehole (bh 2) drilled 2002 in an avalanche slope at Flüelapass (A), and the corresponding ground-temperature profiles T with depth z, measured six weeks after drilling (B).

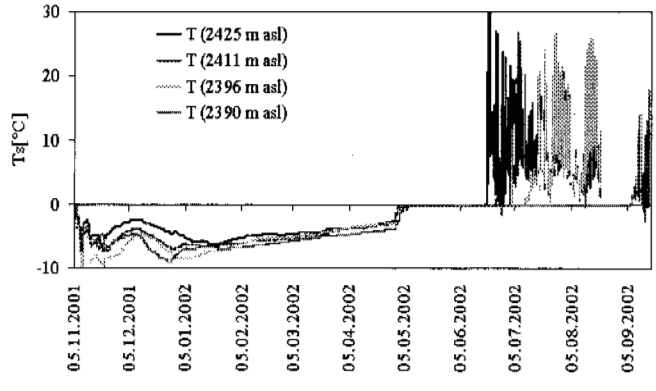

Figure 2. Ground surface temperatures (Ts) measured in 2001/02 between the two borehole positions in the avalanche slope at Flüelapass show a temperature inversion with altitude.

ACKNOWLEDGEMENTS

The borehole drilling presented here was carried out by Stump Bohr AG. This work was partly funded by the Swiss National Science Foundation (Nr. 21-65263.01).

REFERENCES

Haeberli, W. 1975. Untersuchungen zur Verbreitung von Permafrost zwischen Flüelapass und Piz Grialetsch (Graubünden). Mitteilung der Versuchsanstalt für Wasserbau, Hydrologie und Glaziologie der ETH Zürich 17: 221.

Keller, F. 1994. Interaktion zwischen Schnee und Permafrost. Mitteilung der Versuchsanstalt für Wasserbau, Hydrologie und Glaziologie der ETH Zürich 127: 145.

Bartelt, P. and Lehning, M. 2002. A physical SNOWPACK model for the Swiss avalanche warning. Part I: numerical model. Cold Regions Science and Technology 35(3): 123-145.

Lerjen, M., Kääb, A., Hoelzle, M. and Haeberli, W. 2003. Local distribution pattern of discontinuous mountain permafrost. A process study at Flüela Pass, Swiss Alps. 8th International Conference on Permafrost, Zurich, Switzerland.

Research on the relationship between wave velocity and the drillability of frozen clay

*Q. Y. Ma, *W. Ma, **M. F. Cai and ***Z. H. Zhang*

Anhui University of Science and Technology, Huainan Anhui 232001, China

**University of Science and Technology of Beijing, Beijing 100083,China*

**State Key Laboratory of Frozen Soil Engineering, Cold and Arid Regions Environmental and Engineering Researching Institute, CAS, Lanzhou 730000, China*

***University of Science and Technology of Beijing, Beijing 100083,China*

****Anhui University of Science and Technology, Huainan Anhui 232001, China*

From studies on the theory of elasticity we know that the propagation of an acoustic wave in rock or frozen ground is closely related to the character of the medium. Once the longitudinal wave velocity and the transverse (shear) wave velocity have been determined, the corresponding characteristics of elastic deformation are also defined. The propagation velocity of the acoustic wave, as measured in frozen ground, reflects the likely drilling properties of this frozen ground. The propagation velocity of frozen ground represents some typical physical properties. Using this basic principle the relationship between wave velocity and the drillability of frozen ground was derived. The measurement of wave velocity has certain advantageous characteristics. This test is quick to perform and not intrusive, hence it causes no disturbance to the ground. Using the wave velocity to determine the drillability of frozen ground is of great practical value.

A segment of frozen clay at a depth of 219.93~224.82m in a mine shaft in the Anhui province of China was chosen. The density of clay was 1710kg/m^3 and had a water content of 21.42%.

In the experiment, a UVM-2 acoustic wave instrument was used. This instrument can, via the sing-around method, perform a delayed determination so that it is not affected by multiple reflection waves and the velocity of the acoustic wave in the material can be measured rapidly and accurately. The method used is as follows: the sensor is covered with petroleum grease and placed on both sides of the sample. The receiver position is adjusted while observing the signal through an oscilloscope. The location and width of the oscilloscope display should be adjusted so that the whole ultrasonic pulse can be seen in the window and an optimal wave form is attained. The measured propagation time is the measured acoustic cycle minus both the sensor delay and the fixed delay. The acoustic velocity can be calculated on this basis.

The diameter of the experimental sample was 61mm, the height of both the longitudinal and transverse wave samples was 50.7mm. The experimental system had a fixed delay of 2.99s for the longitudinal wave and 2.00s for the transverse wave. A specially made constant temperature device for frozen clay and an axial pressure coupled measuring shelf were used to do the experiment. Measurements were made to a precision of ±0.1 °C at six temperatures of: -5°C, -7°C, -10°C, -12°C, -15C°,,and -17°C respectively. The experimental results are shown in Table 1.

Table 1. The experimental results of longitudinal wave velocity and transverse wave velocity of frozen clays

name	temperature °C	longitudinal wave velocity, m/s	transverse wave velocity, m/s
clay C1	-5	2363	1001
clay C2	-7	2477	1077
clay C3	-10	2594	1170
clay C4	-12	2653	1224
clay C5	-15	2725	1279
clay C6	-17	2749	1300

Measuring the drillability of frozen clay requires that the crushing instrument or chisel should follow an identical course to the actual drilling hole so that the measured indexes of the drillability do not vary with time, position or person, this leads to an objective and scientific index. Besides, using the chiseling work per unit volume to reflect the drillability of frozen clay makes it very comparable. The impact is easily controlled and sufficient load may be applied, even from a portable instrument, to crush frozen clay of any typical hardness. Referring to the research on the available experimental equipment for drilling in rock, a chiselling instrument made by East North University has been chosen.

The experimental method is as follows.

(1) The moisture content and particle size distribution should be measured before the experiment.
(2) The sample should be fixed to the test frame within the low-temperature room.
(3) A disc, graduated into 24 equal parts, with a central hole of 60mm diameter was fixed to the sample.
(4) For accuracy, it was necessary to carry out the experiment using a new or repaired drill bit. The chiselling instrument was positioned over the hole in the appara-

tus. One person needs to ensure that the angle setting knob does not move while the other operates the hammer. It must be ensured that the hammer can drop freely without any restriction.

(5) The angle setting knob was turned 15° after each impact. The pieces of frozen clay that fell to the bottom of the hole were cleaned out after each five revolutions. In addition, the hole depth was measured after 240 impacts (10 revolutions) and 480 impacts (20 revolutions).

(6) The hole depth was measured with special vernier calipers on the left edge, in the middle, and on the right edge of the hole, with a precision of 0.1mm. Assuming the frozen clay surface was smooth, the measured average value was regarded as the hole depth.

(7) The chiseling work per unit volume can be calculated with the chiseling depth as follows:

$$a = \frac{A}{V} = \frac{40NA_0}{\pi d^2 H}$$

Where a is the chiseling work per unit volume, kgm/cm^3; N is the number of cycles, its actual value is 480; A_0 is the work from each impact with an actual value of 3.9kg.m; d is the diameter of the drilled hole, the actual diameter is 1mm greater than that of the drill bit so, value d is 4.1cm; H is the depth of the drilled hole in mm and V is the volume in cm^3. The experimental results are shown in Table 2.

Table 2. Drilling depth and chiseling work per unit volume of frozen clays

Temperature, C°„	drilling depth, mm	chiseling work per unit volume, kg°¶m/cm^3
-5	122.20	11.90
-7	116.57	12.48
-10	86.27	16.86
-12	74.27	19.58
-15	67.17	21.65
-17	57.50	25.30

It can be seen from the data in Table 2 that the longitudinal wave velocity, the transverse wave velocity and the chiseling work per unit volume of frozen clay all appear to display a tendency to increase as the temperature decreases. The equation relating the longitudinal wave velocity, the transverse wave velocity and the chiseling work per unit volume can be established according to the principle of regression analysis.

The regression equations are expressed as follows:

$a = 0.807°¡10^{-4}c_p^2 - 0.379c_p + 457.66$, R=0.988

Where: c_p= longitudinal wave velocity, m/s.

$a = 1.171°¡10^{-4}c_s^2 - 0.227c_s + 121.33$, R=0.990

Where: c_s= transverse wave velocity, m/s

The multi-variable regression equation for longitudinal and transverse wave velocity and chiseling work per unit volume is expressed as follows:

$a = -0.158c_p + 0.244c_s + 139.849$, R=0.973, F= 54.507

The value of F is 54.507 and can be derived. It is known that $F_{0.01}(2,3)$=30.8, $F_{0.005}(2,3)$=49.8 and $F_{0.001}(2,3)$=148.5 from the F distribution table. From this we get $F > F_{0.005}(2,3)$, which signifies that the regression effect is excellent and that the result of the multi-variable linear regression is acceptable.

From the results of the experiment we know that the longitudinal and transverse wave velocity and the chiseling work per unit volume of frozen clay all tend to increase as the temperature decreases. While the longitudinal and transverse wave velocity is higher and the frozen clay is harder, the drilling is more difficult; conversely, when the longitudinal and transverse wave velocity is lower, the drilling is relatively easy. The relevant equation between the longitudinal and transverse wave velocity and the drillability of frozen clay can be established fairly easily by adopting the method of multi-variable regression analysis. It indicates that using the longitudinal and transverse wave velocity to evaluate the drillability of frozen clay is feasible.

ACKNOWLEDGEMENTS

The authors wish to express their gratitude to The Outstanding Youth Foundation for Scientific and Technological Research of Anhui Province (2001-28), State Key Laboratory of Frozen Soil Engineering and Education Department of Anhui Province of China for their financial support.

REFERENCES

Peng, W. W. and Yuan, Y. Q. 2000. Developing of a broadband ultrasonic transducer of frozen soils. Journal of Glaciology and Geocryology 22 (1): 85-89.

Ma, Q. Y., Peng, W. W. and Zhu, Y. L. 2002. Relationship among longitudinal and transverse wave velocities and temperature of artificially frozen clay. Chinese Journal of Rock Mechanics and Engineering 21 (2): 290-294.

Zhang, Z. H. and Ma, Q. Y. 2001. Research present situation and analysis on classification of rock drillability, Chinese journal of Coal Science and Engineering 7(1): 39-45.

Permafrost active layer as the concentrator of contaminants in northern regions

V. N. Makarov

Permafrost Institute SB RAS, Yakutsk, Russia

Soils are said to be the "self-purification filters" of nature. However, they lose their decontaminating properties in permafrost zones. The reasons are: thinness of the soil profile, inadequate drainage, thermohydrogeochemical barrier to the migration of contaminants, annual freezing and consequent concentration of soil water contaminants, low geochemical and lowered chemical activity of soils (because of low temperatures), short biological life of soils during the year. These conditions cause increasing soil pollution under the pressure from industrial zones.

Regional permafrost aquicludes at shallow depth from the ground surface and low negative temperatures cause a specific geochemical situation in the northern territories and a widespread development of cryogenic metamorphoses in underground waters. The common direction of this process is to rise mineralization; the amounts of chloride and sulfate increase in the waters and heavy metals accumulate. During repeated freeze-thaw cycles the majority of dissolved contaminants become concentrated in gravitational waters while forming cryopegs. Cryopeg formation is due to the intensity and duration of industrial activity and results in its localization in the older parts of populated areas (Makarov, Venzke 2000).

Studies of soil solution behavior indicate their functional peculiarities during annual cycles. The most contrasting changes of macro- and microelement fluxes, pH value and oxidation-reduction potential (these determine migration in the geochemical environments of the upper horizons of seasonally thawed layers) are observed before and after the cold period when sharp temperature changes and moisture phase transitions occur. Before the beginning of the cold period, the upper horizons of seasonally thawed layers accumulate most of the components that come from industrial geochemical fields. Cryogenic concentration and the migration of soluble contaminants deep into seasonally thawed layers, induced by freezing front action, results in a depletion of the high horizons in seasonally thawed layers during winter. It causes a reduction in the concentrations of contaminant components by the beginning of the warm period. Maximum seasonal fluctuations in the intensity of geochemical fields is typical for components such as Cr, Ag, Pb, Mo, S, Ca, Na, Cl, Mg, Sn whose concentration in pore water changes by 3 to 30 times (Fig. 1).

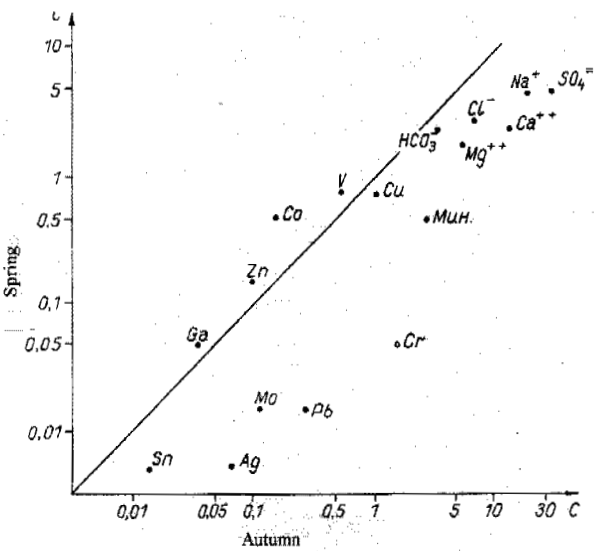

Figure 1. Seasonal variations in the concentration of chemical components in soil's pore water in Yakutsk

The penetration of anomalous industrial components to the top of permafrost depends on the concentration gradient and the geochemical properties of the chemical elements forming the anomaly.

Because of the similarity in some chemical properties and ion radii, iron and manganese hydroxides can sorb heavy metals from a suspension and co-precipitate with other metals (Ponnamperuma 1969). Heavy metal retention by iron and manganese hydroxides increases with time due to metal diffusion into the solid phase. During periods of thawing soils become hydromorphic. This promotes the formation of a large number of amorphous iron hydroxides which increases the maximum adsorption of heavy metals (Ostroumov 1998). However, the presence of organic matter, even in small amounts, retards the crystallization of iron hydroxides, thus causing increased metal mobility. The highly mobile components of organic matter in frost-affected soils form stable organometallic components which have a high ability to migrate. Metal mobility in organic soils is strongly influenced by microbial metabolism. Thus, metal mobility in frost-affected organic soils and permafrost is controlled by the complex interac-

tion of three soil components, iron components, organic matter and microbial communities.

The complicated combination of simultaneously occurring processes determines the content ratio of elements in the solid and liquid phases of industrial geochemical fields. We can summarize the effects of the processes using the thickness ratio of the chemical elements aureole zone in the solid and liquid phases. Absorption of the solid phase is predominant for some elements and dissolution in water predominant for others.

The majority of contaminant solid phases is accumulated in the upper parts of the ground at depths of 15-20 cm. The depth of contaminant penetration can reach 2.5-2.7 m, including the top of the permafrost, depending on the source of industrial contaminants and the intensity of the cryogenesis processes (Makarov 1986). It is caused by the transition of components in soil solutions and ground waters and by further sedimentation on various sorbents (Fig. 2).

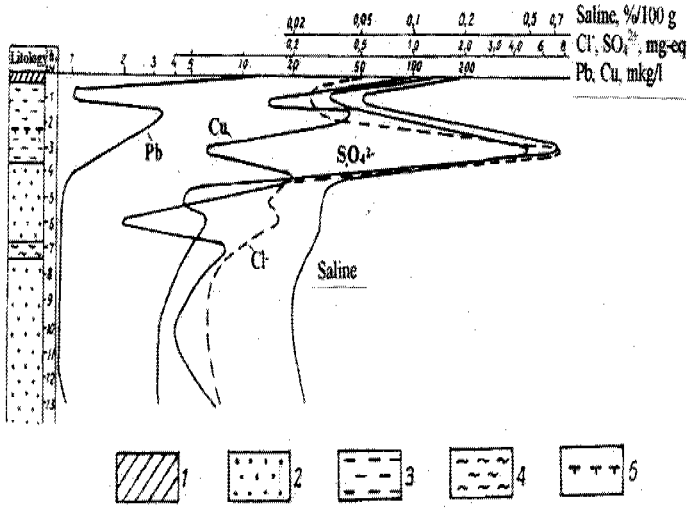

Figure 2. Distribution of chemical components in the active layer and permafrost. 1 – anthropogenically affected soils; 2 – sand; 3 – sandy silt; 4 – clay; 5 – permafrost.

The thickest and ecologically most dangerous contaminant anomalies – Hg, Pb, P, S, Ag, Sn, Cu, Y, Zn, Cr are forming at the thermohydrogeochemical barrier in urban zones.

REFERENCES

Makarov, V.N. 1986. Geochemistry of frost-affected soils in urban areas. In: Geochemistry of Technogenesis, Novosibirsk, Nauka: 118-124.

Makarov, V.N., Venzke, J.-F. 2000. Umweltbelastung und Permafrost in den Stadt- und Agrarokosystemen in Zentral-Jakutien, Sibirien. Geographische Rundschau 12, Braunschweig: 21-26.

Ostroumov, V.E. 1998. Ion redistribution in soils upon freezing. Pochvovedenie 5: 614-619.

Ponnamperuma F. N., Loy, T. A. and Tianco, E. M. 1969. Redox equilibria in flooded soils: The Manganese oxide systems. Soil Science, 108, 1: 48-57.

Borehole and active-layer monitoring in the northen Tien Shan (Kazakhstan)

S. S. Marchenko

Permafrost Institute, Russian Academy of Sciences, Kazakhstan Alpine Geocryological Laboratory, Almaty, Kazakhstan

The Zhusalykezen Mountain pass (43°05'N, 76°55'E, 3330 m a.s.l.) is located within the discontinuous permafrost area of the Transili Alatau Range (frontal range of northern Tien Shan). The location is close to the city of Almaty, and therefore offers an opportunity for geocryological and ecological investigations of the natural system and systems affected by human activities.

The Upper Pleistocene and Holocene moraines from the mountain descend into the nearby valleys. Vegetation cover is dominated by Kobresia. Mean annual, January and July air temperatures at the elevation 3300 m a.s.l. are -3.5°C, -13.7°C and 6.7°C, respectively. The maximum annual precipitation is about 1000 to 1100 mm. The snow cover develops in October. By the beginning of June, the thickness of snow cover varies from 1 to 5 cm up to 100 to 120 cm, relative to topography and wind activity.

Depending on geomorphology and microclimatic conditions, the thickness of permafrost varies from 10 to 15 m to 80 to 90 m on the northern slopes and is absent on the southern slopes. Temperatures of permafrost vary from –0.1°C to –0.45°C. There are 10 thermometric boreholes located on different slopes and aspects within an area of 3 km^2. Active layer thickness is determined by temperature measurements made in boreholes from 3 m up to 70 m in depth. Several CALM sites are located near a mountain pass. Initial results of the Circumpolar Active Layer Monitoring were reported previously (Brown et al. 2000).

Ground temperatures up to 25 m in depth have been measured since 1973 (Gorbunov and Nemov 1978). Both interpolation of temperature measurements and excavations in the moraines revealed active-layer thickness in the late summer for 1973 and 1974 (Table. 1). The table includes mean active-layer thickness during 1974-1977 for C1(K0) and C2(K1) sites. The average increase in mean annual air temperature for the last 100 years in the central part of Transili Alatau Range has been 0.02°C/yr. The average ten-year temperature for 1991-2000 has increased by 0.3°C in comparison with 1981-90. The greatest increase of temperature for the same period has been mean winter (0.4°C), maximum winter (0.9°C) and minimum summer temperature (0.5°C). The warmest years for the last decade of the 20th century were 1997, 1998 and 1999, when mean annual air temperature was higher than the long-term average temperature by 1.1°C, 1.49°C and 0.93°C, respectively. Analysis of meteorological conditions for summer time has shown that the summer temperatures and precipitation figures are currently rising (Fig. 1).

Table 1. Active-layer thickness near Zusalykezen Mountain pass for 1973-1977.

Excavations	Altitude	Depth of pits and boreholes	Active layer thickness
	m a.s.l.	m	m
Pits			
No 1	3337	6.0	4.5
No 2	3334	4.0	4.0
No 4	3334	4.3	3.5
No 5	3337	9.3	4.0
No 10	3336	9.0	3.8
No 12	3334	4.2	3.7
Boreholes			
C1 (K0)	3337	25.0	3.2
C2 (K1)	3328	14.0	3.4
C3a	3337	10.3	4.3
C7	3334	11.7	3.5
C11	3335	13.0	3.7

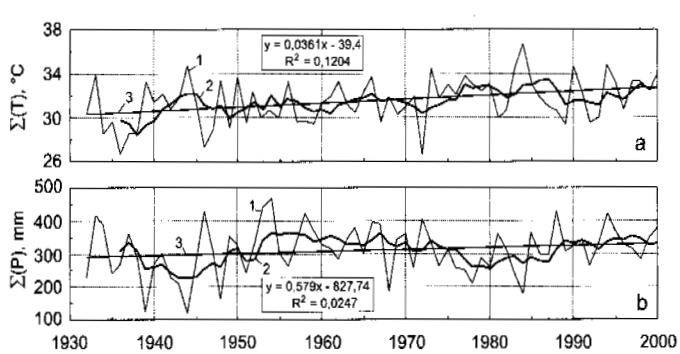

Figure 1. Air temperatures (a) and precipitation (b) for the summer time (Central Transili Alatau Range, 2500 m a.s.l.). 1 – annual, 2 – five-year average, 3 – linear trend.

Thus, climatic processes during the 20th century and especially during the last two decades have a great influence on the contemporary thermal state of permafrost. Geothermal observations indicate permafrost warming in the northern Tien Shan for the last 30 years. The permafrost temperatures increased during 1973 - 2002 by 0.2 to 0.3°C for undisturbed systems, and up to 0.6°C of those affected by human activities.

In accordance with interpolation of borehole temperature data, active-layer thickness showed a significant increase during the last 30 years from values of 3.2 to 3.4 m in the 1970s to a maximum of 5.2 m.

The average active-layer thickness for all measured sites increased by 23% in comparison with the early Seventies. But compared with the thawed depths for the new CALM sites (K0, K1, C7) the increase is much greater at 42%. For example, at the CALM K1 site during 1974-1977, the average active-layer thickness was 3.4 m and maximum value of 3.5 m. During 1990-2000 at the same site the average active-layer thickness was 4.85 m with a maximum value of 5.2 m. At the CALM site K0, the average and maximum active-layer thickness were 3.2 m and 3.3 m for 1974-1977 and 4.8 m and 5.1 m during 1990-2000.

As mentioned earlier, 1998 was the warmest year on record in Transili Alatau since 1964. As a result, in the following year the ground temperature at a depth of 4.6 m had increased significantly. For example, the average temperatures at 4.6 m were -0.2, 2.24, 0.10, 0.06 and 0.04 in 1998, 1999, 2000, 2001, and 2002, respectively. This deep penetration of seasonal thawing into the ground initiated the appearance of a residual thaw layer deeper than 5 m at the CALM K1 site. Normally seasonal freezing penetrates from 4.5 to 5.2 m.

Using data obtained from boreholes, geologic and geomorphologic data, and knowledge about the extent of snow cover and vegetation, an attempt was made to calculate spatial distribution of active-layer thickness for Zhusalykezen Mountain pass area. An area of 1.5x2 km^2 near the mountain pass was selected for the computations of depth of seasonal thaw. The deterministic model (Marchenko 2001) with regular grid spacing of 50x50 m was used for computation. Figure 2 shows the calculated spatial changes in active-layer thickness within selected areas.

Because in high mountain areas permafrost is one of the dominant factors affecting slope stability, knowledge about tendencies of active layer development is of great interest. Model calculations of active-layer thickness allow for the assessment of surface processes, landscape dynamics and natural hazards.

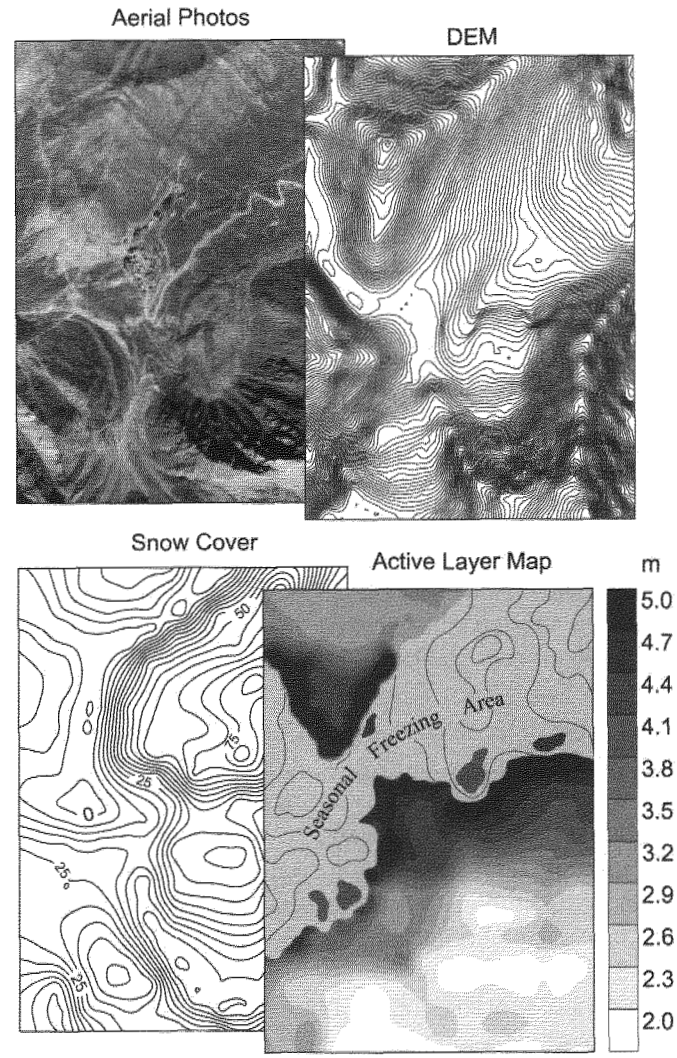

Figure 2. Computed active-layer thickness distribution for Zhusalykezen Mountain pass area using complex data.

REFERENCES

Brown J., Hinkel K. M. and Nelson F. E. 2000. The Circumpolar Active Layer Monitoring (CALM) Program: research design and initial results. Polar Geography 24 (3):165-258.

Gorbunov A. P. and Nemov A. E. 1978. The research of temperature of loose deposits of the high mountain Tien Shan. Cryogenic Phenomena of High Mountains. Nauka, Novosibirsk: 92-99.

Marchenko, S. S. 2001. A model of permafrost formation and occurrences in the intracontinental mountains. Norsk Geografisk Tidsskrift - Norwegian Journal of Geography 55: 230-234.

Active layer temporal and spatial variability at European Russian Circumpolar Active Layer Monitoring (CALM) sites

*G. Mazhitova, *G. Ananjeva-Malkova, **O. Chestnykh and **D. Zamolodchikov*

Institute of Biology, Komi Science Centre, Russian Academy of Science, Sytyvkar, Russia

**Earth Cryosphere Institute, Siberian Division, Russian Academy of Sciences, Moscow, Russia*

***Centre for Ecology and Productivity of Forests, Russian Academy of Sciences, Moscow, Russia*

Three sites were established in European Russia in the framework of the "Circumpolar Active Layer Monitoring" NSF-funded project (Brown et al. 2000). The Bolvansky site [R24] (68°18`N, 54°30`E) located at the western limit of the continuous permafrost zone in Europe has four years of records; Ayach-Yakha [R2] (67°35`N, 64°11`E) with seven years of record and Talnik [R23] (67°20`N, 63°44`E) with five years represent "cold" and "warm" extremes of the range of permafrost conditions in the discontinuous permafrost zone. This report was developed as a result of the CALM synthesis workshop held in November 2002 at the University of Delaware.

The sites represent permafrost with temperatures from –0.5 to –2.0 °C, and sensitive to even decadal-scale climatic changes (Oberman and Mazhitova 2001). Data from weather stations show synchronous MAAT fluctuations in the European Russian Arctic. MAAT is –4.4°C at the maritime R24, whereas at the continental R2 and R23 it is -5.9°C. The difference is due to winter temperatures, whereas annual sums of positive temperatures (DDT) are equal (Fig. 1).

In spite of similar DDT, differences in thaw depths between the three sites occurred in all years of record; end-of-season thaw averaged for the period of record was 101 cm at R24 and 102 cm at R23 versus 68 cm at R2. The differences are due to effects of local factors, first of all, snow thickness. The two sites with deeper thaw, R24 and R23, reveal remarkable similarity in thaw values and dynamics (Fig. 1). Regressions of thaw depths with $DDT^{0.5}$ using a form of the Stefan solution (Fig 2) clearly indicate that the same increases in DDT cause much smaller increases in thaw depths at the cold R2 than at the two "warmer" sites.

An inter-annual node variability (INV) index has been proposed by Hinkel and Nelson (in press) to characterize the consistency of thaw response to thermal forcing. The site average index is 10% at R23, 16% at R24 and 23% at R2 ranging from 3 to 69%, from 0 to 37%, and from 1 to 88%, respectively.The values indicate a more consistent and predictable response of the warmer R23 and R24, as compared to the cold R2. At R2, the highest INV values are characteristic for the grid nodes located in a hollow with very dynamic soil water content and in the area where bedrock is closer to the soil surface.

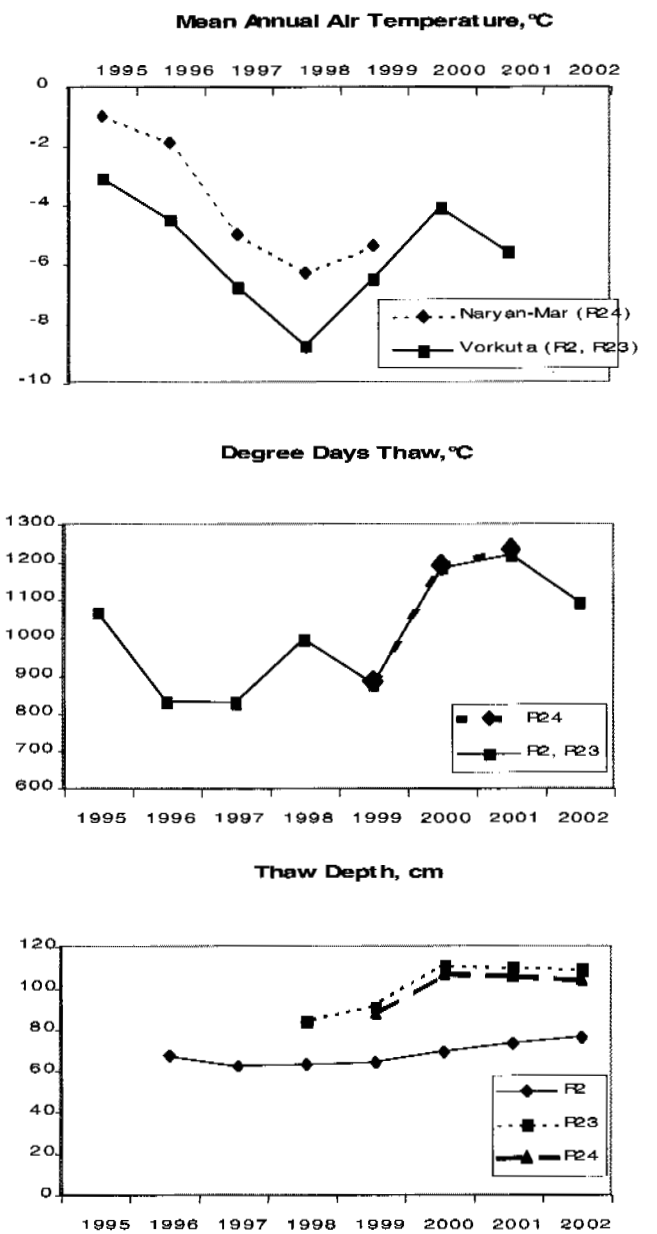

Figure 1. Climate parameters and active layer depths at European, Russia's CALM sites.

Effects of various landscape factors on thaw depth were analyzed. Snow thickness, which is one of the main controls over permafrost distribution patterns at both regional and meso-scale (Oberman 1998) may also work at a scale as detailed as that of 100-m CALM grids, if the range of snow thickness within a site is large enough. Thus, at R24 a talik occurs in a depression under an annually developing snow drift. Surface topographic forms (ridges, basins, etc.) from several meters to several dozen meters in size and a depth to bedrock (R2) are the most powerful controls on thaw depth. The second important factor is organic layer thickness, which can be correlated to thaw depth both negatively and positively, depending on the topographic form. The positive correlation is observed at depressions and hollows where soils are saturated with water. A statistical analysis conducted for R24 showed that a peat soil layer up to 22 cm thick produces a stronger effect on thaw depths than do vegetation and a sodden soil layer. Still, thaw depths under major vegetation classes differ clearly at all three sites. At R2, frost boil dynamics are correlated to average thaw depths: three cold summers in sequence with shallow thaw caused new boils to develop, whereas during the following three warm summers with deeper thaw all boils became covered with at least primitive vegetation.

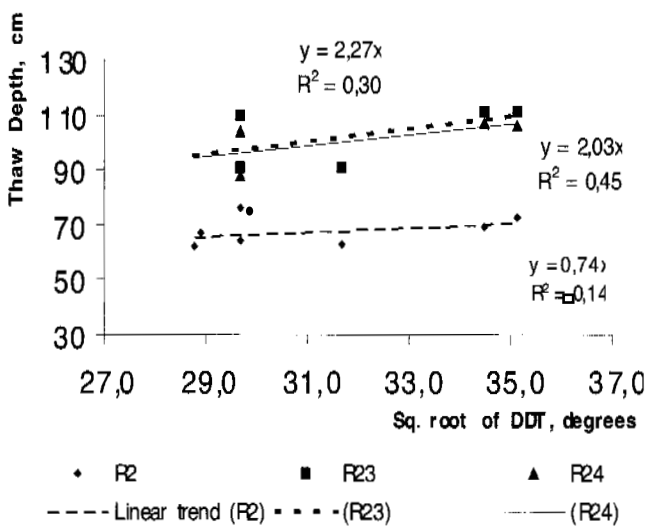

Figure 2. End-of-season thaw depth versus square root of thaw degree days.

Surface subsidence was assessed at R2 by repeated leveling of each grid node. Over a four-year period site subsidence averaged 3 cm in total. Thus, permafrost vertical retreat is underestimated if one bases conclusions on thaw depths alone.

REFERENCES

Brown, J., Hinkel, K.M. and Nelson, F.E. 2000. The Circumpolar Active Layer Monitoring (CALM) Program: Research Designs and Initial Results. Polar Geography 24(3): 165-258.

Hinkel, K.M. and Nelson, F.E. in press. Spatial and Temporal Patterns of Active Layer Thickness at Circumpolar Active Layer Monitoring (CALM) sites in Northern Alaska, 1995-2000.

Oberman, N.G. 1998. Permafrost and cryogenic processes in the East-European Russian Subarctic. Eurasian Soil Science 31(5): 540-550.

Oberman, N.G. and Mazhitova, G.G. 2001. Permafrost dynamics in the north-east of European Russia at the end of the 20th century. Norwegian Journal of Geography 55 (4): 241-244.

Comparative analysis of active layer monitoring at the CALM sites in West Siberia

E.S. Melnikov, M.O. Leibman, N.G. Moskalenko and A.A. Vasiliev

Earth Cryosphere Institute, Russian Academy of Sciences, Siberian Branch, Tyumen, Russia

The main objective of the study is to report on recent analyses of spatial and temporal active layer variations from the CALM grids within several bio-climatic and permafrost zones of West Siberia (Melnikov et al. 2001). These sites were established in the framework of the "Circumpolar Active Layer Monitoring" NSF-funded project (Brown et al. 2000). In addition to the short-term CALM data, other terrain information and longer records are utilized.

The zones covered by the monitoring data are typical tundra (sites *"Marre-Sale"* and *"Vaskiny Dachi"*), and northern taiga (site *"Nadym"*). Tundra is characterized by variable landscapes of hilly plains. The northern taiga has a less-complicated landscape structure and generally more subdued or flatter topography compared with the typical tundra. Distinguishing features of the three CALM monitoring grids are:

Marre-Sale [R3] (69°43'N, 66°45'E; 1000-m grid). Marine-influenced, vast areas of blowout sands, highly dissected surface, sparsely distributed peat-moss cover.

Vaskiny Dachi [R5] (70°17'N, 68° 54'E; 100-m grid). Landslide affected, some blowout sands, saline clay near the surface, highly dissected surface, sparsely distributed peat-moss cover.

Nadym [R1] (65°20'N, 72°55'E; 100-m grid). Technogenic impact outside the grid, permafrost occurs mainly with peatlands and frost-heave mounds, rather flat surface, thick peat and widespread moss. Zonal changes in the thickness of the active layer are controlled by a combination of factors. The summer temperature as well as the thickness of the organic mat and coverage decreases northward. The maximum active layer in peat increases respectively from 80 cm in the taiga to 50 cm in tundra, and in sand from 3 m in the taiga to 2 m in tundra. The difference in thaw rates in various climatic environments has common features with a slight rise of thaw rate northward in mineral soils associated with the reduction of thaw depth.

Active layer landscape interrelation is controlled to a high degree by the composition and wetness of soils. Maximum active layer depth is characteristic of sands, especially at the blowout hollows. In addition to blowout sands, maximum active layer is found on the wettest landscapes, (1) in northern taiga, in mires and tundra with peaty hummocks, (2) in typical tundra, in ravines. Comparison of active layer in different zones is possible within similar landscape types.

Marre-Sale has been the site of long-term observations since 1978 (Vasiliev et al. 1998) at several grids and transects. Minimum thaw depth was observed in 1999 (87 cm) following the low summer air temperature. Maximum thaw depth in 1984, and 1995 (133 cm) is in agreement with high summer air temperature (6.8 to 7.0°C), while peak thaw in 1990 (132 cm) was not connected with summer temperature, which was moderate (5.8°C), but was probably due to rather low summer precipitation.

The Vaskiny Dachi site has been active since 1990 (Leibman 2001). The minimum active layer (81 cm) was observed in 1992 (transect) and 1997 (CALM grid), and the maximum was in 1995 (98 and 94 cm, respectively). The interannual active layer variability does not directly depend on the air temperature fluctuations, but also on atmospheric precipitation and its regime, at least for the minimum active layer depth.

At the Nadym transect (Moskalenko at al. 2001) starting in 1972, minimum thaw was observed in 1972 and 1992 (100 cm), while maximum thaw occurred in 1989, 1995 and 1998 (190cm). At the CALM grid since 1997 the maximum thaw (143 cm) was observed in a year 2002, the year with rather a moderate air temperature but high summer precipitation. Minimum active layer occurred in 1999 (125 cm). There is a correlation (average coefficient -0.6) between the peat thickness and active layer depth at the Nadym CALM grid.

Thaw depths for the tundra CALM grids at Marre-Sale and Vaskiny Dachi are compared (Fig. 1). The trend is similar at sandy sites, though a certain difference in the active layer depths is observed. Since the climatic situation for both sites is rather similar and data is taken from the same source, the explanation may be found in surface conditions reflected in ground temperature. Comparing observed ground temperature at both sites we conclude that blowing and removal of the snow in winter from the hilltops of Vaskiny Dachi determines a rather low ground temperature, about –7 °C, while at Marre-Sale ground temperature averages –5 °C.

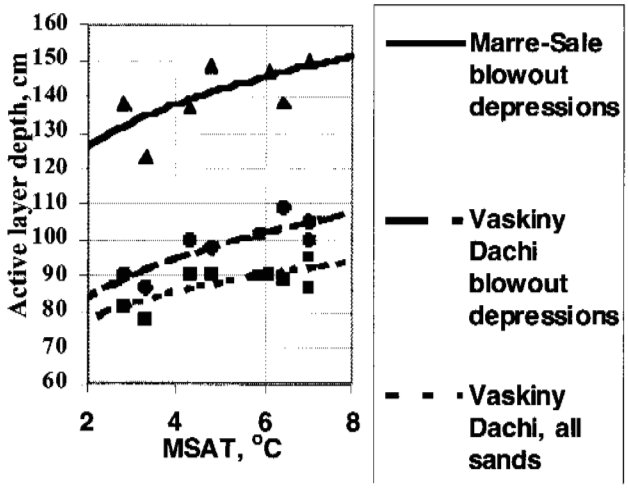

Figure 1. Correlation between the mean summer air temperature (MSAT) and the active layer depth at the sandy surfaces of Marre-Sale and Vaskiny Dachi CALM grids.

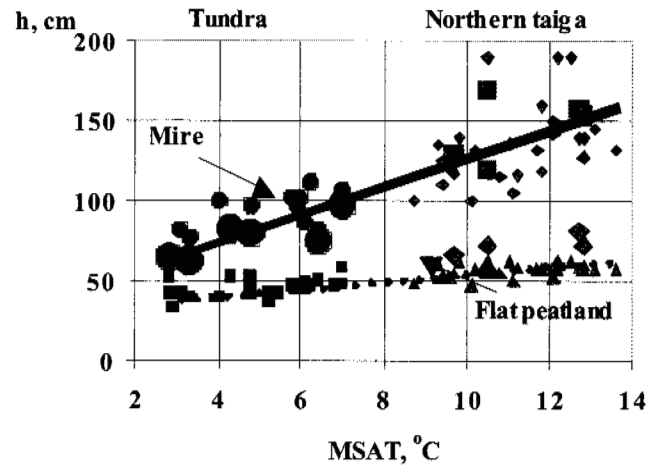

Figure 2. Model of the climate warming: correlation between mean summer air temperature (MSAT) and active layer depth (h). Larger symbols refer to the CALM grids, smaller ones to transects; black markers refer to Marre-Sale (the tundra zone), and shaded markers are for Nadym (the taiga zone).

The long-term data from transects and CALM grids for tundra and taiga are presented in Figure 2. Landscape types are characterized by specific response to the atmospheric warming, independent of the bio-climatic zone. A comparison was made of mires: wetlands with water table near the surface, and peatlands with thick peat. As follows from the trend slope on Figure 2, the response of mires (the upper set of points on the diagram, Fig. 2) to possible warming is more strongly expressed as compared with peatlands (the lower set of points on the diagram, Fig. 2).

Thus, temporal and spatial variations of maximum thaw depth in two bio-climatic zones of West Siberia are under study. The following conclusions are drawn.

1 Various bio-climatic and permafrost zones in West Siberia show little or no warming trends during the study period. In tundra, no trend is noted. In taiga, the average trend is 0.03°C per year.
2 A slight trend can be discerned for thaw depth. In the typical tundra and mires of the northern taiga of West Siberia, active layer thickness increases by 0.2 % and 0.5% per year, respectively. During the last several years, the north of West Siberia was characterized by drier summers; therefore the possible reason for increased depth of the active layer is atmospheric precipitation rather than air temperature changes.
3 Response of the active layer to climate fluctuations differs for various landscapes. In both bio-climatic zones, peatlands are most passive due to the existence of a thick insulating organic layer. In tundra, the most active response is determined for wet terrains. In taiga, mires are the most responsive.

ACKNOWLEDGEMENT

This report was developed as a result of the CALM synthesis workshop held in November 2002 at the University of Delaware.

REFERENCES

Brown, J., Hinkel, K.M. and Nelson, F.E. 2000.The Circumpolar Active Layer Monitoring (CALM) Program: Research Designs and Initial Results. Polar Geography 24 (3): 165-258.

Leibman, M.O. Active layer dynamics and measurement technique at various landscapes of Central Yamal. Earth Cryosphere V(3): 17-24 (in Russian).

Melnikov, E.S., Vasiliev, A.A., Malkova G.V. and Moskalenko N.G. 2001. Monitoring of the active layer in the Western part of the Russian Arctic. First European Permafrost Conference, Rome, 26-28th March 2001. Abstracts.

Moskalenko, N.G., Korostelev, Yu. V. and Chervova, E.I. 2001. Monitoring of Active Layer in Northern Taiga of West Siberia. Earth Cryosphere V(1): 71-79 (in Russian).

Vasiljev A.A., Korostelev Yu. V., Moskalenko N.G. and Dubrovin V.A. 1998. Active layer monitoring in West Siberia under the CALM program (database). Earth Cryosphere II(3): 87-90 (in Russian).

Recent evolution of permafrost in both Becs-de-Bosson and Lona glacier/rock glacier complexes (western Swiss Alps)

*S. Métrailler, R. Delaloye and *R. Lugon*

Dept. Geosciences, Geography, University of Fribourg, Switzerland

**University Institute Kurt Bösch, Sion, Switzerland*

INTRODUCTION

Geoelectrical and BTS (Bottom Temperature of the winter snow cover) measurements were repeated a decade after the first investigations on two neighbouring sites of the Valais Alps (Switzerland, 46°9'N, 7°31'E) where glaciers largely overrode rock glaciers during the Little Ice Age (LIA). The main objective of the present study is to provide an overview of the recent evolution of permafrost in these glacier/rock glacier complexes. Two different time scales associated with specific processes are involved: (a) the LIA and the impact on permafrost bodies produced by the glacier advance, and (b) the last decade of the 20th century and the response of permafrost to climate warming.

Tenthorey (1993) and Gerber (1994) investigated both glacier/rock glacier complexes of Becs-de-Bosson (2630 - 2900 m a.s.l) and Lona (2640 - 3000 m a.s.l.) during the period 1989 to 1991. By means of geophysics, these authors observed that the permafrost distribution within the rock glaciers had been affected by the glacier advance that had occurred during the Little Ice Age (LIA).

Most of the numerous vertical DC (direct current) resistivity soundings which were carried out around 1990 were repeated in 2002, as far as possible at the same places. The data were supplemented by further geoelectrical and BTS measurements.

METHODS

Twenty-eight DC resistivity soundings were performed in 2002, of which ten were new ones. Contrary to the 1990 soundings, when only the symmetrical Schlumberger array was used, the dissymmetrical Hummel configuration was systematically applied for the more recent acquisitions. Such a configuration allowed lateral changes in the ground resistivity to be detected. It was difficult to relocate the exact location of the soundings that were carried out a decade earlier at the Becs-de-Bosson rock glacier. At Lona, Gerber (1994) marked the position of the soundings with wooden stakes. It was therefore possible to reiterate exactly the same soundings.

A resistivity mapping was carried out in the rooting zone of the Becs-de-Bosson rock glacier. The apparent resistivity was investigated at a pseudo-depth of about 10-15 m (20 m inter-electrode spacing, Wenner configuration, 177 measurements).

A BTS map based on 281 measurement points was drawn for the Becs-de-Bosson rock glacier. A similar task is planned at Lona.

Finally, 30 minidata loggers (UTL-1) were dispatched on both sites in September 2002 in order to control the thermal state of the ground surface during at least one year.

IMPACTS OF THE LITTLE ICE AGE

Becs-de-Bosson

The small Becs-de-Bosson glacier had completely disappeared by the middle of the 20th century. During the LIA, the glacier covered the upper half of the rock glacier. Several push moraines were formed.

The BTS map largely fits with geo-electrical data and therefore permits the discontinuous distribution of permafrost in the rooting zone of the rock glacier to be illustrated (Fig.1). The zone where the BTS values are above -2°C points to the current probable absence of permafrost. Most of this area was covered by the glacier during the LIA and probably at least until the end of the 19th century. Colder BTS values indicate permafrost occurrence. They correspond either to push moraines or to the intact lower part of the rock glacier. The foot of the northern steep slope of the Becs-de-Bosson peak is cold as well.

Lona

During the LIA, the Sasseneire glacier almost completely overrode the Lona rock glacier. In some places, the glacier appears to have gone beyond the rock glacier extent. Only a few ice patches remained at the foot of the Sasseneire headwall in 2002.

Geoelectric data showed that only pieces of the rock glacier have continued to exist since the LIA glacier advance. Today, there is almost no ground ice whatever left in the en-

tire glacier/rock complex. However, permafrost was detected, notably, in the terminal part of the rock glacier. This frozen body seems to have been pushed down by the glacier towards a more sunny area and far away from any source of debris.

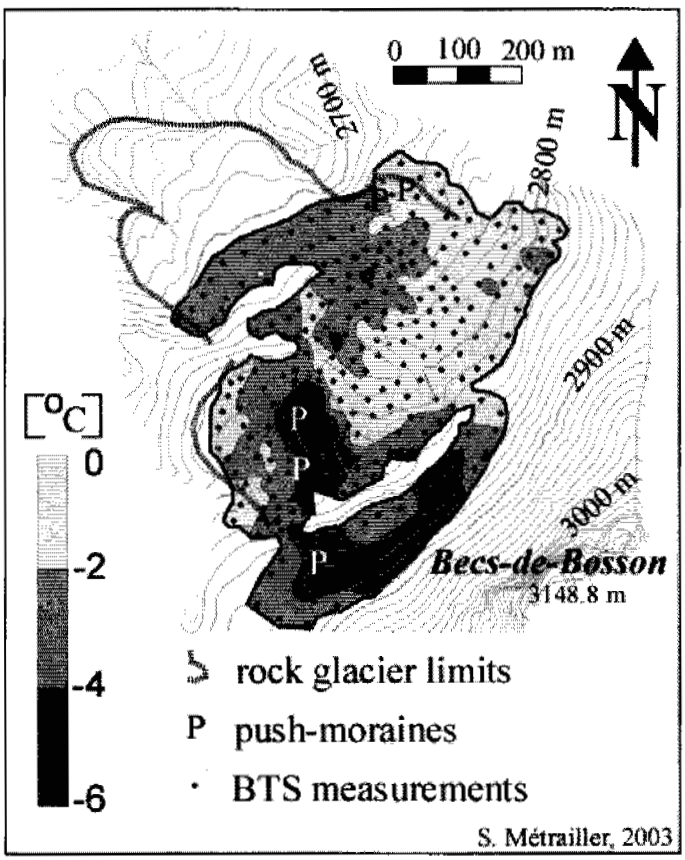

Figure 1. BTS map on the upper half Becs-de-Bosson rock glacier.

CHANGES BETWEEN 1990 AND 2002

The comparison between the 1990 and the 2002 data shows an evident change for only two of the resistivity soundings. The other sixteen soundings for 2002 were not significantly different than those from a decade earlier.

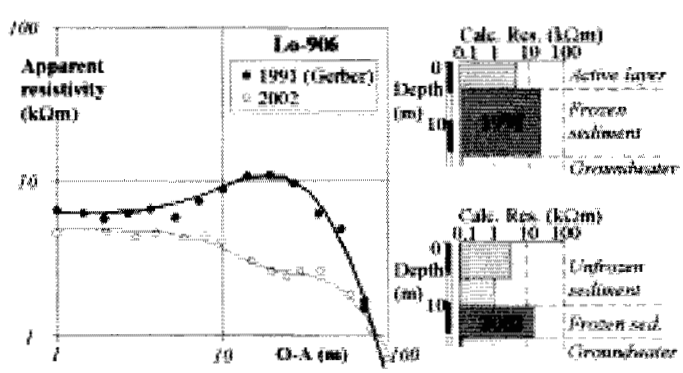

Figure 2. Vertical resistivity sounding Lo-906 repeated at a decade interval on the terminal part of the Lona glacier/rock glacier complex.

The two different soundings were performed at the front of the Lona rock glacier. Similarly, they indicate a decrease of the resistivity in the uppermost former frozen layer (Fig. 2). This could be interpreted as a dramatic increase in ground temperature and probably a melting of permafrost between about 4 and 10 m depth.

CONCLUSIONS

The permafrost and ground ice distribution within the two glacier/rock glacier complexes reflects the glacial history over the last centuries. The investigated rock glaciers have been considerably remodelled by the LIA advance of small glaciers. Some perennially frozen materials were displaced, while others had melted completely.

Over the last decade of the 20th century, no tangible evolution of the permafrost geometry, that could be attributable to changing climatic conditions, was detected by means of DC resistivity soundings in both glacier/rock glacier complexes.

The permafrost modifications observed at the front of the Lona glacier/rock glacier complex are attributed rather to the current unfavourable location of this permafrost consecutive to LIA glacier/rock glacier dynamic. This melting of the permafrost had begun a certain time before 1990, as Gerber (1993) already observed a settlement of about 1 m in the same area by comparing aerial photographs taken in 1972 and 1992.

ACKNOWLEDGEMENTS

This project was supported by the Valaisian Society of Natural Sciences, the University Institute Kurt Bösch and the Department of Geosciences at the University of Fribourg.

REFERENCES

Gerber E. 1994. Geomorphologie und Geomorphodynamik der Region Lona-Sasseneire (Wallis, Schweizer Alpen) unter besonderer Berücksichtigung von Lockersedimenten mit Permafrost. PhD thesis 1060. Fac. Sciences, Univ. Fribourg, Switzerland (in German).

Tenthorey G. 1993. Paysage géomorphologique du Haut Val de Réchy (Valais, Suisse) et hydrologie liée aux glaciers rocheux. PhD thesis 1044. Fac. Sciences, Univ. Fribourg, Switzerland (in French).

Application of quantitative land-surface analysis methods in geocryology

A.V. Mitusov and O.E. Mitusova

Institute of Physical, Chemical and Biological Problems of Soil Science of the Russian Academy of Sciences, Pushchino, Moscow region, Russia

INTRODUCTION

When Digital Elevation Models (DEM) are used for land surface analysis, quantitative characteristics or morphometric variables (MVs) must be used. Physical phenomena, which could be described by MVs, might be subdivided into the following 4 groups:

- Morphometric conditions of surface run-off and soil throughflow.
- Geometrical landforms.
- Morphometric conditions of thermal regimes on slopes.
- Morphometric conditions of altitude zonality, i.e.,the change of atmospheric properties with elevation.

All 4 groups occur in the cryolithic zone.

MORPHOMETRIC VARIABLES

The land surface can be described by regional and local MVs. In the first case, the influence of remote sites is taken into account, in the second case it is not. In this study, a system of 18 MVs of general geomorphometry was used (Shary et al. 2002).

Morphometric conditions of runoff

The planar land surface is regionally described by maximum catchment area (MCA) and maximum dispersal area (MDA). MCA for a given matrix element (square on a map) shows the maximum area from which material moving downslope may be collected. MDA describes the maximum area on which materials moving downslope may be diffused.

The planar dimension and profile of the land surface are locally described by horizontal (kh) and vertical (kv) curvatures. The differentiation of land surfaces with respect to kv and kh allows us to group them into four local landform types (Troeh 1964).

Algorithms are frequently used which integrate slope gradient and aspect (GA) to simultaneously describe both planar and profile characteristics. The most popular formula is the topographical index (Beven and Kirkby 1979). This method, however, tends to approach infinity with GA→0 and makes its application incorrect for a lot of land surfaces. MV's are available now with the correct regional and simultaneous description of planar and profile characteristics of land surfaces (Shary et al. 2002).

Geometrical landforms

Geometrical landforms are land surface forms which do not need to take gravitational fields into account for their description. For example, ridge and valley forms are referred to as geometrical forms if they are defined independently from their orientation in gravitational fields. Locally, maximum and minimum curvatures describe such forms.

APPLICATION OF MORPHOMETRIC VARIABLES

Here we consider the application areas of an MV system in geocryology but have not considered the morphometric conditions of altitude zonality and of the thermal regimes of slopes. The primary possibility concerns the analysis of runoff directions and potential flowspeeds (movement of water, avalanches, glaciers, lava, etc.).

The MCA map reflects both potential and real hydrological channel networks without distinguishing them (Fig. 1 and 2); during calculation, the locations and depths of all depressions were also computed. This MV is of a critical value and determines free water at the surface. The places of output of land surface waters and their areas of their origin are well described.

For the definition of potential runoff rates it is necessary to take the slope profile along the length of the flow path into consideration. Areas of relative flow deceleration always coincide with the concave parts of the profiles, while areas of relative flow acceleration correspond to the convex parts.

The development of cryogenic processes such as thermokarst and solifluction, the formation of frost mounds and alas etc. is connected with the occurrence of water in the soil/ground. This allows the prediction of position and potential intensity based on the correlation of the soil/ground moisture content (and some other parameters) with the MVs. It is important to note that in some of the terrains from the 18 studied

MVs, only the geometrical form provided a strong correlation with soil moisture.

Already existing cryogenic landforms can be found as a result of morphometric analysis of DEMs. In general, landforms of different genesis can be found. Landforms with geomorphometric structures typical for cryogenic landforms can be separated from other landforms but only by the application of all 18 MVs.

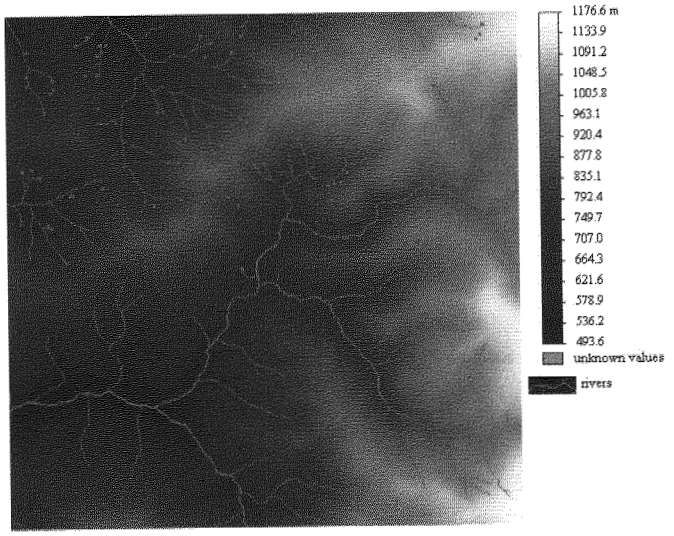

Figure 1. Example of an elevation matrix (digital elevation model – DEM) 4x4 km. The information on the rivers contains an additional vector layer.

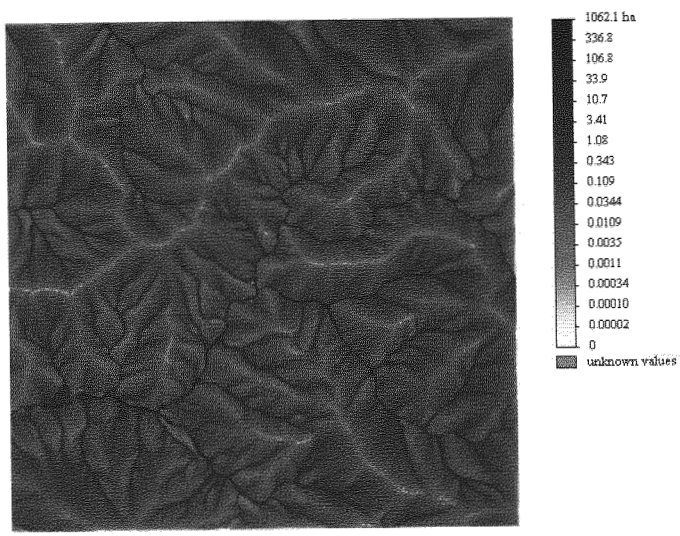

Figure 2. Example of a matrix with MCA calculated from the DEM given in Figure 1. The map of MCA allows to predict the location of rivers. It follows from comparison between Figure 1 and Figure 2 that the locations of rivers coincides with areas of the large MCAs.

CONCLUSIONS

The application of an extended system of quantitative land surface analysis methods in cryology - except for the morphometric conditions of thermal regimes on slopes and altitude zonality - allows us to:

(1) define a direction and potential speed of flow movements for various substances (water, glaciers, lava, landslides, snow avalanches, etc.); on this basis it is possible to forecast the potential irrigation of a territory and to estimate the hazards.

(2) predict the places of development of cryogenic processes (thermokarst, solifluction, formation of frost mounds and alases, etc.) as well as their potential intensity.

(3) reveal cryogenic landforms on DEM and separate them from other landforms (geological, etc.).

ACKNOWLEDGEMENTS

The authors are grateful to P.A. Shary for providing Analytical GIS Eco with data and Dr O.I. Khudyakov for advice in the geocryology field.

REFERENCES

Beven, K.J. and Kirkby, M.J. 1979. A physically based, variable contributing area model of basin hydrology. Hydrological Sciences Bulletin 24: 43-69.

Shary, P.A., Sharaya, L.S., and Mitusov, A.V. 2002. Fundamental quantitative methods of land surface analysis. Geoderma 107 (1-2): 1-35.

Troeh, F.R. 1964. Landform parameters correlated to soil drainage. Soil Science Society of America Proceedings 28: 808-812.

Modeling permafrost distribution in the northern Alps using global radiation

*O. Mustafa, M. Gude and *M. Hoelzle*

Department of Geography, University of Jena, Germany

**Glaciology and Geomorphodynamics Group, Department of Geography University of Zurich, Switzerland*

INTRODUCTION

In order to reduce natural hazards in alpine areas high mountain permafrost became an important objective of research within the last decade. Many investigations were made in the central Alps. Here, the spatial distribution of permafrost is well documented because a high number of field measurements and computer models give reasonable results. But the adaptation of these findings to the northern Alps margin is assumed to cause problems due to the different climatic conditions controlling the permafrost regime. A regional analysis should especially account for the higher diffuse radiation compared to direct radiation. Therefore, the CLOUDMAP model is developed as a variant of the PERMAMAP model.

THE TEST SITES

The investigation area in the mountains of Wetterstein is situated at the northern margin of the Alps at 47°25′N and 10°59′E. It is crowned by Germany's highest peak, the Zugspitze (2962 m a.s.l.) and the lowest elevation is at 1580 m a.s.l. A 20 m grid is used for model runs at this site. For calibration and comparison a secondary test site in the central Alps south of Zermatt (Valais) was chosen (47°02′N, 7°45′E). The 25 m DEM of this site reaches from 1675 to 3424 m a.s.l. Climatic parameters with relevance to the models are listed in Table 1.

Table 1: Climatic parameters of the test sites.

	Wetterstein	Zermatt
0°C-Isotherme [m NN]	2101	2363
Temp. gradient [K/100 m]	0.60	0.51
Daily sunshine [h]	5.7	6.0
Cloudiness [1/10]	6.9	4.1

The Zermatt test site has, for years, been the site of intensive permafrost research. A great deal of field data are collected and various computer models were applied (e.g. Gruber and Hoelzle 2001). In contrast, there is only little information about the permafrost situation at the Wetterstein test site (Ulrich and King 1993).

Permafrost-mapping was accomplished by long-term measurements of BTS and bedrock temperature and analysis of observed permafrost and permafrost related features (Gude and Barsch 2003). For spatial extrapolation of the measurements, GIS-based modeling was undertaken with two different models, which will be presented.

PERMAFROST DISTRIBUTION MODELS

The PERMAMAP model (Hoelzle 1994) calculates the spatial distribution of alpine permafrost by applying a statistical relation of field measurements of BTS (bottom temperature of snow) with elevation and direct solar radiation during summer.

To account for the more humid and, therefore, more cloudy conditions in the northern Alps the CLOUDMAP model was developed. CLOUDMAP relates the BTS to elevation and global radiation (Fig. 1). An approach by Arck & Escher-Vetter (1997) is the basis for the calculation of global radiation. In contrast to the PERMAMAP model, CLOUDMAP needs the input of meteorological data for cloudiness and duration of sunshine.

RESULTS

Both models were applied to both test sites. Due to the inaccessibility of large parts of the Wetterstein during winter it was not possible to get enough BTS-data to generate the statistical relations the models need. Hence, a regional calibration by climatic parameters was applied to the statistical relations of the Zermatt test site in order to transfer them to Wetterstein.

A comparison of the model results for the Zermatt test site shows only minimal differences. In contrast, the results for the Zugspitze test site differ significantly (Fig. 2). The difference concerns most notably the north-exposed slopes, where the lower limit of permafrost rises about 250 m of elevation.

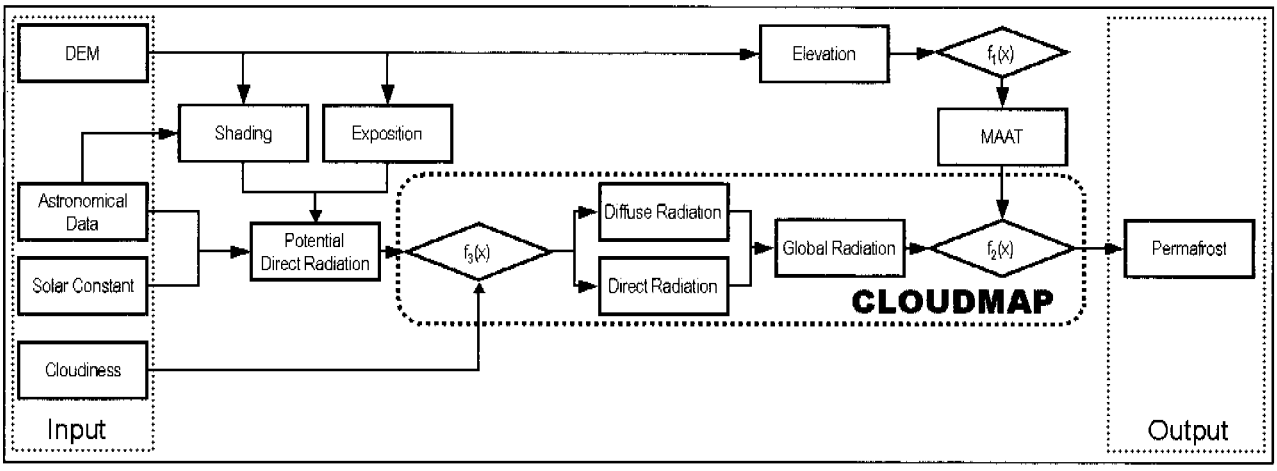

Figure 1. Structure of CLOUDMAP as an insertion to PERMAMAP; $f_{1\text{-}3}(x)$ – empirical functions

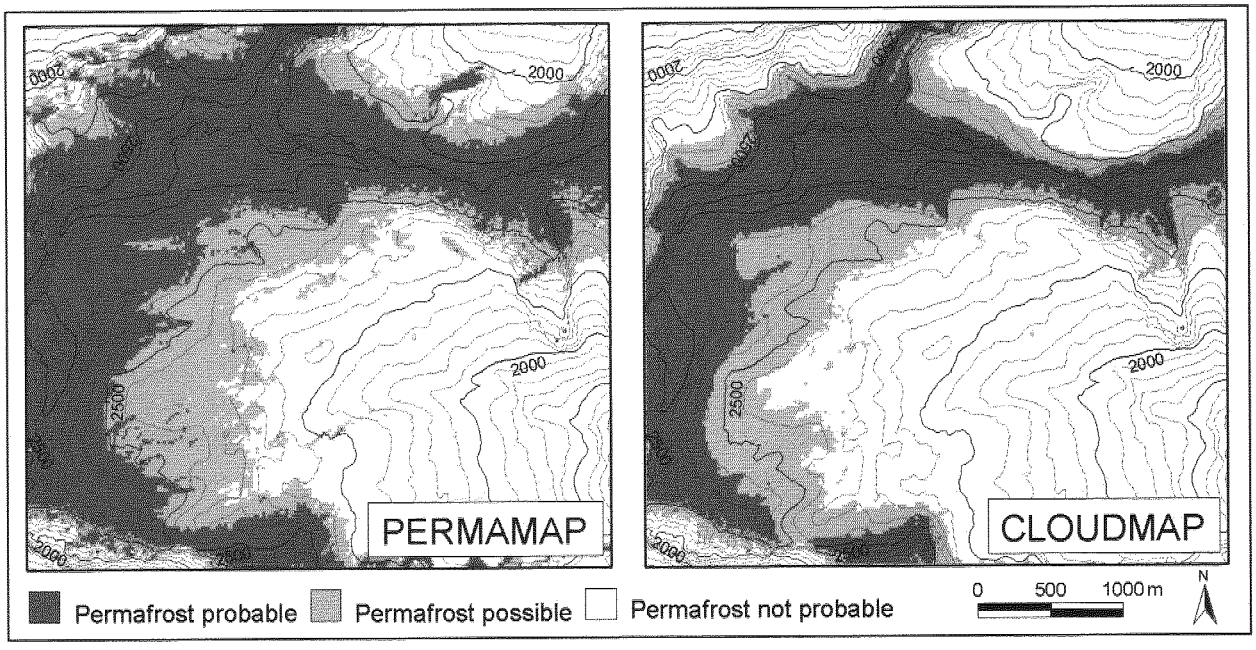

Figure 2. Modelled permafrost distribution at the Wetterstein test site (glaciers are not considered).

REFERENCES

Arck, M. and Escher-Vetter, H. 1997. Topoclimatological analysis of the reduction of the glaciers in the Zugspitz region, Bavaria. Zeitschrift für Gletscherkunde und Glazialgeologie IX(1-2): 57 - 72.

Gruber, S. and Hoelzle, M. 2001. Statistical modelling of mountain permafrost distribution: Local calibration and incorporation of remotely sensed data. Permafrost and Periglacial Processes 12(1): 69 – 77.

Gude, M. and Barsch, D. 2003 (in print). Assessment of geomorphic hazards in connection with permafrost occurrence in the Zugspitze area (Bavarian Alps). Geomorphology.

Hoelzle, M. 1994. Permafrost und Gletscher im Oberengadin. Grundlagen und Anwendungsbeispiele für automatisierte Schätzverfahren. Mitteilungen der VAW 132. ETH Zurich.

Ulrich, R. and King, L. 1993. Influence of mountain permafrost on construction in the Zugspitze mountains, Bavarian Alps, Germany. Sixth International Conference on Permafrost, Beijing, Proceedings 1: 625 – 630.

The circumpolar active layer monitoring (CALM) program: Recent Developments

*F. E. Nelson, N. I. Shiklomanov, *K. M. Hinkel and **J. Brown*

Department of Geography, University of Delaware, Newark, DE USA
**Department of Geography, University of Cincinnati, Cincinnati, OH USA*
***International Permafrost Association, Woods Hole, MA USA*

The Circumpolar Active Layer Monitoring (CALM) program was established to observe the long-term response of the active layer and near-surface permafrost to changes in climatic parameters. Initial foci of the program included "data rescue" activities and creation of a data archive, building an alliance of active field scientists willing to share data, execution of critical field experiments, and development of data-collection protocols. Most aspects of these tasks were implemented by the mid-1990s. Details are provided in the volume by Brown et al. (2000).

Data produced from the CALM network have proven useful in many contexts, including model validation. Owing to the limited observational record at most sites, it is not yet possible to arrive at definitive conclusions about long-term changes or trends in the temperature and thickness of the active layer. The few long-term data sets available from high-latitude sites in the Northern Hemisphere show very substantial interannual and interdecadal fluctuations. The spatial variability of active-layer thickness is large, even within geographic areas of very limited extent (e.g. 1 km^2). Most sites in tundra environments show a strong, positive relation between summer temperature and the thickness of the active layer. This relation is weaker in boreal environments. Increases in thaw penetration, subsidence, and development of thermokarst terrain have been observed at some sites, particularly in subarctic regions.

Strong bonds have been forged between CALM and several international monitoring and global change programs. CALM is part of the International Permafrost Association's Global Terrestrial Network for Permafrost (GTN-P), which also incorporates a network of boreholes for monitoring permafrost temperatures (Romanovsky et al. 2002). GTN-P is itself part of the Global Terrestrial Observing System (GTOS) and the Global Climate Observing System (GCOS), co-sponsored by a consortium of international organizations, including the World Meteorological Organization and the International Council of Scientific Unions, among others. Further details are provided in Burgess et al. (2000).

Only a little more than a decade into its existence, CALM has produced a large body of scientific literature, much of it reviewed in a monograph-length paper by Brown et al. (2000). Under the aegis of the IPA's Permafrost and Global Change Working Group, meetings and discussions devoted to CALM have been held at most of the annual cryosphere conferences in Pushchino, Russia and at several of the American Geophysical Union's Fall Meetings in San Francisco. The current phase of CALM, supported by the U.S. National Science Foundation (NSF), reached its apogee in November 2002, when 35 scientists from six countries attended an NSF-sponsored workshop in Lewes, Delaware. This workshop provided an opportunity for CALM scientists to learn details about research programs at various sites, to discuss progress and problems in the network, to implement unified data-analytic procedures, and to plan future activities.

The CALM network currently includes 130 active sites with 15 participating countries. An additional 20 secondary sites are co-located with these primary sites, resulting in a total of 150 sites that report active-layer thickness on an annual basis. Of the total, 100 sites are collecting soil and permafrost temperature data; of these, 60 are from boreholes between 3 m and 884 m deep (Smith et al, this volume, discuss metadata information on GTN-P boreholes). Most sites in the CALM network are located in Arctic and Subarctic lowlands, although 20 boreholes are in mountainous regions of the Northern Hemisphere above 1300 m elevation. A new Antarctic component is forming and currently contains 13 sites.

The 2002 CALM workshop focused synthesis activities on the 70 sites in six countries from which gridded data are available. The workshop resulted in preparation of seven extended regional abstracts for this volume (Table 1). Several other papers report details from these same CALM sites (Romanovsky et al. 2002, Hinkel and Nelson 2003) Other CALM related papers appear in the Proceedings and Abstract volumes for Mongolia (Sharkhuu), Kazakhstan (Marchenko), Canada (Tarnocai et al.), and Antarctic (Guglielmim et al.).

Extended discussions about CALM's future directions, strategies, and activities took place at the Delaware workshop, culminating in the CALM Workshop Resolution.

The Resolution consists of the following main recommendations:

- To continue the CALM observations and improve the thematic representativeness of the network;
- To improve linkages with other networks and international programmes such as WCRP (CliC), IGBP and the proposed Circumarctic Environmental Observatories Network (CEON);
- To better understand active layer dynamics through observations of borehole temperatures, subsidence, snow cover, soil properties (moisture, surface organics, texture), topography and vegetation;
- To ensure continued operation, maintenance and enhancement of CALM and borehole temperature databases (GTN-P) and websites;
- To provide input for improvement of permafrost-climate model development, model result comparison, and verification;
- To prepare reports to disseminate results of data analyses beginning with the 8th ICOP and a special journal publication; and
- To develop strategies for remote sensing-based methods of monitoring geocryological parameters over extensive areas, consistent with the GHOST observation scheme

Table 1. Extended abstracts resulting from 2002 CALM workshop (senior author listed for abstract in this volume).

1. Nordic Region: Christiansen et al.
2. Lower Kolyma River: Fyodorov-Davydov et al.
3. West Siberia: Melnikov et al.
4. European Russia: Mazhitova et al.
5. West Siberia: Vasiliev et al.
6. Chukotka: Zamolodchikov et al.
7. Modelling: Oelke and Zhang

ACKNOWLEDGEMENTS

The CALM program work was supported by the U.S. National Science Foundation under grants OPP-9732051, 0094769, 0095088, and 0225603. Views expressed in this abstract are the authors' and do not necessarily reflect those of NSF.

REFERENCES

Brown, J., Hinkel, K.M. and Nelson, F.E. 2000. The Circumpolar Active Layer Monitoring (CALM) program: research designs and initial results. Polar Geography 24(3): 165-258.

Burgess, M., Smith, S.L., Brown, J., Romanovsky, V. and Hinkel, K. 2000. Global Terrestrial Network for Permafrost (GTNet-P): permafrost monitoring contributing to global climate observations. Geological Survey of Canada, Current Research 2000-E14.

Hinkel, K.M. and Nelson, F.E. in press. Spatial and temporal patterns of active layer thickness at circumpolar active layer monitoring (CALM) sites in northern Alaska, 1995-2000. Journal of Geophysical Research-Atmospheres.

Romanovsky, V., Smith, S., Yoshikawa, K. and Brown, J. 2002. Permafrost temperature records: indicators of climate change. Eos, Transactions, American Geophysical Union 83(50): 589 and 593-594.

Life in the terrestrial permafrost: a possible key to the search of Life in Space

*K.A.Novototskaya-Vlasova, D.A.Gilichinsky, *A.A. Abramov and **V.S. Soina*

Soil Cryology Laboratory, Institute of Physicochemical and Biological Problems in Soil Science, Pushchino, Moscow Region, Russia

**Department of Geocryology, Moscow State University, Moscow, Russia*

*** Department of Soil Biology, Moscow State University, Moscow, Russia*

Sterile frozen samples were taken from boreholes (Fig. 1) near the Laptev Sea coast (East Siberia) and in Beacon Valley (Antarctica) for "classical" microbiological analyses. The examined Arctic sediments were formed about 10-400 thousand years ago (Schirrmeister et al. 2002). The sediments are ice-rich (up to 80-90%) and have a low mean annual temperature (-10 to –15°C). We also investigated ancient Antarctic permafrost, several million years old (Sugden et al. 1995) taken from boreholes drilled in the region of the Dry Valleys, which have mean annual temperatures ranging from -20 to -22°C with ice contents lower than in Arctic deposits (40%). The magnitude of unfrozen water and total organic matter content (TOC) in Arctic loam is 3-5%. In Antarctic sands, both these values are close to zero, i.e., at levels impossible to record with presently available instrumental methods.

Special procedures were used to determine the biological activity in the thawed samples. The number of viable cells was counted using the plate method. In the model experiments, the long-term viability of isolated species of both spore-forming and non spore-forming bacteria was maintained, for 1 to 4 months in a diluted nutrient medium, that is tryptic soy broth and water suspensions at room and lower (7°C) temperatures.

The communities of micro-organisms inhabiting the ancient permafrost could be easily recovered. These communities are chiefly represented by bacteria concentrations varying from 10^2 to 10^7 cells/gdw (Fig. 1).

Taxonomic identification of isolated aerobic bacteria showed that such biotopes contain the same diversity of bacteria as modern tundra cryosols. The taxonomic diversity revealed the tendency to survive predominantly as non spore-forming, presumably psychrotrophic bacteria able to grow on nutrient media at temperatures of 4 to 22°C. Increase in the microbial (=permafrost) age or decrease in temperature of Antarctic sediments in comparison with Arctic ones result in the decrease of proliferating cell numbers. This suggests that part of the permafrost microbial community may either undergo deep anabiosis, or be preserved in stable, so-called viable, but non-cultivable forms. As mentioned in an earlier study (Vorobyova et al. 1997), the ratio between cultivable and non-cultivable microbial cells might indicate the physiological response of microorganisms to environmental conditions.

The ability of bacteria to survive in frozen sediments may be explained by specific mechanisms of the cell differentiation into forms that enable bacteria to sustain conditions unfavorable for growth and multiplication (cold stress, starvation, etc.). The colony-forming units (CFU) in long-stored cultures decreased from 10^8 down to 10^2. Nevertheless, as may be seen by electron microscopy, the majority of the cells are intact and resume their activity without additional procedures in conditions favorable for growth. Bacteria *Bacillus sp.*, and *Azotobacter sp.*, isolated from permafrost, are known to produce typical resting forms - spores and cysts in their life cycles. However, for long-term storage under conditions of starvation and subzero temperatures, they produce other forms (Fig. 2). Such specific cell forms as observed in the stored cultures may be regarded as one of the reversible dormant types of both, non spore-forming bacteria and bacteria which are known to produce specific resting cells that can be formed in permafrost. Probably, this mechanism of survival in extreme conditions might also work in an extraterrestrial environment. The investigated deposits may be considered approximately similar to Martian permafrost which, according to the most recent data, contains ground water ice (Mitrofanov et al. 2002). The existence of thermo-resistant viable bacterial cells with specific ultrastructure (similar to dormant forms) in terrestrial permafrost is a reason for advancing the hypothesis that Martian permafrost might contain Life.

ACKNOWLEDGEMENT

This work was supported by the Russian Foundation for Basic Research, grant 01-05-65043.

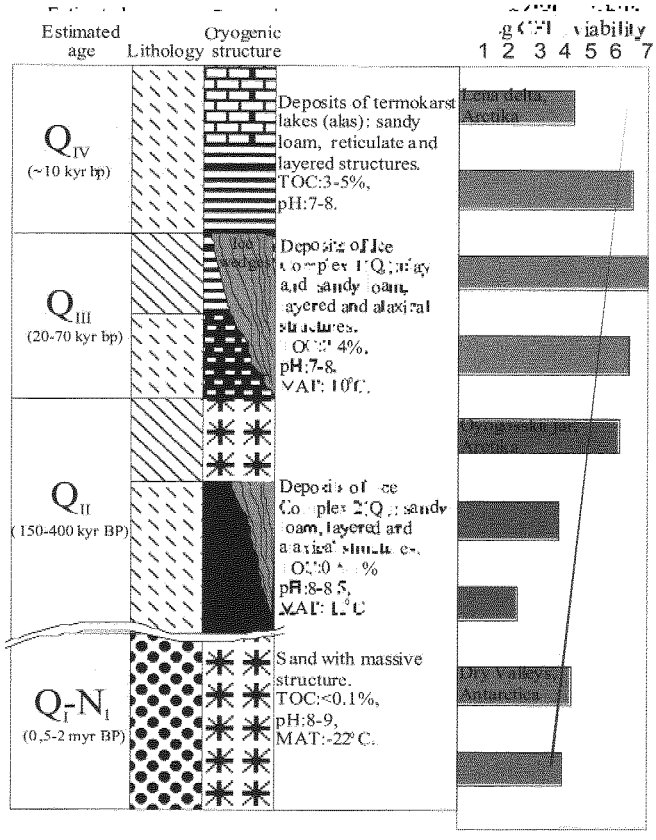

Figure 1. Schematic geological profile of the studied areas and number of viable cells (CFU/g), isolated from Arctic and Antarctic permafrost sediments at +20°C.

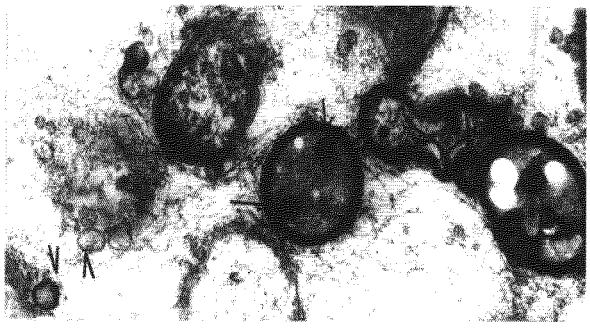

Figure 2. Cyto-morphological forms of *Azotobacter sp.* 5-10, isolated from Antarctic permafrost in cultures stored during 4 months in water suspensions at +7°C: cyst-like cells (single arrow) and nanoforms (double arrow).

REFERENCES

Gilichinsky D. 2002. Permafrost as a microbial habitat. Encyclopedia of Environmental Microbiology,Willey: 932-956.

Mitrofanov I. et al. 2002. Maps of Subsurface Hydrogen from the High Energy Neutron Detector, Mars Odyssey. Science 297: 78-81.

Schirrmeister L. et al. 2002. Paleoenviromental and paleoclimatic records from permafrost deposits in the Arctic region of Northern Siberia. Quaternary International 89: 97-118.

Sugden D. et al 1995. Preservation of Miocene glacier ice in East Antarctica. Nature 376: 412-414.

Vorobyova E. et al. 1997. The deep cold biosphere: facts and hypothesis. FEMS Microbiology Reviews 20: 277-290.

Comparing thaw depths measured at CALM field sites with estimates from a medium-resolution hemispheric heat conduction model

C. Oelke and T. Zhang

National Snow and Ice Data Center, Crysospheric and Polar Processes Division, CIRES, University of Colorado, Boulder, Colorado, U.S.A.

INTRODUCTION

The Circumpolar Active Layer Monitoring (CALM) program (Brown et al. 2000) was initiated in the late 1980s to observe and understand the response of the active layer and near-surface permafrost to climate change. This systematic study focuses on active layer processes and monitoring thaw depth. It currently incorporates measurements from more than 100 sites involving 15 investigating countries. The CALM site data were collected primarily over 100 m x 100 m or 1000 m x 1000 m test areas. CALM data are available from the CALM website at http://k2.gissa.uc.edu/~kenhinke/CALM/. Here we compare these field measurements of thaw depth with results from a numerical heat conduction model.

Heat Conduction Model

A finite difference model for one-dimensional heat conduction with phase change (Goodrich 1982) is used. This model has been shown to provide excellent results for active layer depth over permafrost and soil temperatures (Zhang et al. 1996) when driven with well-known boundary conditions and forcing parameters at specific locations. A detailed description of the model is given by Goodrich (1982) and Zhang et al. (1996). Our intent is to model the soil freeze/thaw state for the whole Arctic drainage area. We run the model one-dimensionally and assume no lateral heat transfer among the 25 km x 25 km grid cells with depths of 15 m. Soil is divided into three major layers (0-30 cm, 30-80 cm, and 80-1500 cm) with distinct thermal properties of frozen and thawed soil, respectively. Calculations are performed on 54 model nodes ranging from a thickness of 10 cm near the surface to 1 m at 15 m depth. Details about model settings and the forcing data sets (surface air temperature, snow thickness, soil bulk density, soil moisture content) are given by Oelke et al. (2003). The model is spun up for 50 years in order to obtain more realistic start conditions for temperatures of all model layers. The model is applied to the whole Arctic area drainage comprising 39,926 north polar Equal-Area Scalable Earth (EASE) grid cells with an area of 24.7×10^6 km^2. We use a daily time step for the 22 years of our simulation (1980 through 2001). Oelke et al. (2003) show fields of thaw depth for this area at three-month intervals, together with the active layer depth and the length of freezing and thawing periods.

COMPARISON WITH CALM THAW DEPTH MEASUREMENTS

Arctic Drainage Area

We compare our model results for the year 2000 with measurements of thaw depth (D_T) for the same year, made at 66 locations in regions of continuous or discontinuous permafrost. Measurements from Canada, Greenland, Russia, Svalbard, and Alaska are included. Figure 1 shows the comparison for the day when the measurement was taken in the field, which is usually close to the annual late summer maximum. Also shown are bars of ±1 standard deviation for 48 grid sites. Modeled thaw depth is a distance-weighed average between the four grid cells around the CALM site location.

The comparison between modeled thaw depths based on 625 km^2 averages of temperature, snow depth, and soil bulk density and a measured thaw depth on a much smaller scale (1 ha or 1 km^2) should be viewed as an indication of model performance rather than a true validation. The modeled values nevertheless agree reasonably well with the measured values within their standard deviation, and capture the general picture of high-Arctic active layers. The high standard deviation of the grid measurements points to large spatial variability of thaw depth, even on these small scales.

Grid cells with modeled thaw depths much lower than measured depths are located in Greenland, Svalbard, or Baffin Island fjords at lower elevations than those of the higher, and consequently colder, corresponding model grid cells. The resulting modeled thawing seasons are shorter and the thaw depths are shallower. The RMS er-

ror without seven such sites (marked by diamonds in Figure 1) is reduced from 32.1 cm to 23.7 cm. The comparison to 70 CALM sites for 1999 shows a similar behavior as for 2000, with a RMS error of 29.7 cm. It is reduced to 26.7 cm without six sites that experience a strong cold bias adjacent to mountain ranges.

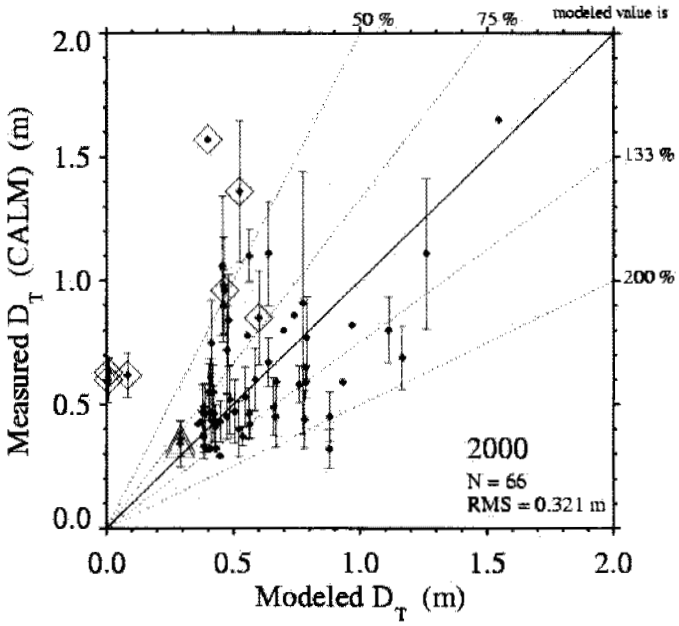

Figure 1. Modeled vs. measured thaw depth (D_T) for the day when the measured value was observed in 2000. Bars give the ±1 standard deviation for CALM sites measured on grids. Diamonds mark sites adjacent to mountains or high plateaus; therefore, modeled thaw depths are too shallow.

Local Time Series

The comparison between modeled and measured thaw depth for the two CALM sites near Barrow (north slope of Alaska at 71° 19′N and 156° 36′W) shows D_T close to the diagonal at about 0.3 m (triangles in Figure 1). A 22-year time series (1980–2001) of active layer depth (ALD) for the model grid cells near Barrow is shown in Figure 2. Only a very small positive linear trend of 0.029 cm/a is calculated. The solid bold line gives thaw depth (D_T) for the day of year the CALM measurements were taken, and is therefore lower than the ALD. This modeled thaw depth is compared to measurements at CALM sites U1 (Barrow, 1000 m grid, dotted line) and U2 (Barrow, CRREL 10 m plots, dashed line). Both modeled and measured values show an increase in thaw depth from 1991 to 1994. The model value then decreases before rising to a maximum in 1998. From 1998 to 2001 there is a steady decline in thaw depth at Barrow. A correlation coefficient r_{U1} of 0.421 is calculated between modeled and measured thaw depth at U1 (1992–2001). For the site U2, R_{U2} is slightly higher at 0.609 (1991–2001). Modeled and measured curves are almost parallel after 1994, with differences up to 5 cm. The correlations become much stronger when starting the analysis in 1995 with r_{U1}=0.961 and r_{U2}=0.936. Differences in U1 and U2 thaw depths are up to 2 cm, due to the different location and size of the sites, and different probing dates.

Measured and modeled thaw depths agree quite well, taking into account the considerable differences in scales and the large spatial variability measured on the very much smaller CALM grids.

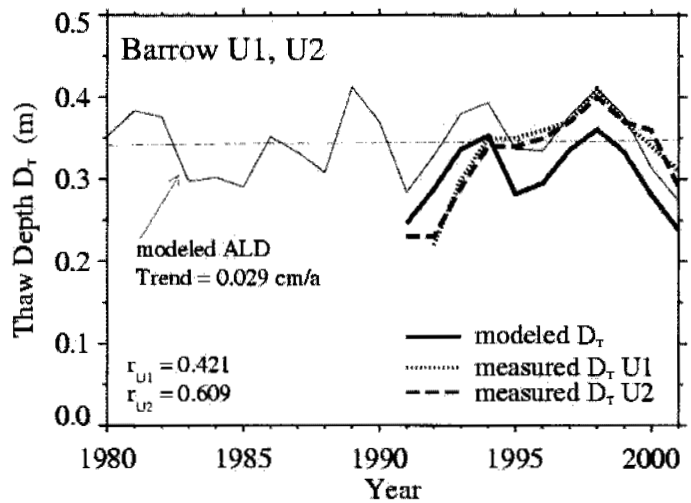

Figure 2. Modeled active layer depth (ALD) at Barrow, Alaska, for 1980–2001, including the linear trend (dash-dotted line). Bold dotted lines are measured thaw depths (D_T) at CALM sites U1 (1992–2001) and U2 (1991–2001), and the solid bold line is the modeled thaw depth for the actual day of measurement.

ACKNOWLEDGMENTS

This report was developed as a result of the CALM synthesis workshop held in November 2002 at the University of Delaware. This study was supported by NASA through grant NAG5-6820 and by NSF through grant OPP-9907541.

REFERENCES

Brown, J., Hinkel, K.M. and Nelson, F.E. 2000. The Circumpolar Active Layer Monitoring (CALM) Program: Research Designs and Initial Results, Polar Geography, 24(3): 163—258.

Goodrich, L.E. 1982. Efficient numerical technique for one-dimensional thermal problems with phase change, International Journal of Heat and Mass Transfer, 21: 615—621.

Oelke, C., Zhang, T. Serreze, M. and Armstrong. R. 2003. Regional-scale modeling of soil freeze/thaw over the Arctic drainage basin, Journal of Geophysical Research 108(D10): 4314, doi: 10.1029/2002JD002722..

Zhang, T., Osterkamp, T.E. and Stamnes, K. 1996. Influence of the depth hoar layer of the seasonal snow cover on the ground thermal regime, Water Resources Research, 32(7): 2075—2086.

Coastal dynamics of the Pechora Sea under human impact

S.A. Ogorodov

Faculty of Geography, Moscow State University, Moscow, Russia

The so-called Pechora Sea is located in the south-eastern part of the Barents Sea. The Pechora sector of the Barents Sea is characterised by loose permafrost coasts. These coasts are relatively stable under natural conditions but are rapidly destroyed under human impact. A case in point is the Varandei industrial area where expeditious measures to protect industrial buildings and living accomodation are necessary. Human impact upon the Varandei area activates coastal erosion because of improper exploitation that does not take peculiarities of coastal relief and dynamics into account. Coastal erosion of the Varandei area brings a threat to the settlement, oil terminal (Fig. 1) and airport.

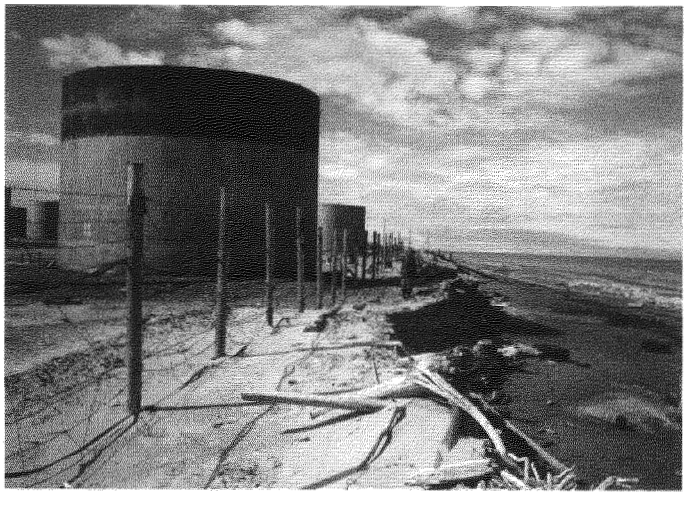

Figure 1. Wave-cut cliff near the Varandei oil terminal

Active exploitation of the Varandei industrial area and Varandei Island started in the seventies. Varandei Island is a typical sand barrier beach in the Pechora sea. The shoreface of this accumulative form is covered with a dune belt (avandune) of 4 to 7 m high. Laidas or high-water surge berms occupy the inner part of the barrier beach behind the dune belt. Varandei Island was subjected to very strong technogenic impacts. The main industrial base was built and Novyi Varandei, a settlement for 3.5 thousand inhabitants. A well-drained dune belt of the barrier beach, made up of sand beds with low ice content, was chosen as a place for the settlement, oil terminal and storehouses because it seemed to be more stable from the engineering-geological point of view than the surrounding swampy tundra lowland.

Construction of the settlement and industrial base, along the edge of the erosional coastal cliff, was acompanied by repeated removal of sand and sand-pebble sediments for building materials from the avandune and beach. This is absolutely wrong for the zones of wave energy divergence, especially in those that already suffer erosion.

Within the zone of industrial exploitation, the coastal bluff and the coastal zone experienced considerable mechanical deformations of landforms because of transport, mechanical leveling of coastal declivities and other technogenic disturbances. A systemless use of transportation and construction techniques, including caterpillars, caused degradation of soil and plant cover of the whole dune belt of Varandei Island. Under conditions of deep seasonal melting the dune belt, formed of fine sands, is subjected to deflation and thermoerosion. The extent and rate of these processes are so great that in places the surface of the island became 1-3 m lower than before the period of exploitation began. Deflation hollows became widespread. Numerous deflation-thermoerosional gullies were formed in the coastal cliffs. As a result the cliffs become lower, their homogeneity had been disturbed, the coastal zone loses sediments and, finally, the rate of coastal retreat increases.

During the 2000 field season we measured the rates of deflation and thermoerosion with specially equipped stations. The averaged data of repeated measurements at more than 50 reference squares has shown that the thickness of the sand layer blown away by the wind was 10 to 14 cm in technogenically-deformed territories. At the same time, eolian accumulation took place in the territories that were not affected by human activity. At the "erosional" station, we observed the formation of a new big gully (up to 4 m deep) in the coastal bluff. Up to 400 m^3 of sand were removed from the gully itself and from its catchment area during the two weeks of snow melting in June. The coast near the Novyi Varandei settlement is a

region of wave energy flow divergence and correspondingly, formation of sediment flows. As a result, coastal protection in the area close to the Novyi Varandei settlement caused a decrease in sediment supply to the adjacent areas and, hence, their erosion.

The height of storm surges increased after an earth-dam and a bridge were constructed in the eastern part of Varandei Island. The latter is an important factor in coastal dynamics. Previously, during high surges that corresponded in time with tides, water flowed partly into branches and channels, thus lowering the surge height and decreasing its influence upon the coast.

The erosion rate increased considerably under human impact in the middle-late seventies. In some years it was up to 7-10 m/year. It decreased slightly, down to 1.5-2 m/year, after the coastal protection near the Novyi Varandei settlement was constructed. However, it remained high in the adjacent areas. Recent measurements during 1987-2000 have shown that the rate of coastal retreat in the region, outside of the settlement, have increased and reached 3-4 m/year (fig. 2), that is twice as high as in similar regions that have no human activity.

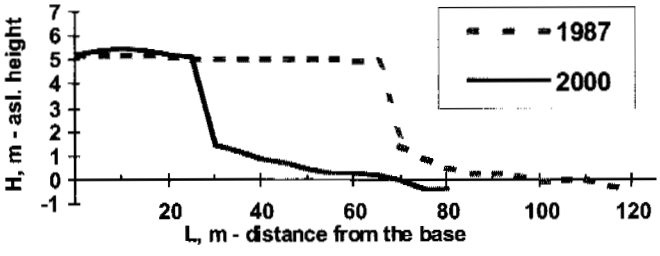

Figure 2. Dynamics of the coast near Varandei settlement.

The geoecological situation on Varandei Island is nearly critical. Industrial exploitation of the territory has resulted in not only the destruction of the natural coastal system but also caused considerable damage to human activities. Several housing estates and industrial constructions have already been destroyed due to coastal retreat. This damage will increase every year following the cliff retreat towards the center of Varandei settlement. Oil terminal, airport and other industrial objects are endangered. It is therefore necessary to thorough analyze coastal morpholithodynamic schemes before natural environments are disturbed.

Active industrial exploitation of the Pechora region demands a well-thought-out strategy of territory development and the finding of proper areas for new constructions. This negative example from the Varandei region shows that a well-developed ecologically grounded approach to further exploitation of coastal regions is necessary. After many years of investigations in the Pechora Sea region, the Research Laboratory of the Geoecology of the North, MSU, has worked out a special methodology of morpholithodynamic research and created a database on the coastal morpholithodynamics of this area that will be a basis for solving both fundamental and applied problems arising in the course of coastal reclamation.

ACKNOWLEDEMENT

This work was supported by INTAS grant no. 1489.

Permafrost processes inducing disastrous effects in engineering constructions. Medvezhje gas-field, Western Siberia

Y. V. Panova

Earth Cryosphere Institute, SB RAS, Moscow, 119991, Russia, yanusia@mail.tascom.ru

The Medvezhje gas-field is located in the northern part of Western Siberia. There are three main gas pipelines constructed above ground, they have diameters of 1420 mm and 1020 mm. The average gas temperature is more than 15 °C. The permafrost in the area is discontinuously distributed and consists of sedimentary soil of Quaternary age (mainly at the Kazanskaya and Salexardskaya sites; Nedra 1989, Express information 1980). A number of earlier investigations have been conducted in the area under study (Galiulin et al. 1997).

The Medvezhje gas pipeline system (MGP) is in need of reconstruction because of the increasing amount of deformations that occur. MGP was investigated from the air and in the field to assess its stability.

Besides the engineering issues, a geocryological map of 1:100'000 scale was prepared for the area. Locations of exploration and the associated findings were marked on the map and listed in a table. For a small selection see Table 1. Inspection of the MGP revealed 66 damage sites: 18 were a little deformed, 35 middle deformed and 13 badly deformed.

The most widespread type of deformation (i.e. bending of the pipeline) occurs in a horizontal plane. Usually the pipeline sags and it results in subsequent ground contact.

An indication for the initiation of pipeline deformation is the appearance of an apparently superfluous length of pipeline. The observed pipeline deformations are caused by different processes (Degtyarev 1974):

- temperature deformations;
- deformations from inner pressure in the pipeline;
- deformations caused by the incorrect loading of the pipeline or by other engineering constructions on and around the MPG;

Deformation or loss of support of the ground underneath the pipeline also determines the character and degree of deformation. The latter deformations are influenced by the interaction of the pipeline with permafrost and geotechnical / geocryological conditions along the MGP route:

- the pipeline embankment or the pipeline itself hinder surface water runoff;
- the frozen foundation melts under the thermal influence of the gas pipeline and the skeleton of the foundation is compressed;
- the pipeline is clamped on watersheds (e.g., hills), but is without support between such fixed points. This may lead to differential sagging of the pipeline under its own weight, and, thus, to incorrect pipeline loading (Fig. 1).

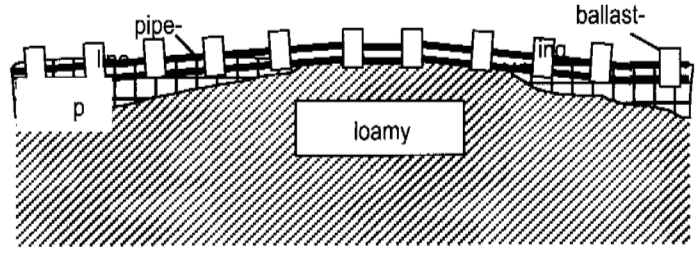

Figure 1. Schematic of an incorrectly ballasted pipeline.

Various combinations of the above listed processes have been found.

Deformations, caused by the wrong loading of the pipeline due to the influence of additional engineering constructions are:

- destruction of the MGP embankment and the subsequent relocation of the embankment ground;
- part of the pipeline is compressed by the superimposed road embankment that crosses it (Fig. 2).

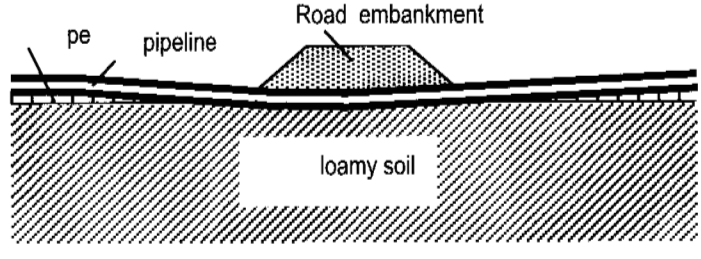

Figure 2. Schematic image of the vertical deformation of the gas-pipeline as it crosses a highway.

After inspection of the MGP and analysis of the field data we marked out the general exogenous and geologi-

cal processes which cause changes in the MPG location and result in its deformation.

During the operation of the MGP the bog zones in the area were found to increase under the thermal influence of the pipeline, as has been confirmed by air-photos over the years. If the foundation ground is ice-rich and able to subside, water often initiates thermokarst processes. Particularly bog water, temporary or constant brooks, subsurface water, within or above the active layer, influence the pipeline. In a number of cases drainage was found to occur lengthwise along the pipeline embankment, for instance, in the line trench. For elevated sites, the concentration of water flow in this trench leads to water inundation into the rock.

At the beginning of gas extraction holes began to form in the foundations, by thawing, because of missing heat-insulation. On ice-rich sites, the thawing was accompanied by the formation of thermokarst slumps. The most typical types of subsequent deformations are:

- non-uniform pipeline slumps accompanied by bends in the vertical and horizontal planes;
- emergence of the pipeline from water, accompanied by bends in the vertical and horizontal planes.

The pipeline, initially and most frequently, was built on ice-rich highland, 2-3 m above the ground. Initially it contained vertical bends, they slowly straightened due to the ice-rich ground settling because of ice melt.

Beside the thermokarst processes within the slopes of a river or brook, water erosion also plays a part in the formation of settlements.

An enhanced deformation of the MPG occurs at permafrost sites containing ice wedges due to the melting of the ice bodies. Investigated sites that developed such thermokarst phenomena are confined to polygonal peat soil with ice wedges or with ice inclusions. In extensive peat soil areas the pipeline comes out, in general, into the drained trench which is supported by local peat-material or by mineral ground with only a thin layer of peat. Many sites are deprived of an embankment and the open trench forms into a pond which becomes a thermokarst center along the ice wedge. Heat transferred by water-flow forms an initial trench in the ice wedges. They increasingly melt forming growing trenches filled with water.

The pipeline itself is a powerful heat source, especially in the summer time. A broken embankment leads to a change in albedo and thus, to ground warming. As a result of the deformation and destruction of the melting peat at the base it is possible for the pipeline to sink to the foundation ground owing to the thermal influence of the trench water on the peat soil, even if the ground contains no ice. This effect lasts until all the peat from the pipeline base has been pushed away and firm mineral soil has been reached.

REFERENCES

"Geocryology of USSR Western Siberia" "Nedra" Moscow 1989.

Degtyarev, 1974. "Instruction on account and choice of designs of holev with thermal protection in a permafrost" Moscow "VSRIgas" 72.

Galiulin Z., Ismailov I., Dubinin P. and Samsonova L.N. 1997. Increase of efficiency of development of gas deposits of Far North Moscow "Science" 655

Express information, release 3, Moscow. 1980. Gas industry series: Geology, drilling and development of gas deposits.

Table1. Example of MGP data taken in file research, summer 1999

Site No.	Geomorphologic type of site	Length (L), amplitude (A) and type of MGP deformation (m) in horizontal plane	in vertical plane	Filling up the ponds with water round the pipeline (m)	Type of construction method and preservation of the embankment	Degree of deformation
46-2	flood-plain of brook	-//-	sagging, L~70	there is	above ground, destroyed by water embankment	middle deformed
504-1	bog landscape	right bend A~2,5; left bend A~2	-//-	there is	above ground, destroyed by water embankment	strongly deformed

Frozen ground data information: advances in the IPA Global Geocryological Data (GGD) system

*M. A. Parsons, T. Zhang, R. G. Barry and *J. Brown*

National Snow and Ice Data Center/World Data Center for Glaciology, Boulder, CO, USA

** International Permafrost Association, Woods Hole, MA, USA*

BACKGROUND

Permafrost regions occupy about 23.9% and seasonally frozen ground regions underlie on average of approximately 57.1% of the exposed land surface in the Northern Hemisphere (Zhang et al. 2003). Data and information on frozen ground collected over many decades and in the future are critical for fundamental process understanding, environmental change detection and impact assessment, model validation, and engineering application in seasonal frost and permafrost regions (IPA DIWG 1998). However, many of these data sets and information remain widely dispersed and relatively unavailable to the national and international science and engineering community, and some are in danger of being lost permanently.

The International Permafrost Association (IPA) has long recognized the inherent and lasting value of data and information and has worked to prioritize and assess frozen ground data requirements and to identify critical data sets for scientific and engineering purposes. The groundwork of the IPA strategy for data and information management was laid during the 1988 IPA Conference in Trondheim, Norway. Barry (1988) presented a paper on status and needs of permafrost data and information and organized an informal workshop on requirements for permafrost data and information that attracted more than 100 attendees. The IPA Data and Information Working Group (DIWG) was established and a formal workshop was held during the 1993 IPA Conference in Beijing, China. The DIWG has subsequently organized workshops in Southampton and Oslo (1994), Potsdam (1995), and Boulder (1996). The Global Geocryological Data (GGD) project was initiated by the DIWG during the Boulder workshop in 1996. During the 1998 IPA Conference in Yellowknife, Clark and Barry (1998) provided an update on IPA permafrost data and information management. The first Circumpolar Active Layer Permafrost System (CAPS) CD-ROM was published and delivered to the delegates. The IPA Standing Committee on Data, Information and Communication (SCDIC) was established, replacing the former IPA DIWG.

FROZEN GROUND DATA CENTER (FGDC)

To continue the IPA strategy for data and information management and to meet the requirements by cold regions science, engineering, and modeling community, the World Data Center (WDC) for Glaciology, Boulder in collaboration with the International Arctic Research Center (IARC) has established a new Frozen Ground Data Center (FGDC) as a key node in the IPA's GGD system. The IPA SCDIC has organized two workshops in Boulder (2002 and 2003) on the prioritization and assessment of frozen ground data requirements and identification of data sets. The FGDC has expanded access to the 1998 CAPS data and has augmented data holdings. Data and information for seasonally frozen ground regions from in situ measurements, satellite remote sensing, and model outputs are included. Figure 1 is an example of these new types of data. It shows modeled maximum frozen ground depth for non-permafrost regions in the Arctic drainage basin (Oelke et al. 2003).

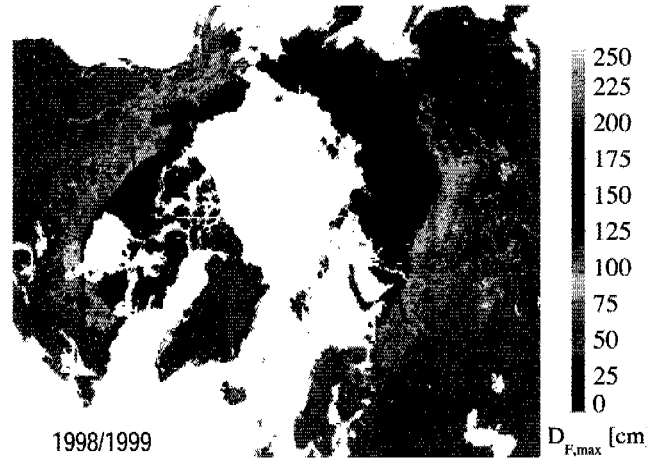

Figure 1. Maximum frozen ground depth 1998/99

The FGDC is distributing a new version of CAPS at the July 2003 International Conference on Permafrost in Zurich. The ultimate goal of the FGDC is to serve as a central access point for frozen ground data and information in

the international permafrost community and scientific community at large.

The FGDC has improved access to existing data through an online search and order system and availability in the Global Change Master Directory. The FGDC has also expanded and updated current holdings with maps of global and regional permafrost, soil temperature, and soil classification in a variety of grids and data formats especially geared to aid the permafrost modeling community.

Publication and distribution of CAPS version 2 marks a milestone for the FGDC and the IPA. CAPS version 2 is a compendium of GGD data and metadata currently available in the FGDC and around the world (see Table 1). It serves as a snapshot of frozen ground and related data holdings available as of spring 2003 and enables access to these data for users lacking ready internet access or high-speed connections.

Table 1. Highlights of CAPS version 2

IPA Program Data
- Metadata from the Global Terrestrial Network for Permafrost's (GTN-P) Borehole Program and the Permafrost and Climate in Europe (PACE) project.
- Annual thaw depth and other summary data from the GTN-P's Circumpolar Active Layer Monitoring (CALM) Program.
- IPA Cryosols Working Group map of Arctic soils
- Metadata, photos, and a specialized bibliography from the Arctic Coastal Dynamics (ACD) project
- Review papers and a specialized bibliography form the Southern Hemisphere Working Group (SHWG)

Maps
- The IPA Circum-Arctic Map of Permafrost and Ground Ice in several new grids and formats.
- Regional permafrost maps from Russia, China, Europe, and Alaska
- Northern Circumpolar Soils Map
- Regional soil maps from Russia and China

Frozen Ground
- Historical soil temperatures from stations across Russia
- Soil temperatures from sites in Alaska, China, Mongolia, and Antarctica.
- Global grids of seasonal frozen ground derived from remote sensing
- Borehole and active layer data from historical sites and other sites outside the GTN-P purview.
- Modelled seasonal frozen ground depth for the Arctic drainage basin.

Bibliographies
- A Comprehensive Permafrost Bibliography current through Decemeber 2002. (A searchable, up-to-date version is available online at the FGDC web site.)
- A bibligraphy of permafrost and related maps
- Specialized bibliographies from the SHWG and ACD.

Other Products
- Output from several permafrost or active layer models.
- Borehole and active layer data from historical sites and other sites outside the GTN-P purview.
- Dozens of regional and site-specific data sets of permafrost, soil properties, snow cover, and related parameters.
- GGD metadata describing over 100 other data sets available from investigators and institutions around the world.

We continue to welcome data submissions for inclusion on the FGDC web site at http://nsidc.org/fgdc/index.html. Identification of additional data and information from all participating countries, organizations, and individuals are requested. Suggestions on data acquisition, management and distribution are always welcome and encouraged. The IPA Standing Committee on Data, Information and Communication will continue to coordinate the GGD and CAPS activities.

ACKNOWLEDGEMENTS

We thank the IPA Standing Committee on Data, Information and Communication for coordinating the GGD and CAPS activities. We especially thank the many data contributors to this important effort. This work was supported by the International Arctic Research Center, University of Alaska Fairbanks, under the U.S. NSF cooperative agreement OPP-0002239. Financial support does not constitute endorsement of the views expressed in this article.

REFERENCES

Barry, R. G. 1988. Permafrost data and information: status and needs. In Senneset, K. (ed.), Proceedings of the 5th International Conference on Permafrost, Trondheim, Norway, 1988. Vol. 1, Tapir Publishes, Trondheim: 119-122.

Clark, M. J. and Barry, R. G. 1998. Permafrost data and information: advances since the Fifth International Conference on Permafrost, in Lewkowicz, A. and M. Allard (eds.), Proceedings of the 7th International Conference on Permafrost, Yellowknife, Canada, 1998: 181-188.

International Permafrost Association, Data and Information Working Group, comp. 1998. An Introduction to Circumpolar Active-Layer Permafrost System (CAPS), in Circumpolar Active-Layer Permafrost System (CAPS), version 1.0. CD-ROM available from National Snow and Ice Data Center, Boulder, Colorado.

Oelke, C., Zhang, T., Serreze, M. and Armstrong, R. in press. Regional-scale modeling of soil freeze/thaw over the Arctic drainage basin. Journal of Geophysical Research.

Zhang, T., R., Barry, G., Knowles, K., Ling, F. and Armstrong, R. L. 2003. Distribution of seasonally and perennially frozen ground in the Northern Hemisphere. Proceedings of the Eighth International Conference on Permafrost, Zurich, Switzerland, July 21-25, 2003.

Mapping of rock glaciers with optical satellite imagery

F. Paul, A. Kääb and W. Haeberli

Glaciology and Geomorphodynamics Group, Department of Geography, University of Zurich, Switzerland

There is a growing concern about permafrost degradation as a result of ongoing global warming. In particular, rock fall events and debris flows from now unstable mountain slopes are expected (Haeberli and Beniston 1998). Hence, the great effort to map the distribution of mountain permafrost in the Alps. Rock glaciers are indicative of permafrost conditions and can easily be recognized on aerial photography due to their typical shape. Time series analysis of the derived orthophotos allows the calculation of flow fields and mass changes (Kääb 2002) but is not practical for large area mapping on a small scale.

The potential of high-resolution panchromatic satellite sensors to detect rock glaciers has been analysed in order to validate the results of permafrost distribution models at large scales and in remote areas. The investigated sensors range from 15 m spatial resolution ETM+ to the 1 m Ikonos sensor. The sensors also differ in the spectral range and ground area covered as well as costs per km^2 (Table 1). In general costs increase with higher resolution while the area covered decreases.

Table 1. Some characteristics of the pan sensors examined.

	ETM+	SPOT	IRS-1C	Ikonos
Resolution [m]	15	10	5	1
Spectral range [mm]	0.52-0.9	0.51-0.73	0.5-0.75	0.45-0.9
Area covered [km]	180x180	60x60	70x70	11x100
Costs per km^2 [US$]	0.02	0.33	0.51	ca. 30

In Figure 1 the comparison of the three pan bands from ETM+, SPOT and IRS-1C is shown together with a ground based photo of a complex rock glacier system near Piz d'Err (Grisons). The ETM+ sensor (Fig. 1a) captures the rock glaciers quite well as the sensor is also sensitive in the near infrared where the high reflection of vegetation contrasts well with the low reflection of bare rock. However, details of the ridge structure are not visible and the spatial resolution is thus, not appropriate for a clear identification.

In the SPOT image (Fig. 1b) the typical ridges become visible and identification and large area mapping of rock glaciers seems feasible. However, the outline of the lower (relict) part is difficult to recognize as the reflections from the surrounding meadow and bare rock are quite similar in this spectral range.

The IRS-1C image (Fig. 1c) reveals only few new details, as compared to SPOT, but seems to be more noisy (nominal resolution is 6.8 m). The surrounding meadow is slightly brighter than seen with SPOT although the spectral range covered is quite similar.

A comparison between SPOT and Ikonos imagery (draped over a DEM with 25 m spatial resolution) is shown in Figure 2 (view to south) for the comparable small Gigli rock glacier (near Sustenpass, Uri). Although some of the rock glacier ridges are visible in the SPOT imagery (see inset), it is by no means comparable to the level of detail visible from Ikonos. Here also, the typical larger rocks at the rock glacier surface and the very fine debris at the front can be discerned. A DEM allows the creation of 3D perspective views which enhance the identification of further rock glaciers (white arrows). A large number of breaches from former debris flows across historic (1850) moraines can be identified as well.

The regions of likely and probable permafrost are indicated as high-lighted areas in Figure 2. The model simulates BTS, a threshold of -2.0 (-3.0) °C is chosen to assign regions with likely (probable) permafrost (Gruber and Hoelzle 2001). It seems that the rock glaciers originate in regions with likely permafrost but extend much more further down into permafrost free terrain. This has also been observed for many other rock glaciers (Frauenfelder et al. 2001).

We propose that contrast enhanced SPOT pan imagery can be used to identify and map rock glaciers for large and remote areas at comparably low costs. The 10 m spatial resolution seems appropriate for validation of permafrost distribution maps obtained from 25 m spatial resolution DEM data. For further detailed studies of interesting regions the 1 m resolution Ikonos imagery is a valuable alternative to aerial photography but about three times more expensive.

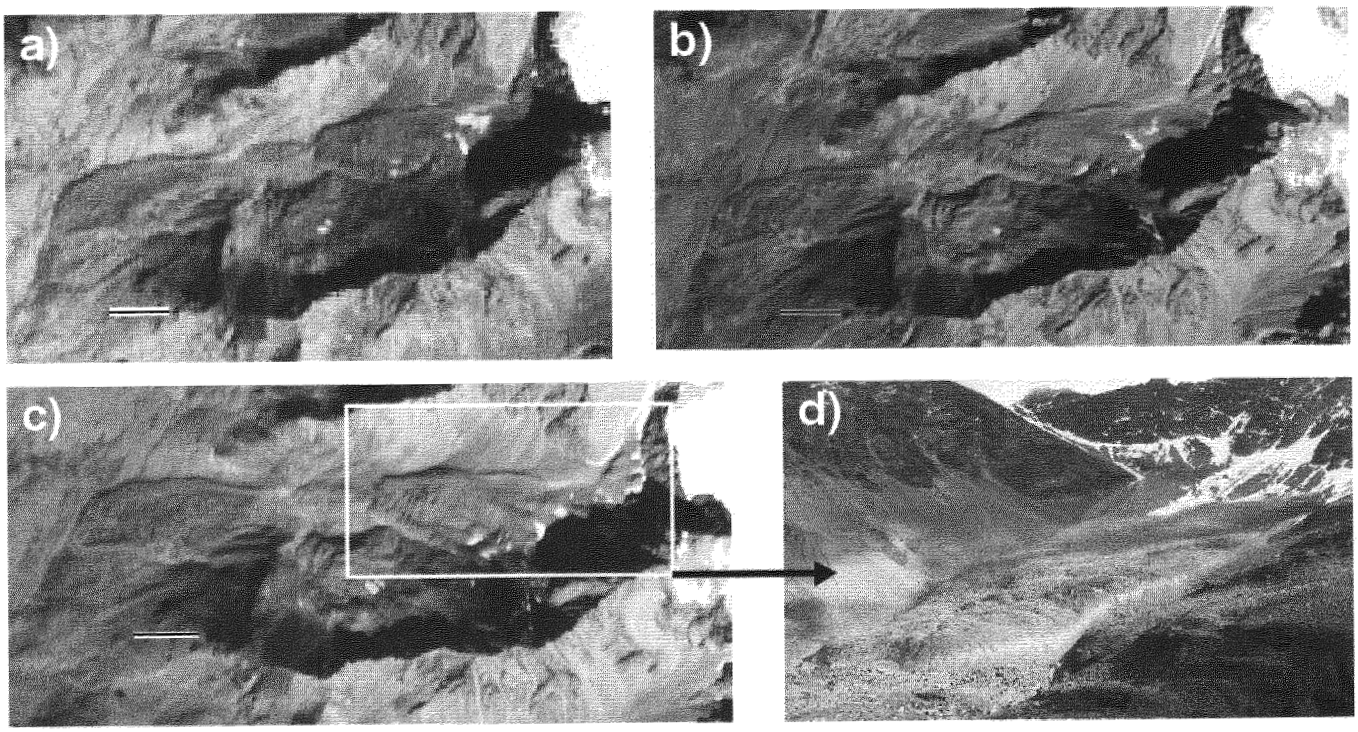

Figure. 1. A complex rock glacier system near Piz d'Err (Grisons) as seen by three satellite sensors (scale bar is 300 m): a) ETM+, b) SPOT and c) IRS-1C. d) Shows a ground based photograph for comparison (taken by M. Reuschenbach).

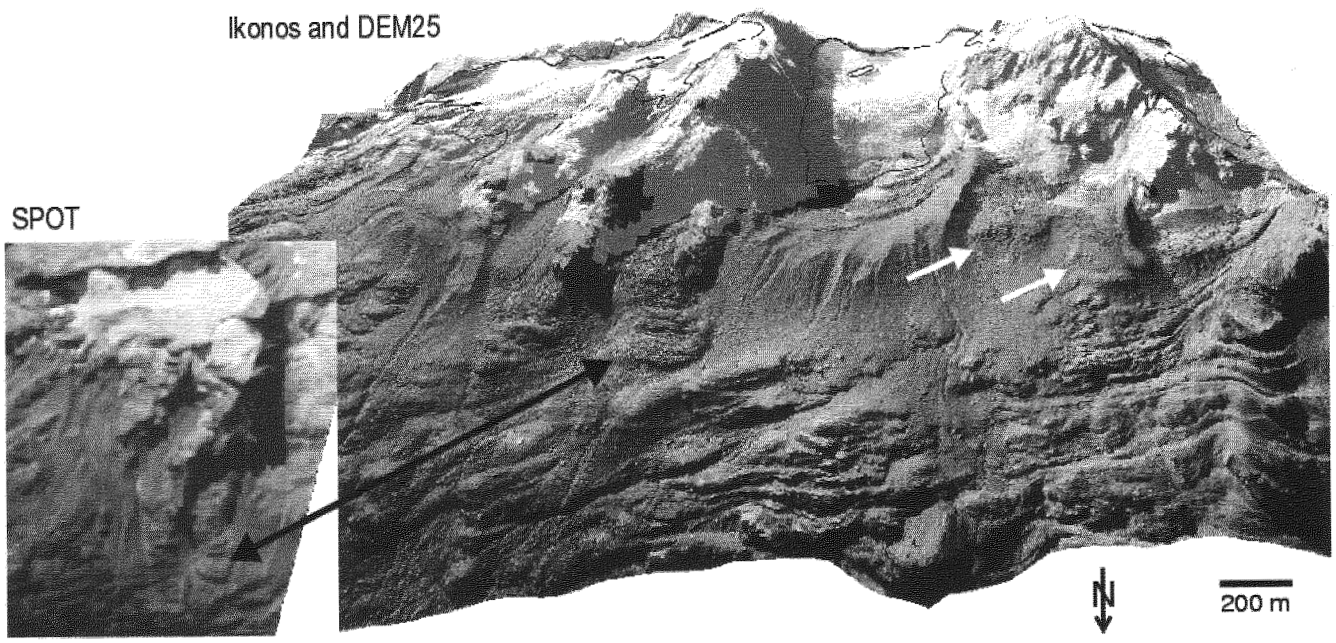

Figure. 2. 3D view of rock glaciers, permafrost distribution (high-lighted) and 1973 glacier outlines (black) near the Sustenpass from Ikonos imagery. The inset shows SPOT imagery for comparison. DEM25: © 2003 Swisstopo (BA 035256).

REFERENCES

Frauenfelder R, Haeberli W, Hoelzle M. and Maisch M. 2001. Using relict rockglaciers in GIS-based modelling to reconstruct Younger Dryas permafrost distribution patterns in the Err-Julier area, Swiss Alps. Norwegian Journal of Geogra-phy 55 (4): 195-202.

Haeberli, W. and Beniston, M. 1998. Climate change and its impacts on glaciers and permafrost in the Alps. Ambio 27 (4): 258-265.

Gruber, S. and Hoelzle, M. 2001. Statistical modelling of mountain permafrost distribution: local calibration and incorporation of remotely sensed data. Permafrost and Periglacial Processes 12 (1): 69-77.

Kääb, A. 2002. Monitoring high-mountain terrain deformation from repeated air- and spaceborne optical data: examples using digital aerial imagery and ASTER data. ISPRS Journal of Photogrammetry and Remote Sensing 57 (1/2): 39-52.

Morphogenetic classification of the Arctic coastal seabed

*Y. Pavlidis and S. Nikiforov and *V. Rachold*

P.P. Shirshov Institute of Oceanology, Moscow, Russia

**Alfred Wegener Institute for Polar and Marine Research, Potsdam, Germany*

INTRODUCTION

A precise and standardized classification on the variety of relief forms of the Arctic shelf is essential for both scientific and applied purposes. The evolution of the Arctic coastal zone, which is controlled by the interactions of modern wave and ice factors and the influence of numerous glaciations and large-scale sea level fluctuations, significantly differs from other coastal areas of the World Ocean. Glaciations have left coastal traces in the western part of the Russian Arctic, whereas its eastern part was almost completely drained during glacial periods and the subaerial paleorelief is characterized especially by cryogenic forms: thermokarst, thermoabrasion, thermodenudation and cryodislocation.

Earlier classifications of the coastal seabed relief suggested by Ionin et al. (1990) for the World Ocean or by Shepard (1977) according to the peculiarity of geological structures or sedimentation processes could not characterize the variety of forms and regional features in the Arctic zone. The classification presented in this paper is based upon scientifically evidenced information on morphology, origin and age as well as geological and neotectonic characteristics of the seabed relief. This kind of simultaneous analysis of complex of interactive factors can be called a "morphogenetic" approach.

The investigations are based on the results of long-term research with the application of modern equipment including narrow-beam and multi-beam echo sounders, Parasound, side-looking radars, bathymetric maps and the analysis of numerous sediment samples. According to the Science and Implementation Plan of the Arctic Coastal Dynamics (ACD) project (IASC 2001), the classification will be formulated for integration into a circum-Arctic coastal Geo Information System (GIS).

RESULTS AND DISCUSSION

The seabed evolution is determined by both modern and paleogeographical processes such as vertical tectonic and glacio-isostatic movements. Among the exogenic and endogenic coastal processes it is possible to allocate active processes, which directly contribute to the formation of the shelf relief, and passive processes, which predetermine the display of the active processes and direct the course of their development. Active processes can be modern (hydrogenic, gravitational, etc.), paleogeographical (glacial, erosional, etc.), and in some cases anthropogenic processes. Structural forms, with few exceptions, are related to passive morphogenetic factors. By using such an approach it is possible to designate three major categories of the seabed relief: structural, structural-sculptural and sculptural. This kind of subdivision is relative in many respects because the majority of relief forms are caused by both endogenic and exogenic factors and processes. It is necessary to determine the prevailing value of various factors of concrete seabed forms. A certain cannot be avoided subjectivity in allocating structural and sculptural forms of a relief, and in their morphogenetic division into active and passive factors. The need to characterize the relief "layer by layer" arises inevitably when specialized geomorphological maps have to be produced and a database to be used in a GIS environment within in international network has to be designed. As an example the following layers could be used: first layer - endogenic background; second layer - relief forms linked to the action of paleogeographic factors; third layer - modern relief forms caused by the action of endogenic processes.

Typical structural forms are large seabeds predetermined by geological structures and created by endogenic processes, i.e., folded and/or fault-fracture tectonics, volcanism, vertical movements of the Earth's crust, etc. Geological structures underlie all forms of the shelf relief and determine the position of large relief forms, such as synclinal underwater depressions, anticlinal and brachyanticlinal underwater raisings, monoclinal plains, flexure ledges etc. This large group can be further divided into two genetic types and some subtypes. (1) The *tectogenic type* includes plicated forms, i.e., anticlinal, brachyanticlinal, synclinal, brachysynclinal, monoclinal, uniclinal; disjunctive, i.e., fault and grabens, horsts, fracture-blocks; and non-broken structural dislocations, i.e., subhorizontal and inclined plains. (2) The *volcanogenic type* includes magmatic and mud volcanic subtypes. Usually relief forms created by volcanic processes like lava domes and mud volcanic cones

(Norwegian Sea) are located in water depths of more than 200 m.

In our morphogenetic classification, structural-sculptural forms are assigned to a category of transitive, often relict formations. These forms can be divided into the following subtypes: (1) *erosion-tectonic, i.e.,* structural-erosive with fluvial or glacial relief, structural-erosive-gravity created by turbidity currents, (2) *glacial-tectonic, i.e.,* structural depressions in internal basins of fjords and covered by glacial-marine deposits, structural swells with accumulative superstructure, structural forms with a surface of glacial ablation corresponding to fjords and adjacent underwater trough valleys, structural forms with glacial ablation and accumulative marginal troughs and anticlinal swells blocked by moraines.

Exogenic subaerial and subaquatic processes are the most active ones. The sculptural relief of the seabed is created by destructive and accumulative processes such as ablative and accumulative activity of Late Quaternary glaciers on the shelves of the marginal and internal seas of polar and subpolar climatic zones. Glacial forms are most typical among the relict exogenic sculptural relief forms within the limits of the glacial shelf in the Arctic. The sculptural relief forms can be divided into seven types and several subtypes: (1) *glaciogenic, i.e.,* glacial-ablative, glacial-accumulative and glacial-dynamic, (2) *cryogenic, i.e.,* thermokarst relict forms such as extended underwater depressions and hollows documented by echosounding and acoustic profiling in the Laptev, East Siberian and Pechora Seas; the origin of these negative relief forms is connected with the thermal destruction of ice lenses and wedges during the late glacial transgression, the size ranges from 2 to 10 m depth, 10 to 100 m width and extension of 3 to 4 km depending on the thickness of the lenses of repeatedly-cavern-load ice; in the Chukchi Sea, the relict thermokarst relief forms are large depressions which are covered by a 7 to 10 m thick Holocene sediment layer; cryodislocative relief forms represented by folds and frost mounds have a local distribution in the Arctic, for example Western Yamal Peninsula, (3) *hydrodynamic, i.e.,* wave abrasion forming modern cliffs and benches and paleo underwater terraces, wave accumulation with ancient underwater accumulative forms and coastal barrier islands, spits, beaches, etc., abrasive-accumulative processes forming modern underwater coastal slopes, mainly subglacial accumulative and tidal forms such as sandy waves and ridges, tidal troughs, step tidal benches, etc., (4) *torrentogenic, i.e.,* accumulative and erosive as, for example, in the Bering Strait where, due to strong quasistationary currents, a subhorizontal plain lacking modern deposits is formed in the central zone while as a result of deposition, underwater cones are generated in the adjoining southern Chuchi Sea, (5) *fluvial, i.e.,* fluvio-glacial and potamogenic forms with ice-marginal valleys and channels of paleo-rivers, ancient and modern deltas, river mouth bars, etc., (6) *gravitational, i.e.,* rockfall-landslides, turbidity currents, and (7) modern *anthropogenic, i.e.,* constructive forms connected with ground spoil, artificial islands, basements of port constructions, oil derricks etc., destructive forms with artificial cuts, port channels, waterways in gulfs and other near-port constructions within shallow water.

CONCLUSIONS

The Arctic shelf can be described as a zone witch evolved in the couse of long-term endogenic and exogenic interactions. The initial structure was created by the basement surface which was and is constantly reworked by a complex of paleogeographical and modern processes within various glacial and interglacial periods and sea level fluctuations. The classification suggested in the present article is based on scientifically evidenced data on morphology, origin and age, and on the geological and neotectonic features of the seabed relief, and it also takes into account a multitude of natural factors and their interactions and evolution in time. Three types of major relief-forming processes were distinguished and further subdivided: structural, structural-sculptural (transitive), and sculptural (formed by modern and paleogeographical exogenic processes).

ACKNOWLEDEMENT

This study was supported by INTAS (project number 2001-2332).

REFERENCES

IASC 2001. Arctic Coastal Dynamics (ACD). Science and Implementation Plan, International Arctic Science Committee, Oslo, April 2001.

Ionin, A., Pavlidis Yu. and Yurkevich, M. 1990. Relief of arctic eastern shelf of Russia and its classification. In A. Aksenov (eds), Geology and geomorphology of shelf and continental slope. Moscow, Nauka: 24-50.

Shepard, F.P. 1977. Geological oceanography. N.Y.

Near-surface ground temperatures and permafrost distribution at Gornergrat, Matter Valley, Swiss Alps

S. Philippi, T. Herz and L. King

Institute of Geography, Justus Liebig University, Giessen, Germany

INTRODUCTION

Due to substantial research during the past fifteen years, permafrost distribution of the Matter valley is known on an overview scale. However, the currently available permafrost distribution models do not consider local soil properties which can vary significantly within short distances in high mountain environments. Besides other local factors such as air temperature, solar radiation and snow cover, changes in substrate and moisture conditions strongly influence the ground thermal properties (Williams and Smith 1989) and consequently, the distribution pattern of mountain permafrost. The zone of discontinuous permafrost is characterized by rather warm ground temperatures insignificantly below zero, which makes permafrost at its lower limit very susceptible to increasing air temperatures. Active layer thickening, rising of the lower limits of permafrost and permafrost reduction by basal melting could be possible responses to long-term climate changes (Williams and Smith 1989).

The current investigations will provide quantitative insights into ground thermal regimes and will correlate measured soil temperatures with different soil properties and their possible effects on the discontinuous permafrost pattern.

The Gornergrat area is located between 2700 and 3200 meters a.s.l. at the end of the Matter valley surrounded by some of the highest peaks of the Alps. The continental climatic conditions cause a high glacier equilibrium line associated with a periglacial belt of large vertical extent. According to King (1996), discontinuous permafrost can be expected in an altitudinal range between 2800 and 3500 meters a.s.l. and is indicated by the presence of numerous active rock glaciers.

SELECTED STUDY SITES

The east-west running crest between Gornergrat (3135 meters a.s.l.) and Hohtälli (3286 meters a.s.l.) divides the study area into a northern part called 'Kelle' and a southern part named 'Tuft'. Both areas are located within the zone of discontinuous permafrost showing a rich periglacial morphology such as solifluction lobes, patterned ground and rock glaciers. However, the local permafrost pattern is not yet known.

Shallow ground temperature measurements are performed at eight vertical profiles differing in substrate (cf. Table 1) and moisture conditions. The measurements are carried out in order to obtain an insight into the various reasons for the variability of ground thermal properties over short distances within the zone of discontinuous permafrost.

In terms of local soil characteristics, each of the four instrumented profiles in the Tuft corresponds to a profile in the Kelle. The substrates of location T (Tuft) 1 and K (Kelle) 1 show a rather high soil moisture content, T2 and K2 were installed in substrates with moderate water content, whereas T3 and K3 are comparatively dry locations. All sites show a sparse vegetation cover of moss, lichen and grass and are located at approax 3000 meters a.s.l. (cf. Table 1).

According to Harris and Pedersen (1998) the differing thermal properties of blocky materials seem to explain permafrost occurrences below the regional lower limit. In order to compare the thermal regimes of soils and coarse debris two additional locations (K4 and T4) within the surface layer of active rock glaciers were chosen.

Meteorological data are available for the 'Kelle' and the permafrost monitoring site at Stockhorn plateau (3410 meters a.s.l.) close to the research area.

GROUND TEMPERATURE MEASUREMENTS

Measurement setup

In August 2002 eight data loggers with an accuracy of 0.02 °C were installed, measuring shallow ground temperatures at different levels (cf. Table 1). The measurement interval was set at 15 minutes during summer and autumn, while from October on hourly recordings are made. So far, data are available from the end of August until the end of October 2002.

Table 1. Information on the location of near-surface ground measurements at Gornergrat.

Profile	Altitude	depth of sensors	location	soil type (until 100 cm)	humus within upper horizon
	m	cm		cm	%
T1	3005	2, 25, 50, 100, 160	moist plain	0-15 loam 15-100 sandy loam	9.7
T2	3000	2, 25, 50, 100, 180	solifluction lobe	0–100 loam	15.0
T3	3000	2, 25, 50, 100, 150	knoll	0–100 sandy loam	4.5
T4	3010	50, 120, 190, 255	active rock glacier		
K1	2950	2, 25, 50, 100, 150	moist plain	0–15 loam 15–100 silt loam	9.5
K2	2950	2, 20, 45, 70, 120	plain	0– 40 sand 40–100 loamy sand	2.3
K3	3005	2, 25, 50, 100, 140	knoll	0–100 sandy loam	6.3
K4	2950	100, 160, 220, 280, 360	active rock glacier		

Preliminary results

The observed smaller temperature ranges at the moist profiles K1 and T1 compared to the drier locations, could be explained by the low thermal conductivity of water. This effect is shown in Figure 1, comparing the measured ground temperatures at the northern site K1 (moist) with the south-exposed site T3 (dry).

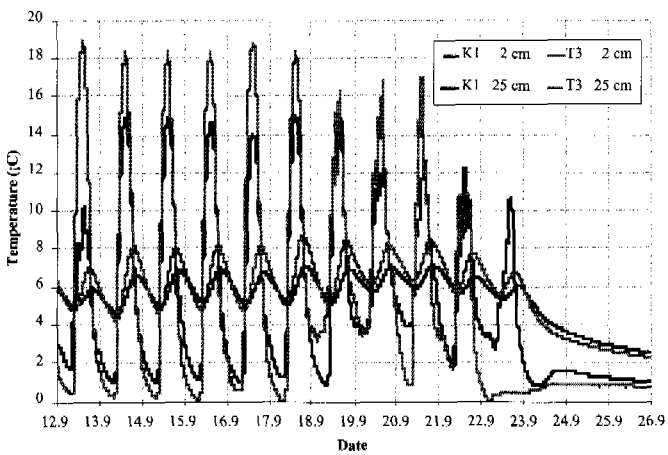

Figure 1. Near-surface ground temperatures in 2 cm and 25 cm depth in the profiles K1 and K2 (12.09.-26.09.2002).

Differences in aspect due to solar radiation mainly affect the surface ground temperatures (cf. Figure 1). With increasing depth local soil properties - especially moisture conditions - seem to have a major impact on the thermal regime. Apart from the surface ground temperatures, which are considerably higher at the southern location, the two moist profiles show similar temperatures and temperature ranges at all other measured levels - independent of their aspect.

The temperature amplitude at all measured levels is significantly greater within the rock glaciers. The phase lag between surface and soil temperature changes increasing with depth is missing at the rock glacier profiles. Similar to the soil locations, the coarse blocky layers also show a decreasing amplitude with depth, but without any time delay. Rapid air movement through the gaps seem to be the main process of heat transfer (Harris and Pedersen 1998) and would explain the direct response of the temperature changes within the block layers to a change in air temperatures at the surface.

OUTLOOK

To verify the local permafrost pattern, measurements of the Basal Temperature of Snow cover (BTS) and further soil temperature readings will be carried out before the ICOP 2003 and will be discussed in the poster presentation.

The study area will be visited during one of the post-conference excursions in July 2003.

REFERENCES

Harris, S.A. and Pedersen D.E. 1998. Thermal Regimes Beneath Coarse Blocky Materials. Permafrost and Periglacial Processes 9: 107-120.

King, L. 1996. Dauerfrostboden im Gebiet Zermatt – Gornergrat – Stockhorn: Verbreitung und permafrostbezogene Erschliessungsarbeiten. Z. Geomorph. N.F., Suppl. Bd. 104: 73-93.

Williams, P.J. and Smith, M.W. 1989. The Frozen Earth. Cambridge: University Press.

Results of the engineering geocryological mapping of the Pechora Sea arctic coast (the key site of the Varandey Peninsula)

A. A .Popova

Industrial and Research Institute for Engineering of Construction, Moscow, Russia

INTRODUCTION AND STUDIED AREA

Natural conditions are complex in Arctic Sea coastal areas. At present, it is necessary to study this area in detail in connection with oil and gas recovery and all the associated pipework.

The studies were performed in the Pechora Sea coastal band with a width of 8-10 km: from the Varandey Cape in the west to the Khaipudyr Bay in the east. The average annual air temperature is –5.6 °C. The studies were performed on the laida (absolute elevation 0-3 m) and the first sea terrace (absolute elevation 5-15 m). The sea terrace surface is complicated by numerous shallow lakes and sedge-moss bogs. Laida is a low part of the coast and subject to flooding during tides and storms. Saline sea water penetrates, through the river valleys, up to 10 km deep into the continent.

The thickness of the Quaternary sediments is 40-50 m in the area under study. They are represented mostly by sandy and clayey soils in the first terrace and laida, respectively.

The Varandey Peninsula is located in the zones of continuous and discontinuous permafrost with a total thickness of about 250 m. The average annual temperature of the perennially frozen ground (PFG) varies from 0 to -4 °C (Geocryology of the USSR 1988).

On the first sea terrace (>95% of the area), PFG is continuous. Part-through taliks (zones of unfrozen ground) with a thickness of 5-10 m are confined to small lakes and rivers. Through taliks are located below large lakes and rivers. In the first sea terrace, PFG has a thickness of 40 to 100 m and is underlain by cooled salinized ground with lenses of saline water (cryopegs). Cryopeg salinity reaches 40-50 g/l. The average annual temperature of the ground is the lowest (from -2 to -4 °C) at hillocky peatbogs and in areas without vegetation. The temperatures are the highest (from -0.5 to -2 °C) within wide swampy runoff bands, khasyreyas (thermokarst depressions), and the valleys of small streams.

On the coastal part of the area (laida) PFG is discontinuous. The upper section (to a depth of 3-4 m) is composed of cooled ground at a positive temperature. Cooled salinized ground at negative temperatures (from -1.5 to -3 °C) composes the lower section. The freezing point of silty clay at a salinity of 2% is -3 °C. Therefore, frozen ground occupies only 50-90% of the laida area in spite of a continuous distribution of ground temperature from 0 to -4 °C. The physical properties of a cooled ground correspond to those of a thawed ground. Therefore, we can state that PFG is discontinuous within the laida. The surface of the frozen ground is also broken by part-through and through taliks below saline rivers and lakes. The thickness of part-through taliks can exceed 50 m.

Physical geological processes and formations, including cryogenic heaving, thermokarst and thermal erosion and polygonal microrelief are widespread within the first sea terrace. Coastal erosion is observed at the high cliffs of the first sea terrace.

METHODOLOGY

Engineering geocryological zoning is the main method used in this study. It is performed according to the genetic principle and is based on landscape zoning. Topography, vegetation, and surface drainage are described for each landscape. The landscape zoning has been performed using data from field studies and the deciphering of aerial photographs. Geocryological areas were distinguished as a result of this zoning. Genesis and lithology of subsurface sediments, temperature, thickness and the occurrence of frozen, cooled and thawed ground and cryogenic processes, were determined for each area.

The performed studies included the drilling of 25 boreholes, borehole thermometry, geophysical works (VES and electric profiling) and the analysis of ground composition and properties to a depth of 15 m.

RESULTS AND DISCUSSION

The map of engineering geocryological zoning of the Varandey Peninsula coast was constructed based on the performed studies. Figure 1 is only a fragment of this map. The zoning shows the relationship between the geomorphological level, genesis, lithology, landscape and average ground temperature.

Three typical ground sections were distinguished depending on the salinity: (I) the entire section (to a depth of 15 m) is composed of salinized ground; (II) non-salinized and salinized ground occur in the upper (to a depth of 3-4 m) and lower sections, respectively; (III) non-salinized and salinized ground occur in the upper (to a depth of 10-12 m) and lower

sections, respectively. During the zoning it has been established that geocryological conditions depend directly on landscape conditions. Genetic types, lithology, temperature of the ground and landscape type are shown on the map for each distinguished area, the shading of each area corresponds to the average annual temperature of the ground.

The section types with a different distribution of salinity (see above and Fig. 1) are shown by independent indices (I, II, III).

CONCLUSION

The area under study includes continuous and discontinuous permafrost. Thawed ground and part-through taliks are local. The presence and non-uniform distribution of salinized cooled ground are responsible for specific geocryological conditions in this area. This is especially evident within laidas, where the frozen ground is discontinuous because of high salinity in the upper section. As a result, although all grounds have negative temperatures they exhibit the properties of thawed soils. Slightly salinized ground also occurs in the bottom sections of the first sea terrace.

ACKNOWLEDGMENTS

This work was supported by the Russian Coast Protection Program and INTAS grant 2332.

REFERENCES

Geocryology of the USSR. European Part. 1988. Moscow: Nedra (in Russian).

Rivkin F., Popova A., and Eospa A. 2001. The Permafrost Conditions along the Pechora Sea Coast (the Varandey Peninsula, European North of Russia). In Proceedings of 1st European Permafrost Conference, Rome: 38.

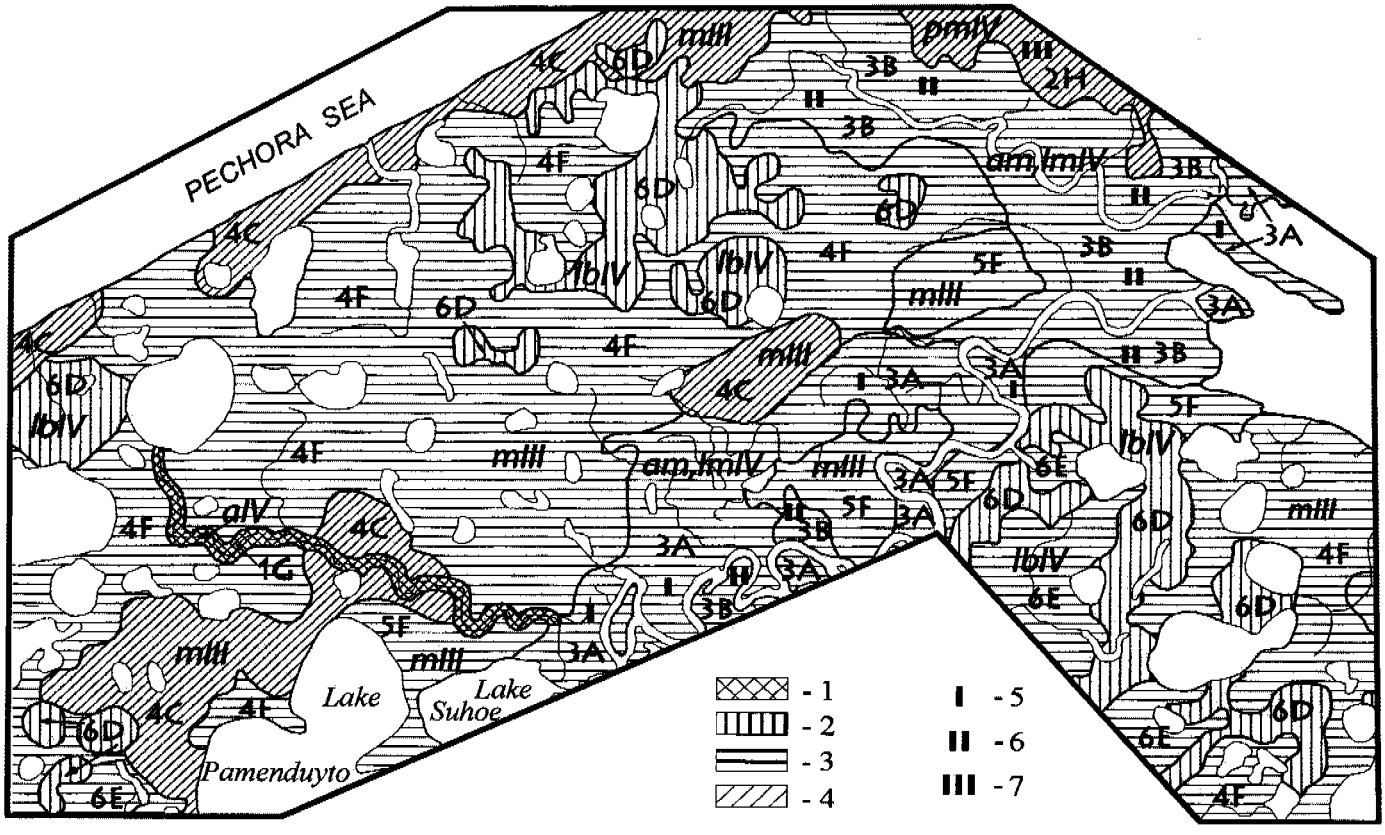

Figure 1. The map of engineering geocryological zoning of the Varandey Peninsula coast. 1-4 – average ground temperature: 1) >0-°C 2) -0.5 to -1.5 -°C 3) -1.5 to -3.0 °C, 4) -2.0 to -4.0 °C; 5-7 – the section types with different distribution of salinity (I, II, III)

An active rock glacier in the southernmost permafrost environment of the Alps (Argentera Massif, Italy): four years of surface ground temperature monitoring

A. Ribolini

Dipartimento di Scienze della Terra, University of Pisa, Via S. Maria 53, 56126 Pisa, Italy; ribolini@dst.unipi.it

The Argentera Massif corresponds to the south-ernmost permafrost environment of the European Alps, being only 50 km far from the Mediterranean Sea (Fabre and Ribolini 2003). This alpine sector is highly sensitive to environmental changes as demonstrated by last century glaciers disappearing. The surface ground temperature (SGT) is used in the analysis of the relationship between the near surface soil temperature and the non-conductive seasonal soil heat transfer processes, forcing permafrost growth/degradation (Kane et al. 2001). Four years-ground thermal regime at the snow-ground interface of the Portette rock glacier will be analysed by means of hourly monitoring of soil temperature using a miniature digital data logger (DTL). In this rock glacier, located in the south-eastern sector of the Argentera Massif, previous geoelectrical sounding indicated the presence of permafrost between 5-20 m depth (Fabre and Ribolini, 2003).

SGT data cover the November 1998-November 2002 period (Fig. 1). Four onsets of autumn freezing and spring-summer thawing periods are recognizable. During winter months the temperature remains well below 0°C, except for the 2000-2001 winter, when it did not descend below -2°C. The October-May SGT reached the lowest value during 1998, when the highest annual "cold content" (degree day of frost, DDF) was experienced. The winter records show both a regular temperature decrease/increase (1999-2000, 2000-2001) and a temperature trend characterized by several "spike-like" anomalies (1998-1999, 2001-2002).

To better understand the ground thermal behavior, the hourly temperature change DT (°C/h) at the DTL depth (25 cm) was calculated (Fig. 2). Four seasonal thermal regimes can be identified: summer thawing (ST), zero curtain (ZC), autumn-winter freezing (FR) and snow melt (SM).

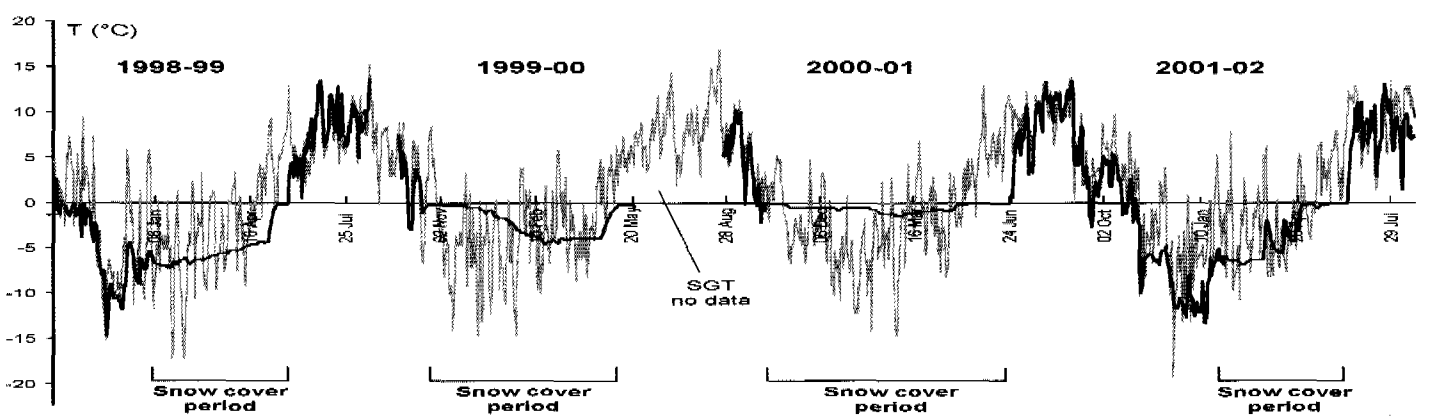

Figure 1. Daily air (grey) and Surface Ground Temperature

The large hourly temperature change characterizing the ST regime can be considered to represent the rapid response of the active layer to weather fluctuations.

The ground freezing thermal behavior is characterized by a lapse of time during which the temperatures show a reduced variation and maintain themselves at a constant value below 0 °C. This behavior can be attributed to the "Zero Curtain Effect" (ZC), i.e. the compensation of the upward heat loss associated with the drop in air temperatures by the freezing latent heat of the soil. The hourly temperature change of the autumn-winter FR regime shows positive (warming) and negative (cooling) "spike-like" fluctuations, that are sharp in the first and last winter, suggesting atmosphere-ground interaction. At the end of

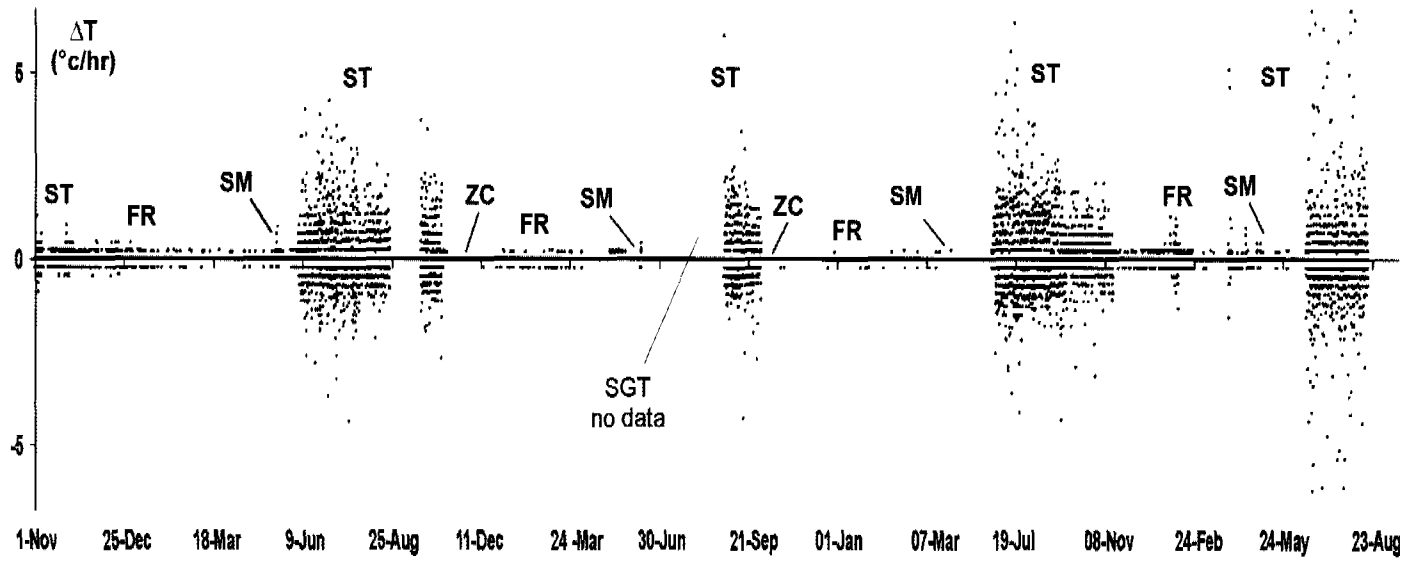

Figure 2. Hourly temperature change (DT, °C/hr) at DTL depth

every FR regime a rapid increase in SGT occurs, followed by a close 0 °C temperature plateaux (SM). These sharp temperature rises are decoupled from the daily air temperature variations and could be referred to non-conductive processes such as snow melt-water infiltration. The 0 °C flat trace of several days, that follows every rapid increase (Fig.1), could represent the ice-water phase change. In order to evaluate the relations between the presence of snow on the rock glacier surface and non conductive processes, the ground-air thermal signal coupling/decoupling could be considered. The magnitude of ZC effect strongly depends on the soil water content, being longer in response to enhanced moisture. The relation between snow cover and the limited/absence of ZC for the 1998 and 2000 autumn suggests that the air temperature lowering affected a well drained ground without a consistent water content. During the 1999 and 2001 FR regimes, the snow cover presence assured a relative water content inside the block voids, triggering and prolonging the ZC effect. The 1998-99 and 2000-01 winter recordings (FR) clearly show coupled air-ground thermal traces, with trends evidently disturbed by abrupt SGT. Funnels in the thin snow cover likely allow the replacement of warm air present in the block voids by dense cold air descending from the atmosphere. Spike-like thermal anomalies are absent or very limited during 1999-00 and 2000-01, because the snow cover isolates the ground from external air fluctuations. The warming magnitude relative to snowmelt water infiltration in the frozen soil (SM) mainly results from the infiltrated water volume/temperature and soil porosity. The coarse-grained ground surface of the Portette rock glacier allows rapid infiltration of snow meltwater. To this non-conductive process corresponds a high thermal impact resulting in an up to 4-5 °C increase within a few days. Finally, the long-lasting snow cover until late spring insulates the ground from the incoming solar radiation and prevents the ground from heating up.

The Portette rock glacier shows SGT trends characterized by non-conductive and seasonally driven heat transfer processes, i.e. release of latent heat during phase change, snow melt infiltration and air circulation. The ground-air temperature comparison suggests that the permafrost growth/degradation strongly depends on the timing of snow appearance/disappearance at the rock glacier surface. Delayed and thin snow cover in autumn represents a forcing factor for permafrost maintenance/growing because it allows i) strong penetration of cold into the ground, ii) lacking/reducing of the ZC effect and ii) downward funnelling of cold air.

REFERENCES

Fabre, D. and Ribolini, A. 2003. Limite actuelle des glaciers ro-chers actifs dans le massif de l'Argentera (Alpes Maritimes italiennes). Réunion du Société Hydrotechnique de France, March 2003, Grenoble.

Kane, D.L., Hinkel, K. M., Goering, D.J., Hinzman L.D. and Outcalt, S.I. 2001. Non-conductive heat transfer associated with frozen soil. Global and Planetary Change 29: 275-292.

Undercooled scree slopes covered with stunted dwarf trees in Switzerland - abiotic factors to characterize the phenomenon

*A. Rist, M. Phillips and K. Auerswald**

Swiss Federal Institute for Snow and Avalanche Research (SLF), Davos Dorf, Switzerland
**Chair of Grassland Sciences, Department of Plant Sciences, Technical University of Munich-Weihenstephan, Freising, Germany*

INTRODUCTION

Large-scale permafrost distribution can be estimated using numerical models simulating the spatial distribution of permafrost in complex topography (Hoelzle et al. 2001). The phenomenon can exist sporadically far below the alpine timberline as azonal permafrost (Haeberli 1978) at special locations with extreme shadow and a significant lower mean annual ground temperature than their surroundings. Sites satisfying this definition are called undercooled scree slopes by Wakonigg (1996) including locations which are not frozen perennially, but significantly longer than their surroundings. Undercooled scree slopes are characterized physiognomically by a coverage of stunted dwarf trees (Fig. 1), whose growth is limited by the cold (Sieghardt et al. 2000).

Already in the 19th century an air stream through the voids of the coarse blocky material of the scree slope changing its direction seasonally was regarded as the causal process for the exceptionally cold temperatures. This can be explained by the relatively constant temperature of the air in the underground compared to the seasonal temperature fluctuations in the above-ground atmosphere: in summer the relatively cold air inside the scree slope sinks downwards through the big voids between the blocks and thereby draws warm atmospheric air through the upper openings of the scree slope. On its way through the underground the air cools down on contact with the cold blocks and comes out as an icy wind at the slope foot. In winter, when the rock is relatively warm, the air stream changes its direction: cold atmospheric air streams into the lower openings of the scree slope, warms on the blocks, which thereby cool down, and ascends due to its lower density in order to escape into the atmosphere at the upper end of the scree slope. This theory only explains why the ground temperatures of an undercooled scree slope are significantly lower than the surrounding air temperature in summer.

However, out of this it can not be derived that the mean annual ground temperature of this site is lower than in the surroundings, because the lack of energy in winter might be compensated by the surplus of energy in summer. The presented theory can only be kept if the winter effect preponderates the summer effect. Therefore an asymmetry in the system has to be looked for. However, the energy balance of an undercooled scree slope has to be lower than in its surroundings and negative if azonal permafrost is to occur. The energy balance at a site is determined by four energy balance factors: radiation balance, ground heat flux, sensitive heat flux and latent energy flux.

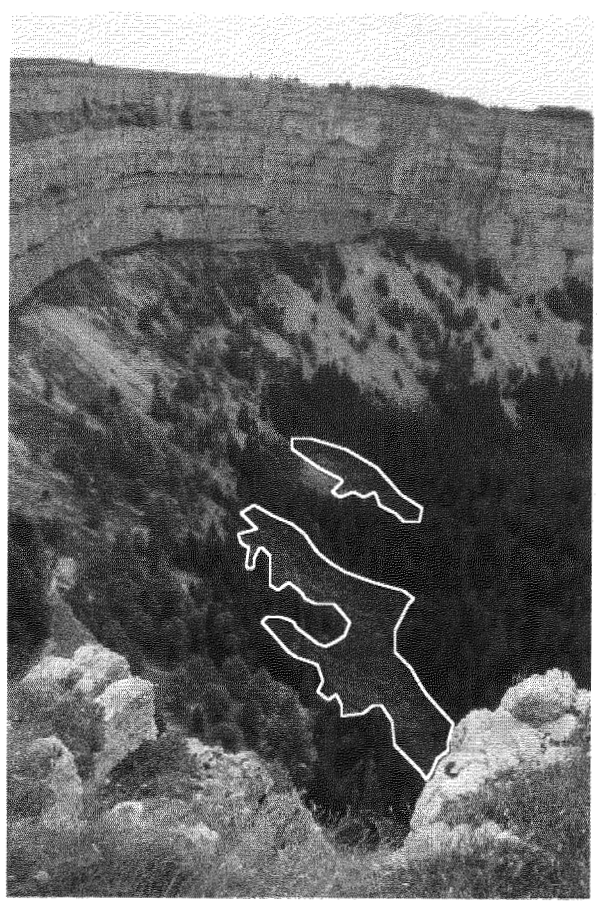

Figure 1. Undercooled scree slope Creux du Van in the Swiss Jura mountains. The stunted dwarf trees (white frames) indicate undercooled conditions.

Our objective was to determine the abiotic factors of undercooled scree slopes. In Switzerland 36 sites were investigated. On the landscape scale, climatic, relief and ground parameters were determined with GIS-techniques and compared with the equivalent values of 495 reference sites with zonal forest. Ten of the undercooled scree slopes were stud-

ied in more detail by comparing each with its reference site with zonal forest in the immediate surroundings in respect to climatic, relief, surface and ground parameters. For that purpose each study slope was divided vertically into a high (HZ), middle (MZ) and low zone (LZ) and horizontally into a transect of stunted dwarf trees and one of zonal forest at the slope foot (Fig. 2).

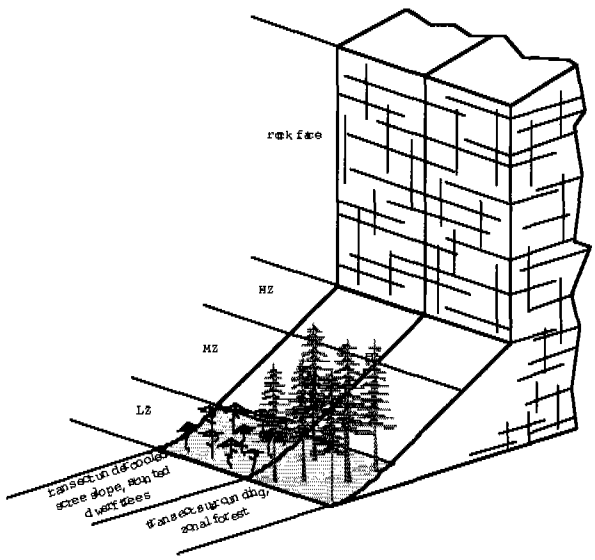

Figure 2. Zoning of an investigated slope horizontally in functional transects, vertically in a high (HZ), middle (MZ), low zone (LZ) and the rock face.

The investigated undercooled scree slopes are located in areas with a mean annual precipitation between 1700 and 2000mm and at a mean altitude of over 1000m a.s.l. The presence of undercooled scree slopes is therefore restricted to mountain regions, but not to an exceptionally cold zonal climate. Undercooled scree slopes are characterized by special local factors: the slope and the rock face above (present in 90% of cases) have a northerly aspect, are shady, and the slope inclination is at least 20°. The rock face – if present – is at least 75m high and 40° steep. These relief parameters cause a low annual radiation balance of about 2.3 GJ/m² on average over the slope profile. In the transect of the stunted dwarf trees respectively the undercooled scree slope the surface area of open scree (about 40%) is more than twice as high as in the proximate transect with zonal forest. Therefore the absorption of radiation will be less in the first transect, as the short wave albedo of rock is higher than that of soil and vegetation. Furthermore the air convection flux through the coarse blocky material, which is important for the low energy balance of an undercooled scree slope (Delaloye and Reynard 2001), can be ascribed to the large surface area of open scree and to the wide pore diameters (increasing from 4 cm on average at the head of the scree slope to 10 cm at its foot). The soil depth of the undercooled scree slope (8 cm on average) is less by about one third than in the surrounding zonal forest. The outcome of this is a reduced thermal insulation of the undercooled scree slope. In combination with the stronger air convection this may lead to a faster cooling of the undercooled scree slope in comparison to the surrounding forest in autumn. When the snow cover reaches about 1 m, the lower energy level will be conserved by thermal insulation. In spring this can result in a delayed snowmelt, i.e. the undercooled scree slope will become snowfree later than the surroundings. Due to the higher short wave albedo of snow in comparison with soil and vegetation this will further decrease the annual areal radiation balance of the undercooled scree slope as compared to its surroundings.

Most of the investigated parameters differ only slightly between an undercooled scree slope and its surroundings and therefore the differences of the energy balances are also marginal. Nevertheless, the physiognomical forms of forest at the compared sites are different. Thus undercooled scree slopes are labile systems and therefore represent a rare phenomenon and an ecosystem worthy of protection.

REFERENCES

Delaloye, R. and Reynard, E. 2001. Les éboulis gelés du Creux du Van (Chaîne du Jura, Suisse). Environnement Périglaciaires. Notes et Comptes-Rendus du Groupe Régionalisation du Périglaciaires 8: 118-129.

Haeberli, W. 1978. Special aspects of high mountain permafrost methodology and zonation in the Alps. Proceedings of the Third International Conference on Permafrost, NRC Ottawa, 1, 379-384.

Hoelzle, M. Mittaz, C. Etzelmüller, B. and Haeberli, W. 2001. Surface energy fluxes and distribution models relating to permafrost in European Mountain Permafrost areas: an overview of current developments. Permafrost and Periglacial Processes 12: 53-68.

Sieghardt, H., Punz, W. and Reimitz, R. 2000. Vergleichend-anatomische Studien an Pflanzen der Eppaner "Eislöcher". Verhandlungen der Zoologisch-Botanischen Gesellschaft in Österreich 37.

Wakonigg, H. 1996. Unterkühlte Schutthalden. Arbeiten aus dem Institut für Geographie der Karl-Franzens-Universität Graz Beiträge zur Permafrostforschung 33: 209-223.

Formation and evolution of the Shalbatana Valley System, Mars: A case study for the interaction between magmatism and permafrost

*J.A.P. Rodriguez, S. Sasaki, *R.O. Kuzmin and **R.Greeley*

Department of Earth and Planetary Sciences, University of Tokyo, Japan

**Vernadsky Institute of Russian Academy of Sciences, Moscow, Russia*

***Department of Geological Sciences, Arizona State University, Arizona, U.S.A*

INTRODUCTION

A large concentration of seemingly collapsed features and associated outflow channels are found between western Lunae Planum and western Arabia Terra in the cratered highlands (units Npl1 and Npl2) and the volcanic plains (unit Hr). Comparisons with terrestrial flood channels, such as those of Channeled Scablands in eastern Washington, suggest that the Martian channels were eroded by catastrophic floods. Most of the Martian channels originate from chaotic terrains interpreted to represent areas where the ground collapsed as water (confined under the permafrost) was released under high hydrostatic pressures within artesian basins. Understanding the geologic history of the Shalbatana Valley System (SVS) can improve our knowledge of groundwater recharging and extraction mechanisms, and the derivation of the history of valley formation in the highlands. Shalbatana Vallis was interpreted as an outflow channel excavated by water flow from an ice-covered paleolake in Ganges Chasma (Nedell et al. 1987) and from catastrophically releases from confined aquifers as the permafrost seal (Clifford, 1987) was disrupted at three locations, forming chaotic regions (Cabrol et al. 1997). Rodriguez et al. (2003) proposed that the excavation of SVS also involved water released from an extensive underground cavern system produced by magma and permafrost interaction. They also proposed an alternative hypothesis for the origin for the Shalbatana upstream chaotic region; they suggest that a highly degraded late Hesperian impact crater (SE part) collapsed over the putative cavernous system. In this work, we have used 128 pixels/degree MOLA DEMs to derive alternative hypotheses for the origin the Basin-A and its chaotic material, as well as for the origin of the flanking Valley system III (Fig. 1A).

THE BASIN A

The abrupt widening of the main Shalbatana Valley occurs at the junction between VS-I and B-A (Fig. 1B). This is also the transition of the main valley from incision into the Noachian plateau (bounded by unit Npl2 to the east) and to the West by VSIII (Hesperian highland unit Hr). The chaotic terrain in B-A was used as evidence that this basin resulted from collapse over an aquifer (Cabrol et al. 1997). The east margin of the main SVS valley shows a change in orientation where it bounds B-A, which resemble intercepted craters. The topographic region TL1 partly bounds the basin at an elevation of about 700 meters above TL2 and TL3 (Fig. 1B). A channel (Chn) extends from VSI into B-A, the margins of which are partly bounded by TL1-A and TL1-B. This suggests that the topography was continuous prior to channel formation. The topographic and roughness characteristics of these terrains resemble those of Crater A (Fig. 1B and Fig. 2). Moreover, unit TL1-C occurs along the flanks of the arcuate cliff section. These observations are consistent with this unit representing the floor of collapsed craters intercepted by SVS. The karst-like features (seen on the top edges of B-A), are consistent with collapse processes for this part of the valley and suggest that the permafrost might have been relatively shallow in the past and/or there are efficient mechanisms of vertical transport of volatiles from a deeper permafrost region, such as fractures produced by surface extension over intrusive non-emergent dikes. Structural control (Cabrol et al. 1997) over the main valley determined the deep and narrow U-shaped VSI, which is incised into the Noachian highlands. Structural control along the eastern flank of the main valley is suggested by the orientation, depth and slope characteristics and we propose that the abrupt widening of the main valley resulted from a change in lithologies. This hypothesis is consistent with the distribution of the chaotic terrain, which is rougher, more abundant, and topographically higher on the flanks of VSIII. This suggests that the chaotic material was shed from the VSIII upland. The position of the deepest and smoothest topographic unit (TL3) is consistent with its being a depositional area for material carried by the channel (Chn). We propose that flow from VS-I intercepted a series of collapsed craters in this region and possibly formed a crater-lake system, which might have extended as far as the end of VS-II. The geological materials composing the western margin of this lake system were apparently volatile rich and suggest that the permafrost at a regional scale was/is unequally distributed and/or has undergone different geological processes.

THE VSIII COMPLEX

It has been proposed (Cabrol et al. 1997) that water from the B-A region successively drained and excavated the d1 and d2 channels in the Hesperian plateau (Fig. 2). These two channels were abandoned following the deepening of the main channel towards the Simud valleys (Cabrol et al. 1997). We have observed that this region forms a complex system of valleys, which includes rimless quasi-circular depressions, elongate depressions, pit chains and deep U-shaped valleys. The roughness of this region reveals a high frequency, low amplitude component, which would be consistent with extensive thermokarstic activity and other subsurface degradation processes (Rodriguez et al. 2003; Kuzmin et al. 2002).

The d2 system: The contact between the d2 system and B-A forms a wide valley (Fig. 2, yellow dotted line), which narrows and is incised by a relatively narrow, south-dipping central region (d2a). Channel d2a joins with d2b to the north, forming a deep U-shaped valley. B-A drainage by the d1 and d2 channel systems is consistent with the temporal ponding of VS-1, B-A and VS-II, which was subsequently lowered as flow toward the Simud valley occurred (Kuzmin et al. 2002).

We propose that in a first stage flow took place from B-A to the north, forming a drainage channel of which only the northern d2b section remains. After drainage from B-A ceased the northern margin of B-A became unstable and recession occurred preferentially headward along the preexisting drainage channel. Recession happened mainly as debris flows, fed by material shed from the valley flanks to its central region, flowed towards B-A, which resulted in valley widening, excavation of the central channel d2a, and the deposition of most of the chaotic unit TL2.

The d1 system: This system forms an N-trending series of depressions, which includes wide shallow regions (Fig. 2, WSR), narrow enclosed-and elongate-regions (Fig. 2, NEER), and deep, rimless quasicircular depressions (Fig. 2, RQCD). This association does not seem to be the result of surface flow and it is more consistent with subsidence related to long-lasted subsurface degradation, possibly by water flowing through underground conduits (Rodriguez et al. 2003). Other features in the region consistent with large subsurface processes include the floor of Crater A, which shows surface modifications and an elongate depression that extends south from the margin of crater A, forming a sequence of pits, which shallow up and become narrower to finally disappear near the margin of the VS II. The presence of dike like ridges at the bottom of grabens located within the VSIII complex are suggestive of the observed featured to be genetically related to interactions between intrusive magmatism and permafrost (Rodriguez et al. 2003).

FINAL REMARKS

These regions of the SVS demonstrate the importance of lithological and structural controls over the morphological characteristics of highland valleys. Our observations suggest that processes possibly related to debris flows and thermokarstic degradation produced the knobby material in the chaotic region within B-A. The observing evidence for extensive underground denudation apparently had resulted in different degrees of subsidence, which might have been related to the development of cavernous systems. These issues are important to understand the complexity of hydrological processes involved in the formation of the SVS, to quantify the amount of water involved, and the amount of material eroded during its excavation and to stress the complexity and great age range of the processes involved in the Martian permafrost.

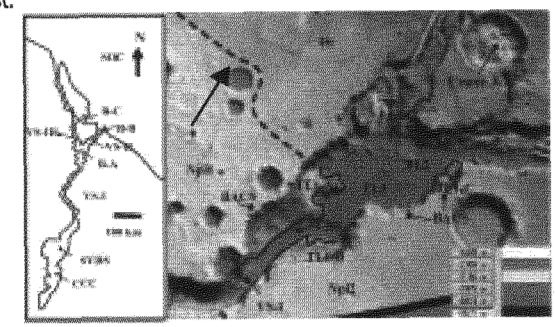

Figure 1A. (left) Feature map. CCC: Collapsed Conduit Complex, SVHS: Shalbatana Valley Headwater System, VS-I to III: Valley systems I to III, B-A to C: Basins A to C, SOC: Simud Outflow Channel.

Figure 1B. (right) MOLA DEM of B-A. Crater A is 35 km across. Npl1, Npl2: Noachian plains 1 and 2. Hr: Hesperian ridges. BACS: Bounded arcuate cliff sections, TL 1-3: Topographic levels 1 to 3.

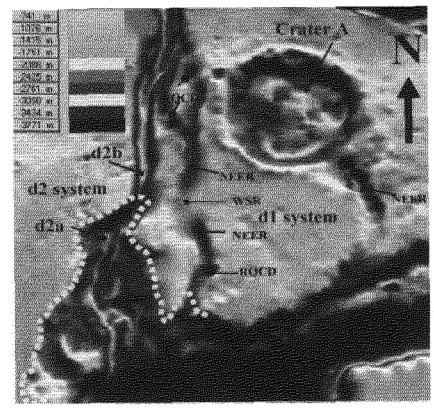

Figure 2. MOLA DEM of VS-III. Crater A is 35 km in diameter. The d1 system includes RQCD: Round quasicircular depressions, NEER: Narrow enclosed elongate depressions, WSR: Wide shallow region. The d2 system includes channels d2a and d2b.

REFERENCES

Nedell, S.S., Squyres, S.W. and Andersen, D.W. 1987. Origin and evolution of the layered deposits in the Valles Marineris, Mars. Icarus, 70: 409-441.

Clifford, S.M. 1993. A model for the hydrologic and climatic behavior of water on Mars. Geophys. Res. Lett., Vol. 98 No.E6, 19073-11016.

Cabrol, N.A., Ednmon, A. G. and Dawidowicz, G. 1997. Model of outflow generation by hydrothermal underpressure drainage in volcano-tectonic environment, Shalbatana Vallis (Mars), Icarus, 125: 455-464.

Rodriguez, J.A.P., Sasaki, S. and Miyamoto, H. 2003. Nature and Hydrological relevance of the Shalbatana complex underground cavernous system ,Geophys. Res. Lett., Vol. 30 No.6, 1304, 10.

Kuzmin, R.O., Greeley, R. and Nelson, D. M. 2002. Mars: The morphological evidences of late Amazonian water activity in Shalbatana Vallis. Lunar and Planetary Science conference XXXIII. Abstract 1087.

Distribution of ramparted ground-ice depressions, Llanpumsaint, southwest Wales.

*N. Ross, C. Harris, P. Brabham and *S. Campbell*

School of Earth, Ocean and Planetary Sciences, Cardiff University, Cardiff, Wales

**Department of Earth Sciences, Countryside Council for Wales, Bangor, Wales*

INTRODUCTION

Geomorphological features recognised as 'ramparted ground-ice depressions' are well represented in the Welsh landscape. These features have been interpreted as some of the finest examples of relict open-system pingos in the UK, formed within discontinuous permafrost during the Late Devensian or Loch Lomond Stadial (GS-1; Watson 1972). Landforms include horseshoe-shaped, circular or complex ramparts, enclosing water- and/or peat-filled basins.

Although they are distributed throughout Wales (Fig. 1), previous research indicates a remarkable density in the southwest, particularly within the tributaries of the Afon Teifi (e.g. Cledlyn Valley), northwards towards Aberystwyth (Watson 1972).

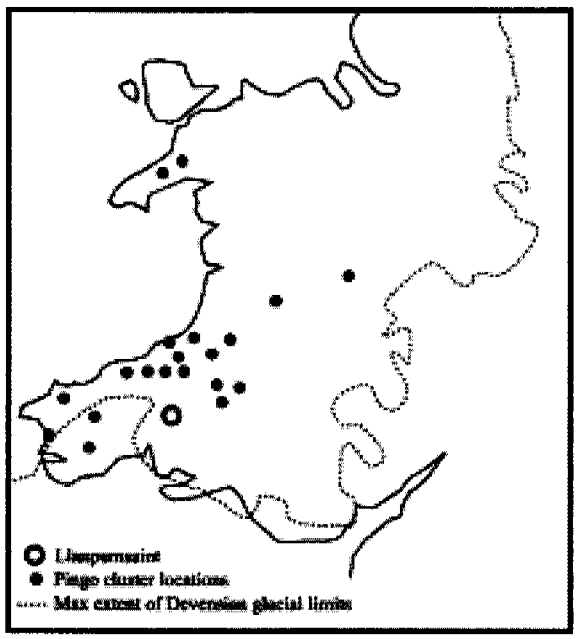

Figure 1: Distribution of ramparted ground-ice depressions in Wales (Adapted from Ballantyne and Harris 1994).

The known distribution of ramparted depressions in Wales is however, thought to represent only a proportion of the total number of potential sites. Research aimed at establishing their distribution, morphology, structure and origin has been initiated to develop a framework for their conservation. This paper concentrates on the spatial distribution and density of these features, presenting preliminary results from a representative location where ramparted depressions are documented, but no rigorous investigation has previously been conducted.

LOCATION AND RESULTS

Ramparted depressions were identified near Llanpumsaint by Watson and Watson (1974) in a series of papers on ramparted depressions in southwest Wales during the 1970s. Their research focused predominantly on the features of the Cledlyn and Cletwr valleys however, and although other locations were illustrated in maps in various publications, the exact map references of these sites were never published. Re-identification and geo-referencing of these "dots on maps" is therefore a current research priority.

The ramparted depressions of Llanpumsaint are located within an area of approximately 20 km^2 in the tributaries of the Afon Gwili at altitudes between 90-150 m. Aerial photography has enabled the identification of numerous impressive landforms with ramparts enclosing depressions and impounding marshland. In excess of 100 clearly defined ramparts are identifiable, not including areas of complex micro-topography that may also represent ramparted depressions. A particularly impressive subset of features is located to the south of Llanpumsaint at SN 420275.

Preliminary mapping of this locality indicates a remarkable density (>15 per km^2) of identifiable ramparts (Fig. 2), representing approximately 25% of the total number of identifiable ramparted depressions proximal to

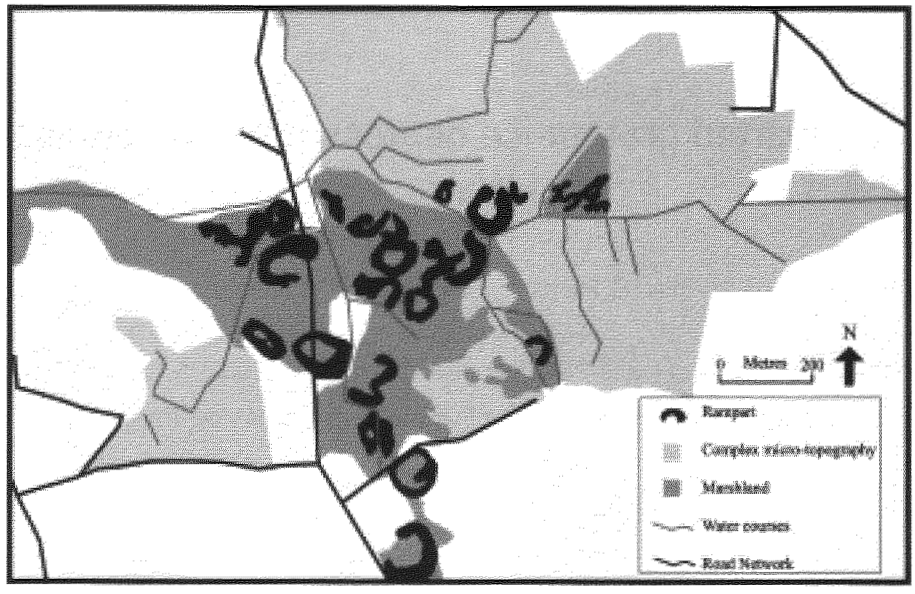

Figure 2. Ramparted ground-ice depressions near Llanpumsaint, southwest Wales.

Llanpumsaint. The relationship between the distribution of these features and water courses is of note, with well-developed forms located in the areas adjacent to, or between, channels. Without the support of field verification however, the impact of channel modification for agricultural purposes cannot be assessed, and the current network of water courses may not reflect the natural state. Like the features of the Cledlyn valley, those at Llanpumsaint are clustered on valley bottoms and on low gradient slopes. This common morphology and geographical setting suggests a common mechanism of formation.

WIDER IMPLICATIONS AND FURTHER RESEARCH

Preliminary fieldwork and a review of aerial photography resources confirm the initial assessment that the distribution of ramparted depressions in Wales is much more extensive and of a higher density than previously recorded. This has important implications for the genetic origin and age of these features.

The context necessary for the formation of contemporary ground-ice mounds depends not only on climate, but also on an array of geological and hydro-geological factors. The remarkable number and density of ramparted depressions in southwest Wales is therefore indicative of a combination of factors that facilitated their development. Potentially, these include the interaction of i) topography, ii) superficial geology, iii) structural geology, iv) the extent and influence of the Late Devensian ice sheet, v) subsurface hydrology, and vi) geothermal flux.

Recently, a hypothesis that the ramparted depressions of the Cledlyn and Cletwr valleys may represent the relict forms of mineral palsas has been propagated in the literature (Gurney 1995). In our opinion the origin of these features remains an open question. Investigation of their internal structures remains critical in addressing this issue, together with the location, morphology, volume of the ramparts, hydrological setting and distribution of sediments susceptible to ice segregation. The apparent similarities of morphology and geographical setting of the Llanpumsaint ramparted depressions with those of the Cledlyn valley means that a similar mechanism of formation can be tentatively inferred.

The assignment of all ramparted depressions recorded in Wales to the Loch Lomond Stadial (GS-1) period must be questioned. Ground-ice mounds producing ramparted depressions of this number, size and density are unlikely to have formed within 1ka.

To test these initial hypotheses, more detailed investigations are planned to:

i. produce a complete inventory of ramparted depression localities in Wales using aerial photography;
ii. define the extent of ramparted depressions within identified sites, and assess their relative conservation status;
iii. investigate selected sites utilising a suite of geophysical techniques and vibrocoring to determine internal structure and stratigraphy.

REFERENCES

Ballantyne, C.K. and Harris, C. 1994. The Periglaciation of Great Britain. Cambridge University Press, Cambridge.

Gurney, S.D. 1995. A reassessment of the relict Pleistocene "pingos" of west Wales: hydraulic pingos or mineral palsas? Quaternary Newsletter 77: 6-16.

Watson, E. 1972. Pingos of Cardiganshire and the Latest Ice Limit. Nature 236: 343-344.

Watson, E. and Watson, S. 1974. Remains of pingos in the Cletwr basin, south-west Wales. Geografiska Annaler 56A: 213-225.

Groundwater under deep permafrost conditions

*T.Ruskeeniemi, L.Ahonen, M.Paananen, R.Blomqvist, • P.Degnan, ** S.K.Frape, *** M.Jensen, **** K.Lehto, L.Wikström, ***** L. Moren, I. Puigdomenech and ****** M. Snellman*

*Geological Survey of Finland, Espoo, Finland; * UK Nirex Ltd., UK; ** University of Waterloo, Waterloo, Canada*

**** Ontario Power Generation, Toronto, Canada; **** Posiva Oy, Olkiluoto, Finland*

****** Svensk Kärnbränslehantering AB (SKB), Stocholm, Sweden*

******* Consulting Engineers Saanio & Riekkola, Helsinki, Finland*

INTRODUCTION

According to the geologic disposal concept in Scandinavia, spent nuclear fuel will be sealed in corrosion-resistant and watertight canisters, and then emplaced in holes drilled at the bottom of tunnels excavated into the bedrock. The canisters are to be surrounded with bentonite clay, which expands when it absorbs water. In Scandinavia the depth of any repository is to be approx 500 m below ground surface. When the last canisters have been emplaced, the tunnels are to be filled, e.g., with a mixture of bentonite and crushed stone, and the shafts leading to the repository closed.

In assessing the safety of the geologic disposal concept, it is essential to assess what physical and chemical conditions could evolve within the repository and surrounding environment. The objective of performance and safety assessments is to demonstrate the long-term safety of a repository for long-lived radioactive waste and most management agencies consider scenarios up to 1 my into the future.

During at least the past 2 million years, repeated cycles of glaciation have occurred in the Northern Hemisphere. At present, a major part of the area to the north of latitude 60°N is under permafrost conditions, although within Fennoscandia at the same latitudes, temperate conditions prevail. Climate models based on astronomical forcing predict a cold period after approximately 60 000 years. Cold, dry periods favour the formation of periglacial conditions and the development of deep permafrost, such that permafrost is expected to reoccur in northern and central Europe and North America.

In order to predict the long-term performance of a geologic repository the influence of periglacial and glacial conditions must be considered. A key goal of this research project is to enhance the scientific basis for safety and performance assessment and to derive constrained permafrost scenarios relevant to the evolution of crystalline groundwater flow systems.

A number of issues were identified as possible targets of study: 1) Freezing rate and depth extent of permafrost in crystalline bedrock; 2) Cold saline water segregations (cryopegs) and their role in transport processes, 3) Role of non-frozen areas (taliks) as pathways for groundwater flow, 4) Aggregation of solid methane hydrates (clathrates), and 5) Effects of freezing on bedrock stability.

All these aspects are related to the long-term stability of hydrogeological and hydrogeochemical conditions. Some of these phenomena are reviewed at length in the literature and much is known about their role in shallow systems or in sedimentary environments. However, much less has been published regarding cryogenic processes and hydrogeology in crystalline rock under deep permafrost conditions.

This PERMAFROST project is a co-operative international undertaking jointly funded by the participants from Finland (Geological Survey of Finland and Posiva), Sweden (Svensk Kärnbränslehantering, SKB), Great Britain (UK Nirex Ltd) and Canada (Ontario Power Generation and University of Waterloo). After a short feasibility phase, the research at Lupin started in late 2001 (Ruskeeniemi et al. 2002).

THE STUDY SITE

Although the occurrence of permafrost is wide-spread in the Northern Hemisphere today, there are only a few locations at which permafrost in crystalline terrain can be investigated. Such is the case at the Lupin gold mine in Canadian Arctic (Nunavut Territory), approximately 1300 km north of Edmonton, and some 80 km south of the Arctic Circle. The distance to the White Sea in the north is about 300 km.

The site is within the continuous permafrost zone. Today the depth of the permafrost in the area extends to depths between about 400 and 600 m. The temperature measurements conducted in the mine indicate that permafrost persists down to 541 m. It is assumed that much of the deep permafrost in this part of Canada has been formed during the Holocene, i.e., during the past 10,000 years.

The region is located in the continental sub-arctic climate zone well above the timberline. The vegetation is

typical for tundra: grass and low-growing shrub species and dwarf birch. The mean annual air temperature is –11°C, and the annual extreme values range from –49°C to +31°C. The annual mean precipitation is low, about 270 mm.

The Lupin gold deposit is located in an Archean metaturbidite sequence. The formation of the ore is dated at 2.5 Ga. The major lithological units at the site are crystalline rock types, phyllite and quartz-feldspar gneiss. However, their sedimentary counterparts mudstone and graywacke/quartzite are locally preserved and recognizable. The gold ore is hosted by an amphibolitic iron formation.

RESEARCH AT LUPIN

To support an evaluation of the feasibility of the site and to develop a preliminary conceptual geosphere model, the research at Lupin began with the compilation of the available historical information on the lithostratigraphy, structural geology, hydrogeology, mine hydrology, Quaternary geology, etc. The mine site investigation focused on the collection of groundwater samples from the mine at existing boreholes and drift-exposed discontinuities.

In general the mine is dry (mine discharge about 50 000 m^3/a), with the majority of the inflow occurring from a few long exploration boreholes and, to a lesser extent, from certain fracture zones. One of the fracture zones is repeatedly cut by the spiral mine access ramp, which provided an opportunity to collect dripping water to the 680 m level at which the seepage apparently drains. Water samples were obtained from a vertical cross section between the 87 m and 1130 m levels.

As suspected, all the samples from frozen levels turned out to be contaminated by Na-Cl brines used for drilling in permafrost. In comparison, the boreholes at lower levels provided insight into the chemistry of the deep groundwaters below the permafrost. These waters are brackish to saline, Na-Cl dominant, with dissolved solids (TDS) ranging between 2 to 29 g/L and lacking all indication (high SO4, NO3 and tritium) of contamination.

One of the key activities at Lupin is to explore whether the outfreezing process can result in the formation of a saline groundwater layer at the base of the permafrost in crystalline bedrock. An electromagnetic sounding carried out in the area gave indications of a subhorizontal conductor in the depth range of 400 to 700 m. It is assumed that this conductor would mark the location of the base of the permafrost. According to model calculations, a saline water layer with TDS of 5-30g/L could explain the observed anomaly. Parallel to the field research, laboratory freezing experiments were carried out at the University of Waterloo, Canada with various groundwaters collected from Canada and Scandinavia. In addition to detailed information on the behaviour of major and trace elements and isotopic fractionation during outfreezing, the experiments demonstrated that it was difficult to generate significant volumes of concentrated fluids from the small volume of groundwater available in crystalline bedrock. This result appears to contradict the results from the geophysical field study.

To resolve this dilemma, and to support other hydrogeochemical studies, two 400 to 500 m long low-angle research boreholes were drilled from mine adits in late 2002 in an attempt to intercept fractures close to the base of the permafrost that might contain uncontaminated groundwater.

The preliminary results suggest that the groundwater table has declined and unsaturated conditions may exist below the permafrost. Similar information is determined from hydraulic pressure head measurements in boreholes on the 890 and 1130 m levels. Currently it is too early to say whether this is typical for deep permafrost conditions in an area with limited recharge and low hydraulic gradients, or if it is simply the effect of 20 years of mine operation. A small amount of groundwater is seeping into the new boreholes from the overlying permafrost. Geochemical and isotopic geochemical charaterization of these samples is underway.

CONCLUSIONS

The overall goal of the studies at the Lupin mine is to study permafrost features and processes, which could have relevance in assessing the performance and safety of a repository at depth. Thus information obtained must be transferable from observations in the Lupin mine to a generic nuclear waste repository in a similar geological environment. The research at Lupin will continue to address the hydrogeochemical questions, but major efforts are also directed towards improving the understanding of the hydrogeology below the permafrost, in particular, the influence of taliks on groundwater flow conditions.

REFERENCES

Ruskeeniemi, T., Paananen, M., Ahonen, L., Kaija, J., Kuivamäki, A., Frape, S., Moren, L., and Degnan, P. 2002. Permafrost at Lupin: Report of Phase I. Geological Survey of Finland, Nuclear Waste Disposal Research. Report YST-112, 59 p.

A new approach to dating firn accumulation in an ice cave in the Swiss Jura mountains

*F. Schlatter, M. Stoffel, M. Monbaron and *M. Luetscher*

Department of Geosciences, Geography, University of Fribourg, Fribourg, Switzerland

**Swiss Institute for Speleology and Karstology (SISKA), La Chaux-de-Fonds, Switzerland*

INTRODUCTION

Located at 1359 m a.s.l. on the south east side of the Swiss Jura range (Bière/VD, 6°17'50"/ 46°33'47"), a collapsed doline with a diameter of about 40 m acts as an important source of snow accumulation during the winter season. The particular morphology and the sufficient depth (-45m) of the cavity enable the trapping of cold air. This causes the freezing of infiltration water and the transformation of the snow into ice. Over sixty ice caves are recognized in the Swiss Jura. The St Livres ice cave is the second largest in the range. In 1976, its volume was estimated at 3,500 m3 (Gigon 1976). Due to the significant melting of ice in the recent past, its volume is now reduced to approximately one-third (i.e. 1200 m3).

Next to its vertical pit, the cavity has a horizontal development of 60 meters (Fig. 1). Ice flows along for about 40 m, leading to the lower part of the cavity. In this place, an overhanging ice wall forms the front of this small glacier. Thus it is possible to observe an almost continuous outcrop of the glacier. The presence of organic matter in the ice allows the identification of different layers. Moreover, great number of branches and trunks are trapped in the ice (Fig. 2). In several places, deformations of the ice layers confirm the presence of significant flow of the ice filling. This flux is also responsible for the transport of woody material that fell down in the accumulation zone, that is, tree trunks and branches slowly movingto the deepest part of the cavity.

In the past, the front of the glacier was completely covered by a big stalagmite of ice forming a dome. Freezing water infiltration originating from the roof of the cavity formed this ice. In the last ten years however, the ice cave melted considerably and the ice dome totally disappeared. Furthermore, the front of the glacier also retreated, liberating trunks and branches. The ice contains essentially four tree species, namely European beech (Fagus sylvatica L.), Great maple (Acer pseudoplatanus L.), European silver fir (Abies alba Mill.) and Norway spruce (Picea abies (L.) Karst.). In contrast to the wood trapped in the ice, only the two conifer species are abundant in the local forest next to the ice cave.

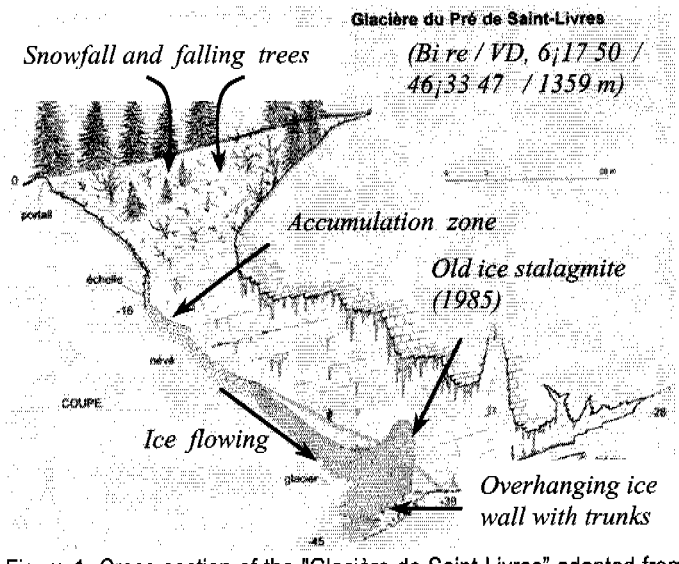

Figure 1. Cross section of the "Glacière de Saint-Livres" adapted from Audétat and Heiss 2002.

OBJECTIVES

This study aims to date (relative age) all ice layers with woody material. Dendrochronological methods (Schweingruber 1996) are used to cross-date the single layers containing subfossil tree trunks and branches. Analysis of living trees outside the ice cave will reveal the link between the living and the subfossil samples, permitting an absolute dating of the single layers. This work is expected to provide important data on the process of firn accumulation in ice caves.

METHODOLOGY

First, the front of the glacier in the ice cave is mapped in detail. Special focus is placed on the identification of different accumulation layers and the position of some 60

subfossil trunks and branches of Norway spruce (Picea abies (L.) Karst.) trapped in the ice. Cross sections of every tree are made using a chainsaw. In the laboratory, the samples are dried and polished using sandpaper. In order to determine the age and the yearly increment of the samples, tree-ring widths are measured, detrended and averaged (Schweingruber 1996). The resulting series of the 60 sections are then crossdated in order to build a floating chronology (relative age).

In a further step, living trees outside the ice cave are sampled in order to obtain growth patterns of undisturbed living trees in the neighbouring forests. From each tree, at least two cores are extracted with increment borers. The resulting reference curve covers approximately the last 200 years.

Finally, the absolute reference curve of living trees is cross-dated with the floating chronology of trapped wood inside the cave in order to close the gap between the youngest subfossil and the oldest living trees.

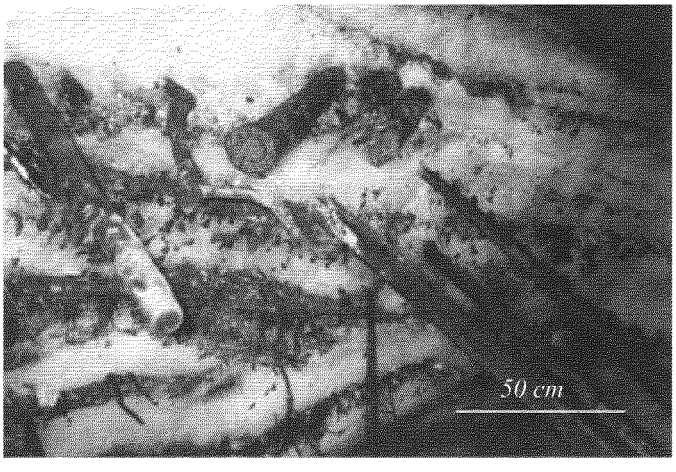

Figure 2. Organic strata at the front of the ice filling in the "Glacière de St. Livres".

CONCLUSION

Dendrochronological investigations in ice caves have only rarely been attempted to date ice layers and the accumulation of firn. Nevertheless, this approach will help to better understand the processes at the origin of such ice filling and will significantly improve our knowledge of these particular permafrost occurrences, without distur-bing the subterranean environment too much. Preliminary results will be presented on the poster.

REFERENCES

Audétat M. and Heiss G. 2002. Inventaire spéléologique du Jura vaudois, partie ouest. Académie suisse des sciences naturelles, La Chaux-de-Fonds: IRL Renens

Gigon R. 1976. Inventaire spéléologique du canton de Neuchâtel. Société helvétique des Sciences Naturelles. Neuchâtel.

Schweingruber, F.H. 1996. Tree Rings and Environment. Dendroecology. Swiss Federal Institute for Forest, Snow and Landscape Research WSL/FNP. Birmensdorf:

Rock glacier inventory of the Adamello Presanella massif (Central Alps, Italy)

*R. Seppi, *C. Baroni and **A. Carton*

Dipartimento di Scienze della Terra, Università di Pavia, Pavia, Italy and Museo Tridentino di Scienze Naturali, Trento, Italy

**Dipartimento di Scienze della Terra, Universià di Pisa and CNR, Istituto di Geoscienze e Georisorse, Pisa, Italy*

***Dipartimento di Scienze della Terra, Università di Pavia, Pavia, Italy*

The rock glacier inventory of the Adamello Presanella Group (Central Alps, Italy) was carried out by means of field and topographic surveys as well as aerial photograph analysis. The study area is characterized by a series of valleys descending from the summit of the massif with a centripetal pattern. Geomorphology is dominated by mass wasting (talus slopes, debris cones, debris-flow cones and lobes), and glacial (erosional landforms and moraines) and periglacial (mainly rock glaciers) landforms. Lithology is characterized by the Adamello–Presanella–Monte Re di Castello intrusive rock complex (tonalites and granodiorites). The metamorphic basement and volcanic and sedimentary rocks of the Permian-Cretaceous sequence outcrop at the external margins of the batholite. The mountain summit area hosts the largest glacier of the Italian Alps (Adamello Glacier, 17.66 km^2); more than 90 glaciers are to be found in the northern and central sectors of the massif.

In the study area 216 rock glaciers have been identified and mapped by means of GIS (ArcView 3.2). They have been divided into (a) active/inactive (83 rock glaciers, 38%) and (b) relict (133 rock glaciers, 62%), according to Barsch (1996). The average elevation of the front of active/inactive rock glaciers is 2493 m a.s.l. (minimum value 2180 m a.s.l.). The average of the maximum elevations of the same rock glaciers is 2614 m a.s.l. (maximum value 2940 m a.s.l.). The average elevation of the front of the relict forms is 2071 m a.s.l. (minimum value 1700 m a.s.l.). The average maximum elevations of the same rock glaciers is 2183 m a.s.l. (maximum value 2650 m a.s.l.). Active/inactive rock glaciers are on average 291 m long and 163 m wide, whereas the relict ones are on average some 290 m long and 199 m wide. The average area covered by rock glaciers is 0.041 km^2, varying from 0.039 km^2 for the active/inactive forms and 0.043 km^2 for the relict ones. The largest form (A75 in the inventory), located in Val di Lares, is a lobate type and extends over 0.27 km^2.

In terms of orientation, 61% of rock glaciers face N, NE and NW, whereas 17% are exposed to the S, SE, SW. The remaining ones face E (13%) and W (9%), respectively. The elevation of the front of active/inactive and relict rock glaciers facing N, NE and NW is considerably lower than the elevation those facing S, SE and SW (Fig. 1). In the active/inactive forms this difference is 202 m, whereas in the relict ones it is 89 m.

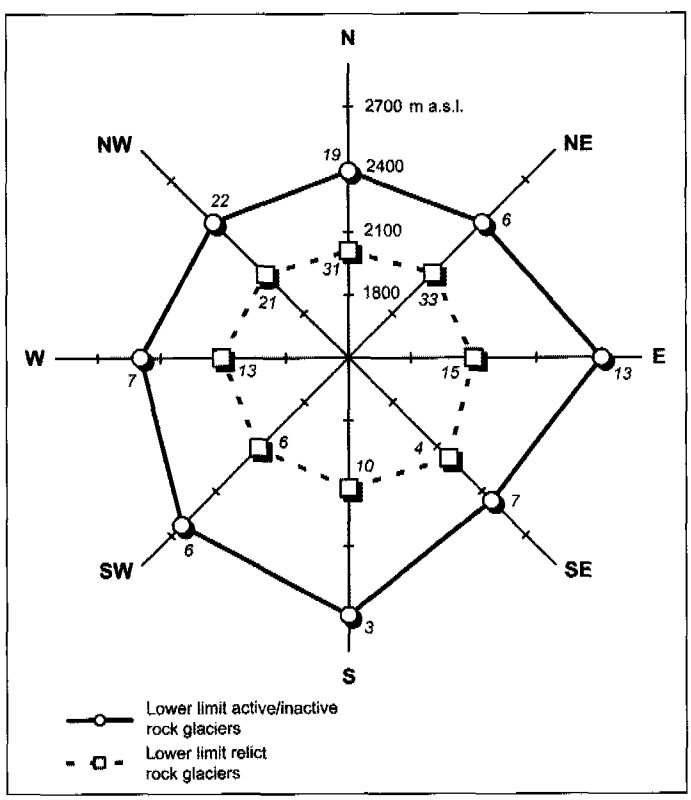

Figure 1. Altitude of the fronts of active/inactive and relict rock glaciers compared with aspect. The number of forms for each orientation is shown.

Measurements of the displacement of rock blocks from two active rock glaciers are in progress. Preliminary survey has been carried out on each of them by means of a theodolit. The position of 25 boulders marked with screw anchors was checked one year after installation on a rock glacier located in the upper Val di Genova (A37 in the inventory). This tongue-shaped rock glacier, which ranges in elevation from 2750 to 2880 m a.s.l., faces SW, is some 280 m long, 100 m wide and covers an area of about 0.023 km^2. The movement of the single monitored boul-

ders ranges between 0.05 m and 0.21 m. The boulders scattered on the frontal and left-sided portions of the rock glacier (points 1–15) are subject to greater displacements, whereas the higher sector is less dynamic (Fig. 2). In any case, the measured movements are rather slow (cf. Barsch 1996, Kaufmann 1996) and generally oriented along the slope's maximum dip. The surface velocity surveyed in the second rock glacier, which is located in Val d'Amola (A42 in the inventory), ranges between 0.02 and 0.16 m/year, with flow vectors oriented in a rather homogeneous way. The eastern portion of the front appears to be more dynamic (0.12–0.15 m/year).

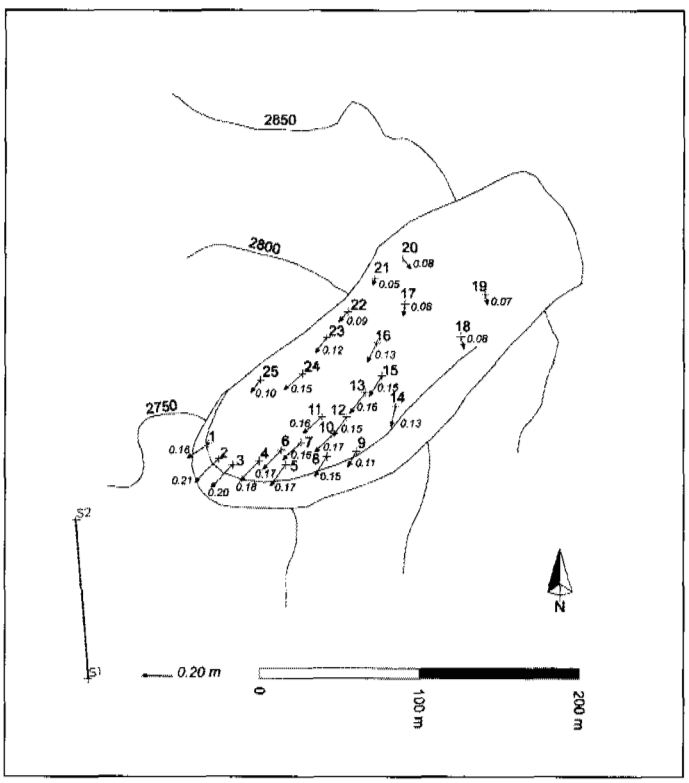

Figure 2. Movement (direction and rate of displacement) of marked boulders (1–25) on the active rock glacier located in Val di Genova (A37 in the inventory). S1=basis of topographic survey; S2=bench mark of topographic survey.

The minimum altitude of active/inactive rock glaciers is utilized as an indicator of the present lower boundary of discontinuous permafrost (Barsch 1996), whereas the elevation of relict forms is used as an indicator of past permafrost conditions. In the study area the difference in altitude between the fronts of the active/inactive and relict forms indicates a increase in the lower boundary of discontinuous permafrost of 420 m. In other alpine areas, the relict rock glaciers have been ascribed to the Late Glacial (Sailer and Kerschner 1999, Frauenfelder et al. 2001, Lambiel and Reynard 2001). If the relict rock glaciers of the Adamello Presanella massif were tentatively correlated to Late Glacial by applying a mean temperature lapse rate of 0.65 °C/100 m to the altitude variation of the lower limit of the discontinuous permafrost, a mean annual temperature rise of about 2.7 °C would be recorded.

Among the active/inactive rock glaciers, about 20 are located in areas occupied by glaciers during the Little Ice Age (LIA) or are fed by glacial deposits from the same period. On the other hand, more forms (about 30) are placed immediately outside the boundaries attained by glaciers during the LIA and do not show any relationship with the glacial deposits of this period. It may therefore be inferred that among active/inactive rock glaciers the most recent forms are ascribable to a period subsequent to the LIA, whereas the other forms are attributable to coeval or preceding Holocene phases.

REFERENCES

Barsch, D. 1996. Rock glaciers: indicators for the present and former geoecology in high mountain environments. Berlin: Springer-Verlag.

Frauenfelder, R., Haeberli, W., Hoelzle, M. and Maisch, M. 2001. Using relict rock glaciers in GIS-based modelling to reconstruct Younger Dryas permafrost distribution patterns in the Err-Julier area, Swiss Alps. Norsk geog. Tidsskr. 55: 195-202.

Kaufmann, V. 1996. Geomorphometric monitoring of active rock glaciers in the Austrian Alps. High Mountain Remote Sensing Cartography; Proc. Intern. Symp., Karlstadt-Kiruna-Tromsø, 19-29 August 1996: 97-113.

Lambiel, C. and Reynard, E. 2001. Regional modelling of present, past and future potential distribution of discontinuous permafrost based on a rock glacier inventory in the Bagnes-Hérémence area (Western Swiss Alps). Norsk geog. Tidsskr. 55: 219-223.

Sailer, R. and Kerschner, H. 1999. Equilibrium-line altitudes and rock glaciers during the Younger Dryas cooling event, Ferwall group, western Tyrol, Austria. Annals of Glaciology 28: 141-145.

Viable protozoa from permafrost sediments and buried soils

A.V. Shatilovich, L.A.Shmakova, S.V.Gubin and D.A.Gilichinsky

Soil Cryology Laboratory, Institute of Physicochemical and Biological Problems in Soil Science, Russian Academy of Sciences, Pushchino, Moscow Region, Russia

INTRODUCTION

A significant number of viable ancient microorganisms is known to be present within permafrost. The age of the cells corresponds to the longevity of the permanently frozen state of the sediments, and the oldest date back to the Pliocene (Gilichinsky 2002). Viable spores of the lower plants (mosses) and seeds of the higher plants were also found within Siberian and Canadian late Pleistocene permafrost; it was shown that they were still able to grow (Porsild et al. 1967; Gilichinsky et al. 2001; Gubin et al. 2003). In order to extend our knowledge of biotic survival on geological time scales within permafrost, we aimed at the detection of viable protozoa. Protozoa represent a considerable part of soil biota and possess a wide spectrum of adaptation abilities.

MATERIALS AND METHODS

The late Pleistocene icy-loess complex, i.e., syngenetically frozen aleurites with the traces of soil (so-called cryopedolite), ice veins and buried soils on Kolyma lowland, has been studied. Cryopedolite contains up to 1% organic matter and thin filamentous roots of grasses. Buried soils belong to Histosols and Gleysols. We also investigated samples from burrows of fossil gopher. The studied material consisted of mixture of aleurites with litter components: seeds, residues of leaves and grasses, wool of animals, etc. (Fig. 1). Radiocarbon age of burrows was determined as 28 to 32 thousand years (Gubin et al. 2001).

In order to find viable protozoa we used a method of soil enrichment cultivation on a poor nutrient non-selective medium (sterile water and Lozina-Lozinskii medium). The cultivation was carried out during one month using two different temperature/light conditions: 20°C with daylight in one case and 5°C without light in the other. Protozoa were observed directly in the soil enrichment cultures and in suspension. Methods of light and fluorescent microscopy were used for their morphological description and identification. Images of protists were obtained by means of a digital camera.

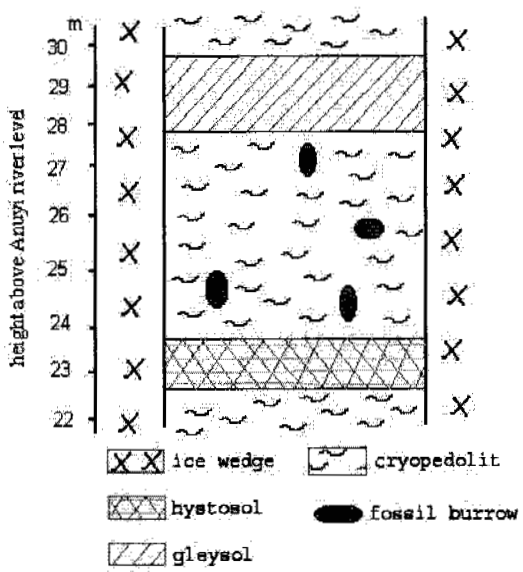

Figure 1. Geological section of icy-loess complex.

RESULTS AND DISCUSSION

Organic matter from burrows contain a large number of elements from late-Pleistocene tundra-steppe ecosystems. This great volume of paleoecological information survived due to the frozen state of deposits from the time of their formation. Viable protozoa were found among other biological objects. Protists were isolated from all samples but one (collected from the top layer of buried Histosol) and were identified as representatives of three large taxones: heterotrophic flagellates, naked amoebae (Fig. 2), and small ciliates. Heterotrophic flagellates were dominant species of recovered communities. It was observed that a succession cycle (species composition change) of permafrost protests community takes approximately 20 days. A tendency appeared to exist for an increase in the number of viable protists and their species diversity in soil samples with high content of fossil plant . It was also observed that protozoa abundance and biodiversity was higher inside fossil burrows than in buried soils. This fact is likely to be due to initial relative abundance of protozoan fauna as well as to more favorable conditions of its cryopre-

servation within the burrows. Following long-term survival in permafrost, the organisms become subjected to the stresses of thawing and exposure to oxygen as the samples are melted in the lab environment at relatively high temperatures. Because the strategies and techniques for the recovery of protozoa from frozen environments are just beginning to be developed, the standard methods for isolation of the protists in pure cultures have not yet delivered positive results. Most protozoa have not been cultured, and many of them died or altered their activity.

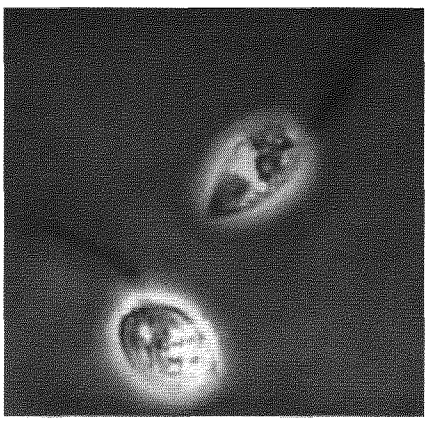

a.

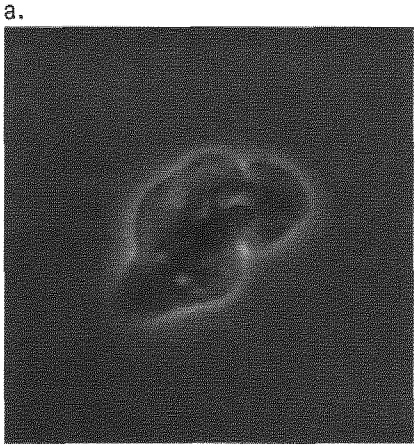

b.

Figure 2. Viable protozoa from permafrost: a – flagellates; b – amoebae.

CONCLUSION

For the first time, viable protozoa were discovered in frozen layers and their ability to survive within permafrost during dozens of thousands of years was shown. This suggests that in such a unique physicochemical environment as permafrost, these organisms keep unknown possibilities of physiological and biochemical adaptation incomparably longer than in any other known habitat. Their ability to survive on geological time scales within the broad limits of natural systems forces us to redefine the spatial and temporal limits of the terrestrial biosphere. On the basis of the obtained results, it is possible to propose the existence of viable protozoa not only in buried soils, but also in deposits rich in organic matter. Permafrost thawing due to natural or anthropogenic processes exposes ancient life to modern ecosystems and the ancient protozoa renew their physiological activity and participate in formation of modern biodiversity on the northern territories.

ACKNOWLEDGEMENTS

This work was supported by the Russian Foundation of Basic Research (grants 01-05-65043 and 01-04-49087).

REFERENCES

Gilichinsky, D. Shatilovich A., Vishnivetskaya T.., Spirina E., Faizutdinova R., Rivkina E., Gubin S., Erokhina L., Vorobyova E., Soina V. 2001. How long the life might be preserved? In (Giovannelli F., ed.), Proceedings of the International Workshop «The Bridge between the Big Bang and Biology», Consiglio Nazionale delle Ricerche of Italy: 362-369.

Gilichinsky, D. 2002. Permafrost as a microbial habitat // Encyclopedia of Environmental Microbiology, 2002, 932-956.

Gubin, S.V. et al. 2001. Composition of seeds from fossil gopher burrows in the ice-loess deposits of Zelyony mys asenvironmental indicator. Earth Cryosphere 5(2): 76-82 (in Russian).

Gubin, S.V. et al. 2003. The Possible Contribution of Late Pleistocene Biota to Biodiversity in Present Permafrost Zone // Journal of General Biology 2003, v.64 _1: 45-50 (in Russian).

Porsild, A. et al. 1967. Grown seeds of Pleistocene age // Science, v. 158: 113-114.

Stress-strain conditions and the stability of arctic coastal slopes: assessments using seismic surveys

A.G. Skvortsov and D.S. Drozdov

Earth Cryosphere Institute, SB RAS, Russia

Within the framework of ACD and INTAS-2332 projects, seismic research for the purpose of slope stability analysis was carried out at the Bolvanskii key-site in the mouth of Pechora river (Barents sea). A special seismic technique for investigations at various types of slopes, mainly at sliding slopes, was used. It is based on theoretical relationships and experimental correlation between seismic characteristics of the ground and stress-strain conditions of the soil. A very important feature of this technique is the possibility to monitor and predict preliminary changes of slope stability before discontinuity occurs. The term of forecast ranges from some months to several years. The uncertainty in spatial allocation of expected discontinuities does not exceed a few meters (Gorjainov et al. 1987, Skvortsov 1989).

In previous years, the most adequate results were obtained for different sites in temperate climatic zones. The geological conditions of some examined sites can be considered to be a model of Arctic frozen slopes in summer time. The most interesting data was gained while investigating a coastal slope where limestone underlies a layer of clay. The processing of seismic data showed that the stable (for the date of research) part of the slope is going to be involved in the sliding process. Mainly the seismic data on the upper horizon of the clay layer were used to trace the position of the predicted crack (Alyoshin et al. 2002). Within a few years, new landslides took place according to the forecast.

The results of this research and numerous other experiments have shown that reliable information on the stress-strain conditions in slopes can be received on the basis of data on compressional wave velocity and its anisotropy in the uppermost part of a geological section (1 m thickness). From the methodical point of view this conclusion is extremely important for assessments of arctic coastal slope stability, since it shows that the stress-strain conditions of the coastal massif can be examined using the distribution of seismic characteristics in the active layer (seasonally-thawed layer).

This conclusion was taken into account while carrying out in-situ field investigations at the northern slope of cape Bolvanskii where sea water undermines the third marine terrace (September, 2002). Three main types of geological cross-sections are observed along the coast: 1) mainly peaty in top part; 2) mainly sandy; 3) mainly loamy. The loams contain many boulders. All soils are permanently frozen. Generally, they have relatively low ice-content (no more than 0.2). The increased ice-content (up to 0.3–0.4) is a characteristic of the upper 2-3 m of loamy cross-sections. The peat bogs are the most ice-rich sites which include thick ice wedges (Malkova et al. 2002).

At the seismic key-site sand prevails in cross-section. The height of the coastal slope is about 25 m and the slope is rather abrupt (30°). However, any modern active processes, including landslides, crumbling and slumping, are not observed now while at nearby sites all these processes occur. Dense bushes, as seen on Figure 1, prove the modern stability of the investigated slope.

The seismic operations were executed at four 50-60 m long profiles located perpendicularly to the coastal line. The profiles cross a sandy surface stretched along a ledge (bright grey band on Fig. 1) and enter a peatbog (grey color). Information about the distribution of compressional and shear wave velocity, both in the active layer and in the top part of permanently frozen ground, was obtained. The preliminarily processing of these results showed obviously that the wave velocity greatly depends not only on the stress-strain distribution and further expected disturbances, but also on the variability of lithology, moisture, density, ice and organic content, etc.

Other geophysical parameters depend less on these factors: the lateral anisotropy of wave velocity, Poisson's ratio and its anisotropy. To obtain them the wave velocity measurements were carried out in lateral rectangular directions (Skvortsov and Drozdov 2002).

The analysis of seismic characteristics of the seasonally thawed ground allows to define two weakened zones in the active layer. Most obvious, these zones are seen at the isoline maps of compressional wave velocity anisotropy and of Poisson's ratio anisotropy (Fig. 2).

The first more sharply expressed weakened zone is situated in the north-western part of the site. It is subparallel to the ledge of terrace and is indicated as a zone with minimum values of wave velocity anisotropy and Poisson's ratio anisotropy.

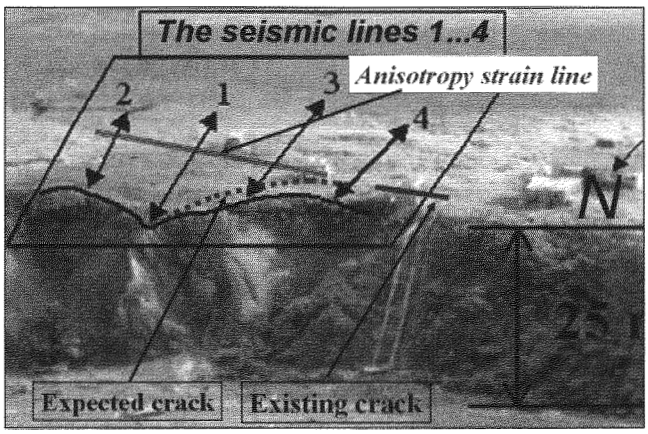

Figure 1. Seismic profiles at the Bolvanskii key-site and the results of the obtained data processing.

An attempt has been undertaken to detect the presence of landscape attributes of this zone at the surface. For this purpose micro-landscape mapping was carried out during which an existing crack in the ground surface has been found 20 m to the west of the key-site in the first zone. That proves the first zone to be a weakened one. The first weakened zone indicates a line along which the separation of relatively small frozen blocks can move ("expected crack" at Figures 1 and 2).

The second weakened zone shows less contrast on isoline maps than the first zone. It is situated at 20-40 meters from the slope, crosses the first zone and ledge and probably is an attribute of larger frozen blocks which can be separated in a comparatively longer future. ("anisotropic ground strain" on Fig. 1 and 2).

The submitted results illustrate a possibility of surface seismic techniques to investigate slope processes, to assess the stability of frozen ground and make spatio – temporal forecasts of coastal retreat at particular sites in the Arctic.

ACKNOWLEDGEMENTS

This project is supported by INTAS (grant 01-2332) and SB RAS grant.

The authors express gratitude for cooperation and assistance with carrying out in-situ field investigations to: Norwegian Geotechnical Institute (manager of Oil Pollution project O. Nerland) and Circumpolar Active Layer Monitoring project (CALM, manager on European Russian sites G.V. Malkova).

REFERENCES

Alyoshin, A.S., Drozdov, D.S., Dubovskoj, V.B. and Skvortsov, A.G. 2002. New opportunities of geophysical monitoring of processes slope. Sergeev reading, issue 4. – Moscow; GEOS: 485-488 (in Russian).

Gorjainov N.N., Bogolyubov, N.M., Varlamov, A.N., Matveev, V.S., Nikitin, V.N. and Skvortsov, A.G. 1987. Studying of landslides by geophysical methods – Moscow; Nedra: 157 (in Russian).

Malkova (Ananjeva), G.V., Drozdov, D.S., Kanevskiy, M.Z. and Korostelev, Yu.V. 2002. The coastal researchs in the area of geocryological station "Cape Bolvanskiy ", the estuary of Pechora river. 3-rd Workshop on Arctic Coastal Dynamics. – Oslo, IPA: 27-28.

Skvortsov, A.G. 1989. Monitoring of sliding slopes stability by use of seismic methods. Investig. of hydro-geol. and engineer.-geol. objects by geophysical and isotope methods. – Moscow: VSEGINGEO: 32-43 (in Russian).

Skvortsov, A.G. and Drozdov, D.S. 2002. The assessment of stress-strain conditions of coastal slope by use of seismoreconnaissance (seismic-service). 3-rd Workshop on Arctic Coastal Dynamics. – Oslo, IPA: 48.

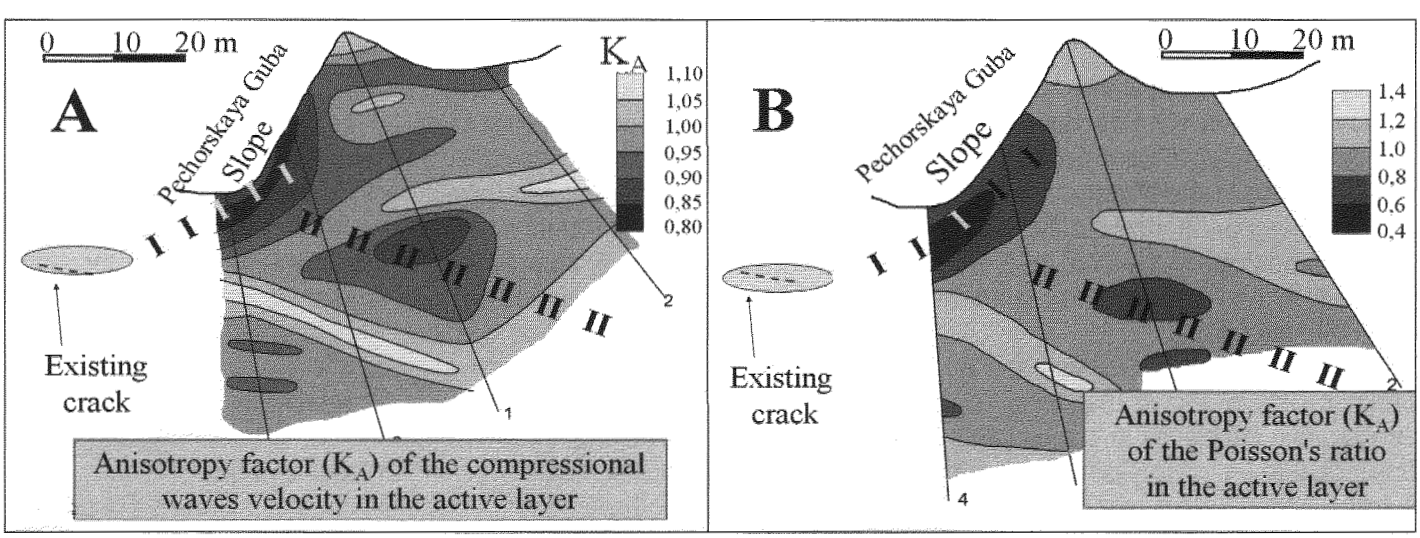

Figure 2. The isoline maps of seismic parameters in the seasonally-thawed layer showing two weakened zones in ground massif.
I I I – first weakened zone – zone of expected crack; II II II – second weakened zone – zone of anisotropic ground strain and long term discontinuity evolution.

Contraction crack dynamics in polygonal patterned ground and soil inflation in the Dry Valleys, Antarctica

R.S. Sletten and B. Hallet

Quaternary Research Center, University of Washington Seattle, WA, USA

INTRODUCTION

The Dry Valleys of Antarctica are believed to be part of an ancient landscape that has remained undisturbed for millions of years. Our recent work suggests, however, that the soils and land surfaces are relatively active due in part to seasonal opening and partial closure of contraction cracks that delineate the pervasive polygonal patterned ground in this region (Péwé 1959). Unlike the relatively moist Arctic where contraction cracks tend to fill with surface meltwater and form ice wedges, contraction cracks in the Dry Valleys tend to fill with sand and form sand wedges. The growth of sand wedges disturbs the ground surface and the development of soil profile. We examined the rates of sand wedge growth by continuing a four decade-long survey of displacements across contraction cracks, and by installing modern instrumentation.

RESULTS AND DISCUSSION

To measure the growth of sand wedges, Robert F. Black and Thomas Berg (Berg and Black 1966; Black 1973) installed over 500 pairs of 60cm vertical rods that span contraction cracks in the Dry Valleys during the early to mid 1960s. They measured crack divergence manually using precision rulers. We revisited and measured Black's 13 sites on three occasions since 1995; we found the rods to be generally in good condition and that crack divergence continued at rates (0.4-2 mm a^{-1}) similar to those measured by Black (Figure 1).

To provide a better understanding and a basis for modeling the annual dynamics of contraction cracks, we installed linear transducers connected to data loggers at 3 sites in Beacon Valley and Victoria Valley in 1998, and have continuously monitored displacements across cracks since that time. In addition, we monitor the micrometerology, soil temperature, soil thermal properties, and other physical parameters.

The total annual crack opening due to thermal contraction of polygons ranges from 0.5 cm to nearly 2 cm at other sites, and lags air temperature (Figure 2). The contraction cracks open during cooling as the ice-rich ground contracts and expands as the ground warms. The net annual crack divergence reflects the amount of fines that fall into the cracks thereby preventing full closure. The 40-year average rate of divergence across the cracks based on Black's rods is 0.6 mm a^{-1} for the lower Beacon Valley site, whereas our continuous measurements for the past 4 years show a net crack divergence rate of 1.4 mm a^{-1}. If the more rapid recent growth is significant, it presumably reflects an increase in either the amplitude of the thermal forcing or the sediment input into cracks.

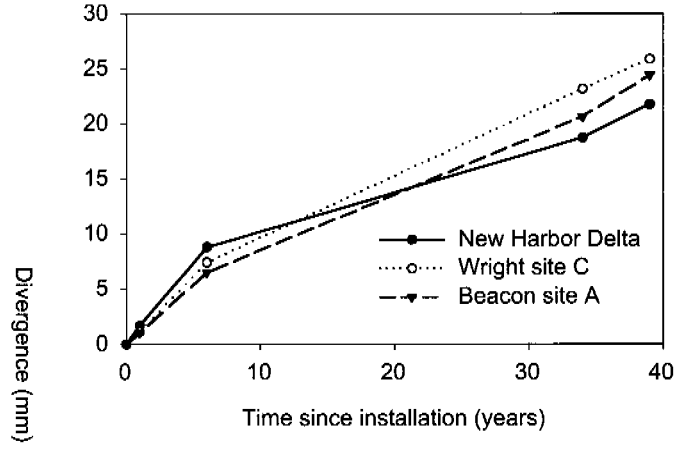

Figure 1. Average contraction crack growth as determined by rods installed at 3 Black's sites and measured manually. Initial and 7-year measurements were made by Black. Our measurements were made 35 and 39 years after the rods were pounded into the permafrost.

The long-term growth of sand wedges has caused an effective inflation of the soils and, in lower Beacon Valley, raised the ground surface by at least 8 m, the depth of our deepest borehole there. Preferential injection of fine-grained material to depth, as the larger rocks do not fit into the open contraction cracks, ultimately results in the accumulation of rocks and boulders on the surface. The sand wedges grow to encompass the entire surface and appear to repeatedly sweep across the surface, thereby building up a complex of sand wedges overlain by rocks.

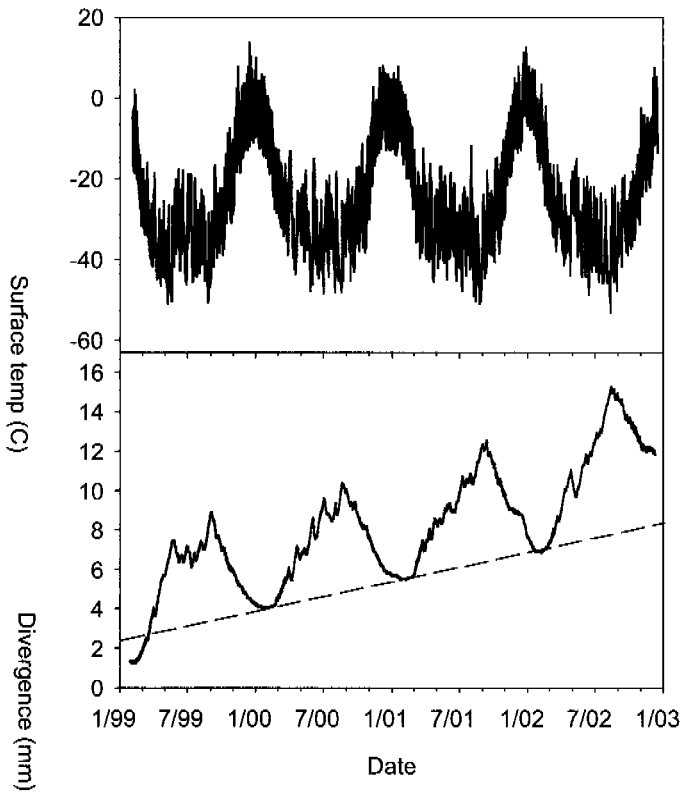

Figure 2. Continuous record of surface temperature and divergence across contraction cracks at the periphery of sand-wedge polygons using linear transducers mounted on rods spanning the cracks. The dashed line indicates a net annual divergence rate of 1.4 mm a^{-1}.

This injection of fine-grained sediment into contraction cracks and the resulting inflation of the surface in the Dry Valleys appear analogous to the formation of the ice complexes in Siberia due to the recurrent build-up of ice in contraction cracks (Schirrmeister et al. 2002). In both cases, soil inflation has been occurring for long periods. Our preliminary cosmogenic isotope data indicate that sand from sand wedges at 5 m depth has been buried for several million years, suggesting long-term burial and inflation and, possibly, shielding by the Taylor Glacier during a former excursion into Beacon Valley.

CONCLUSIONS

Current rates of sand-wedge growth (~1 mm a^{-1}) and polygon sizes (~10 m) suggest that the near-surface layer of polygons would be completely resurfaced, in a period of tens of thousands of years, while rocks remain at the surface indefinitely as sand-wedges grow beneath them. The continuous injection of fines into contraction cracks has created a sand wedge complex that has inflated the surface over 8m. Our findings suggest that landscape surfaces with well-developed polygonal patterned ground in the Dry Valleys are relatively active, which contrasts with suggestions that these surfaces have been undisturbed for millions of years.

REFERENCES

Berg, T. E. and Black, R. F. 1966. Preliminary measurements of growth of nonsorted polygons, Victoria Land, Antarctica. Antarctic Soils and Soil Forming Processes, Antarctic Research Series, Vol. 8. J. C. F. Tedrow. American Geophysical Union, Washington, DC: 61-108.

Black, R. F. 1973. Growth of patterned ground in Victoria Land, Antarctica. Permafrost: The North American Contribution to the 2nd International Conference, Yakutsk, Siberia, National Academy of Sciences: 193-203.

Schirrmeister, L., Siegert, C. Kuznetsova, T. Kuzmina, S. Andreev, A. Kienast, F. Meyer, H. and Bobrov, A. 2002. Paleoenvironmental and paleoclimatic records from permafrost deposits in the Arctic region of Northern Siberia. Quaternary International 89(1): 97-118.

Péwé, T. L. 1959. Sand-wedge polygons (Tesselations) in the McMurdo Sound region, Antarctica-a progress report. American Journal of Science 257: 545-552.

The Global Terrestrial Network for Permafrost (GTN-P) – status and preliminary results of the thermal monitoring component

*S.L. Smith, M.M. Burgess, *V. Romanovsky and **J. Brown*

Geological Survey of Canada, Natural Resources Canada
**University of Alaska, Fairbanks, USA*
***International Permafrost Association, Woods Hole, Mass., USA*

INTRODUCTION

The Global Terrestrial Network for Permafrost (GTN-P) was established in 1999 to provide long-term field observations of active layer and permafrost thermal state that are required to determine the present permafrost conditions and to detect changes in permafrost stability. The data supplied by this network will enhance our ability to predict the consequences of permafrost degradation and to develop adaptation measures to respond to these changes. The GTN-P contributes to the World Meteorological Organization's Global Climate Observing System and Global Terrestrial Observing System. An overview of the GTN-P is given by Burgess et al. (2000).

The active layer component of the GTN-P, the Circumpolar Active Layer Monitoring (CALM) program, has been in operation over the last decade. Organizational efforts of the GTN-P are therefore focused on the recently established borehole thermal monitoring component. This paper describes the present status of the thermal monitoring component and presents preliminary results from North America.

STATUS OF THE THERMAL MONITORING PROGRAM

The permafrost thermal monitoring program consists of a globally comprehensive network of boreholes for ground temperature measurements. Many of these boreholes were drilled for research, geotechnical, or resource exploration purposes in the last two decades and have been maintained as thermal monitoring sites. About 370 boreholes from 16 countries have been identified as candidate sites for inclusion in the GTN-P thermal monitoring system (Fig. 1). The majority of these boreholes are between 10 and 125 meters deep and are in the northern hemisphere. A few sites are located in Antarctica and Argentina. Regional networks include those of the Geological Survey of Canada (GSC) in the Mackenzie region, the University of Alaska's Alaskan transect, the United States Geological Survey's deep boreholes in Northern Alaska and the European Community's Permafrost and Climate in Europe (PACE) program of boreholes largely in alpine permafrost. A web site (http://sts.gsc.nrcan.gc.ca/gtnp) developed by the GSC, provides an inventory of candidate boreholes, and background material on the GTN-P.

Metadata compilation for the candidate boreholes has been conducted over the last two years. Metadata from about 60% of the boreholes has been compiled and posted on the GTN-P website. Over the next year, metadata compilation will be completed and site selection will take place. Compilation of summary historical data for network sites will also occur over the next year.

PRELIMINARY RESULTS

A general discussion of preliminary results from GTN-P sites can be found in Romanovsky et al. (2002). This paper focuses on results from across the North American Arctic.

Analysis of permafrost temperatures, taken in the upper 20 m, from a network of boreholes in Alaska maintained by the University of Alaska Fairbanks indicates that permafrost has warmed over the last 20 to 50 years. At the recently reactivated monitoring site at Barrow, temperatures at a depth of 15 m increased 1°C between 1950 and 2001. Increases of permafrost temperature ranging from 0.6 to 1.5°C between 1983 and 2000 at a depth of 20 m have been observed at sites along the Trans-Alaska pipeline route.

The GSC has operated a network of thermal monitoring sites in the Mackenzie region, Northwest Territories since 1985. At 15 m depth at a site in the central Mackenzie valley an increase of about 0.03°C per year was observed between 1986 and 2001 in permafrost with temperatures of approximately –1°C. In the northern Mackenzie region, in colder permafrost (-7°C), temperatures at a depth of 28 m show an increase of about 0.1°C per year in the 1990s.

At the GSC's high Arctic observatory at Alert, a warming of the permafrost occurred in the late 1990s of 0.15°C per year at a depth of 15 m. Some cooling of permafrost was observed from the late 1980s to the early 1990s in the eastern Canadian Arctic at a depth of 5 m at Environment Canada's borehole at Iqaluit. This cooling however, was following by warming in the late 1990s. This trend is similar to that observed in Northern Quebec, where cooling of about 0.1°C

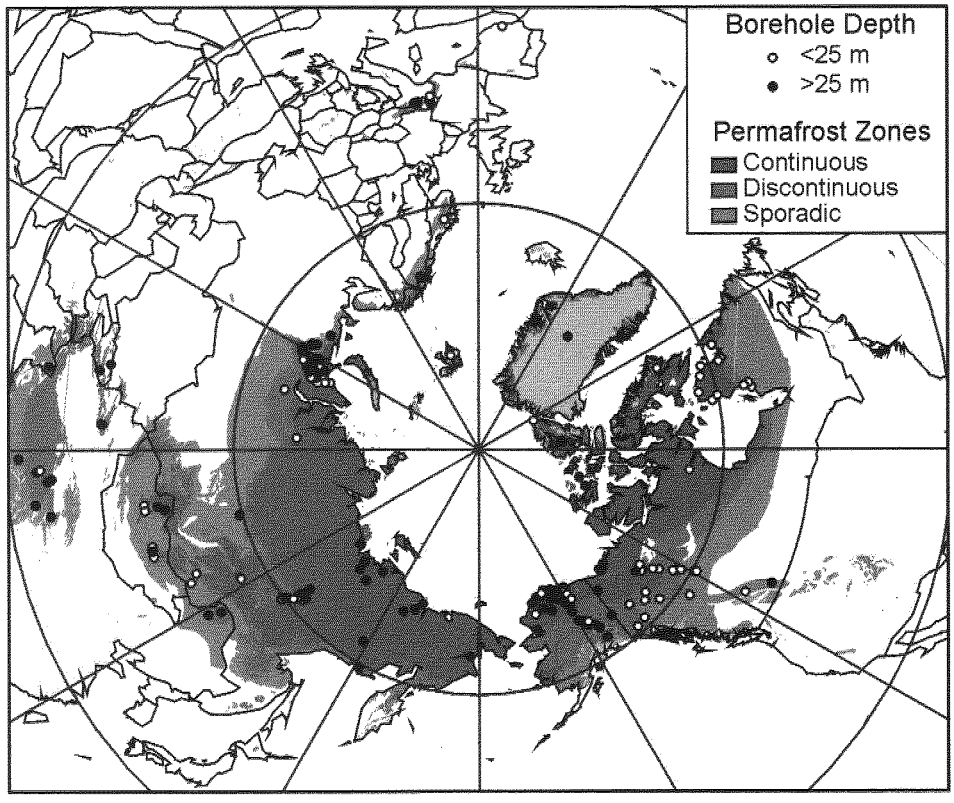

Figure 1. Permafrost distribution in the Northern Hemisphere and location of candidate boreholes for permafrost thermal monitor-

per year was observed from the mid 1980s to the mid 1990s at a depth of 10 m in boreholes maintained by Université Laval (Allard et al. 1995). This was followed by a warming trend starting in 1996 (Brown et al. 2000).

SUMMARY

The GTN-P has been established to provide long-term observations of permafrost conditions that will enable us to address a number of climate change issues in the permafrost regions. The data collected by this network will provide information to scientists studying the cryosphere, and also to stakeholders, politicians and other decision makers. This information is critical in order to evaluate the impacts of climate change and to develop adaptation measures to reduce these impacts.

Results from North America indicate that warming of permafrost occurred in the latter half of the 20th century in Alaska and the western Canadian Arctic. Warming of permafrost is also observed in the Canadian eastern and high Arctic and mainly occurred in the late 1990s. These trends in permafrost temperature are consistent with the increases in air temperature observed since the 1970s in the North American Arctic.

REFERENCES

Allard, M., Wang, B. and Pilon, J.A. 1995. Recent cooling along the southern shore of Hudson Strait Quebec, Canada, documented from permafrost temperature measurements, Arctic and Alpine Research 27: 157-166.

Brown, J., Hinkel, K.M. and Nelson, F.E. 2000. The Circumpolar Active Layer (CALM) program: research designs and initial results. Polar Geography 24: 163-258.

Burgess, M.M., Smith, S.L., Brown, J., Romanovsky, V. and Hinkel, K. 2000. Global Terrestrial Network for Permafrost (GTNet-P): permafrost monitoring contributing to global climate observations. Geological Survey of Canada, Current Research 2000-E14.

Romanovsky, V. Burgess, M., Smith, S., Yoshikawa, K., and Brown, J. 2002. Permafrost temperature records: indicators of climate change. EOS, Transactions of the American Geophysical Union 83 (50): 589.

Satellite radar interferometry for detecting and quantifying mountain permafrost creep

*T. Strozzi, U. Wegmüller, * A. Kääb and R. Frauenfelder*

Gamma Remote Sensing, Muri BE, Switzerland

**Glaciology and Geomorphodynamics Group, Department of Geography, University of Zurich, Switzerland*

Remote-sensing techniques represent suitable tools for integral hazard mapping and monitoring in high mountains, regions that are typically difficult to access. Spaceborne Synthetic Aperture Radar (SAR) systems offer the possibility, through differential SAR interferometry (DInSAR), to map surface displacements at mm to cm resolution in the line-of-sight direction (Bamler and Hartl 1998). Recent studies on rock glacier deformation suggest that the technique is promising also for relatively small objects in mountainous terrain (Rignot et al. 2002; Kenyi and Kaufmann, 2003).

We analyzed a series of SAR images between 1993 and 1999 from the European Remote Sensing Satellites ERS-1 and ERS-2 (C-Band, 5.3 GHz, 5.6 cm wavelength) and the Japanese Earth Resources Satellite JERS-1 (L-Band, 1.3 GHz, 23.5 cm wavelength). From the large number of the possible interferometric pairs we considered interferograms with short baselines acquired during the snow-free period between early summer and mid-fall. The topographic reference was determined from two winter ERS-1/2 Tandem pairs and subtracted from the interferograms. The differential interferograms were orthorectified to the Swiss cartographic system with a pixel spacing of 10 m by use of a Digital Elevation Model (DEM) derived from aerial photogrammetry (Kääb 2002). For the most convincing interferograms the analysis continued with phase unwrapping permitting the quantitative measurement of the displacement field of identified rock glaciers. Phase unwrapping of interferograms in rugged terrain and for complicated displacement fields is a critical task that was successful only for small areas. The line-of-sight displacement was finally transformed in displacement along the slope direction using the DEM.

Results for the Fletschhorn region in the Simplon/Saas valley region, Swiss Alps, were analyzed together with the survey of rock glaciers (Frauenfelder et al. 1998) and displacement maps from digital photogrammetry of repeated airborne imagery (Kääb 2002). Two examples are shown in Figures 1 and 2. For large active rock glaciers such as the Rothorn (Figure 1) JERS DInSAR is able to display the entire flow field with the typical velocity distribution of highest speeds in the rock glacier center. Below the Jegi rock glacier (Figure 2) the advantage of DInSAR for detecting small movements becomes apparent. Field classification gave a transition from active over inactive to relict parts. In the ERS differential interferogram surface deformation can clearly be seen. It is however an open issue whether deformations observed from DInSAR for the inactive and relict parts of the rock glaciers are due to 'active' ice deformation or due to 'passive' pushing by the upper active rock glaciers. Also for the debris slope to the south of the Jegihorn, which was not classified as rock glacier, it is not clear if the small movements are due to deformation of frozen debris.

For rock glacier research and assessment of related slope instability hazards, our study suggests the following prior fields of application for DInSAR: (i) DInSAR is especially useful for area-wide detection of rock glacier activity and order of surface velocity; (ii) the detection of very small movements by DInSAR is feasible and will provide new insights into the behavior of inactive or even relict rock glaciers; (iii) such results reveal valuable parameters for further detailed investigations at selected sites by photogrammetric or field-based methods; (iv) DInSAR is able to provide rock glacier speed for a large number of such landforms and might promote the understanding of the coupling between landscape, climate and rock glacier activity.

The major limiting factors of DInSAR in mountainous terrain arise from temporal decorrelation and the SAR image geometry, both leading to incomplete spatial coverage. Over rock glaciers, where dense vegetation is no longer present, high coherence is regularly observed during the snow-free period. Also, large and incoherent displacements of adjacent scatters may cause decorrelation. Coherence maps may therefore support the detection of displacements. The very rugged topography of alpine regions causes incomplete coverage due to layover and shadowing. Furthermore, there is a privileged slope direction, namely that facing away from the SAR look vector, where the technique is better suited for the monitoring of displacements.

Strozzi, T. et al.: Satellite radar interferometry, permafrost creep...

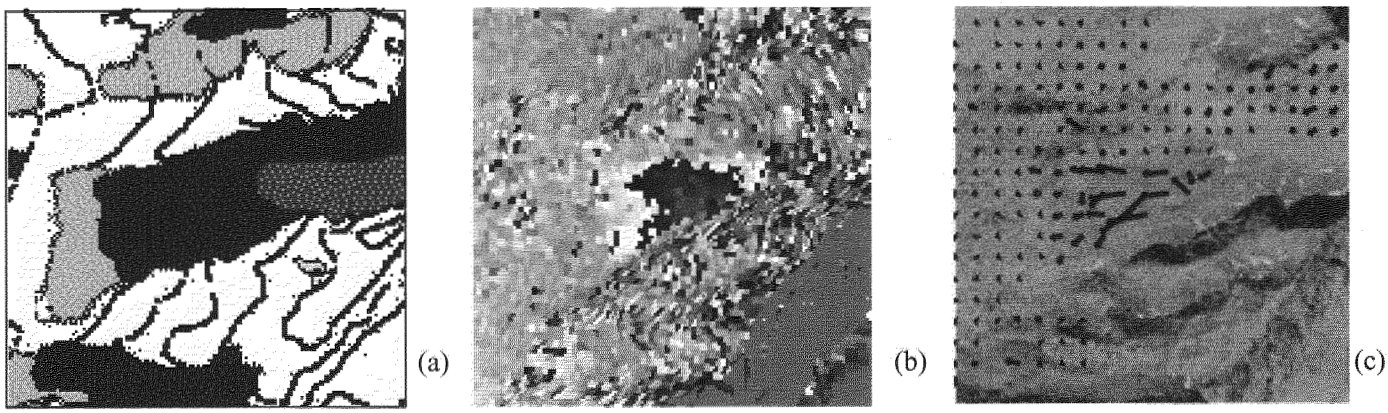

Figure. 1. (a) Rock glacier inventory around the Inner Rothorn from in-situ natural indicators, such as geomorphological interpretation, source water temperatures, existence of perennial snow patches, percentage and composition of vegetation cover, and locations of burrows of hibernating marmots (Frauenfelder et al. 1998). Rock glaciers are classified as active (black), inactive (dark gray), and relict (light gray). Image width is 1.5 km. (b) JERS differential interferogram of 1996.06.21_1996.09.17 with 88 days acquisition time interval and -65 m perpendicular baseline. (c) Surface displacement velocity derived from satellite radar interferometry by assuming creep in the direction of maximum slope (maximum 60 cm/year). Background image is an aerial imagery.

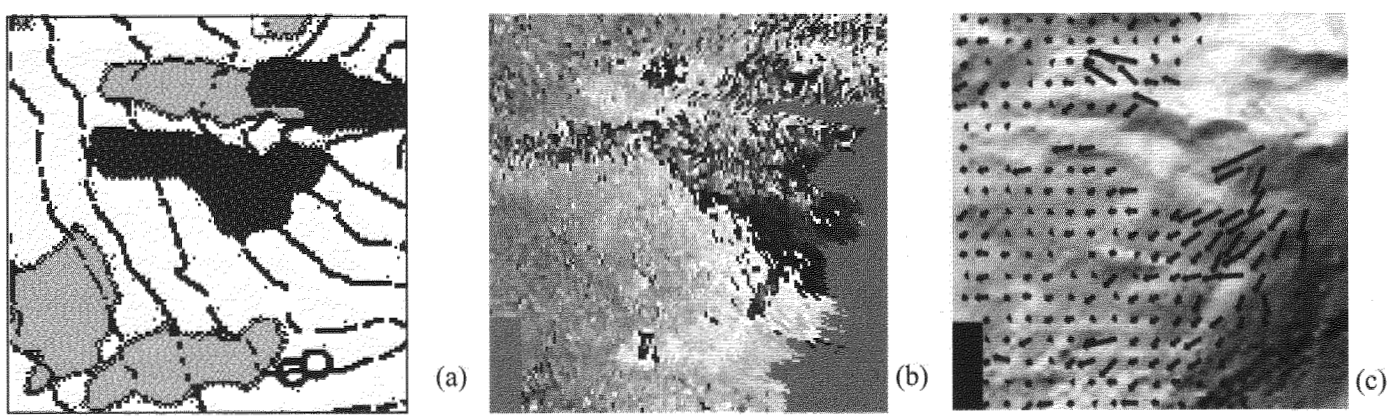

Figure. 2. (a) Rock glacier inventory around the Jegihorn from in-situ natural indicators. Legend as in Figure 1. Image width is 1.5 km. (b) ERS differential interferogram of 1999.07.16_1999.10.29 with 105 days acquisition time interval and 5 m perpendicular baseline. (c) Surface displacement velocity derived from satellite radar interferometry by assuming creep in the direction of maximum slope (maximum 10 cm/year). Background image is a DEM shaded relief.

ACKNOWLEDGEMENTS

ERS SAR data courtesy AO3-178, © ESA, processing GAMMA. JERS SAR data courtesy J-2RI-001, © NASDA, processing GAMMA. Aerial imagery taken by Swisstopo and the Swiss Federal Office of Cadastral Surveys.

REFERENCES

Bamler, R., and Hartl, P. 1998. Synthetic aperture radar interferometry. Inverse Problems, 14, R1-R54.

Frauenfelder, R., Allgöwer, B., Haeberli, W., and Hoelzle, M. 1998. Permafrost investigations with GIS - a case study in the Fletschhorn area, Wallis, Swiss Alps. Proc. 7th Intern. Conf. Permafrost, Yellowknife, Canada, Collection Nordicana. 57: 291-295.

Kääb 2002. Monitoring high-mountain terrain deformation from digital aerial imagery and ASTER data. ISPRS Journal of Photogrammetry and remote sensing. 57(1-2): 39-52.

Kenyi, L.W. and Kaufmann, V. 2003. Measuring rock glacier surface deformation using SAR interferometry. 8th Int. Conference on Permafrost, Zurich.

Rignot, E., Hallet, B., and Fountain, A. 2002. Rock glacier surface motion in Beacon Valley, Antarctica, from synthetic-aperture radar interferometry. Geophysical Research Letters, 10.1029/2001 GL013494, 29 June 2002.

An attempt to obtain paleoclimatic information from the present permafrost distribution in Siberia

*T. Sueyoshi and *Y. Hamano*

Laboratory of Hydraulics, Hydrology and Glaciology, ETH Zürich

**Department of Earth and Planetary Sciences, Univ. of Tokyo, Japan*

INTRODUCTION

The thickness of permafrost changes in response to climate change. Changes in surface temperature are transmitted through thermal conduction, thus, the response time becomes long for thick permafrost.

Siberia is a region in which some of the thickest permafrost is found, sometimes more than several hundreds meters deep. Such thicknesses of permafrost should reflect the surface temperature history of the past. In spite of its importance for the understanding of long-term climatic variability, the terrestrial paleotemperature history of the continental inland is still open to argument because most "high-resolution" paleoclimatic studies are based on marine sediments or ice cores. In this study, we attempt to obtain paleoclimatic information from the present permafrost distribution in Siberia by means of numerical methods.

METHOD

We used a one-dimensional numerical model of permafrost in which the ground temperature profile is calculated in response to the variations of surface temperature change from LGM (Last Glacial Maximum, 21ka) to the present.

We worked with the one-dimensional thermal conduction problem, we took latent heat production into account but neglected soil water diffusion. Latent heat was considered by using the enthalpy method, which generally gives good results when calculating frozen/unfrozen boundary positions. The thickness of the permafrost is obtained by tracking the position of this frozen front.

Three study sites for numerical experiments, Tiksi (71°N), Yakutsk (62°N) and Irkutsk (52°N) were selected in this study to investigate the paleoclimatic variability in east Siberia.

These sites are located along the Lena River and have similar geological conditions. The locations, permafrost thickness and the mean annual air temperature (MAAT) of the sites are shown in table 1.

Table 1.

Site name	Lat.	Log	thickness	MAAT
Tiksi	71.35°N	128.55°E	650m	-14°C
Yakutsk	62.05°N	129.45°E	500m~	-8.8°C
Irkutsk	52.16°N	104.21°E	25m~	~0.0°C

These permafrost thicknesses are based on Nekrasov and Devyatkin (1974) and Harada (2001).

Boundary Conditions:
Conditions considered in this simulation are summarized as follows:

1) Geothermal heatflow value (30 ~ 60 mW/m²)
2) Local climate condition:
   annual mean temperature, seasonal variability
3) Temperature drop during LGM (*DT*)
   a) "normal" paleocliamte scenario:
      same as the ice-core reconstruction (*DT* ~10°C)
   b) "extreme" paleocliamte scenario:
      colder climate (*DT* ~15°C, 20°C, 25°C)
4) Effect of ice sheet existence (only in the Tiksi case)

Top and bottom boundary conditions are necessary to run the model. Geothermal heatflow was given for the bottom boundary conditions and surface temperature was used for the top.

We assumed the value of the heatflow to be constant for the calculated period since the study area is on a stable shield continent. We found this assumption to be reasonable.

Surface ground temperature is substituted by air temperature. Present climatic data was used when considering the climatic conditions of the study sites. Paleoclimate history was obtained from reconstructed temperature-deviation data from Greenland ice cores (GRIP, 1993) in order to represent the outline of climate change. The general pattern of climate change was assumed to be basically the same for all sites, while the temperature drop between Holocene and LGM was treated as a parameter. The blanketing effect of the ice sheet during the glacial period was also considered.

The effect of the ice sheet on ground temperature was also taken into account in the model. The ground temperature un-

der the ice sheet was calculated from the air temperature at the surface of ice sheet and assuming a temperature gradient through the ice sheet. The air temperature on the top of the ice sheet was calculated using the adiabatic gradient of the atmosphere (0.6°C/100m) and assuming the thermal conductivity of ice to be 2.2 [W/k/m]. The thickness of the ice sheet was also treated as a parameter but this condition was considered only for the north-Siberian case. The reconstruction of ice sheet distribution was based on CLIMAP (1976) and Pertier (1994).

RESULTS AND DISCUSSIONS

A series of numerical experiments was performed under the various boundary conditions mentioned in the previous section. We obtained the temporal variations of permafrost thickness for the last 30k years (from LGM to the present).

In this paper, we show the results from the parameter study of the temperature drop during LGM. The target of these experiments was to examine the sensitivity of permafrost thickness to the climate during LGM and to argue to what extent the present thickness of the permafrost has been affected by past climate history.

Figure1 shows the temporal variation of the permafrost thickness around Tiksi, from 30ka to the present, using several different values of temperature drop during LGM (*DT*). In this plot the X-axis represent the years before present while the Y-axis represents the thickness of the permafrost. The arrow at the Y-axis shows the present thickness of permafrost at that location. From the figure we can tell that the present permafrost thickness in this region roughly agrees with the "normal" paleoclimate scenario.

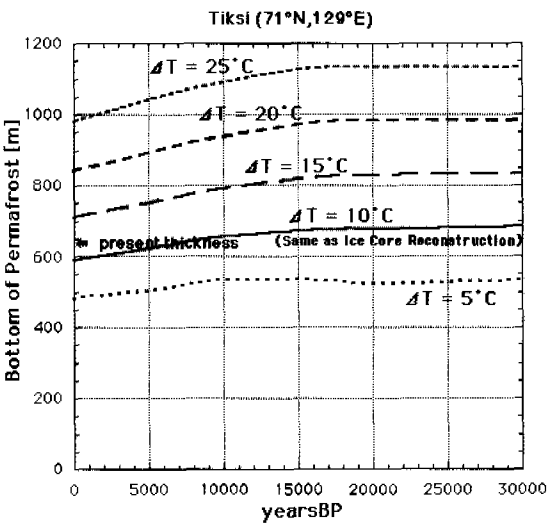

Figure 1. Temporal change of permafrost thickness at Tiksi.

Figure 2 shows the case for Yakutsk in the central part of Siberia.

Comparison with the present thickness suggests that this area could have experienced enhanced cooling during LGM which is different to that obtained from the reconstructed ice core data. If we do not consider this effect the conditions for this region are too mild, the thickness of permafrost should be thinner than it is at present. However, the permafrost thickness around Tiksi can be reproduced by the "normal" paleotemperature scenario, thereby this "extreme" cooling is thought to be characteristic for inland Siberia.

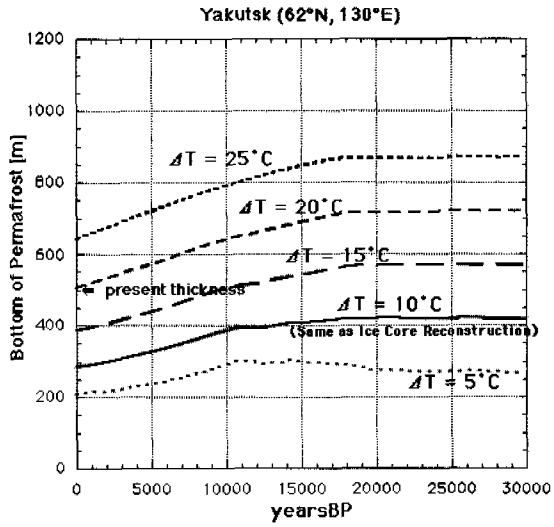

Figure 2. Temporal change of permafrost thickness at Yalutsk.

On the other hand, the distribution of permafrost in the south-marginal area could not be reproduced, even under "extreme" conditions. Since such thin permafrost responds quickly to surface climate change it should not be regarded as a relic of a past cold climate.

CONCLUSIONS

The permafrost thickness in the central (Yakutsk) and northern part (Tiksi) of Siberia cannot be explained consistently by the same paleoclimatic boundary conditions. The present permafrost thickness at Tiksi generally agrees with the value of the calculated thickness, while that at Yakustk requires colder conditions. This suggests that the temperature drop during LGM in the central part of Siberia was larger in the north.

REFERENCES

CLIMAP Project Members. 1976. The Surface of the Ice-Age Earth; Science 191: 1131-1137.

GRIP Members. 1993. Climate instability during the last interglacial period recorded in the GRIP ice core; Nature 364: 203-207.

Harada, K. 2001. Study on detection of permafrost structure., Doctoral Thesis in Hokkaido Univ.

Nekrasov, I.A. and Devyatkin, V.N. 1974. Morphology of permafrost - underlain areas of the Yana River basin and adjacent regions, Nauka Press, Novosibirsk (in Russian).

Pertier, W.R. 1994. Ice Age Paleotopography, Science 265: 195-201.

Isotopic composition of the massive ground ice of the Bovanenkovo geotectonic structure (Yamal Peninsula, Russia)

A. M. Tarasov, I. D. Streletskaya and N. G. Ukraintseva**

"GROUND" CO. LTD, Moscow, Russia

**Moscow State University, Moscow, Russia*

INTRODUCTION

A study of massive ice deposits was carried out within the framework of an engineering geo-cryological survey in the area of the Bovanenkovo gas-condensate field. Ten large ice beds, situated at a distance of 5 to 60 km from each other, were drilled from top to bottom (Kurfurst et al. 1993, Tarasov 1990, 1993). The ice and host deposits were sampled, with an increment of 10-15 cm, to determine their chemical and isotopic composition.

RESULTS AND DISCUSSION

Morphological features of the massive ground ice

It has been established that the large ice deposits stretch for 200-800 m and that their thickness varies from 5 to more than 30 m. They form beds with a horizontal area that can exceed the vertical by up to a dozen times. Deposits of this type are widely spread in sections of the Upper Pleistocene marine plains and lie mainly in the contact zone between the saline marine clays (D_s=0.3-1.5%), and the slightly salinized (D_s=0.02-0.1%) marine-lacustrine sandy-silt sediments that lie at depths from 1-2 m to more than 20-30 m (Dubikov 2002). Massive ground ice bodies are more than 15 m in thickness. In all studied deposits the bottom of the ice beds is flat, sub-horizontal and lies beneath the modern sea level (Fig. 1). The contact is consistent with substrate strike. The ice top is rolling due to diagenetic processes (melting, thermodenudation and thermoerosion). Locally, the bedding is concordant with the covering clay sediments (coarse ice bars). However in some cases, when the ice is covered by solifluction-landslide deposits with cryogenic structure, the contact is sharply discordant, gently sloping and the ice top is melted. Ice has been noted with local inclusion of salty water, cryopegs, voids, cracks and under-ice gases (Streletskaya and Leibman 2002).

Chemical and isotopic composition of the massive ground ice

The chemical composition of massive ground ice was analyzed at study sites 1-88 (central part of the gas field area). An exposure of massive ground ice was found in a west slope relic hill in 1987. The bottom of the massive ground ice body is horizontal and situated at 1-3 m above sea level. The massive ground ice body is flat-layered, ultra fresh, and abundant in mineral inclusions. The salt content in pure ice (melted) is very low and varies from 10 to 80 mg/dm^3. The salt content in massive ground ice with mineral inclusions increases up to 160-180 mg/dm^3. Water-soluble HCO_3^- is the dominant anion and Na^+, Ca^{++} dominated among cations.

The oxygene-18 isotope content ($\delta^{18}O$) in massive ice melts is shown in table 1. The background measurements of $\delta^{18}O$ are the same in all ice bodies even though they can be 30-50 km removed from each other. This proves that the all massive ground ice in this region has a common origin. Meteoric water was the source for the formation of this massive ground ice, marine water did not take part in this process.

Table 1. Oxygene-18 isotope ($\delta^{18}O$) in massive ground ice.

Study Site/ Point	H a.s.l., m	Depth of the ice, m	$\delta^{18}O$ Mean	$\delta^{18}O$ Min	$\delta^{18}O$ Max	n*
1-88/2	6.8	1.2-8.7	-18.4	-17.7	-19.7	13
1-88/3	10.3	1.8-11.0	-18.0	-17,1	-19.0	16
1-88/4	12.1	3.7-14.6	-18.4	-18.0	-19.0	20
1-88/7	14.4	6.4-15.4	-18.5	-18.1	-19.0	7
2-88/1	21.9	6.1-12.0	-18.8	-18.0	-19.7	10
2-88/62	6.4	1.7-7.5	-18.9	-18.6	-19.3	8
2-89/22	15.6	3.3-12.8	-18.9	-17.3	-20.2	18
3-89/1	11.4	3.6-5.3	-19.7	-19.0	-20.6	4
1-90/3	7.0	1.0-15.3	-19.0	-17.7	-22.5	16
2-90/32	16.4	1.8-10.6	-18.8	-17.6	-20.6	11
2-90/1	17.0	1.2-13.2	-18.9	-18.1	-19.3	27
3-90/2	20.2	1.9-7.0	-20.6	-16.8	-22.6	12

*n – number of analyzed samples from indicated boreholes

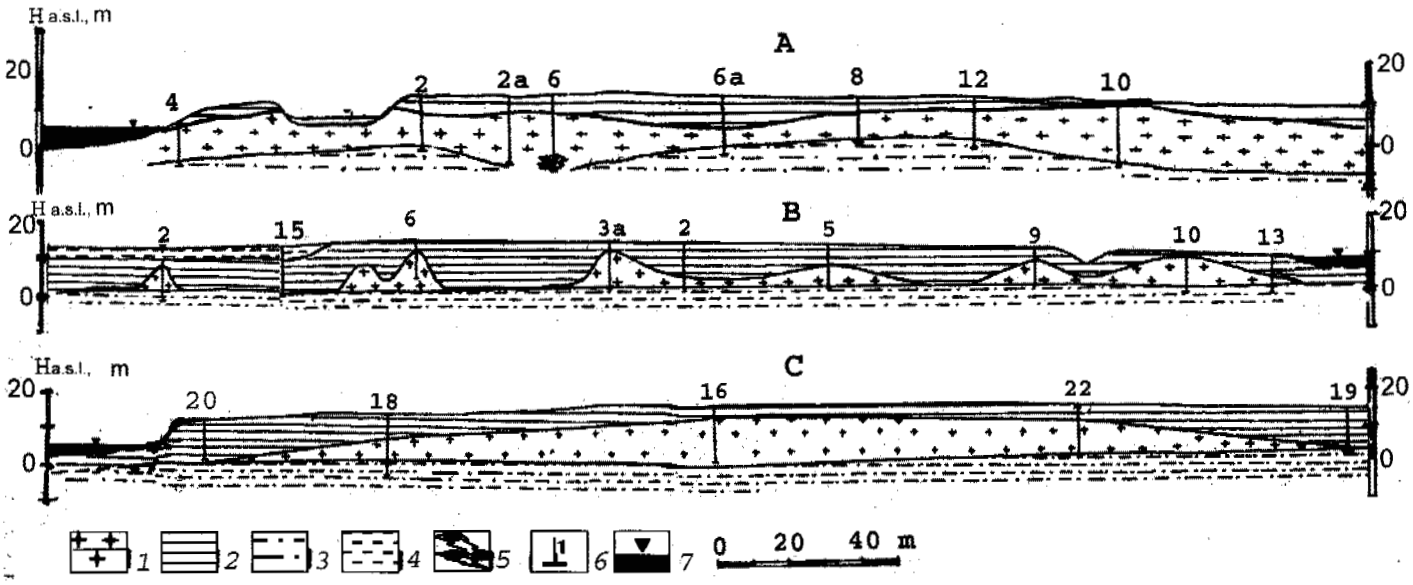

Figure 1. Profiles of geological and ground ice conditions.
A – study sites 1-90, profile 2; **B** – study sites 2-89, profile 1; **C** – study sites 2-89, profile 2. *1* – massive ice; *2* – clay, loam; *3* – silty sand; 4 – loamy sand; 5 – hollows in massive ice; 6 – borehole location and number; 7 – lakes.

CONCLUSIONS

Massive ground ice is widespread in the Bovanenkovo geotectonic structure (Yamal Peninsula).

In all studied deposits the bottom of the ice beds is flat, sub-horizontal and lie beneath the modern sea level. The ice top is rolling due to diagenetic processes (melting, thermodenudation and thermoerosion).

The concentration of oxygen-18 and heavy hydrogen isotopes in the studied massive ice bodies reveals evidence of their genetic relation. The obtained results suggest that the ice had been formed below ground during the freezing of a water-bearing sandy horizon fed by atmospheric water precipitation.

ACKNOWLEDGEMENTS

This work was supported by INTAS (grant 01 - 2329) and RFBR project _ 02-05-64263.

REFERENCES

Dubikov, G.I. 2002. Composition and cryogenic structure of permafrost in West Siberia. Moscow: GEOS Publisher (in Russian).

Kurfurst, P.J., Melnikov, E.S., Tarasov, A.M. & Chervova, E.I. 1993. Co-operative Russian-Canadian engineering Geology Investigations of Permafrost on the Yamal Peninsula, Western Siberia. In Permafrost. Proc. of the 6th intern. Conf. on permafrost, Beijing, 5-9 July 1993, v.1: 356-361.

Streletskaya, I.D. & Leibman, M.O. 2002. Cryogeochemical interrelation of massive ground ice, cryopegs, and enclosing deposits of Central Yamal. Kriosfera Zemli 6(3): 15-24 (in Russian).

Tarasov, A.M. 1990. Experience of applying oxygen-isotope method to study ground ice at engineering-geological survey. In E.S. Melnikov (ed.), Methods of engineering-geological survey: 118-133. Moscow: VSEGINGEO (in Russian).

Tarasov, A.M. 1993. The isotopic composition of the massive ice of the Bovanenkovo gas-condensate field. In 'The Isotope in the Hydrosphere' Abstr. of the 4th intern. Symp., Pjatigorsk, 18-21 May 1993. Moscow: RAS (in Russian).

Mapping of permafrost and the periglacial environments, Cordón del Plata, Argentina

D. Trombotto

Affiliation Unidad de Geocriología, Instituto Argentino de Nivología, Glaciología y Ciencias Ambientales (IANIGLA) - CONICET, Mendoza - Argentina

Regional mapping of periglacial areas and permafrost in the Cordillera Frontal, Mendoza, Argentina is unprecedented in South America – only certain particular sites or valleys have been mapped. A regional approach was made, with a focus on analyzing the surrounding limited periglacial and glaciological environments, and preparation of an inventory of glacial forms. The resulting map is intented to form the basis of the geocryological map of South America.

The study area, Cordón del Plata, lies in the province of Mendoza, in the Argentine Central Andes between 32°40′ and 33°24′S and 69°45′ and 69°12′W. Geologically the mountain ranges belong to the Cordillera Frontal. The study area ranges from a height of 2000 m a.s.l. to a maximum height of 6310 m, which corresponds to the peak of the Cerro El Plata. The minimum height was considered on the basis of geographical and geological limits of the area and its independence as a topographical unit. Three outstanding ranges may be distinguished however: "La Jaula" in the west, the "Cordón del Plata" in the central and northern part on the eastern border, and "Santa Clara" in the southwest. The area comprises ca. 2830 km^2.

The MAAT of the meteorological stations of Aguaditas at a height of 2225 m (1972–1983) and Vallecitos (1976–1985) at 2500 m at its eastern flank are 7.7°C and 6°C, respectively. The meteorological station Balcón I at 3560 m on the tongue of a rock glacier at Morenas Coloradas indicates a MAAT of 1.6°C and precipitation of between 500 mm (April 2001 – April 2002), and 630 mm (1991–1993).

The vegetation ranges from shrubs to the Andean tundra above 3600 m. Above this zone and on the rock glaciers vegetation is extremely scarce.

The map has been initiated by scanning and digitizing topographic maps (scale 1:100.000) using the AutoCad program Map (R) Release 3. The contour intervals are set at 100 m. For georeferencing of the obtained data and for the elaboration of a data base, the program Idrisi for Windows version 2.010 was applied. As a first step the existing data were superposed and updated with landsat images. In a second step the periglacial and glacial data by Corte and Espizúa (1980) obtained from aerial photographs (scale 1: 50.000) between March and May 1963 were translated to the basic map, and corrections applied. For the periglacial environment studied for mapping the "facies" (in sense of Corte) of structural debris and inactive facies were taken from the inventory of glaciers. In the case of the "thermokarst facies", it was considered whether or not they had a direct relation with debris-covered glaciers. They were included if they belonged to the environment of rock glaciers ("structural debris facies") or to debris-covered glaciers. The 1981 inventory shows that the debris-covered glaciers preceded the areas or "facies" with thermokarst, although these are the exceptions. In those cases where moraine terminals were identified, the "roots" of rock glacier are found. This allows for the separation of the two differnet environments.

Permafrost was detected by direct methods, using temperature profiles in surface drillings (up to a depth of 5 m) or indirect methods such as geophysical profiling or geomorphological interpretations by applying aerial photographs and satellite images. Field visits helped to verify the interpreted results. For active rock glaciers with southwesterly orientation the permafrost table was found at 3770 m at a depth of 3 m (Balcón II).

The periglacial forms and types of permafrost were mapped according to (Trombotto 2000).

The geomorphological processes according to the altitudinal levels may be grouped as follows:

1) from 2000 to 3500 m, with periglacial fossil forms, dynamics of seasonal freezing and semi-arid shaping of slopes, eventual relict permafrost;
2) semi-arid periglacial level from 3500 to 4500 m, with different types of permafrost, varied patterned ground, solifluction forms, glaciers, rock glaciers and mainly detrital slopes; and
3) snow-covered level, with snow patches, approximately continuous permafrost, glaciers, rock glaciers and cryoplanation surfaces (Garleff 1977, Trombotto 1991).

With the help of the Andean geomorphologists, involved and by interpretating the cryogenic or cryotic characteristics and cryogenic processes or restrictive factors, the permafrost so far detected by various authors can be classified and the preliminary typology elaborated (Trombotto 2000). Six or possibly seven major groups can be proposed according to their expected ice content, their water potential, and their genesis (Tab. 1).

The glacier zones have decreased, supposedly in relation to global change. As a result of the retreat of glaciers and the thinning of level 3 glacial and snow-covered zone, the periglacial level has enlarged, and the cryogenic surfaces occupy new higher zones with moraines and glacial sediments. However, the variations in the altitudinal periglacial limit (semi-arid or semi-humid) still have to be defined more precisely. A reliable catalogue of catastrophic slope events remains to be compiled. These events have not been described for Level 2 and are important for Level 1 where human settlements are located. While the area above 4500 m is likely to have permafrost occurrence everywhere, the area between 3500 and 4500 m obviously has fewer possibilities of permafrost and is limited preferentially to the rock glacier valleys.

REFERENCES

Corte, A. and Espizúa, L. 1981. Inventario de Glaciares de la Cuenca del Río Mendoza. IANIGLA–CONICET. Imprenta Farras, Mendoza.

Garleff, K.; 1977. Höhenstufen der argentinischen Anden in Cuyo, Patagonien und Feuerland. Göttinger Geographische Abhandungen, Heft 68.

Trombotto, D. 1991. Untersuchungen zum periglazialen Formenschatz und zu periglazialen Sedimenten in der 'Lagunita del Plata', Mendoza, Argentinien. Heidelberger Geographische Arbeiten, Heft 90.

Trombotto, D. 2000. Survey of cryogenic processes, periglacial forms and permafrost conditions in South America. Revista do Instituto Geológico 21: 33-55.

Table 1. Permafrost types and environments (*see Trombotto 2000 for source references).

Ice Content	Hydric Potential	Permafrost Types	Features	Restrictors andAndes Processes	Tropical Andes	Dry Andes Desert Andes (17°30'–31°S)	Dry Andes Central Andes (31°–35°S)	Southern (35°–55°30'S)
+⇑	+⇑	1) Creeping	Active rock glaciers, Cold Discontinuous	Creeping, Energy balance, Precipitation	Active rock glaciers	Chile: Rock glaciers >175 mm/y	Argentina: active rock glaciers as indicators in the sense of Barsch	Argentina: active rock glaciers
+⇑	+⇑	2) Approxi-mate – Continuous	Cold	Topography Energy balance, Exposition	Chimborazo (6275 m), Ecuador: inf. limit: 5250-5300 m a.s.l.	NW Argentina: MAAT –1/–2°C, <300 mm/y, R. denudation slopes (*) 30°S: summit cryoplanation surfaces(5000m)	Argentina: MAAT–2/–4°C, and 500 900 mm/y, cryoplanation surfaces	Argentina: 1) 44°S: 2060 m 980 - 1100 m
-	2) 51°30'S:	3) Dry	Cold Pore ice	Low precipitation, Exposition		South American Dry Diagonal (*)	Argentina: cryoplanation surfaces, detritic slopes	
-⇓	-⇓	4) Sporadic	Isolated patches	Warming, Energ balance		Rock glaciers	Rock glaciers	
	-⇓	5) Insular	Island Isolated patches	Warming, Energy Balance	Chimborazo, Ecuador < 5000 m		Argentina: "cryobasin of cryosediments	
		6) Degraded	Warm	Warming, Degradation, Meltwater		Bolivia, rock glaciers, constant ice temperature at –1.6°C, low resistivities <20000Ω m	Argentina: rock glaciers: thermokarsts, low resistivities in "cryobasin of cryosediments"	
		7) Relict	Relict ice	Thermic problems, Dry condi-		"Mesas" in the Puna de Atacama and Altiplano, Bolivia and Chile	Argentina: rock glaciers	

+/– indicates increase or decrease in ice content or water potential.

New map of seasonal ground freezing and thawing in Mongolia (scale1:1500000)

D. Tumurbaatar, Ya. Jambaljav, D. Undarmaa, M. Enkhtuul and A. Batbold

Institute of Geography, MAS, Ulaanbaatar, Mongolia

INTRODUCTION

In 1971 D. Tumurbaatar compiled a map of seasonal freezing and thawing of the ground around Ulaanbaatar city at a scale of 1:25,000. In 1975 S. J. Zabolotnik created a map of seasonal freezing and thawing of ground at a scale of 1:2,500,000. In 2001 D. Tumurbaatar compiled a new map of seasonal freezing and thawing of ground in Mongolia at a scale of 1:1500000. It is based on 40 years of research on permafrost in Mongolia (Devyatkin 1976, Jambaljav 2001, Kudryavtsev 1978, Tumurbaatar 1973, 1993). For this map we have used data of the physical and thermophysical properties of 2000 samples and climate data from 234 meteorological stations located in the territory of Mongolia.

SEASONAL FREEZING AND THAWING

The following methods were used: (1) field survey and laboratory test analyses, (2) statistical analyses of field surveys and laboratory tests, (3) B.A.Kudryavtsev's equation for the determination of freezing and thawing depths, (4) The winsurfur software drawing the contours of mean annual surface temperature (MAST) and mean annual surface amplitudes of temperature (MASAT).

The map of Quartenary geological deposits of Mongolia, compiled by E.V.Devyatkin, was taken as a base map.

Depths of seasonal freezing and thawing of ground in Mongolia vary separately as follows:

1) Depth of seasonal thawing for sandy loam and loam filling debris of glacial deposits is 2.1 - 3.7 meters, where MAST is 0 - -2°C, MASAT is 21 - 25°C and ground moisture is 14 - 29.1%. Where the MAST is 0 - 4°C, the depth of seasonal freezing and thawing is 1.7 meter in the south and 3.8 meter in the north of the country.

2) Depth of seasonal thawing in alluvial deposits is 2.4 meter for loam filling debris and 4.7 meter for sand filling debris, where MAST is -2 – 0°C, MASAT is 21 - 31°C and ground moisture is 6 - 22%. Where MAST is 0 - 4°C, MASAT is 21 - 25°C and ground moisture is 6 - 22%, the depth of seasonal freezing and thawing is 1.9 meter for sand filling debris in the south and 4.9 meter in the north. Where MAST is 4 - 7°C, depth of seasonal freezing is 1.7 meter in the central parts and 3.5 meter in the south of the country.

3) Depth of seasonal thawing in lacustrine deposits is 2.1 meter in the north, 3.6 meter in the central parts for clay and loam, where MAST is 0 - -2°C, MASAT is 23 - 25°C and the ground moisture is 14 - 29.1%. Where MAST is 0 - 4°C, MASAT is 21 - 31°C and ground moisture is 14 - 29%, the depth of seasonal freezing and thawing is 1.7 meter in the south and 3.7 meter in the north. Where MAST is 4 - 9°C, MASAT is 21 - 25°C, the depth of seasonal freezing is 1.0 meter in the south and 2.8 meter in the central parts of the country.

4) Depth of seasonal thawing in glacial-lacustrine deposits is 2.3 - 3.7 meter for sandy loam and loam, where MAST is 0 - -2°C, MASAT is 21 - 25°C and ground moisture is 14 - 29.1%. Where MAST is 1 - 4°C, the depth of seasonal freezing is 1.9 meter in the south and 3.6 in the north of the country.

5) Depth of seasonal thawing in alluvial-lacustrine deposits is 2.7 - 3.7 meter for sand and sandy loam with debris, where MAST is 0 - -1°C, MASAT is 31°C and ground moisture is 14 - 25%. Where MAST is 0 - 4°C, MASAT is 23 - 27°C, the depth of seasonal freezing and thawing is 1.9 meter in the south and 3.7 meter in the north. Where MAST is 4 - 8°C, MASAT is 21 - 25°C, the depth of seasonal freezing is 1.1 meter in the south and 2.8 meter in the north of the country.

6) Depth of seasonal freezing in proluvial deposits is 2.3 - 3.2 meter for loam and sandy loam with debris, where MAST is 1 - 4°C, MASAT is 21 - 27°C and ground moisture is 7 - 12%. Where MAST is 4 - 9°C, MASAT is 21 - 25°C, the depth of seasonal freezing is 1.3 meter in the south and 2.6 meter in the central parts of the country.

7) Depth of seasonal freezing in proluvial-lacustrine deposits is 2.1 - 3.2 meter for loam and sandy loam with debris, where MAST is 1 - 4°C, MASAT is 21 - 25°C and ground moisture is 7 - 20.5%. Where MAST is 4 - 9°C, the depth of seasonal freezing is 1.2 meter in the south and 2.8 meter in the central parts of the country

8) Depth of seasonal freezing in eluvial deposits is 2.7 - 4.1 meter for sand, where MAST is 1 - 4°C, MASAT is 23 - 31°C and ground moisture is 8%. Where MAST is 4 - 9°C, MASAT is 21 - 25°C, the depth of seasonal freezing is 1.9 - 3.23 meter.

9) Depth of seasonal thawing in volcanic deposits is 4 meter and more for basalt, where MAST is -2 - 0°C, MASAT is 23 - 25°C. Where MAST is 0 - 5°C, the depth of seasonal freezing is less than 4.0 meter.

10) Depth of seasonal freezing and thawing in eluvial deposits is 1.9 - 4.7 meter for debris with loam and sandy loam fill, where MAST is 0 - 4°C, MASAT is 21 - 29°C and ground moisture is 7 - 22%. Where MAST is 4 - 9°C, MASAT is 21 - 23°C, the depth of seasonal freezing is 1.1 meter in the south and 3.5 meter in the central parts and north of the country.

11) Depth of seasonal thawing in eluvial-solifluction deposits is 2.7 - 3.4 meter for loam and sandy loam with debris, where MAST is 0 - -1°C, MASAT is 23 - 25°C and ground moisture is 7 - 22%. Where MAST is 4 - 9°C, MASAT is 21 - 25°C, the depth of seasonal freezing is 2.3 - 3.4 meter.

12) Depth of seasonal thawing in elluvial-deluvial deposits is 3.0 - 4.6 meter for debris with sand fill, where MAST is 0 - -2°C, MASAT is 23 - 25°C and ground moisture is 7 - 22%. Where MAST is 0 - 4°C, MASAT is 21 - 29°C, the depth of seasonal freezing is 1.9 meter in the south and 4.6 meter in the central parts. Where MAST is 4 - 9°C, the depth of seasonal freezing is 1.1 in the south and 4.3 meter in the north of the country.

13) Depth of seasonal thawing in delluvial-solifluction deposits is 3.0 - 4.5 meter for loam and sandy loam with debris, where MAST is 0 - -2°C, MASAT is 23 - 25°C and ground moisture is 7 - 20%. Where MAST is 0 - 4°C, MASAT is 23 - 29°C, the depth of seasonal freezing and thawing is 1.9 meter in the south and 4.4 meter in the north. Where MAST is 4 - 9°C, MASAT is 21 - 25°C, the depth of seasonal freezing is 1.1 meter in the south and 3.4 meter in the central parts.

14) Depth of seasonal thawing in bedrock deposits is more than 4 meter for granites, where MAST is –2 - 0°C. Where MAST is 4 - 9°C, the depth of seasonal freezing is less than 4 meters.

Using this new map, we have divided three regions of seasonal freezing and thawing (Fig. 1).

Region of seasonal thawing:

There is continuous and discontinuous permafrost in this region. The ground thawing begins during the first decade of May and ends in the last decade of October.

Region of seasonal freezing and thawing:

Isolated permafrost is characteristic of this region (2°C). The ground freezing begins in the last decade of October and ends in the last decade of April.

Region of seasonal freezing:

In this region, permafrost does not exist. Ground freezing begins during the first decade of November and ends in the last decade of March.

CONCLUSION

1) On the represented map are shown the MAST, MASAT, superficial deposits and ground freezing and thawing depths.

2) Minimum depth of seasonal thawing is 2.1 meter for clay and maximum depth of seasonal thawing is 4.7 meter for sand. Mean depth of seasonal thawing is 2.2 meter for loam and 3.9 meter for sandy loam.

3) Minimum depth of seasonal freezing is 1.0 meter for clay and maximum depth of seasonal freezing is 4.9 meter for sand. Mean depth of seasonal freezing is 1.5 meter for loam and 4.0 meter for sandy loam.

4) The seasonal thawing of the ground begins in the first decade of May and ends during the first decade of October. The seasonal freezing of the ground begins in the last decade of October and finishes in the last decade of April in the north and central parts of the country. This freezing begins in the first decade of November and ends during the last decade of March in the south of the country.

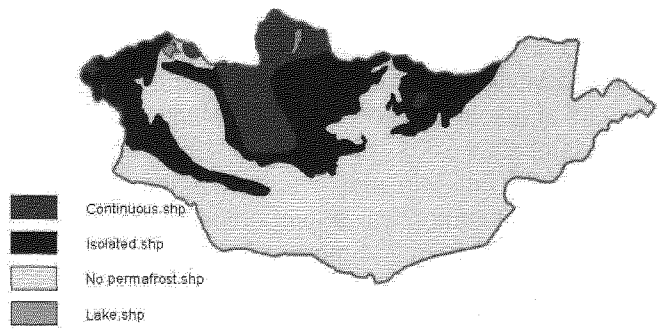

Figure 1. Schematic map of permafrost regions

REFERENCES

Devyatkin, E.V. 1976. Map of Quartenary geological deposits of Mongolia.

Jambaljav, Ya. 2001. Regression equation of maximum and minimum monthly mean ground temperature curves. In proceedings of the International Symposium on mountain and arid land permafrost; 33.

Kudryavtsev, V.A. 1978. General geocryology (In Russian).

Tumurbaatar, D. 1993. Seasonal freezing and thawing grounds of Mongolia. In proceeding of International Conference on permafrost. Bejing, China, Vol.2; 1242-1246.

Tumurbaatar, D. 1973. Seasonal freezing and thawing grounds of Mongolia. (In Mongolian).

Decadal changes in permafrost, land form and land cover near Barrow, Alaska

C .E. Tweedie, R. D Hollister and P. J. Webber

Department of Plant Biology, Michigan State University, East Lansing, USA

INTRODUCTION

A significant challenge in global change science is assessing the impact and feedbacks of climate change and land-use/land-cover change on ecosystem function, namely carbon exchange across the land-atmosphere boundary. In the Arctic, terrestrial carbon balance is regulated by complex spatial and temporal interactions between land cover, climate, land form, hydrologic balance, permafrost, and stochastic events such as fire, herbivory and human disturbance. The importance of arctic regions to global energy balance and biogeochemical and hydrological cycling is well recognized, as is the documented evidence, propensity and sensitivity for these to change (sometimes non-linearly) in response to climate change (Hinzman et al. submitted). The IPCC (2001) forecast Arctic regions as continuing to undergo among the fastest rates of climatic change on Earth over the next century. Clearly, the need for understanding the interaction between permafrost, land form, hydrologic balance, land cover and the response of ecosystem function in Arctic regions to climate change and following surface disturbance has never been greater.

Most investigations of the functional response of Arctic ecosystems to climate change have been derived from manipulative experiments, modelling, and paleoenvironmental investigations with few studies illustrating a thorough and multidisciplinary examination of the interaction between ecosystem properties and processes. Limited by the availability of adequate and long-term datasets, few forecasts of ecosystem function in Arctic regions have been validated by observed changes. In the absence of long-term and integrated multidisciplinary datasets, reoccupation and retrospective analysis of research sites established several decades ago offer the best means by which decadal change in ecosystem function can be assessed or inferred.

This report details careful re-sampling of vegetation plots established at Barrow, Alaska during the Tundra Biome Project of the International Biological Program (IBP 1969-74). Results are discussed in light of other studies in the Barrow region documenting anthropogenic disturbance (Brown et al. 1980 and references therein) and changes in biogeochemical cycling (Oechel et al. 1995, 2000).

METHODS

Plots varied in size from a few square meter plots nested within single land cover units to a 4.3 hectare grid spanning the majority of land cover types in the Barrow region. Following relocation of plot markers between 1999 and 2002, resampling was performed using the original sampling methods. Comparison of seasonal active layer progression, microtopography, vegetation composition and abundance and high resolution land cover maps several decades apart has allowed the direction and magnitude of change in permafrost, land form, hydrologic balance and land cover to be assessed.

RESULTS

Seasonal active layer progression and maximum end of season active layer depths recorded between 2000 and 2002 were on average 2 to 10 cm greater than those recorded across all plots in the early 1970s. Comparison of the range in relative elevation of the ground surface measured at marked grid points between 1973 and 2000 suggest that there has been an increase of up to 10-15cm between polygon trough bases and adjacent rims. At the 4.3 ha landscape level, however, there has been a decrease of 30 cm in the range of relative elevation.

Change in vegetation was greatest in plots established in formerly disturbed or early successional communities situated on alluvial substrates. In undisturbed communities on non-alluvial substrates the greatest change were observed in wet and moist tundra. Dry tundra displayed little change over time. At the landscape scale, wet and moist tundra classes show a reduction in aerial coverage whereas dry tundra classes show an expansion in area. Within the 4.3 ha plot, spatial heterogeneity in land cover increased due to a decrease in patch size and increase in patch number.

DISCUSSION

Differences between measurements made soon after plot establishment and almost three decades later are dramatic. Elevations lack registration relative to points of known height above sea level in initial measurements, which creates difficulty in assessing whether subsidence or soil development (accumulation of organic material) can be attributed to the decrease in the range of relative elevations recorded at the landscape level. Nonetheless, the minimal accumulation of organic matter around marker stakes in the most productive wet tundra land cover classes suggest that the observed change is due to subsidence of polygonized tundra in the gradient studied. The increase in the range of relative elevation between polygon troughs and adjacent rims suggests thermokarsting of ice wedges underlying polygon troughs. Change in vegetation and land cover also supports this hypothesis.

Similar patterns of thermokarst development have been observed in nearby coastal zones where erosion of polygonized tundra is occurring. These elevation changes are potentially significant considering that most of the study area and nearby settlement of Barrow are *ca.* 3 meters above sea level, indicating up to a 10% decrease in elevation relative to sea level and increased susceptibility to storm surges and flooding.

Within the same study area, Oechel et al. (1995) have documented a change from tundra being a net sink for CO_2 to the atmosphere in the early 1970s to being a net source by the early 1990s, implying a positive feedback response to climate change. The increased active layer thickness and change in land cover documented in this study and the well-studied relationship of CO_2 sink activity declining in response to increasing water deficit provides evidence of mechanisms driving patterns documented by Oechel et al. (1995). Although rates of water deficits appear to have increased during the snow-free period in the region over the past few decades (Oechel et al. 1995 2000) and cannot be discounted, we suggest that the above results can be most strongly attributed to a shift in hydrologic balance caused by anthropogenic disturbance and altered land use patterns. These have been dramatic near Barrow since the mid 1940's.

CONCLUSION

This study has illustrated significant changes in ecosystem properties over the last thirty years near Barrow, Alaska and has linked these changes to documented changes in ecosystem function in the region. Ongoing research is investigating the relative importance of climate change, successional change (thaw lake cycle) and anthropogenic disturbance on ecosystem function in the Barrow area. It is proposed that the former IBP Tundra Biome Project study area and the adjacent Barrow Environmental Observatory (BEO) become key sites in the developing Circum-Arctic Environmental Observatories Network (CEON).

REFERENCES

Brown, J., Miller, P.C., Tieszen, L.L. and Bunnell, F.L. (eds). 1980. An Arctic Ecosystem: The Coastal Tundra at Barrow, Alaska. Stroudsburg: Dowden, Hutchinson & Ross Inc.

Hinzman, L. et al. (29 other authors submitted 2003). Evidence and implications of recent climate change in terrestrial regions of the Arctic. Climatic Change.

IPCC. 2001. Climate Change 2001. The Scientific Basis. Contribution of Working Group I to the Third Assessment Report of the Intergovernmental Panel on Climate Change. In Houghton, J.T., Ding, Y., Griggs, D.J., Noguer, M., van der Linden, P.J., Dai, X., Maskell, K. and Johnson, C.A. (eds.). Cambridge: Cambridge University Press.

Oechel, W.C., Hastings, S.J., Vourlitis, G.L., Jenkins, M.A., Riechers G.H. and Grulke, N.E. 1993. Recent change of Arctic tundra ecosystems from a net carbon dioxide sink to a source. Nature 361: 520-523.

Oechel, W.C., Vourlitis, G.L., Hastings, S.J., Zulueta, R.C., Hinzman, L. and Kane, D. 2000. Acclimation of ecosystem CO2 exchange in the Alaskan Arctic in response to climate warming. Nature 406: 978-981.

Contemporary geotechnologies providing safe operation of railway embankments in permafrost conditions

V. Ulitsky, V. Paramonov, S. Kudryavtsev ,K. Shashkin and *M. Lisyuk

St. Petersburg State University of Highways: Moskovsky Pr. 8, Saint Petersburg, 190031, Russia

**Georeconstruction Engineering Co ,Izmaylovsky Pr. 4, Saint Petersburg, 198005, Russia*

Frost heave and thaw related deformation of ground on Russian railways in permafrost conditions and under the influence of deep seasonal frost penetration attract plenty of attention as of the earliest moments of construction and operation of railway subgrades. In order to eradicate actual deformations and stabilise subgrade soils in heave sensitive areas foam polystyrene panels are currently employed (according to the following pattern: effectiveness equals costs plus technological effectiveness plus durability). This method of embankment reconstruction is currently construed to be of prime efficacy in potentially severe conditions. Design of such protective measures requires assessment both of thermophysical characteristics and of stressed-strained ground conditions during freeze-thaw process.

To solve problems of the above-designated type we developed a numerical modelling methodology of such problems incorporated into *FEM models* software created by geotechnical engineers of St. Petersburg (Ulitsky 2000). It allows solution of freeze-thaw problems by means of a thermal conductivity equation with consideration for phase transformations in below zero temperatures range for unsteady heat conditions in 3-D ground medium. In frozen rock phased water (or liquid solution) content varies within a whole range of negative temperatures. This variation occurs under the principle of the dynamic equilibrium state first described by N.A. Tsytovich (Tsytovich 1979). In accordance to this principle the amount of unfrozen water for a certain type of non-saline ground is established based on sub-zero temperature values. As was proved through experiments, a humidity increase in a ground sample considerably higher than the humidity of top plasticity border in frozen state leads to unfrozen water content increase on account of infinitesimal water films found on ice crystals formed during freezing.

Our *FEM-models* software features a function of liquid water content in the ground to assess latent heat of phased transitions being absorbed or released by ground depending on ground water phase fluctuations in below-zero temperatures. Migratory flow directed towards the freeze front at varying distance between the latter and the ground water level (GWL) is established based on experimental data processing. Ground water level location and the average trend thereof in wintertime are assumed based on reference hydrometric materials specific for the given area (GWL – maximum for a monitoring period; trend – minimum for same period).

The stress-strain state is assessed based on temperature fields allowing seasonally dependent definition of deformations and forces in subgrade structures and facilitating the anticipation of procedures targeted at the elimination of heave related adversary effects on the superficial elements of railway tracks. Currently it is possible to establish ground freeze-thaw development as well as to define deformation values of heave related uplift and thaw related settlement of any structures encountered within the ground bulk.

We performed numerical modelling of freeze-heave-thaw sequence on railway embankments of different heights by generalised cross-section profiles established over a period of long-term operation of railways in permafrost soils of Russian Transbaikalia and the Far East.

For the studied Transbaikalia section of the Russian railways (station *Mogocha*, average annual subgrade temperature being in the order of 0-1.0°) foam polystyrene insulation allowed considerable temperature decrease on top of the embankment in winter time, however, with no guaranteed heave elimination. Embankment calculations for different polystyrene application techniques showed that the most effective application was that of 0.12 m and 0.18 m on the top section of subgrade and the bank respectively.

Underneath the insulation panels in the embankment body freezing temperature changed from -2.9 °C to -6.9°C (Fig. 1), thus remaining within the heave temperature range. In warmer periods the applied insulation precludes thaw on top of subgrade thus ruling out embankment deformation in spring-summer time and positively conditioning stressed-strained subgrade structure (Fig. 2).

To ensure safe operation of embankments in permafrost conditions with heaving ground affected by seasonal frost penetration it would be expedient to render geotechnical forecast by means of numerical modelling. Based on such forecast one could advise effective geotechnologies

to apply in subgrade ground stabilisation both for seasonal frost penetration and thaw.

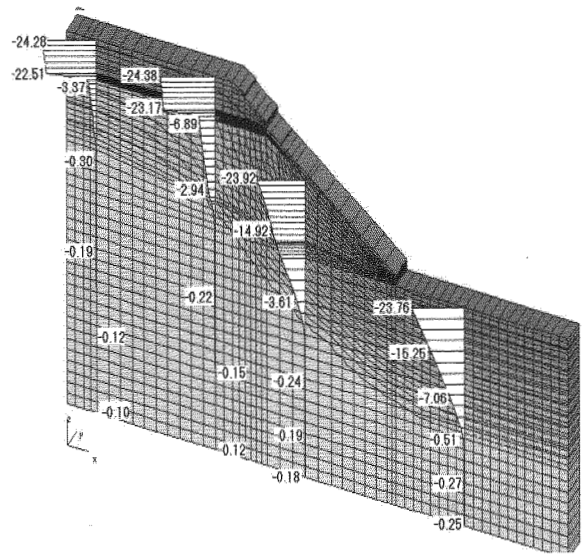

Figure 1. Isolines and epures of temperature distribution in 2 m high embankment with applied insulation in permafrost climate conditions of station Mogocha in Russian Transbaikalia for the month of February: 1- extruded foam polystyrene.

Our calculations and observations demonstrated that application of insulation materials allows reduction and if necessary complete elimination of frost penetration thus fully ruling out the negative influence of heave and thaw related deformations

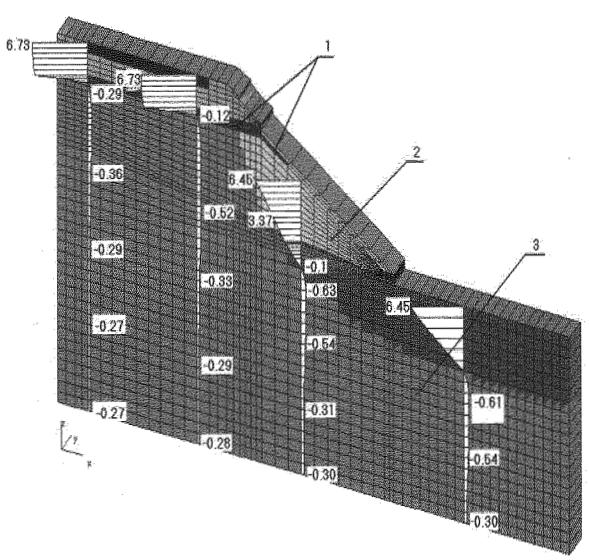

Figure 2. Epures of temperature distribution in 2 m high embankment and subsoil thereof with applied insulation in permafrost climate conditions of station Mogocha in Russian Transbaikalia for the month of September: 1 - extruded foam polystyrene; 2 - thawed ground; 3 – frozen ground.

REFERENCES

Ulitsky, V.M., Shashkin, A.G., Shashkin, K.G. and Paramonov V.N. 2000. FEM models software for modelling and solution of problems in construction and reconstruction by FE method.//Reconstruction of cities and geotechnical engineering/ Saint Petersburg. 2 (in Russian).

Ulitsky, V.M., Paramonov, V.N., Sakharov, I.I., Kudryavtsev, S.A.. and Bakenov H.Z. 2002. Calculation of frozen foundations footings on saline heave sensitive soils with thermal insulation. Proceedings of the international coastal geotechnical engineering in practice. 21-23 May 2002. Atyray, Kazakhstan:145-147.

Tsytovich, N.A. and Chronic, J.A. 1979. Interrelationship of the principal physicomechanical and thermophysical properties of coarse grained frozen soil. Bochum, 1978. - Eng. Geol. 13: 163-167.

A new approach for interpreting active-layer observations in the context of climate change: a West Siberian example

*A. A. Vasiliev, N.G. Moskalenko and *J. Brown*

Earth Cryosphere Institute, Russian Academy of Sciences, Moscow, 119991 Russia
** International Permafrost Association, Woods Hole, MA 02543 USA*

The Circumpolar Active Layer Monitoring (CALM) program provides spatial and temporal observations of seasonal thaw depths at more than 100 sites located in different bioclimatic and landscape conditions of the polar regions (Brown et al. 2000). Many of the sites consist of 100m to 1000 m grids with considerable terrain variation within each grid. Thus the interpretation of these data is complicated because of the diversity of bioclimatic and landscape conditions found within and between monitoring sites. Different landscapes may demonstrate different responses to past, current and future climate changes.

Our analysis, using data from two West Siberian sites, is aimed at developing a new approach to the interpretation of active layer monitoring data. This current report was stimulated in discussions during the CALM synthesis workshop held in November 2002 at the University of Delaware and at recent annual conferences on Earth Cryosphere held in Pushchino, Russia.

There are three CALM grids in West Siberia: Marre-Sale (R3, 69°43' N, 66°52' E); Vaskiny Dachi (R5, 70°17' N, 68°54' E); and Nadym (R1, 65°20' N, 72°55' E). The Marre-Sale and Vaskiny Dachi sites are located in typical tundra; the Nadym site is located in northern taiga. For this report we use data from the Marre-Sale and Nadym sites only, because there are no long-term weather records for the Vaskiny Dachi site. In addition, we use data from previously established auxiliary sites located in the vicinities of CALM grids and having much longer observational records. Active layer depths are considered within the dominant landscapes of the tundra zone (R3) and the taiga zone (R1). For Marre-Sale these include peatland, mire, and five sites within the 1000m CALM grid: dry tundra, ravine, mire, wet tundra, and sand field as described by Melnikov et al. (1983). V. Dubrovin and N. Moskalenko established several of these sites prior to the CALM program (Vasiliev et al. 1998; Moskalenko et al. 2001).

Figure 1 illustrates the dependence of the active layer depth in these landscapes on the sum of positive air temperatures (DDT, degree-days T> 0°C) at the Marre-Sale and Nadym sites. As a first approximation, the linear dependence is used. The slope of the straight line approximation is different for each landscape. We propose that this slope characterizes the active layer response of a particular landscape to climate variation. The maximum inclination is typical of mires (sites 2 and 5); whereas the minimum inclination is typical of flat peatlands (site 1). All other landscapes are characterized by intermediate values of active layer depth versus DDT. As the absolute values of active layer depth are different, it is reasonable to use relative values for comparing responses of different landscapes to climate change with the use of a unified scale.

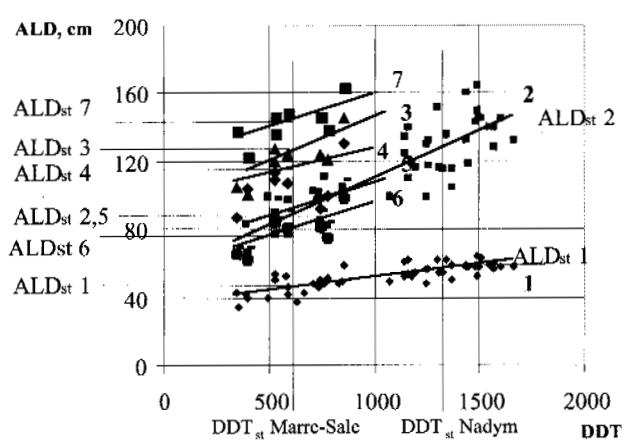

Figure 1. Correlation between the active layer depth (ALD), and DDT for the Marre-Sale and Nadym sites (1- peatland, 2- mire, 3-dry tundra, 4- ravine, 5- mire, 6- wet tundra, 7- sand field. Sites 3- 7 are located on the CALM grid).

The mean value of DDT calculated from long-term air temperature records can be used as a climatic standard for a particular site (DDT_{st}). For the Marre-Sale weather station, DDT_{st} equals 566C degree days (1914-2002) and for the Nadym weather station it reaches 1352C (1965-2002). In Figure 1 the vertical lines for DDT_{st} represent this long-term average. A standard active layer depth (ALD_{st}) for a particular landscape is represented at the in-

tersections of this perpendicular with the corresponding approximation curves. These values are shown along the ordinate axis ($ALD1_{st}$ to $ALD7_{st}$) for Marre-Sale on the left, for Nadym on the right. These are very significant values and can be considered theoretical values of mean active layer depths calculated for particular landscapes. It should be pointed out that these values can be obtained on the basis of relatively short-term observation records (5-10 years). These are the mean active layer depth (ALD_{st} and average active layer depth for observation time (ALD_{av}) in Table 1.

Table 1. Mean active layer depth (ALD_{st}) and average active layer depth (ALD_{av}) for the observation period. Duration of observations enclosed in brackets.

Site	ALD	Landscapes*						
		1	2	3	4	5	6	7
R3	St.	45	87	119	104	86	77	141
	Av.	46.1 (21)	93.3 (15)	121 (8)	105 (8)	87.5 (8)	78.8 (8)	143 (8)
R1	St.	57	130					
	Av.	57.1 (31)	130.8 (31)					

*Landscapes are given in Figure 1 captions

On the basis of these data, we can recalculate all available data on the ALD and DDT into relative units using corresponding standard values, and plot another diagram showing the dependence of the relative active layer depth on the relative sum of positive summer temperatures (Fig. 2). Calculations have been made for contrasting landscapes (mires and peatlands). The resulting curves for the other landscapes should occupy intermediate positions. This diagram makes it possible to assess current tendencies in the active layer development (Fig. 2). If most of the observational data tends to be concentrated in the right part of the diagram, then this indicates climate warming and an increase in the active layer depth. By contrast, the concentration of data in the left part of the diagram attests to a cooling trend with a corresponding decrease in the active layer depth.

Similar calculations have been made for the Nadym monitoring site (northern taiga zone). It is interesting that the resulting diagrams for mires and peatlands have the same shape. The response of these landscapes to the degree of summer warming (DDT values) does not depend on the climatic zone (Melnikov at al., this volume).

The following conclusions can be stated from this analysis:

(1) The suggested method makes it possible to calculate mean maximum depths of the active layer for long-term periods on the basis of relatively short-term observational records.

(2) The response (as manifested by the active layer depth) of seven dominant types of landscapes of the typical tundra zone and two dominant types of landscapes of the northern taiga zone to climate changes is evaluated quantitatively. The active layer depth in mires is very sensitive to climate changes; the least sensitive is typical of peatlands.

(3) The diagram showing the dependence of the active- layer depth on the annual sum of positive air temperatures in relative units can be used for assessing current tendencies of climate variation or changes.

If the values calculated on the basis of actual observational data are generally higher than 1.0, a tendency for climate warming is observed; the reverse is true when calculated values of the relative active layer depth are lower than 1.0. This diagram can also be used for estimating changes in the active layer depth under specific scenarios of climate change.

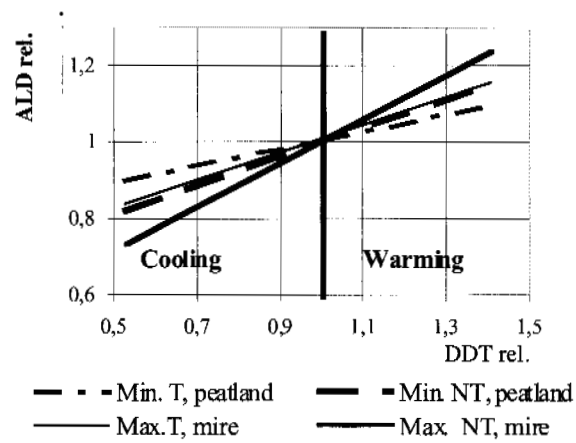

Figure 2. Diagram of the active layer response to warming and cooling in tundra (T) and northern taiga (NT) of West Siberia.

REFERENCES

Brown, J., Hinkel K.M., and Nelson, F.E. 2001. The Circum-polar active layer monitoring (CALM) program: research designs and initial results. Polar Geography 24(3):165-258.

Melnikov, E.S. (ed.) 1983. Landscapes of a permafrost zone in the West Siberian gas province. Novosibirsk: Nauka.

Melnikov, E.S., Leibman, M.O., Moskalenko, N.G., and Vasiliev A.A. 2003. Comparative analysis of active layer monitoring at the CALM spatial variability at European Russian Circumpolar Active Layer (CALM) sites (this volume).

Vasiliev, A.A., Korostelev Yu.V., Moskalenko N.G., and Dubrovin V.A. 1998. Active layer monitoring in West Siberia under the CALM program (database). Earth Cryosphere II(3): 87-90.

Moskalenko, N.G., Korostelev, Yu.V., and Chervova, E.I. 2001. Active layer monitoring in northern taiga of West Siberia. Earth Cryosphere V(1): 71-79.

Influence of seasonal active-layer thickness on broad-scale vegetation dynamics in the permafrost zone

S. Venevsky

Obukhov Institute for Atmospheric Physics, Moscow, Russia and Potsdam Institute for Climate Impact Research, Potsdam, Germany

SPECIFIC BIOLOGICAL AND PHYSICAL PROCESSES IN THE PERMAFROST ZONE

Change of active-layer thickness

Continuous and discontinuous permafrost is the factor most unique for the tundra and taiga environment. Dynamics of the permafrost table, or active-layer thickness depend on the local surface energy balance, reflecting above all air temperature as modified by soil thermophysical properties, vegetation, snow and solar radiation. In particular, the presence of a thick forest floor and organic peat layer significantly lowers soil temperature and active-layer thickness, as low thermal conductivity of the organic matter effectively insulates the mineral soil. A snow cover in autumn limits frost penetration, while in spring it functions as an insulating blanket to delay thawing of soil active-layer. Active-layer thickness and low soil temperature provides a strong feedback on vegetation at high latitudes. Low soil temperatures influence forest productivity by restricting available nutrients due to low decomposition rates and by reducing water uptake by trees due to an increase in root resistance and the viscosity of water. Trees in spring and the first half of summer can also be subject to severe water stress by high evaporation demands when their roots are still frozen and cannot provide the required water uptake.

Forest fires

After climate and soil, fire is the most important natural factor influencing nutrient cycling, chemical and physical processes in soil and forest dynamics (regeneration, growth, species composition and mortality) in a boreal part of the permafrost zone. Depending on flame length and severity of fire, vegetation and topography characteristics, and presence or absence of permafrost, the influence of fire on forest ecosystem is highly variable. Frequent fires can radically change the local biogeochemical status, redistribute and mobilize nutrients and remove the forest floor layer. Therefore, fire in the boreal zone can be considered as a natural rejuvenating force, which rapidly returns climax forests to the initial stage of their development cycle.

SIMULATION OF VEGETATION DYNAMICS IN THE PERAMFROST ZONE

Ecological objective of the study

Annual and seasonal variation of active-layer thickness affects local soil moisture status and, thus regulates the water available to plants and fuel moisture in fire-prone vegetation communities, especially in spring. One should investigate the role played by seasonal and annual variation of active-layer thickness in regional fire regimes, vegetation composition and carbon stocks on a broad scale in the permafrost zone.

Basic vegetation model

The Lund-Potsdam-Jena Dynamic General Vegetation Model (LPJ-DGVM) (Sitch et al. 2003) combines mechanistic treatments of terrestrial vegetation dynamics, carbon and water cycling in a modular framework. Key features include fast feedbacks between photosynthesis and water balance routines and representations of slower ecosystem-level processes including vegetation resource competition, growth, establishment and mortality, soil and litter carbon turnover. To link the fire regime and its effects on vegetation dynamics, a general fire model was incorporated into the LPJ-DGVM. This model estimates fire conditions based on soil moisture.

Principal method of modification of the vegetation model for the permafrost zone

In order to meet the objectives of the study, the LPJ-DGVM was revised and considerably modified for the permafrost zone by including the active-layer thickness as one of the key model variables (Venevsky 2001). Climate variables (daily temperature, precipitation and incoming radiation) define active-layer thickness, soil moisture status and vegetation status. A daily value of the active layer thickness affects water uptake by roots, runoff and percolation of water in the soil and, therefore, vegetation production and soil moisture content. The daily soil moisture content determines the probability of fire, vegetation production status and determines thermophysical properties of soil (and as a result, a current active-layer thickness). Photosynthesis and water uptake by

plants are joint processes which significantly influence daily soil moisture content. Vegetation can be removed by fire in the model and affects fire by an amount of accumulated litter (fuel). The dynamics of the permafrost table, or active-layer thickness, depends on the local surface energy balance, reflecting first of all air temperature as modified by soil thermophysical properties, vegetation, snow and solar radiation (Kudryavtsev et al. 1974). Due to variations in snow cover or vegetation type and corresponding changes in heat transport and radiative energy exchange, surface temperatures may differ from the air temperature by several degrees. A simple periodic trigonometric function with the maximum annual thaw depth as an amplitude was applied to represent daily depth profile of seasonal thawing and freezing, which starts from above. Three regions with measured seasonal thawing depth were taken for validation of the active layer model, two in Siberia (Central Jakutia) and one in Alaska (Kuparuk river basin).

RESULTS OF SIMULATION WITH HISTORICAL CLIMATE DATA

Set of experiments

To assess the influence of permafrost and fire regimes for vegetation structure and carbon pools/exchange, the modified version of the LPJ-DGVM was run in two modes, with and without active-layer processes. For the global historical simulation within the LPJ-DGVM, the CRU05 1901-1995 0.5°x0.5° monthly climate data, provided by the Climate Research Unit, University of East Anglia, UK, was used.

Comparison with observations

Aboveground vegetation biomass differs rather significantly in the runs with and without active-layer processes. The vegetation carbon content in the Asian part of Russia changed from 7.5-12.5 kgC/m^2 to 2.5-10 kgC/m^2 and generally decreased 1.5-2.5 times, when the processes seen in the permafrost zone were included in the LPJ-DGVM. The fire return intervals in western and eastern Siberia decreased two to four times, especially in the continental areas, in comparison with the unmodified model version. The average growing stock of Larch stands by the nine administrative units of Siberia, simulated by the two LPJ-DGVM versions for the year 1993, was compared with the data of Russian Forest State The area of the administrative units varies from 0.4 to 3 10^6 km^2. The mean square relative deviation of simulated against observed growing stock was 26% for the modified LPJ-DGVM version, compared with 70% accuracy obtained with the original version. The growing stock for the largest northern administrative units, Magadanskaia oblast', Sakha (Jakutia) and Evenkiiskaia AO decreased 1.5 to 2 times after the model modification and became close to reality.

CONCLUSION

The significant improvement of results for the vegetation carbon in the permafrost zone is mainly influenced by changes in the hydrological regime with associated transitions in the fire regimes. Therefore, interaction of fire regimes and thaw/freeze processes are very important for vegetation structures in the permafrost zone.

REFERENCES

Venevsky, S. 2001. Broad-scale vegetation dynamics in north-eastern Eurasia – observations and simulations, Universität für Bodenkultur, Vienna, 150 pp.

Sitch, S., Smith, B., Colin Prentice I. and LPJ consortium. 2003. Evaluation of ecosystem dynamics, plant geography and terrestrial carbon cycling in the LPJ Dynamic Global Vegetation Model, Global Change Biology 9: 161-185.

Kudryavtsev, V.A., Garagulya, L.S., Kondrat'yeva, K.A. and Melamed, V.G. 1974. Fundamentals of frost forecasting in geological engineering investigations. Nauka, Moscow, 431pp.

Permafrost Monitoring in Switzerland (PERMOS) in the pilot stage

*D.S. Vonder Mühll, *R. Delaloye, ** W. Haeberli, **M. Hoelzle and ***B. Krummenacher*

Delegate for Permafrost of the Glaciological Commission; Universities of Basel and Zurich, Switzerland

**Institute of Geography, University of Fribourg, Switzerland*

***Glaciology and Geomorphodynamics Group, Department of Geography, University of Zurich, Switzerland*

****Geotest AG, Davos, Switzerland*

INTRODUCTION

The variation of the glacier tongues has been observed systematically in Switzerland since the 1850s. The Swiss Academy of Sciences (SAS) and the Swiss Alpine Club (SAC) were the driving institutions behind ensuring and maintaining the measurements. Permafrost is a thermal phenomenon of the subsurface, and with the snow it complements the cyrosphere. In contrast to glaciers and snow, systematic scientific investigations of Alpine permafrost started some 30 years ago.

The drilling through the Murtèl-Corvatsch rock glacier in 1987 triggered a number of follow-up and parallel activities in permafrost research at several Swiss institutes. Concepts for a Swiss monitoring network on permafrost were developed (Haeberli et al. 1993, Glaziologische Kommission 2000) parallel to efforts initiated by the International Permafrost Association (IPA, Frozen Ground 1995; Brown 1997). While the IPA monitoring strategy was developed mainly for high-latitude plain permafrost areas, PERMOS is adapted to the low-latitude mountain permafrost.

OBJECTIVES

The main goal is to document status and long-term variations of Alpine permafrost. **PER**mafrost **MO**nitoring in **S**witzerland (PERMOS) is based on three elements:

1. recording thermal changes in permafrost, in particular permafrost temperatures in boreholes,
2. determining the lateral distribution pattern near the lower permafrost boundary using the BTS (**B**ottom **T**emperature of the **S**now cover in March) - method in combination with single-channel temperature-loggers, and
3. taking aerial photos to build an archive for photogrammetrical determination of geomorphologic surface changes due to changes in permafrost characteristics.

As a consequence, the processes involved can be investigated and modelled to improve the understanding and knowledge of Alpine permafrost. In addition, long-term development can be analyzed and monitoring parameters adapted if necessary

During the pilot phase, PERMOS comprises 10 boreholes (which all were drilled within scientific projects with mainly non-monitoring aims) and 10 BTS areas (some of which have been observed for several years already) plus about two flights per year for aerial photographs. The distribution of the sites is somewhat random (Fig. 1). Spatial gaps will be filled after the pilot phase.

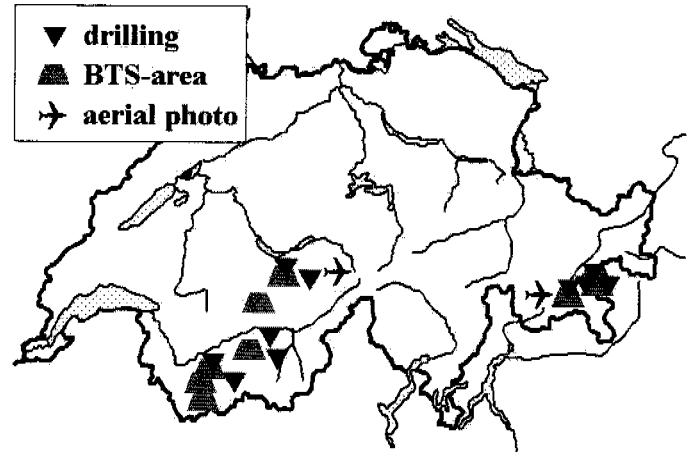

Figure 1. Distribution of the PERMOS sites (drillings and BTS areas) during the pilot phase in the contours of Switzerland.

MANAGEMENT SETUP

The network was initiated by the Swiss Adhering Body of the IPA, and the concept (Glaziologische Kommission 2000) approved by the Glaciological Commission of the Swiss Academy of Sciences (SAS). During the pilot phase, PERMOS is financed by the SAS, the Swiss Forest Agency and the Federal Office for Water and Geology. Measurements are done by eight institutions (Academia Engadina Samedan, ETH Zurich, the Universities of Basel, Bern, Fribourg, Lausanne and Zurich, SFISAR Davos). Annual reports are published by the Glaciological Commission of the SAS.

INITIAL RESULTS

Permafrost temperatures have been recorded at Murtèl-Corvatsch since 1987 (Fig. 2). Processes and causes for variations are discussed by Vonder Mühll (2001). Similar temperature series are recorded at all PERMOS drill sites. Permafrost temperature at 10 m depth range is between –2°C and 0°C. Thickness of the active layer is determined where a data logger records temperatures.

The BTS-area of Alpage de Mille (2220 to 2460 m a.s.l.) has been observed systematically since 1996. Every year at around the same date, BTS values are measured at more that 60 points to investigate variations from one year to another. While the pattern is about the same every year, BTS values vary up to 3°C from one year to the next (Vonder Mühll et al. 2001). The BTS working group of PERMOS is analyzing the set up of the BTS areas and adapting the method for the second pilot phase.

Due to weather conditions, no aerial photos were taken in 2001. In 2002, photos were taken in the Upper Engadin region (Corvatsch-Murtèl).

OUTLOOK

PERMOS is part of the Global Terrestrial Network - Permfrost GTN-P. It is on track to be established and financed by Swiss Federal Departments, together with the Swiss Glacier Network, in about three years. It is important that the measurements are taken, interpreted and coordinated by the scientific community of the Swiss Adhering Body of IPA.

REFERENCES

Brown J. 1997. Disturbance and recovery of permafrost terrain. In: Disturbance and recovery in Arctic lands (Ed. R. M. M. Crawford). Kluwer Academic Publishers: 167-178.

Glaziologische Kommission 2000. Aufbau eines Permafrost-Beobachtungsnetzes in der Schweiz – PERMOS (Konzept und Anhang). 5 plus appendix. http://www.unibas.ch/vr-forschung/PERMOS

Haeberli W., Hoelzle M., Keller F., Schmid W., Vonder Mühll D. and Wagner S. 1993. Monitoring the long-term evolution of mountain permafrost in the Swiss Alps. Sixth International Conference on Permafrost, Beijing, Proceedings 1: 214-219.

Vonder Mühll D. 2001. Thermal variations of mountain permafrost: An example of measurements since 1987 in the Swiss Alps. In Visconti et al (eds.): Global Change in Protected Areas.(Kluwer Academic Publisher): 83-95.

Vonder Mühll D., Delaloye R., Haeberli W., Hölzle M and Krummenacher B. with contributions of 13 others, 2001: Permafrost Monitoring Switzerland PERMOS, 1. Jahresbericht 1999/2000. 32p plus appendix. http://www.unibas.ch/vr-forschung/PERMOS.

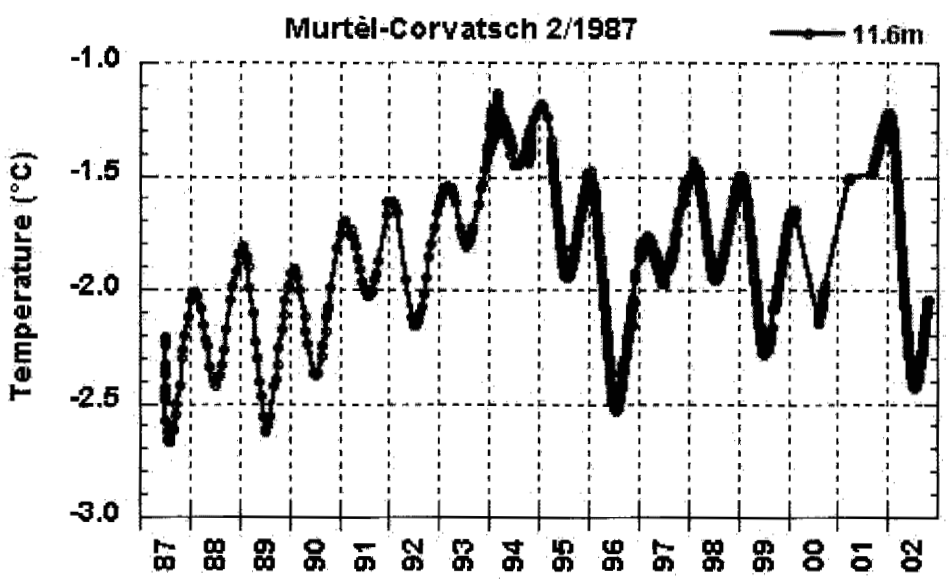

Figure 2. Permafrost temperature at 11.6 m depth in borehole 2/1987 through Murtèl-Corvatsch rock glacier. In the winters 1988/1989, 1995/1996 and 2001/2002 major snowfall came only in January/February, causing a strong cooling of the permafrost.

Methanogenesis under extreme environmental conditions in permafrost Soils: a model for exobiological processes?

D. Wagner, S. Kobabe and E.-M. Pfeiffer

Alfred Wegener Institute for Polar and Marine Research, Research Unit Potsdam, Germany

INTRODUCTION

Permafrost within the solar system exists on seven planets as well as several moons, which are characterized by cold environmental conditions. Of special interest to present-day research in astrobiology is the comparability of environmental and climatic conditions of the early Mars and Earth. Martian and terrestrial permafrost areas show similar morphological structures, suggesting that their development is based on comparable processes. New high-resolution images of the Mars Orbiter Camera (MOC) imply water in liquid form or as ground ice on Mars, which is an essential bio-physical requirement for the survival of micro-organisms in permafrost. Terrestrial permafrost, in which micro-organisms have survived for several million years (Rivkina et al. 1998), is an ideal model for comparative system studies regarding the evolution, adaptation and survival strategy of microorganisms under extreme conditions.

METHANOGENESIS

The microbial methane production (methanogenese) is the terminal step during the decomposition of organic matter in permafrost soils. Responsible for the methane production is a small group of highly specialized microorganisms, called methanogenic archaea, which are considered to be one of the initial organisms from the beginning of life on Earth. They are regarded as strictly anaerobic microbs, which can grow and survive only under anoxic conditions, like in wet tundra environments. Compared to Martian conditions, such a metabolism would be favourable because the atmosphere on Mars is dominated by CO_2 (95.3 %). Furthermore, they are characterized by litho-autotrophic growth, whereby energy is gained by the oxidation of hydrogen, and carbon dioxide can be used as the only carbon source (Deppenmeier et al. 1996). Organic compounds, which were not verified on Mars, are not required for growth. The special metabolism qualities of the methane-forming archaea are the reason that they are regarded as *key organisms* for further investigation in the adaptation strategies and long-term survival in extreme environments such as those with terrestrial permafrost (Wagner et al. 2001).

MICROBIAL METHANE PRODUCTION UNDER EXTREME CONDITIONS

The field investigations were carried out on the Samoylov island (N 72°, E 126°) located in the Lena Delta/Siberia. The study site represented an area of typical polygonal patterned grounds with ice wedges. The permafrost soils were classified as *Glacic Aquiturbels* and *Typic Historthels* with a maximum thaw depth between 30 and 55 cm. The average air temperature was –14.7 °C with a min. of -47.8 °C in January and a max. of +18.3 °C in July.

The investigation of *in situ* methane production revealed methane formation in the boundary layer to the permafrost at temperatures between 0.6 and 1.2°C (Fig. 1) with a rate of about 1.0 nmol CH_4 h^{-1} g^{-1}. Without any additional substrate, the methane production varied between 0.3 and 4.7 nmol CH_4 h^{-1} g^{-1} (Fig. 2). The highest activity could be determined in the peat layer of the upper soil at an average temperature of 10 °C. Nevertheless, the comparison of different vertical profiles to the methane production showed that the activity of the micro organisms is independent of the soil temperature. After addition of methanogenic substrates (acetate, H_2), the activity drastically increased. The methane production in the peat layer with H_2 as substrate was about 2 times higher (13.0 nmol CH_4 h^{-1} g^{-1}) compared with acetate (7.2 nmol CH_4 h^{-1} g^{-1}) as substrate, while above the permafrost table the activity was in the same order of magnitude (approx. 1.5 nmol CH_4 h^{-1} g^{-1}) with both substrates. Even the incubation of soil material from the active layer with H_2 as a substrate showed a significant methane production rate at –3 °C (0.1 – 11.4 nmol CH_4 h^{-1} g^{-1}) and –6 °C (0.08 – 4.3 nmol CH_4 h^{-1} g^{-1}). The existence of a methanogenic community, which has adapted well to the low *in situ* temperature of permafrost soils is assumed by our results.

In accordance with Panikov (1997), psychrophilic bacteria have a significant part in the microbial community in cold environments like permafrost soils. However, the isolation

and characterization of methanogenic archaea from permafrost soils should clarify the possible growth characteristic (psychrophile or psychrotroph) and the ecological significance of these organisms.

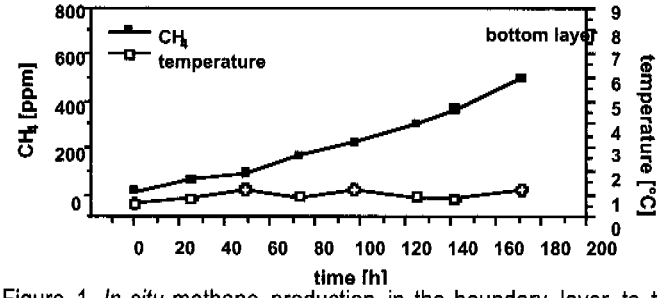

Figure 1. *In situ* methane production in the boundary layer to the permafrost in the soil of the polygon depression.

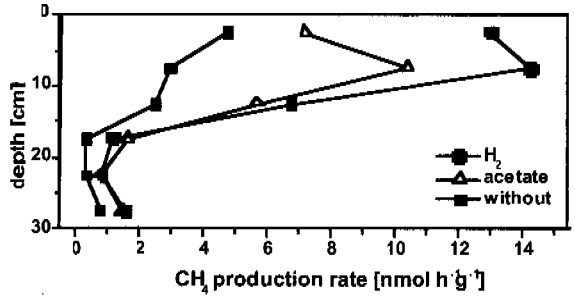

Figure 2. Vertical profile of methane production rates without any additional substrate as well as with H_2 and acetate in the soil of the polygon depression.

First results concerning the diversity of methanogenic microflora by fluorescence *in situ* hybridization (FISH) indicated that H_2-using genera like *Methanobacterium* and *Methanomicrobium* dominated over methylotrophic and acetotrophic methanogenic archaea. Enrichment cultures, which were dominated by the genera *Methanosarcina*, showed that these organisms grow not only with the preferred substrate methanol but also with CO_2 and H_2 as the only carbon and energy source.

CONCLUSIONS AND FUTURE PERSPECTIVES

Methanogenic archaea, which can live solely on the basis of water, minerals, carbon dioxide and hydrogen, survived in terrestrial permafrost for several millions of years. Since they are still active, they had to develop different strategies to resist extreme conditions like salt stress, physical damage by ice crystals and background radiation. The presented results demonstrate an essential basis for the understanding of the origin of life. The studies can be used as a model for exobiological processes to find traces of life in extraterrestrial habitats and to look for possible protected niches e.g. on Mars.

Apart from the presented studies, simulation experiments with permafrost microcosms can supply important results for the understanding of microbial life under extreme conditions (Wagner et al. 2003). Simulation of the freezing-thawing cycle can help to understand the problem in which way the microbial population will be influenced by the natural permafrost system and by the interaction of the combined parameters.

REFERENCES

Deppenmeier, U., Müller, V., Gottschalk, G. 1996. Pathways of energy conservation in methanogenic archaea. Archive of Microbiology 165: 149-163.

Panikov, N.S. 1997. A kinetic approach to microbial ecology in arctic and boreal ecosystems in relation to global change. In W.C. Oechel (ed), Global Change and Arctic Terrestrial Ecosystems Berlin: Springer. 171-188.

Rivkina, E., Gilichinsky, D., Wagener, S., Tiedje, T., McGrath, J. 1998. Biogeochemical activity of anaerobic microorganisms from buried permafrost sediments. Geomicrobiology 15: 187-193.

Wagner, D., Spieck, E., Bock, E., Pfeiffer, E-M. 2001. Microbial life in terrestrial permafrost: methanogenesis and nitrification in Gelisols as potentials for exobiological processes. In G. Horneck, C. Baumstark-Khan (eds), Astrobiology: the quest for the conditions of life Berlin: Springer. 143-159.

Wagner, D., Wille, C., Pfeiffer, E.-M. in preparation. Simulation of annual freezing-thawing cycles in a permafrost microcosm for assessing microbial methane production under extreme conditions. Permafrost and Periglacial Processes, submitted.

A physiognomic-based circumpolar Arctic vegetation map

*D. A. Walker, M. K. Raynolds and, *N. G. Moskalenko*

Alaska Geobotany Center, Institute of Arctic Biology, University of Alaska Fairbanks

**Earth Cryosphere Institute, Siberian Division, Russian Academy of Sciences, Russia*

The Circumpolar Arctic Vegetation Map (CAVM) depicts the distribution of 20 vegetation-physiognomy units in the Arctic (CAVM Team 2003). The map is based on the principle that environmental controls such as climate, topography, soil chemistry and floristic provinces determine which plants grow across the Arctic. The most important environmental control of plant growth in the Arctic is summer temperature. Temperature and vegetation data were used to define bioclimatic subzones.

For purposes of display, the 20 units of the CAVM were summarized into a much simpler map with 7 units (Table 1), based on dominant growth forms. The distribution of these categories by bioclimatic subzone (Fig. 1) is shown in Table 2.

Table 1. Condensed physiognomic legend with CAVM units.

Glaciers: 17. Nunatak area; 18. Glacier
Barren, herbs: 1. Cryptogam, cushion forb barren; 2. Cryptogam barren (bedrock); 3. Non-carbonate mountain complex; 4. Carbonate mountain complex
Graminoid, prostrate shrubs: 5. Rush/grass, forb cryptogam tundra; 6. Graminoid, prostrate dwarf shrub, forb tundra
Prostrate, hemi prostrate shrubs: 9. Sedge/grass, moss wetland; 13. Prostrate dwarf shrub, herb tundra; 14. Prostrate/hemiprostrate dwarf shrub tundra
Graminoid, dwarf shrubs: 7. Non-tussock sedge, dwarf-shrub, moss tundra; 8. Tussock sedge, dwarf shrub moss tundra
Erect dwarf shrubs, low shrubs: 10. Sedge, moss, dwarf shrub wetland; 11. Sedge, moss low shrub wetland; 15. Erect dwarf shrub tundra; 16. Low shrub tundra
Water: 19. Lakes. 20. Ocean

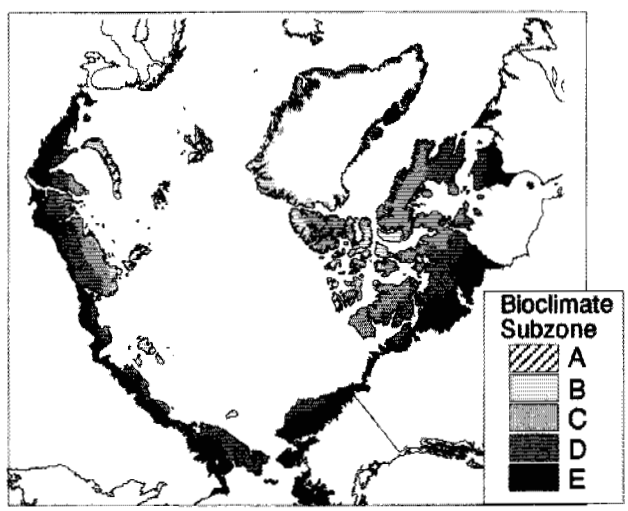

Figure 1. Bioclimate subzones of the circumpolar Arctic.

The glacier category excludes the Greenland Ice Sheet (1697 km^2), which spans numerous bioclimatic subzones. Glaciers cover the largest area in Subzone C, but cover the greatest percentage of Subzone A. Barren vegetation types are common in Subzones A and B, especially on the calcareous soils of the Canadian Arctic Islands. Barren areas in Subzone C are mainly on the Canadian Shield and the Taymyr Mountains; and in Subzones D and E, are due to the mountains of Chukotka and Alaska.

Graminoid-dominated vegetation types with prostrate shrubs are found in the southern Canadian Arctic Islands (Subzones B and C). Graminoid types with erect shrubs (including tussock tundra) are more common in Alaska and Yakutia (Subzones D and E).

Prostrate-shrub dominated vegetation types are common on the southern Canadian Arctic Islands, northern mainland Canada and the Taymyr Peninsula (mainly Subzone C). Erect shrubs are found in western Russia, southern Chukotka, southern Keewatin and the Ungava Peninsula (mainly Subzone E).

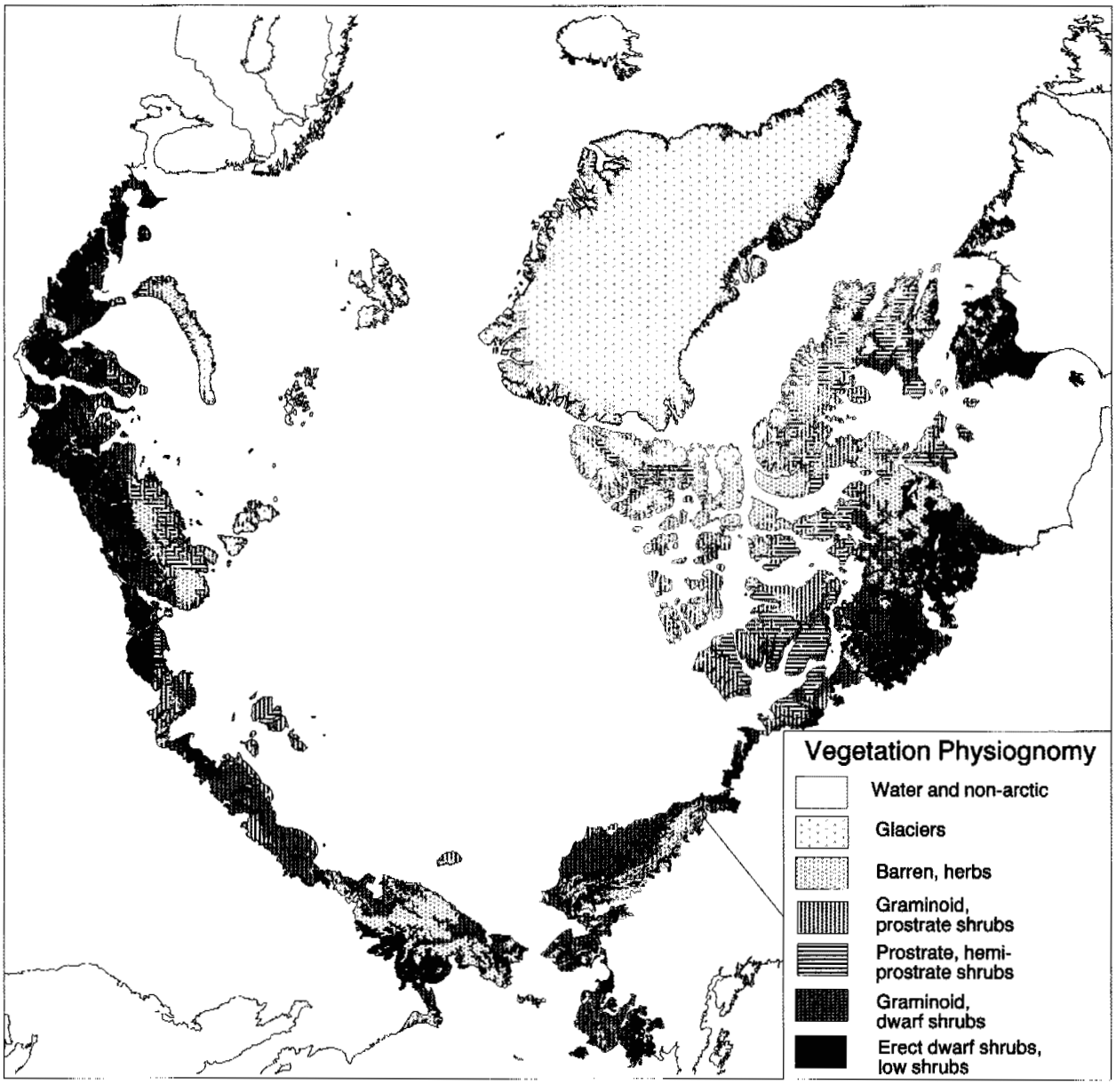

Figure 2. Distribution of vegetation physiognomy in the circumpolar Arctic.

Table 2. Area of physiognomic categories in bioclimate subzones (1000 km²).

Physiognomic Unit	*Subzone*					
	A	*B*	*C*	*D*	*E*	*Total*
Glaciers	95	63	127	74	2	360
Barren, herbs	61	242	332	343	231	1208
Graminoid, prostrate shrubs	2	71	375	162	0	610
Prostrate, hemi-prostrate shrubs	37	130	305	19	68	560
Graminoid, dwarf shrubs	0	0	34	609	505	1148
Erect dwarf shrubs, low shrubs	0	0	0	272	924	1196
Total	194	506	1174	1479	1729	5083

Subzone A is predominantly glaciers and barren. Subzone B is predominantly barren and prostrate shrubs. Subzone C is a mix of barren areas (Canadian Shield); graminoid, prostrate shrubs; and prostrate shrubs. Subzone D is mostly graminoid, dwarf shrubs. Subzone E is a mix of erect shrubs and graminoid, dwarf shrubs.

ACKNOWLEDGEMENTS

This research project is funded by National Science Foundation Grant OPP-9909929, with support from the US Fish and Wildlife Service and the Circumpolar Arctic Flora and Fauna Project.

REFERENCES

Circumpolar Arctic Vegetation Mapping Team. in press. Circumpolar Arctic vegetation. Conservation of Arctic Flora and Fauna (CAFF) Map No. 1. Scale 1:7,500,000. U.S Fish and Wildlife Service, Anchorage, AK.

Permafrost and the Colville River Delta, Alaska

H. J. Walker

Department of Geography and Anthropology, Louisiana State University, Baton Rouge, LA 70803-4105, USA

Although the study of frozen ground has a fairly long history, it was not until 1943 that Siemon Muller first used the word permafrost in a classified volume for the U.S. Army entitled Permafrost or Permanently Frozen Ground and Related Engineering Problems. In 1947, after declassification, this monograph was published as a hard-cover book and then became available to the public (Muller 1947). It can be surmised that Professor Muller, in his Stanford University office, never anticipated that within 20 years there would be an international conference on the subject and that an international permafrost association would soon follow.

Research on the geomorphology of the Colville River delta, which was begun in 1961, included permafrost as a main item of concern. At the First International Conference on Permafrost, held at Purdue University, USA in 1963 (i.e., 40 years ago), a paper on the effect of permafrost and ice wedges on riverbank erosion was presented (Walker and

Arnborg 1966). Measurements collected included the depth (horizontal) of thermo-erosional niches (a term borrowed from the Russian termerosionaja niza) in the permafrost-bound banks of the delta's distributaries. Additional surveys were made of the included ice wedges along which block collapse occurred (Fig. 1) and benchmarks were established to monitor thaw rate of bank retreat. These stations were occupied periodically for the next 30 years. A number of seasons of measurements show that the rate of bank retreat varies with bank composition, bank height, and exposure to erosional processes (Walker 1983).

Lakes within the delta are highly variable in size, shape, and origin. All are affected by permafrost to some extent. Those sufficiently deep have a talik beneath but most are shallow and floored by permafrost with only a thin active layer developing during the summer. The most numerous bodies of water are those present in low-centered polygons bordered by ice wedges (Fig. 2).

Possibly the most unique of the lakes affected by permafrost in the delta are those perched in the sand dunes. Perched lakes can only continue to exist so long as there is an aquaclude between the lake's water table and the regional water table; in the case of the Arctic this aquaclude is often permafrost. Drainage of these ponds occurs by overflow as the accumulated snow melts and by flow through the surrounding sand as the active layer develops. The maximum thickness of the active layer within the dunes of the Colville delta by the end of the summer is generally less than two metres. Thus, those ponds in interdune depressions and in blowouts that are more than two metres deep retain water throughout the year (Walker 2002).

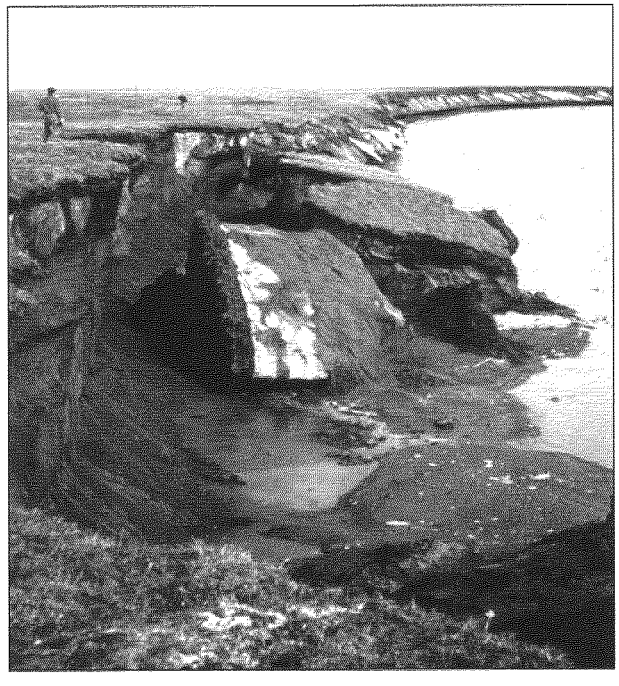

Figure 1. Block collapse along ice wedges in the Gubik Formation. Note the thermo-erosional niche in the background.

Morphologically, lake tapping provides some of the most sudden and drastic changes in the delta. Both lake expansion and river-channel migration lead to tapping which usually occurs between polygons because the ice wedges thaw faster than the surrounding permafrost. Once tapping occurs, lakes fluctuate in level with stage. At

low stage lake depths are reduced sufficiently so that permafrost begins to form in bottom materials. They also become subject to deposition during the river's flood stage and deltas form at the lake's entrance.

Sixty years ago, Muller emphasized the engineering problems associated with permafrost. During most of the subsequent period of time, most of the permafrost-related research in the Colville delta was basic. However, in the 1990s, with the exploration for and development of the oil industry in the delta, research became more applied. It was aimed at providing "... information essential for engineering design and evolution of potential environmental impacts..." (Jorgenson et al. 1998). Such research, which is being conducted by a variety of research teams, is providing much more detailed information about the role of permafrost in the formation and modification of delta forms.

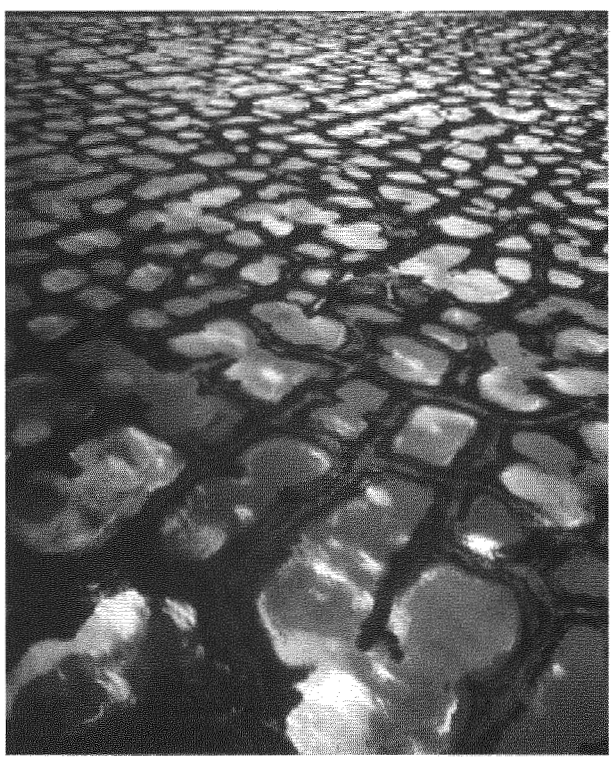

Figure 2. Typical ice-wedge polygon ponds in the Colville River delta.

REFERENCES

Jorgenson, M. T., Shur, Y. L., and Walker, H. J. 1998. Evolution of a permafrost-dominated landscape on the Colville River delta, Northern Alaska. Proceedings: Seventh International Permafrost Conference, Centre d'études nordiques, Université Laval: 523-529.

Muller, S. W. 1947. Permafrost or Permanently Frozen Ground and Related Engineering Problems. Ann Arbor: J. W. Edwards Press.

Walker, H. J. and Arnborg, L. 1966. Permafrost and ice-wedge effect on riverbank erosion. Proceedings: First International Permafrost Conference, National Academy of Science, National Research Council, Washington D. C, Publication 1287: 164-171.

Walker, H. J. 1983. Erosion in a permafrost-dominated delta. Proceedings: Fourth International Permafrost Conference. National Academy of Science Press, Washington D. C.: 1344-1349.

Walker, H. J. 2002. Landform development in an arctic delta; the roles of snow, ice and permafrost. In M. K. Hewitt et al. (eds), Landscapes of Transition, Dordrecht: Kluwer Publishers: 159-183.

Establishing four sites for measuring costal cliff erosion by means of terrestrial photogrammetry in the Kongsfjorden area, Svalbard

*B. Wangensteen, T. Eiken, J. L. Solid, *R. S. Ødegård*

Department of Physical Geography, University of Oslo, Norway

**Gjøvik University College, Norway*

The Kongsfjorden area is situated at the western coast of the Svalbard archipelago (Fig. 1). The area has continuous permafrost with measured depths around 140 meters near the shores of Ny-Ålesund (Liestøl 1976). The mean annual air temperature in Ny-Ålesund is -5.8° C (1975 to 2000) (Ketil Isaksen, pers. comm.). The tidal range is about 2 meters. The shores of the area are a mixture of cliffs in unconsolidated material, cliffs in bedrock and glacier fronts terminating in the sea. The selected four sites consist of low cliffs in bedrock and unconsolidated material, both with stony beaches in front (Ødegård et al. 1987). The geology at three of the sites is lime- and dolostone (Carbon and Perm) while one site is in an area of gneiss (upper Proterozoic). The unconsolidated beach material is of Quaternary origin (Hjelle 1993). The area has earlier been subjected to some related research activities concerning coastal processes e.g., cryogenic weathering of cliffs (Ødegård and Sollid 1993).

At all sites a fixed point for global reference was established; a bolt was drilled into the bedrock and its position measured by GPS. The positions of the camera stations were measured by GPS and surveyed from the fixed point to create both a global and a local reference. The photos were acquired with a stereo overlap using a Hasselblad camera with a 60 mm lens. At two of the sites bolts to be used as photogrammetric control points were drilled into the cliff wall as well. At the sites consisting of unconsolidated material no control points were established. The distance between the camera stations and the cliff wall varied between 7 and 15 meters for the four sites. The distance between the camera stations was approximately half of the photo distance. The coordinate system is transformed in a manner to simulate the geometry of aerial photogrammetry. The z-axis is pointing out of the cliff and the xy-plane is parallel to the cliff wall and also the line between the photo stations. The camera was mounted on top of the theodolite with a special device making it possible to measure the exact position of the camera and to ensure that the photo stations are on line parallel to the cliff wall. The camera positions are also used in the photogrammetric orientation of the scenes. For the scenes from the sites of unconsoli dated material this set-up also gives the opportunity to measure the photo angle used for exterior orientation of the scenes. This is important since no control points are available. The photos were scanned at a resolution of 11 μm (2,300 dpi) and imported into the Z/I Imaging digital photogrammetric workstation software. To be able to use the Z/I Imaging software the coordinate system had to be rotated, as explained earlier, and all coordinates up-scaled by a magnitude of 100, both to simulated aerial photography. After the photo pair or triples have been used to create a photogrammetric stereo model it is possible to automatically generate a high-precision digital terrain model (DTM). The Match-T algorithm in Z/I Imaging utilizes cross-correlation to detect the same points in the different photos of the stereo model and then measures the elevation by measuring the y-parallax. Photo distances in the range of 7 to 15 m give a scale of 1:117 to 1:250. With the above-mentioned scanning resolution the XY-resolution is in the order of 1.2 to 2.5 mm. The accuracy of elevation measurements done by photogrammetry is about 0.20 to 0.40‰ of the photo distance. This gives a theoretical elevation accuracy (Z-direction) of 1.4 to 2.8 mm for the 7 m photo distance and 3.0 to 6.0 mm for the 15 m photo distance.

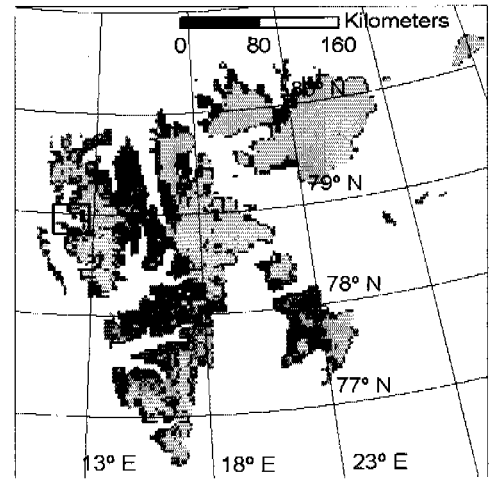

Figure 1. Map showing location of the investigated area.

The automatically-generated DTM for one of the sites is shown in Figure 2 as contour lines on top of an orthophoto of the cliff wall. The height and width of the area covered by the model is 3.3 m and 2.8 m respectively. When investigated in the digital photogrammetric workstation, the terrain model follows the terrain quite nicely. Precision estimates within the Z/I Imaging software gives a value of 1 to 2 mm for the Z-accuracy at this site. The photo distance used here was 7 meters.

Figure 2. Contour lines of 5 cm equidistance draped over an orthophoto. The size of the model area is 3.3 by 2.8 meters (height and width respectively).

The method of close up digital terrestrial photogrammetry seems suitable for creating accurate digital terrain models of coastal cliffs and hence promising for calculating erosion rates in the order of mm/year. The intention is to acquire a new set of photos of the same sites in 2004 to generate new terrain models that will enable the erosion rate calculations. André (1997) reports a rock wall retreat in the range 0 to 1.58 mm/year in the same area. The coastal cliff erosion rate is unknown but believed to be higher than the rock wall retreat rate and hopefully greater than the accuracy of the technique used.

The fieldwork was financially supported by the INTAS-project "Arctic coasts of Eurasia: dynamics, sediment budget and carbon flux in connection with permafrost degradation" (INTAS-2001-2329) and the Norwegian Research Council on behalf of the Norwegian Polar Committee.

REFERENCES

André, M.-F. 1997. Holocene Rockwall Retreat in Svalbard: A triple-rate evolution. Earth Surface and Processes and Landforms 22: 423-440.

Hjelle, A. 1993. Geology of Svalbard. Polarhåndbok No. 7, Norsk Polarinstitutt, Oslo.

Liestøl, O. 1976. Pingos, springs and permafrost in Spitsbergen. In Norsk Polarinstitutts Årbok 1975:7-29.

Ødegård, R., Sollid, J.L. and Trollvik, J.A. 1987. Coastal Map Svalbard A 3 Forlandssundet 1:200.000. Department of Physical Geography, University of Oslo.

Ødegård, R. Sollid, J.L. 1993. Coastal cliff temperatures related to the potential for cryogenic weathering processes, western Spitsbergen, Svalbard. Polar Research 12(1): 95-106.

Laboratory experiments towards better understanding of surface buckling of rock glaciers

M. Weber and A. Kääb

Glaciology and Geomorphodynamics Group, Department of Geography, University of Zurich, Switzerland

Wahrhaftig and Cox (1959) assumed permafrost creep to be the main transfer process in rock glacier flow. A number of boreholes on active rock glaciers give insight into material properties, rheology and the thermal conditions involved (Haeberli et al. 1998). Information on kinematics of rock glaciers has been obtained from terrestrial measurements and computer-aided aerial photogrammetry (Kääb 1998). Numerical modelling showed that transverse ridges might develop after a change in slope if two layers with different viscosity exist (Loewenherz et al. 1989).Yet still many questions concerning the interaction between kinematics and structure of a rock glacier remain unanswered. The characteristic topographic surface structures on rock glaciers, namely transverse ridges, can be regarded as a physical expression of these interactions. Within the framework of a diploma thesis aiming to analyze the occurrence of surface structures in combination with surface parameters, a creeping mass has been physically modelled in a laboratory experiment to qualitatively estimate possible processes involved in such surface buckling. The study addresses the following questions: is there a suitable substitute for the debris-ice mixture of a real rock glacier to be used in laboratory simulations? Is a decrease in longitudinal slope sufficient to trigger the evolution of transverse ridges in a viscous material? If not, which material properties allow transverse ridges to develop?

In our experiments the food additive Xanthan Gum (E415) has been tested. Xanthan gum is a microbial polymer prepared commercially in a pure culture fermentation of the bacterium Xanthomonas campestris. The molecular structure of Xanthan Gum results in pseudo plastic flow behaviour. Xanthan Gum is used in food engineering as well as cosmetics, and the petrochemical industry in order to control flow processes. Our experiments were carried out on a ramp built from perspex. The ramp is constructed such that its slope can be varied. (The discontinuity between the ramp and the horizontal base is referred to here as the "break of slope"). A container is fixed to the top of the ramp, used to provide equal starting conditions for each experiment. In changing the mixture of two compounds differing in viscosity and in solids content such as sand and/or gravel, the rheological behaviour of the material has been varied in a systematic way.

In summary, the experiments showed the following trends:

- No or only very minor transverse ridges at or near the break of slope are created if the material was well mixed and "homogeneous" (i.e., no solids content).
- If two components of different viscosities but no solids content are only slightly mixed ("heterogeneous"), fine transverse ridges could develop near the break of slope. After sufficient material has crept downwards and starts to accumulate in the horizontal, ridges develop above the break of slope.
- Ridges also develop if sand and/or gravel are added to a single-component mass.
- If a mass comprised of sand- and gravel-containing parts of different viscosity is only slightly mixed or applied in two separate layers, distinctive ridges appear.
- In another experiment, where a slightly mixed mass with sand and gravel ("heterogeneous") formed the bottom layer covered by a dry gravel brittle top layer, distinctive ridges developed. Moreover, due to the compression at the point of break in slope, single gravel particles were dislocated and fell into the newly-formed furrows. Viscous material was pushed from underneath to the surface forming ridges of increasing amplitude.

The findings from these experiments exhibit analogies to real rock glaciers. Although the observed processes are certainly not equivalent to those occurring in nature, the experiments yield structures comparable to those of real rock glaciers. A development model for transverse ridges can be deduced from the experiment described above in which a brittle layer has been forced up through viscous material. According to this model, it may be possible that transverse ridges on rock glaciers can develop due to the compressing flow of the viscous ice-debris-mass and its interaction with an overlying brittle layer (i.e., the active layer). It may also be possible that viscous ice-debris-mass be pushed up at places

due to the entire flow process. In any case, a heterogenous variation of viscosities, or solids content, respectively, seems to favour or even be a prerequisite for transverse surface structures to develop. Such conceptual models are presently being investigated in relevant high-precision field surveys.

ACKNOWLEDGEMENTS

Special thanks to STAERKLE & NAGLER AG, Zollikon, Switzerland for providing Xanthan Gum.

Figure 1. Mass comprised of sand- and gravel-containing parts of different viscosity, only slightly mixed: Distinctive ridges appear (exp. no. 14).

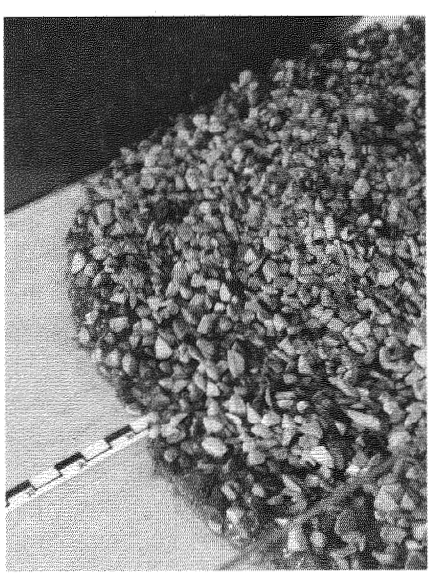

Figure 2. Slightly mixed mass comprised of sand and gravel heterogeneously covered by a brittle layer of dry gravel: Distinctive ridges appear, single gravel particles are dislocated, viscous material is pushed from underneath to the surface and amplitude of ridges increases (exp. no 18).

REFERENCES

Haeberli, W. 1985. Creep of mountain permafrost: internal structure and flow of alpine rock glaciers. Mitt. Versuchsanst. Wasserbau Hydrologie Glaziologie ETH Zürich. 77 pp.

Kääb, A., Gudmundsson, G.H. and Hoelzle, M. 1998: Surface deformation of creeping mountain permafrost. Photogrammetric investigations on Murtèl Rock Glacier, Swiss Alps. Proceedings of the Seventh International Conference on Permafrost, Yellowknife, Canada, Collection Nordicana 57: 531-537.

Loewenherz, D. S., Lawrence, C. J., Weaver, R. L. 1989: On the development of transverse ridges on rock glaciers. Journal of Glaciology 35 (121): 383-391.

Wahrhaftig, C., Cox, A. 1959: Rock Glaciers in the Alaska Range. Bulletin of the Geological Society of America 70: 383-436.

Weber, M. 2003: Oberflächenstrukturen auf Blockgletschern. Diploma thesis, University of Zurich.

Russian Information Transfer Programme

P. J. Williams and I. M. T. Warren

Scott Polar Research Institute, Cambridge, United Kingdom

The longest tradition of permafrost knowledge and the largest body of accumulated information is Russian. Russian studies can be traced back centuries, while it was only in the second world war that permafrost became of broad practical interest and an object of much scientific investigation in North America. In Finland, Norway and Sweden with their cold climates, and elsewhere, occasional studies have been made over two centuries at least. But apart from the contributions of several key figures, for example Taber, Beskow or Troll, only in Russia were there large-scale organised studies of frozen ground and permafrost and the corresponding technologies, through the first half of the twentieth century.

This Russian contribution continues and will increase, considering how many people live in a permafrost environment there, the extent of industrial (oil, gas, mineral development) and other human activities (including those of many native peoples). Development of Alaska and its natural resources and of northern Canada has brought similar intense interest in the scientific, industrial, geotechnical and general environmental conditions of the permafrost regions there. Such is modern society, permafrost is of global significance.

Most permafrost literature is in Russian or English, both major languages but not, for most individuals, interchangeable. The difficulties concern engineers, financiers, politicians and many others now involved with the cold regions. Accessibility to the information, however, is of the utmost importance - it may be extremely costly in financial and in human terms, to remain unaware of the hard-won expertise of others.

The Russian Information Transfer Programme of the Scott Polar Research Institute in Cambridge, England, is designed to bring the significance of 'permafrost' literature in the Russian language to those who cannot read it. It goes further than translation: it is a scholarly undertaking to ensure that the Russian work is as meaningful to English- language readers as to the Russian authors themselves. The history of the twentieth century was such that studies relating to Siberia, to the oil and gas industry, to military interests, and to the cold regions generally were not widely revealed to those outside the Soviet Union. Even more important was that the general lack of scientific exchange resulted in the development of concepts and models distinctly Russian on the one hand and distinctly 'English language' or 'Western' on the other. And however etymologically-polished a translation may appear, it loses much of its value if it is not quite understood by the specialist reader. Think merely of 'cryolithological regions', 'massive permafrost', 'basal ice'- terms quite acceptable to a first-rate translator but full of uncertainty to the permafrost-savvy English language reader.

The first undertaking under the nascent Programme was Professor Yershov's Obshchaya Geokriologiya - General Geocryology (1998), which is a comprehensive overview of Russian permafrost science and technology. The aim was to publish the book to a comparable standard to that if had been authored in English. This was a challenge but, even if we were not completely successful in meeting it, the book has given to English language readers a unique insight into the depth of Russian knowledge and its implications.

Building on this experience, an English-language folio volume was prepared to accompany the original maps of the 16-sheet highly informative Geocryological Map of Russia and Neighbouring Republics. All legends are translated, with additional explanations and a glossary. The Map set has immediate practical applications in planning, and for major engineering and other works. It gives insight into permafrost distribution and origin, active layer conditions and many other features, as well as into the manner in which such information is interpreted and utilised. The second edition (Williams and Warren 2003) of this folio volume (together with the maps) is being published shortly to meet the increased global interest in oil and gas especially, and in other aspects of the Russian cold regions. It includes refinements of the glossary, the translations and other components of the volume. Both Yershov's book and the Map have led to extensive discussions of interpretation with numerous specialists.

The next major undertaking has been the preparation of a volume of selected articles from Kriosfera Zemli - Earth's Cryosphere, the leading Russian journal devoted to permafrost and related topics. This work too has been carried out as a scholarly undertaking and, because of the diversity and importance of topics covered (for example, electrical and mechanical properties of frozen ground; permafrost distribution in coming years; gas hydrate stability; geotechnical foundation techniques; biological activity in permafrost) the advice of even more specialists (some never before involved with permafrost), has been sought. The aim is to continue to publish an English language version of this unique journal - but this will depend on the degree of financial support achieved through sales and other sources.

The Programme has benefited from a generous, collaborative approach from both the Russian and English-language sides, and especially from the authors, editors and publishers of the Russian studies. The Programme has led to new linkages and has given those working with it a fuller bibliographic insight, as well as a depth of understanding of the people and organisations that are contributing to our knowledge of geocryology. Consequently the Programme is also able to make other contributions in the form of advice, and, when funds are available, of literature searches and analyses and 'custom' translations. European Union funds have been awarded for visits to meetings by Russian specialists, especially relating to pollution in permafrost regions, strengthening the Programme in this topic.

Political developments and the significance of the permafrost regions point to a growth in coming years of the Russian Information Transfer Programme, but this will depend on the response of those who utilise it. Most agencies funding research doubtless see these activities as being peripheral to their responsibilities. Yet it is cheaper to benefit by the experience of others than to rediscover the problems and the expense of uncertain solutions, especially when the costs of making such knowledge available are small indeed compared to the financial and other dangers of proceeding in ignorance.

REFERENCES

Yershov, E. 1998. General Geocryology: (originally published as Obshchaya Geokriologiya, Nedra, Moscow). Cambridge University Press, 580pp ISBN 0 521 47334 9.

Williams, P.J. and Warren I.M.T. 2003.The English Version of the Geocryological Map of Russia and Neighbouring Republics.2nd. Edn. Original maps, guide, folio, I-X, & 21pp. Cambridge University, Carleton University, University of Moscow. Ottawa: Collaborative Map Project. ISBN 0-9685013-0-3.

Permafrost as a natural cryobank of late pleistocene and modern plant germplasm

*S. G. Yashina, E .N .Gakhova and *S. V. Gubin*

Institute of Cell Biophysics, Russian Academy of Sciences, Pushchino, Moscow Region, Russia

**Institute of Physicochemical and Biological Problems in Soil Science, Russian Academy of Sciences, Pushchino, Moscow Region, Russia*

INTRODUCTION

Conserving the world's biological diversity has recently become a global problem. The scientific community is now ready to use the advances in cryobiology to initiate long-term strategic and sustainable genetic resource cryobanks for saving endangered species, in addition to the traditional means such as nature reservation, botanical gardens, etc. (Gakhova 1998, Tikhonova and Yashina 1998). In recent years, the viable spores of mosses (Gilichinsky et al. 2001) and seed embryo cells of the higher plants (Yashina et al. 2002) have been discovered within Siberian late Pleistocene permafrost. It was demonstrated that they were able to develop and grow. In connection with this, new prospects have been revealed for cryopreservation and long-term banking germplasm of the modern wild plant. In this study we show current research on vital functions of higher plant seeds from permafrost deposits and present some data for the use of permafrost for the conservation of modern plant seeds.

MATERIALS AND METHODS

The seeds and unripe fruits were evoked from the fossil barrows of ground squirrel in the late Pleistocene ice-loess sediments of North Yakutiya (Gubin and Khasanov 1996). The burrows were found in the constant annual subzero temperature layer at a depth of 10 to 18 m. Radiocarbon age of the paleontological material was determined to be an average of 30 thousand years. Seeds were identified by means of a collection of plant seeds from the Kolymsko-Indigiskaya lowland (Yashina et al. 2002). The fossil seeds were introduced into *in vitro* culture on an agar nutritious medium to ascertain their vital capacity. Methods of plant tissue culture and clonal micropropagation of plant *in vitro*, light microscopy and microphoto were used.

The long-term experiments on storage of modern wild plant (14 species) seeds were performed in a permafrost zone at various temperature conditions. Viability of modern plant seeds was determined by periodic control over the laboratory germinating capacity.

RESULTS AND DISCUSSION

Seeds of sufficient diversity were found in the burrow studied (up to 10 species). Attempts at seed germination were undertaken for each species, but physiological viability of seeds was discovered only in 3 species: stenophyllous campion (*Silene stenophylla* Ledeb.) of the pink family (Caryophyllaceae) and 2 species, identified accurate to the genus: arctous (*Arctous spp.*) of the heather family (Ericaceae) and persicaria (*Polygonum spp.*) of the persicaria family (Polygonaceae). The plantlet of persicaria seed has germinated *in vitro* culture to cotyledon leaf stage (Fig. 1). Callusing from endosperm cells of arctous seeds has been obtained also in culture. It turned out that campion seeds are more tolerant to long-term storage at a subzero temperature. The initial stage of embryonal root growth and callus formation from the resulting roots cells has been induced on several of campion seeds. Development of embryonal roots has not occurred because of degradation of the storage tissue. At the same time, fragments of embryonal tissue in unripe fruits of campion have been shown to have the properties of enlargement (Fig. 2) and organogenesis formation. At present, the plant material obtained provides the basis for clonal micropropagation and the subseguent recovery of plants of full value. The long-standing experiments on storage of wild plant seeds are performed in a permafrost zone at different temperature regimes in order to use permafrost for conservation of the plant genetic resources. Part of the seed samples were placed into the glacier (Kolymsko-Indigiskaya lowland) at mean annual temperatures of -15°C, the rest were placed into an underground depository in the Melnikov permafrost Institute of SD RAS (Yakutsk) and stored at -2,7°C. Research on viability of seeds by determination of laboratory germination capacity over 1.5, 2 and 5 years have shown that glacier conditions had some advantages over the underground storage of seeds. At the same time the seeds of some species had more high germination capacity in underground storage in relation to control (laboratory storage at +4°C). It is interesting that microbiotic seeds (*Anemone sylvestris* L., *Pulsatilla patens* (L.) Mill.) preserved high viability in the glacier as well as in the underground depository, whereas these seeds rapidly lost germination capacity at +4°C. Both easily germinat-

ing seeds (*Dianthus fischeri* Spreng, *D. superbus* L., *Leucanthemum vulgare* Lam.) and seeds with biological dormancy (*Lilium martagon* L., *Lavatera thuringiaca* L.) had high viability after storage in the glacier. Seeds of several species in the pink family demonstrated especially high viability after storage in the glacier for 5 years. It is noteworthy that the viable fossil stenophyllous campion belongs to this same family.

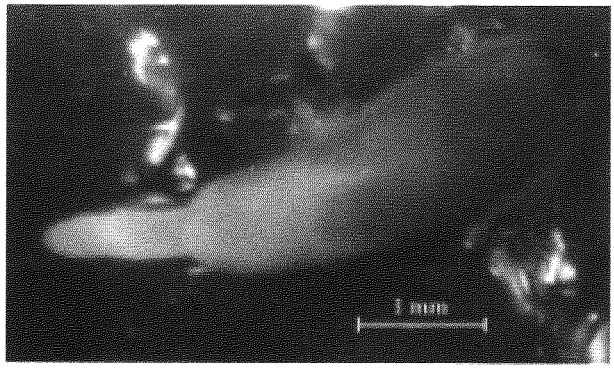

Figure 1. The plantlet of fossil persicaria seed

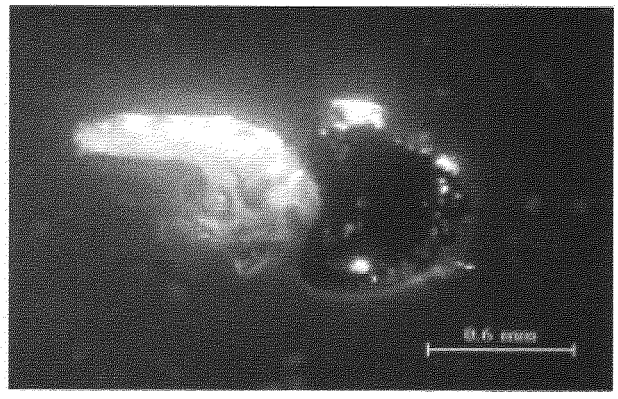

Figure 2. The fossil campion seed with fragment of enlarging embryonal tissue

CONCLUSION

For the first time, it has been demonstrated that cells of fragments of unripe fruits of stenophyllous campion and seed embryo cells of this species, as well as seed embryo cells of two unidentified species of the genera arctous and polygonum, preserved viability during thirty thousand years in permafrost. Physiological activity of seed cells has been discovered by the *in vitro* cultural method. This pioneering method for the conservation of seeds of modern wild species under permafrost conditions may be promising because this type of permafrost storage is protected from natural disasters and anthropogenic effects, is relatively inexpensive, and can maintain a stable subzero temperature. Many importance questions remain to be resolved including the identification of natural mechanisms of adaptation that allow plant cells and tissues to preserve vital capacity for thousands of years at subzero temperatures. Also, there is a need to study temperature regimes and other physicochemical conditions for the long-term storage of plant germplasm in permafrost.

ACKNOWLEDMENT

This work was supported by the Russian Foundation of Basic Research (grants 99-04-49369, 01-04-49087 and 02-04-49369).

REFERENCES

Gakhova, E.N. 1998. Genetic cryobanks for conservation of biodiversity. The development and current status of this problem in Russia. Cryo-Letters, suppl.1: 57-64.

Gilichinsky, D.A. et al 2001. How long the life might be preserved? In (Giovannelli F., ed.), Proceedings of the International Workshop «The Bridge between the Big Bang and Biology», Consiglio Nazionale delle Ricerche of Italy: 362-369.

Gubin, S.V. and Khasanov, B.R. 1996. The fossil barrows of Mammalia from permafrost sediments of Kolymsko-Indigirskaya Lowland. Dokl.Akad.Nauk 346(2): 278-279 (in Russian).

Tikhonova, V.L. and Yashina, S.G. Long-term storage of endangered wild plant seeds. Physiol. Gen. Biol. Rew. 13(1): 1-33.

Yashina, S.G. et al. 2002. Viability of higher plant seeds of late pleistocene age found in permafrost deposits as determined by in vitro culturing. Dokl.Akad.Nauk 383(5): 714-717 (in Russian).

Active layer monitoring in Northeast Russia: regional and interannual variability

*D. Zamolodchikov, *A. Kotov, **D. Karelin and ***V. Razzhivin*

Centre for Ecology and Productivity of Forests, Russian Academy of Sciences, Moscow, Russia

**Scientific Center "Chukotka", Anadyr, Russia*

***Biological department, Moscow State University, Moscow, Russia*

****Komarov Botanical Institute, St-Petersburg, Russia*

The CALM network (Brown et al. 2000) presently includes three sites in northeast Russia (Chukotka district). The first site, Cape Rogozhny, was established in 1994 on the northern coast of Onemen Bay (64°49'N, 176°50'E) of the Bering Sea. The second site, Mount Dionisy, started in 1996 and is located about 25 km south of Anadyr city (64°34'N, 177°12'E). Both sites are dominated by cotton-grass tussocks on Gleyi-Histic Cryosols. Frost cracks and frost boils are well developed. The third site, Lavrentia, was initiated in 2000 in the vicinity of Lavrentia settlement (65°36'N, 171°03'W). The site consists of wet sedge-*Salix* mosses tundra without developed microrelief on Gleyi-Histic Cryosols. This report was developed as a result of the CALM synthesis workshop held in November 2002 at the University of Delaware.

Grids (100x100 m) are used for active layer monitoring at the above sites. Thaw depth is measured using a steel rod (121 points per grid). The surface soil moisture is monitored at the Lavrentia site with a Vitel hydra probe (*Hydra soil moisture probe* 1994). Only end-of-season data are available for Cape Rogozhny and Mount Dionisy. Seasonal measurements were done at the Lavrentia site (3-4 point per summer).

The climate conditions at Cape Rogozhny and Mount Dionisy are well described by data from the Anadyr weather station (64°47'N, 177°34'E). The closest weather station to the Lavrentia site is at the Uelen settlement (66°10'N, 169°50'W).

The mean annual air temperature at the Anadyr and Uelen stations weather stations are fairly similar (Fig. 1*A*) in absolute values and interannual dynamics (R=0.89). Some temperature increase is observed from 1999 to 2002, but the warmest period was 1995 to 1997. For the period of CALM observations (1994-2002), a trend in the mean annual temperature is not noticeable.

An important climatic predictor of seasonal thawing is thawing degree days (DDT) value (Brown et al. 2000). The DDT values are different in the Anadyr and Uelen stations (Fig. 1*B*). The difference is explained by colder summers in the more marine conditions of Uelen and Lavrentia locations. The warmer winters at the above locations lead to similarities in the annual temperature regimes.

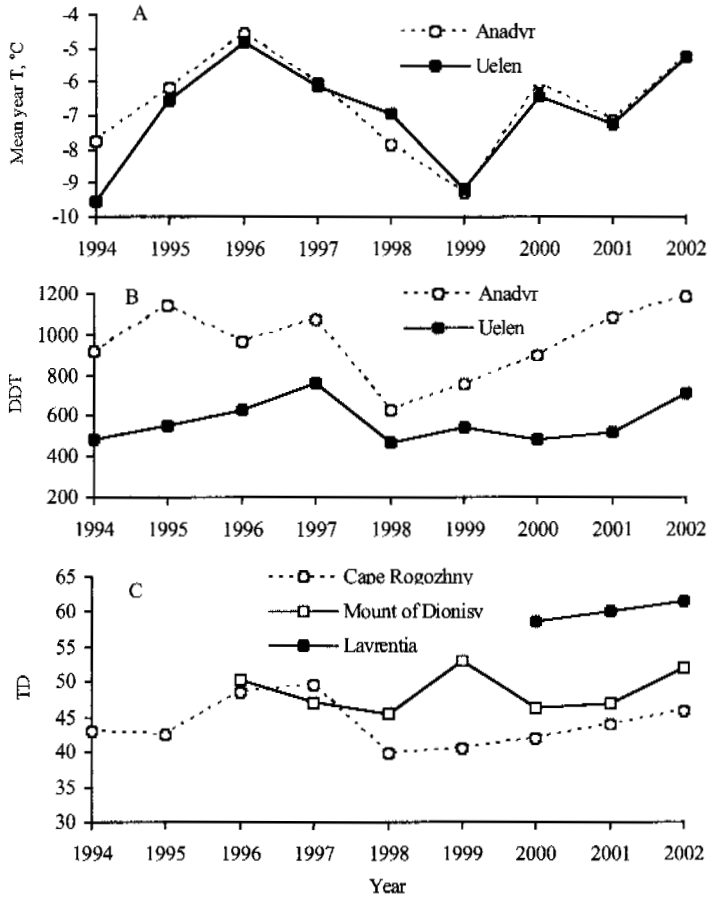

Figure 1. Dynamics of (A) mean annual air temperature, (B) DDT, and (C) end-of-season thaw depth at the CALM sites in northeast Russia.

The mean end-of-season thaw depth in Cape Rogozhny is 44 cm with interannual variations from 38 to 50 cm (Fig. 1*C*). The peak of seasonal thawing was registered in 1996 and 1997 (48 and 50 cm respectively).

The mean end-of-season thaw depth at Mount Dionisy is 49 cm with interannual variations of 45 to 53 cm. The most northern CALM site (Lavrentia) is characterized by the largest end-of-season thaw depth (60 cm), with small interannual variations (59 to 61 cm).

End-of-season thaw depth at Cape Rogozhny is correlated (R=0.62) with the square root of DDT (Fig. 2). The correlation is more pronounced (R=0.71) for thaw depth

and mean annual temperature. This result stresses the role that warm winters play in determining frozen ground temperatures and corresponding lower energy requirements for the thawing season.

The correlation of end-of-season thaw depth and $DDT^{0.5}$ is poor at the Mount Dionisy site (Fig. 2). This has two reasonable explanations. The first is related to the early dates of measurements (near 10 August) in some years (1997, 2000). Actual end-of-season thaw depth can be different from the measured values in these years. The second is due to landscape position of the site where the underground water flows determine the spatial patterns of soil thawing. Under these conditions the actual thaw depth is determined more by summer precipitation than by air temperatures.

The end-of-season thaw depth for the Lavrentia site is well-correlated with $DDT^{0.5}$ (R=0.96). However, the time series are limited for the site (n=3).

Analysis of the current CALM grid data allows us to characterize the main influences of spatial variability on thaw depth. At the Cape Rogozhny site the above factors are disturbances of vegetation and soil cover (frozen boils, tracks of all-terrain vehicles). In the Mountain Dionisy site, the spatial variability of the active layer is determined by subsurface water flows, corresponding to depressions of mesorelief. Frost boils also input to active layer variability at this site. The main control factor of end-of-season thaw depth at the Lavrentia site is the thickness of the soil organic layer.

Seasonal pattern of measurements at the Lavrentia site make it possible to reveal the changes of spatial variability control factor during soil thawing. At the beginning of the warm season, the thickness of organic soil layer, surface soil moisture and thickness of moss cover demonstrate approximately the same relation to thaw depth (absolute values of R coefficients vary from 0.3 to 0.4). In the course of the season the role of organic layer increases (R achieves -0.6), while the input of other factors decreases (absolute value of R diminishes to 0.2).

The present review of regional CALM studies in northeast Russia results in the following conclusions:

- there are no evident trends in end-of-season thaw depth in northeast Russia;
- drainage ways, surface disturbances and the thickness of the organic soil horizon have a major influence on the spatial variations of the end-of-season thaw depth;
- the influence of different factors on the thawing process is seasonally specific.

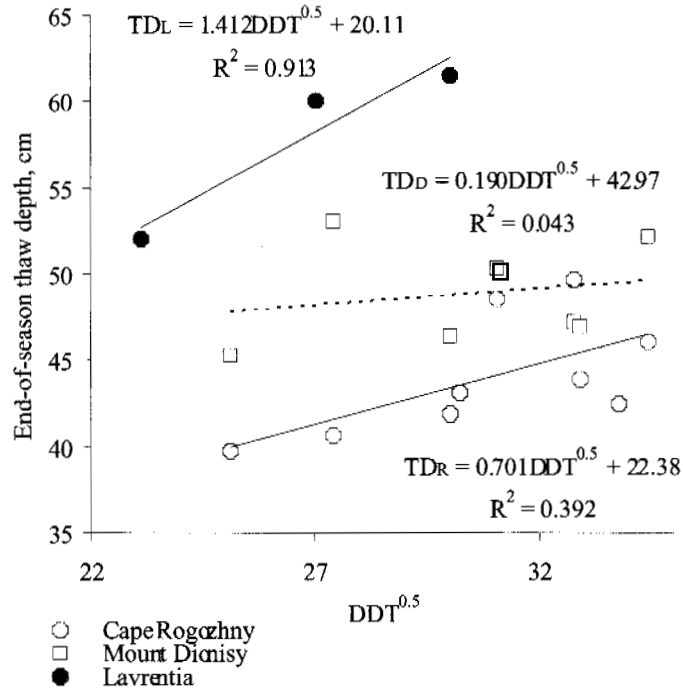

Figure 2. End-of-season thaw depth versus square root of thawing degree days for three CALM sites in northeast Russia.

ACKNOWLEDMENT

The fieldwork at the Lavrentia site was supported by the National Science Foundation (USA), Arctic Systems Science, Land-Atmosphere-Ice-Interactions Program (OPP-9216109), as part of flux studies in Arctic ecosystems (Zamolodchikov et al. 2003).

REFERENCES

Brown, J., Hinkel K.M. & Nelson F.E. 2000. The Circumpolar Active Layer Monitoring (CALM) program: research designs and initial results. Polar Geography 24(3): 166-258.

Hydra soil moisture probe user's manual. Version 1.2. 1994. Vitel, Inc., Chantilly, VA, 24 pp.

Zamolodchikov D.G., Karelin D.V., Ivaschenko A.I., Oechel W.C & Hastings S.J. in press. CO_2 flux measurements in Russian Far East tundra using eddy covariance and closed chamber techniques. Tellus. Special Issue.

Pedogenesis of carga thermochrone paleosols in North-East Russia

O. G. Zanina and S. V. Gubin

Soil Cryology Laboratory, Institute of Physicochemical and Biological Problems in Soil Science, Russian Academy of Sciences, Pushchino, Moscow Region, Russia

INTRODUCTION

Late Pleistocene soils buried in ice-loess deposits were used for reconstructing environments of the Carga thermochrone. The Carga thermochrone (50 to 28 thousand years BP) is a period of late Pleistocene time. In the Northeast of Russia paleosols developed during this period. These paleosols are characterised by a complex organisation; the deposits contain epigenetic and synlithogenetic soils (cryopedolite). Epigenetic pedogenesis in the period of the Late Pleistocene was repeatedly replaced by synlithogenetic pedogenesis. The terms "synlithogenetic" and "epigenetic" are used for the description of soil developments during this period. Epigenetic soil formation refers to processes where differentiation of the active layer material takes place in genetic horizons and soil profiles develop. Synlithogenetic soil formation occurs when material of deposits is transformed by pedogenetic processes in the absence of soil profiles. The different approaches for studying these layers are determined by their genesis.

METHODS

Buried soils contain a set of fossil organic materials in their organic horizons (peatland, humic-peatland). Conditions of soil formation are reconstructed using traditional paleosol methods on the basis of analyzed organic remains and of other soil properties. For studying synlithogenetic soils, detritus, spores and pollen existing in the deposits are analysed. Fossil rodent burrows of Carga cryopedolite are most informative for reconstruction due to their high content in biological matter.

OBJECTS

Paleosols were investigated in eight outcrops of the lower course of the Kolyma River. As a result of long-term research in the Kolyma lowland, buried soils including the two pedocomplexes – early Carga complex and late Carga complex - were determined (Gubin 1994). Layers of loess with attributes of synlithogenetic soil formation are covered by buried epigenetic soils.

Epigenetic pedogenesis

Paleosols of early Carga pedocomplex. Early Carga paleosols were formed during an initial thermochrone stage. The age of soils exceeds 37 thousand years. Paleosols of this period do not have the attributes of wood-soil formation. Their profiles are well differentiated into genetic horizons. Large wood remains are found within humic horizons of these paleosols.

Paleosols of late Carga pedocomplex. Soil formation took place during later periods of Carga time, 35 to 28 thousand years ago. Pedocomplexes include three buried soils of different ages. Structures of paleosol profiles which were formed during the initial stage of pedogenesis within the pedocomplex (the first and the second soils) are best developed. Paleosols are represented by Histosols and Gleysols, which are divided by layers of cryopedolite.

The organic horizons of Gleysols differ with respect to structure, properties and thickness. In these soils the hydromorphic characteristics and gleying are well expressed. The thickness of profiles varies between 1 to 2 m. The structure of organic horizons in moss and sedgy peat is different. The upper (third) soil has badly marked structures. It was formed under drier and even arid conditions of a harsh climate.

The organic horizons often consist of shallow layers of dry peat with high amounts of mineral material. The paleosol properties of the late Carga pedocomplex show a gradual trend towards harsher climatic conditions in this period.

Synlithogenetic pedogenesis

The cryopedolite forms under the influence of synlithogenetic soil formation. There is no differentiation of the active-layer material into genetic horizons. Concentrations of organic material are low and other soil properties weakly developed. Modern investigations of ice-loess deposits are conducted using spore-pollen analysis along with paleontologic and paleopedologic studies. For reconstruction of synlithogenetic soil formation the use of these methods is not sufficient. During the past years, ground squirrel burrows of the subgenus *Urocitellus* and of other rodents (lemmings and mice) were found in Late Pleistocene ice-loess deposits of North-East Eurasia. These objects differ with respect to depth of location inside the deposits, to structure and to content of frozen materials. The radiocarbon age of burrows is about 32 to 28 thou-

sand years. The formation of the burrows thus relates to the Carga thermochrone. The analysis of contents of fossil burrows and the ice-loess deposits containing them enables an impression to be gained about the environments of corresponding local habitats.

The structure of a number of fossil ground squirrel burrows has allowed to determine the thickness of the active layer at 60 to 80 cm during the time of their construction. The presence of sublimation ice in the central parts of chambers proves the absence of their flooding and low moisture of the bottom parts of the active layer during maximum thaw. Uniform distribution of burrows within Late Pleistocene polygons allows to assume plain character of a surface near the burrows. The simple structure of burrows, especially the absence of branching and platforms of excrements close to the entrance, points to a short-term existence of these constructions and rapid blocking of the surface by deposits from active eolian processes.

Fossil burrows of ground squirrel contain organic matter in excellent condition and obviously introduced from the surface. Remains of higher plants, including seeds and fruits, chitin remains of insects and their larvae, eggshells, feathers, excrements, bones and woolly mammals as well as their tissues were found among the contents of fossil burrows. The wool of large mammals found in burrows belongs to bisons and musk oxen which are widely distributed in tundra-steppe landscapes.

The amount of seeds and fruits from higher plants can reach hundreds of thousands of units inside feeding chambers. The great volume of fruit and seeds from fossil burrows belongs to the family of *Brassicaceae, Ranunculaceae, Cariophyllaceae, Poaceae* and *Carex*. The seeds *Silene stenophylla* Ledeb, *Bistorta vivipara* (L.) S.F. Gray, *Potentilla nivea* L and other species of sedges were found more frequently in burrows. The plant seeds from buried rodent burrows show the development of predominant tundra vegetation during the Carga thermocrone with the existence of pioneer and steppe species (Gubin et al. 2001).

Among the remains of fossil insects, various species such as leaf-beetle (Chrisolina rufilabris Fald, Ch. brunnicornis bermani Medv., Galeruca dahurica Jeann), billbug (Stephanocleonus eruditus Faust, S. fossilatus Fisch, Coniocleonus cf. ferrugineus Fahr) and larvae of several species of fly were discovered. These species are typical for the lower course of the Kolyma River during Late Pleistocene times. Almost all species are connected to steppe conditions. Collops obscuricornis Motsch (beetle of the family of Melyridae) was found in the west Chukotka area with modern relict steppe. This confirms that dry steppe conditions existed in the Northeast of Russia during Late Pleistocene time periods.

CONCLUSION

The Carga thermochrone in the investigated area is characterized by changes from synlithogenetic to epigenetic soil formations. Epigenetic soils buried during the Carga thermochrone from 40 to 28 thousand years ago provide information for reconstructing conditions of soil development. The periods of epigenetic soil formation were characterised by a decreasing intensity of eolian sedimentation, a slow increase in humidity and a warm climate. Synlithogenetic soil formation took place under conditions of dry tundra landscape with steppe vegetation as well as active accumulation of eolian deposits at the surface.

ACKNOWLEDGEMENTS

We thank Dr. S.V. Kiselev and Dr. G.G. Boeskorov for help with the identification of material collected from fossil burrows. This original research was supported by the Russian Foundation for Basic Research, grants *01-05-64496, 01-04-49087*.

REFERENCES

Gubin, S.V., Maksimovich, S.V. and Zanina, O.G. 2001. Composition of seeds from fossil gofer burrows in the ice-loess deposits of Zelyony mys as environmental indicator, Russia, Earth Cryosphere, 5 (2): 76-82.

Gubin S.V. 1994. The Late Pleistocene soil formation at the coastal lowlands of northern Yakutia, Russia. Soil Science 8: 5-14.

Changes in permafrost distribution and active layer thickness in Canada during the 20th century: a model assessment of climate change impact

*Y. Zhang, W. Chen, J. Cihlar, *S.L. Smith and *D.W. Riseborough*

Canada Center for Remote Sensing, Natural Resources Canada, Ottawa, Canada
**Geological Survey of Canada, Natural Resources Canada, Ottawa, Canada*

INTRODUCTION

Paleoclimate records and instrumental measurements show that the Arctic during the 20th century is the warmest in the past four centuries, and air temperature in the northern high latitudes has increased at a higher rate than the global mean. The Arctic is extremely vulnerable to climate change, and potential impacts include changes in permafrost distribution and active layer thickness, hydrological dynamics and carbon sink/source, which may positively feedback to the climate system. This paper presents our recent results about the transient changes in permafrost distribution and active layer thickness in Canada during the 20th century simulated by a process-based model at 0.5-degree latitude/longitude resolution.

METHODOLOGY

A process-based model to simulate permafrost thermal regimes was developed by combining the strength of existing permafrost and land surface process models. Soil temperature and active layer thickness (ALT) were determined by solving the heat conduction equation, with the upper boundary conditions being determined using the surface energy balance, and the lower boundary conditions being defined as the geothermal heat flux at a depth of 35 m, where heat flux is not very sensitive to climate variations. We assumed that the heat flux at this depth does not change with time during the simulation period. The model integrated the effects of climate, vegetation, soil features and hydrological conditions based on energy and water transfer in the soil-vegetation-atmosphere system (Fig.1). The model was validated against the measurements at four sites in Canada. The simulation results were in agreement with the measurements of energy fluxes, snow depth, soil temperature and thaw depth (Zhang et al. submitted).

Using this model, we simulated the transient response of permafrost distribution and ALT in Canada to climate change in the 20th century. The climate data were obtained from a 0.5-degree latitude/longitude gridded monthly dataset from 1901 to 1995 (New et al. 2000). A scheme was developed to scale down this monthly dataset to half-hourly intervals (Chen et al. submitted). Other input data include land cover types, leaf area index, surface and soil organic matter, soil texture, the geothermal flux and ground ice content. They are converted to 0.5-degree latitude/longitude, corresponding to the spatial resolution of climate data. The initial conditions are determined by iteratively running the model for an initial year until annual soil temperature is stabilized.

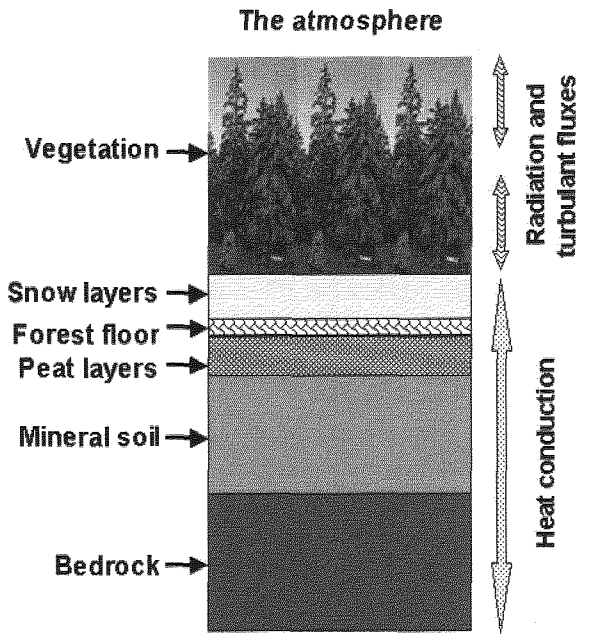

Figure 1. The components of the system considered in the model, and energy fluxes between soil, vegetation and the atmosphere.

RESULTS AND ANALYSIS

Figure 2 shows the simulated spatial distribution of ALT and its change. It also shows the distribution of permafrost areas and their change as well. The simulated permafrost distribution is similar to the permafrost map of Canada (Heginbottom et al. 1995), which is delineated based on permafrost site measurements, physiographic information and air temperature. (It largely represents permafrost conditions in the recent decades, but we show it in all the panels for spatial refer-

ence). Permafrost disappearance mainly occurs in the central part of western Canada, where air temperature increases have been the greatest over the last century. Permafrost also disappeared at the southern margins of the permafrost zone in the rest of Canada. Based on the number of grid cells underlain by permafrost, permafrost areas decreased 3% during the 20th century. ALT shows more gradual change with time and space. ALT ranges from a few centimeters in the north to more than 2.5 m in the south, reflecting the combined effects of both atmospheric climate and ground conditions. For example, ALT is thin in Mackenzie valley and in the southern Hudson Bay because of the wet and thick organic matter. From the 1900s to the decade of 1986-1995, ALT increased in most of the permafrost zone (92% of the permafrost grid cells), especially in western Canada; but ALT decreased in southern Hudson Bay and northern Quebec areas, and with some expansions in permafrost in these areas. These spatial distribution patterns correspond to the change in patterns of air temperature. Average ALT increased by 0.3 m for grid cells where ALT increased, and decreased by 0.1 m for grid cells where ALT decreased (excluding grid cells where permafrost disappeared or formed over this period). For all the permafrost grid cells ALT increased an average of 29% from the 1900s to the decade of 1986-1995.

CONCLUSIONS

Using a process-based model and inputs from climate records, soil features and remotely-sensed vegetation parameters, the transient response of permafrost distribution and active layer thickness in Canada to climate change during the 20th century was simulated. The results show that the land area underlain by permafrost decreased by 3% and ALT increased by 29% during the 20th century. However, permafrost degradation and changes in ALT differ with space and time.

REFERENCES

Chen, W., Zhang, Y., Cihlar, J., Smith, S.L. and Riseborough, D.W. submitted. Changes in soil temperature and active layer thickness during the 20th century in a permafrost region in western Canada. Journal of Geophysical Research.

Heginbottom, J.A., Dubreuil, M.A. and Harker, P.A. 1995. Canada Permafrost. In; National Atlas of Canada 5th edition, Natural Resources Canada, Ottawa, Canada.

New, M.G. Hulme, M. and Jones, P.D. 2000. Representing twentieth century space-time climate variability, Part II: Development of 1901-1996 monthly terrestrial climate fields. Journal of Climate 13: 2217-2238.

Zhang, Y., Chen, W. and Cihlar, J. submitted. A process-based model for quantifying the impact of climate change on permafrost thermal regimes. Journal of Geophysical Research.

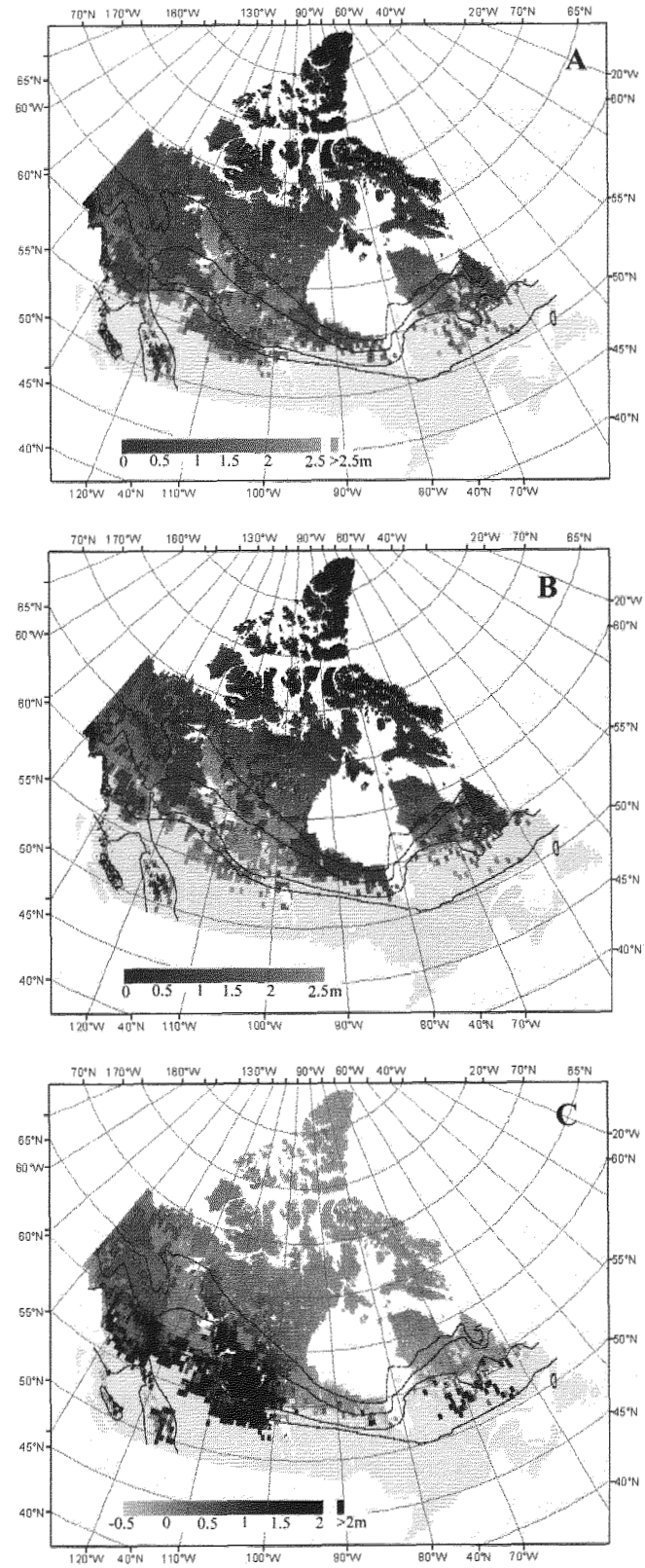

Figure 2. Active layer thickness during A) the 1900s, B) the decade of 1986-1995, and C) its change from the 1990s to 1986-1995. White color is for water bodies or outside Canada, and light gray in the south is for non-permafrost areas. A value of zero was used for glaciers. The curves are the southern boundaries of permafrost types (continuous, extensive discontinuous, sporadic discontinuous, and isolated patches from top to bottom, respectively) delineated in the map of Canada Permafrost (Heginbottom et al., 1995).

Author Index